THE STRETCH-SHORTENING CYCLE OF ACTIVE MUSCLE AND MUSCLE-TENDON COMPLEX: WHAT, WHY AND HOW IT INCREASES MUSCLE PERFORMANCE?

EDITED BY: Wolfgang Seiberl, Daniel Hahn, Geoffrey A. Power, Jared R. Fletcher and Tobias Siebert

PUBLISHED IN: Frontiers in Physiology

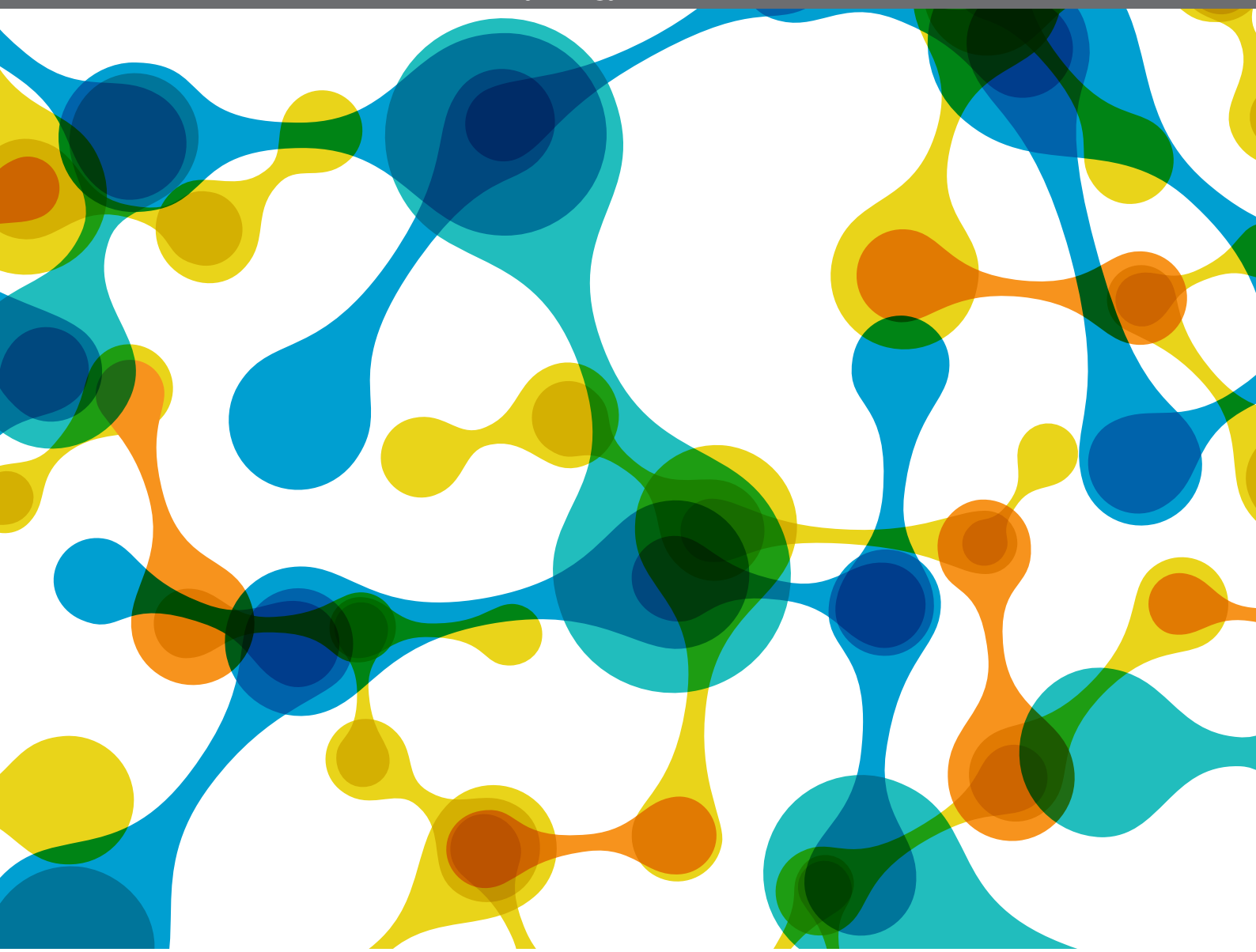

frontiers Research Topics

ISSN 1664-8714
ISBN 978-2-88966-993-6
DOI 10.3389/978-2-88966-993-6

About Frontiers

Frontiers is more than just an open-access publisher of scholarly articles: it is a pioneering approach to the world of academia, radically improving the way scholarly research is managed. The grand vision of Frontiers is a world where all people have an equal opportunity to seek, share and generate knowledge. Frontiers provides immediate and permanent online open access to all its publications, but this alone is not enough to realize our grand goals.

Frontiers Journal Series

The Frontiers Journal Series is a multi-tier and interdisciplinary set of open-access, online journals, promising a paradigm shift from the current review, selection and dissemination processes in academic publishing. All Frontiers journals are driven by researchers for researchers; therefore, they constitute a service to the scholarly community. At the same time, the Frontiers Journal Series operates on a revolutionary invention, the tiered publishing system, initially addressing specific communities of scholars, and gradually climbing up to broader public understanding, thus serving the interests of the lay society, too.

Dedication to Quality

Each Frontiers article is a landmark of the highest quality, thanks to genuinely collaborative interactions between authors and review editors, who include some of the world's best academicians. Research must be certified by peers before entering a stream of knowledge that may eventually reach the public - and shape society; therefore, Frontiers only applies the most rigorous and unbiased reviews.
Frontiers revolutionizes research publishing by freely delivering the most outstanding research, evaluated with no bias from both the academic and social point of view. By applying the most advanced information technologies, Frontiers is catapulting scholarly publishing into a new generation.

What are Frontiers Research Topics?

Frontiers Research Topics are very popular trademarks of the Frontiers Journals Series: they are collections of at least ten articles, all centered on a particular subject. With their unique mix of varied contributions from Original Research to Review Articles, Frontiers Research Topics unify the most influential researchers, the latest key findings and historical advances in a hot research area! Find out more on how to host your own Frontiers Research Topic or contribute to one as an author by contacting the Frontiers Editorial Office: frontiersin.org/about/contact

THE STRETCH-SHORTENING CYCLE OF ACTIVE MUSCLE AND MUSCLE-TENDON COMPLEX: WHAT, WHY AND HOW IT INCREASES MUSCLE PERFORMANCE?

Topic Editors:
Wolfgang Seiberl, Bundeswehr University Munich, Germany
Daniel Hahn, Ruhr University Bochum, Germany
Geoffrey A. Power, University of Guelph, Canada
Jared R. Fletcher, Mount Royal University, Canada
Tobias Siebert, University of Stuttgart, Germany

Citation: Seiberl, W., Hahn, D., Power, G. A., Fletcher, J. R., Siebert, T., eds. (2021). The Stretch-shortening Cycle of Active Muscle and Muscle-tendon Complex: What, Why and How It Increases Muscle Performance?. Lausanne: Frontiers Media SA. doi: 10.3389/978-2-88966-993-6

Table of Contents

frontiers in Physiology

EDITORIAL
published: 20 May 2021
doi: 10.3389/fphys.2021.693141

Editorial: The Stretch-Shortening Cycle of Active Muscle and Muscle-Tendon Complex: What, Why and How It Increases Muscle Performance?

Wolfgang Seiberl[1]*, *Daniel Hahn*[2,3], *Geoffrey A. Power*[4], *Jared R. Fletcher*[5] and *Tobias Siebert*[6,7]

[1] Human Movement Science, Department of Human Sciences, Bundeswehr University Munich, Neubiberg, Germany, [2] Human Movement Science, Faculty of Sport Science, Ruhr University Bochum, Bochum, Germany, [3] School of Human Movement and Nutrition Sciences, University of Queensland, Brisbane, QLD, Australia, [4] Neuromechanical Performance Research Laboratory, Department of Human Health and Nutritional Sciences, College of Biological Sciences, University of Guelph, Guelph, ON, Canada, [5] Department of Health and Physical Education, Mount Royal University, Calgary, AB, Canada, [6] Department of Motion and Exercise Science, University of Stuttgart, Stuttgart, Germany, [7] Center for Simulation Science, University of Stuttgart, Stuttgart, Germany

Keywords: eccentric contraction, passive elastic energy, stretch-reflex, performance enhancement, history dependence, plyometric exercise

Editorial on the Research Topic

The Stretch-Shortening Cycle of Active Muscle and Muscle-Tendon Complex: What, Why and How It Increases Muscle Performance?

OPEN ACCESS

Edited and reviewed by:
Giuseppe D'Antona,
University of Pavia, Italy

***Correspondence:**
Wolfgang Seiberl
wolfgang.seiberl@unibw.de

Specialty section:
This article was submitted to Exercise Physiology, a section of the journal Frontiers in Physiology

Received: *09 April 2021*
Accepted: *19 April 2021*
Published: *20 May 2021*

Citation:
Seiberl W, Hahn D, Power GA, Fletcher JR and Siebert T (2021) Editorial: The Stretch-Shortening Cycle of Active Muscle and Muscle-Tendon Complex: What, Why and How It Increases Muscle Performance? Front. Physiol. 12:693141. doi: 10.3389/fphys.2021.693141

INTRODUCTION

During a stretch-shortening cycle (SSC), a muscle is first actively stretched before it actively shortens (Cavanagh and Komi, 1979). Intriguingly, the force, work, and power output during the shortening phase of a SSC is enhanced compared with shortening that is not preceded by active stretch (Cavagna et al., 1965). Since then, the SSC-effect has fascinated researchers and several mechanisms underlying the SSC-effect have been considered. These mechanisms include neuromuscular pre-activation, stretch-reflex contributions, and recoil of elastic energy stored in tendons (van Schenau et al., 1997). Furthermore, it was suggested that following the initial stretch, the force production is enhanced at the sarcomeric level during shortening of SSCs (Cavagna et al., 1968). While this force enhanced mechanism hasn't received much acceptance, it was recently revisited and linked to the plastic history-dependent properties of muscle (Seiberl et al., 2015). Since then, a new series of SSC studies focused on the history-dependent properties of stretch-induced force enhancement provided strong support for their relevance in SSCs. Therefore, the aim of this Research Topic was to reignite a holistic debate on the mechanisms contributing to the SSC-effect (**Figure 1**), as well as on the relevance of SSCs for movement and training.

CONTRACTILE MECHANISMS UNDERLYING SSC

Four papers in this Research Topic focused on the underlying contractile mechanisms that might contribute to the SSC-effect. Tomalka et al. (a) used skinned single fiber preparations to show that part of the SSC-effect is sarcomere based. By using a cross-bridge inhibitor, their data indicates

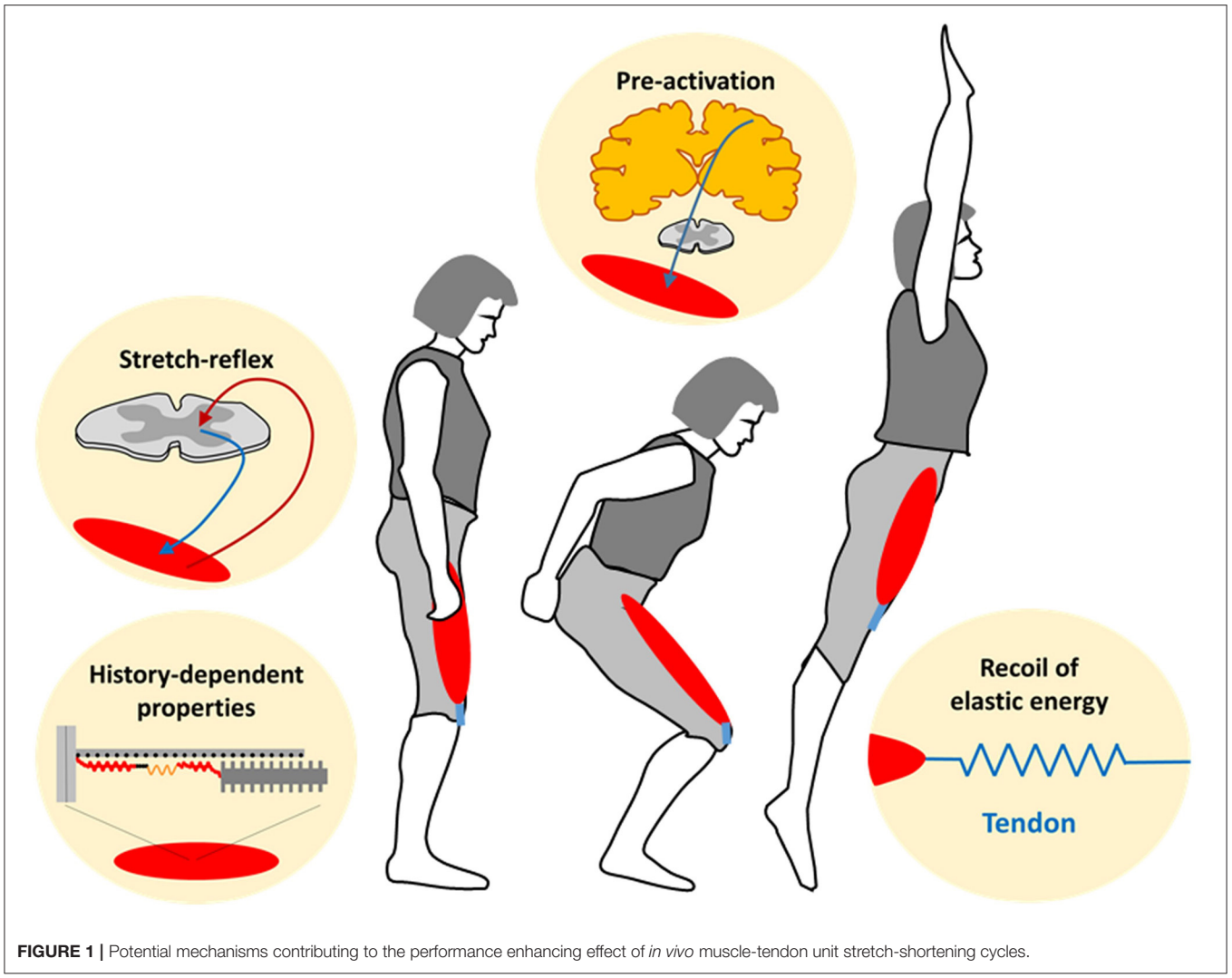

FIGURE 1 | Potential mechanisms contributing to the performance enhancing effect of *in vivo* muscle-tendon unit stretch-shortening cycles.

that a non-cross bridge viscoelastic element contributes to the SSC-effect. This suggestion was further supported by Hessel et al. who, in their study, also used skinned muscle fiber preparations and a myosin inhibitor, as well as a whole muscle preparation from *mdm* mice, which had a small deletion of titin's N2A region. Based on the combined results from both papers, the giant spring-like protein titin appears to contribute to the SSC-effect. In their second study, Tomalka et al. (b) showed that the SSC-effect in skinned fibers increases with SSC velocity. This again points toward a contribution of non-cross-bridge structures to the SSC-effect, which might be explained by the viscoelastic properties of the structural protein titin. The fourth study that used skinned fibers by Joumaa et al. investigated the energy cost of force production following SSCs and following shortening contractions of identical speed and magnitude. While their data support the contribution of history-dependent muscle properties to the SSC-effect (Seiberl et al., 2015), energy cost per unit of force was not different during an isometric steady-state following SSCs compared with shortening without preceding stretch. Joumaa et al. suggest that the increase in total force observed following SSCs was achieved with an increase in the proportion of attached cross-bridges and titin stiffness. As their data mainly refer to the steady-state following SSCs, no conclusion can yet be drawn regarding the metabolic cost *during* SSCs.

IN VIVO HUMAN SSC

Another four studies in this Research Topic focused on SSCs of *in vivo* human muscles. Similar to the *in vitro* studies described above, Groeber et al. investigated whether the history-dependent properties of muscle contribute to the SSC-effect in the human quadriceps femoris. For electrically and voluntarily activated contractions at activation levels ranging from 20 to 100%, they observed a consistent SSC-effect. Residual force depression following SSCs did not differ or was less compared with shortening contractions without preceding stretch. As residual force depression is known to increase with the work

produced during shortening (Chen et al., 2019), their finding provides indirect support for the contribution of history-dependent muscle properties to the SSC-effect. Similarly, but in a more applied setting, Held et al. found a SSC-effect in terms of a 10% higher power output during rowing, when rowing was performed with a countermovement before leg extension compared with a leg extension without such countermovement. However, in their study, the question remains whether a SSC occurred in the muscle, the tendon or both. This question was investigated by Aeles and Vanwanseele for the medial gastrocnemius during jumping. In their study, by using B-mode ultrasound, they found that for this specific movement a SSC did occur at the level of the muscle-tendon unit and the tendon but not the muscle fascicles. Accordingly, related to where the SSC occurs, different mechanisms are likely at play. To better understand SSCs of *in vivo* human muscles, Wearing et al. performed a proof of concept regarding the reliability of transmission mode ultrasound in quantifying the instantaneous modulus of elasticity of human Achilles tendon during repetitive submaximal hopping. Their results showed that the technique allows to reliably monitor ultrasound velocity and to detect changes in the instantaneous elastic modulus of the tendon, which may provide further insights into *in vivo* SSC performances.

SHORT- AND LONGTERM ADAPTATIONS TO SSC

Finally, four articles of this Research Topic dealt with short- and long-term adaptation of the muscle-tendon unit to SSCs and whether SSCs are a suitable training tool, typically referred to as plyometric training. Kositsky et al., demonstrated acute main effects after exhaustive SSCs: decreased voluntary strength and joint stiffness, and increased resting fascicle lengths of medial gastrocnemius muscle. On a larger timescale, Hammami et al. showed that a 10 weeks upper and lower limb plyometric training program improved many measures of physical performance in young female handball players. Similarly, after a 6-week plyometric training intervention, Ruffieux et al. found significant increases in jump performance. More specifically, they concluded that (at least for non-professional female volleyball players) training with a high percentage of slower SSC jumps, such as counter-movement jumps, is more effective than a training with a high percentage of fast SSCs, such as drop-jumps. Therefore, slower SSCs during CMJs seem to be more specific for these players and tasks. To better understand the time-course of changes in muscle function and morphological parameters in response to SSCs, Monti et al. compared muscle torque and power combined with muscle architectural changes after 2, 4, and 6 weeks of plyometric training. They showed rapid increases in muscle volume, fascicle length, pennation angle, torque, and power in healthy younger adults following the training. They also pointed out that SSC exercise is likely beneficial for neuronal adaptations to performance, as not all enhancements in muscle power were explainable by increases in cross-sectional area or muscle volume.

LIMITATIONS AND FUTURE PERSPECTIVES

The main limitations of the studies covered in this Research Topic are that (1) skinned muscle fiber experiments provide insight into potential contractile mechanisms but that they do not necessarily represent muscle function under physiological conditions. Conversely, (2) the *in vivo* studies represent physiological muscle function but suffer from the problem of identifying underlying mechanisms. A major limitation of (3) the training studies is that the mechanisms that trigger specific adaptations remain unclear and that it is very difficult to match different training regimes to make them comparable. Especially for *in vivo* human muscle research, this Research Topic showed that it is crucial for future studies to distinguish between the behavior of the muscle-tendon unit, the tendon, and the muscle fascicles. Further, although a broad field of SSC research is covered in this Research Topic, the interplay of potential mechanisms is not yet well-understood, and research on neuromuscular factors and modeling approaches are missing in this collection. Accordingly, SSCs remain a topic of high relevance and great scientific interest.

AUTHOR CONTRIBUTIONS

All authors contributed to the manuscript and approved the final version.

FUNDING

TS, DH, and WS were supported by the German Research Foundation (DFG) under grants SI841/15-1, SI841/17-1, HA 5977/5-1, and SE 2109/2-1, respectively. JF and GP were supported by the Natural Sciences and Engineering Research Council of Canada's (NSERC) Discovery Grants program.

REFERENCES

Cavagna, G. A., Dusman, B., and Margaria, R. (1968). Positive work done by a previously stretched muscle. *J. Appl. Physiol.* 24, 21–32. doi: 10.1152/jappl.1968.24.1.21

Cavagna, G. A., Saibene, F. P., and Margaria, R. (1965). Effect of negative work on the amount of positive work performed by an isolated muscle. *J. Appl. Physiol.* 20, 157–158. doi: 10.1152/jappl.1965.20.1.157

Cavanagh, P. R., and Komi, P. V. (1979). Electromechanical delay in human skeletal muscle under concentric and eccentric contractions. *Europ. J. Appl. Physiol.* 42, 159–163. doi: 10.1007/BF00431022

Chen, J., Hahn, D., and Power, G. A. (2019). Shortening-induced residual force depression in humans. *J. Appl. Physiol.* 126, 1066–1073. doi: 10.1152/japplphysiol.00931.2018

Seiberl, W., Power, G. A., Herzog, W., and Hahn, D. (2015). The stretch-shortening cycle (SSC) revisited: residual force enhancement contributes to increased performance during fast SSCs of human m. adductor pollicis. *Physiol. Rep.* 3:e12401. doi: 10.14814/phy2.12401

van Schenau, G. J. I., Bobbert, M. F., and Haan, A. de. (1997). Mechanics and energetics of the stretch-shortening cycle: a stimulating discussion. A stimulating discussion. *J. Appl. Biomech.* 13, 484–496. doi: 10.1123/jab.13.4.484

Conflict of Interest: The authors declare that the research was conducted in the absence of any commercial or financial relationships that could be construed as a potential conflict of interest.

frontiers in Physiology

ORIGINAL RESEARCH
published: 13 December 2019
doi: 10.3389/fphys.2019.01504

Do Stretch-Shortening Cycles Really Occur in the Medial Gastrocnemius? A Detailed Bilateral Analysis of the Muscle-Tendon Interaction During Jumping

Jeroen Aeles[1,2]* *and Benedicte Vanwanseele*[2]

[1] School of Human Movement and Nutrition Sciences, The University of Queensland, Brisbane, QLD, Australia, [2] Department of Movement Sciences, KU Leuven, Leuven, Belgium

The effect of stretch-shortening cycles (SSCs) is often studied in laboratory settings, yet it remains unclear whether highly active muscle SSCs actually occur during *in vivo* movement. Nine highly trained jumping athletes performed single-leg pre-hop forward jumps at maximal effort. We hypothesized that these jumps would induce a SSC at the level of the muscle in the medial gastrocnemius. Kinematic and kinetic data were collected together with electromyography signals (EMG) and muscle fascicle length and pennation angle changes of the medial gastrocnemius of both legs and combined with a musculoskeletal model to calculate the stretch-shortening behavior of the muscle (fascicles) and tendon (series-elastic element). The length changes of the fascicles, longitudinal muscle displacement, series-elastic element, and whole muscle-tendon unit further allowed for a detailed analysis of the architectural gearing ratio between different phases of the SSC within a single movement. We found a SSC at the level of the joint, muscle-tendon unit and tendon but not at the muscle. We further found that the average architectural gearing ratio was higher during the stretching of the series-elastic element as compared to when the series-elastic element was shortening, yet this was not statistically tested because of low sample size for this parameter. However, we found no correlation when plotting the architectural gearing ratio as a function of the fascicle velocities at each instance in time. Despite the athletes having a clear preferred leg for jumping, we found no differences in any kinematic or kinetic parameter between the preferred and non-preferred leg or any parameter from the muscle-tendon interaction analysis other than a reduced longitudinal muscle shortening in the non-preferred leg ($p = 0.008$). We conclude that, although common at the level of the joints, MTUs, and tendon (series-elastic element), highly active SSCs very rarely occur in the medial gastrocnemius, even in movements that induce high loading. This has important implications for the translation of *ex vivo* findings on SSC effects, such as residual force enhancement, in this muscle. We further conclude that there is no precise tuning of the architectural gearing ratio in the medial gastrocnemius throughout the whole movement.

Keywords: jumping, architectural gear ratio, fascicle behavior, muscle-tendon unit, tendon dynamics

OPEN ACCESS

Edited by:
Daniel Hahn,
Ruhr University Bochum, Germany

Reviewed by:
Neil Cronin,
University of Jyväskylä, Finland
Urs Granacher,
University of Potsdam, Germany
Martino V. Franchi,
University of Padua, Italy

***Correspondence:**
Jeroen Aeles
j.aeles@uq.edu.au

Specialty section:
This article was submitted to Exercise Physiology, a section of the journal Frontiers in Physiology

Received: *27 September 2019*
Accepted: *28 November 2019*
Published: *13 December 2019*

Citation:
Aeles J and Vanwanseele B (2019) Do Stretch-Shortening Cycles Really Occur in the Medial Gastrocnemius? A Detailed Bilateral Analysis of the Muscle-Tendon Interaction During Jumping. Front. Physiol. 10:1504. doi: 10.3389/fphys.2019.01504

INTRODUCTION

The stretch-shortening cycle (SSC) is a common phenomenon in many naturally occurring movements and has long been identified as a performance-enhancing mechanism (Bosco et al., 1982; Seiberl et al., 2015). It is defined as the rapid stretching of a pre-activated muscle prior to shortening of that same muscle (Nicol et al., 2006). This speed aspect is important because the time for muscles to produce high forces during SSCs *in vivo* is often limited (Farris et al., 2016) and would require muscles to shorten at very high velocities, impeding their capacity to produce high forces. To cope with this, the muscles rely on tendons to store elastic energy, extending the time available for active muscle contractions, allowing the muscle to shorten at lower velocities, which forms a large component of the performance enhancement from a SSC (Cavagna et al., 1965).

A SSC can be found at different levels, from the joint level muscle and tendon separately. Indeed, ever since the discovery of the decoupling of the contractile and elastic elements from the whole muscle-tendon unit (Griffiths, 1984, 1987), it has become apparent that a SSC of a muscle or tendon can occur without a SSC at the joint level. The squat jump is a typical example where a SSC is found in the tendon, but not in the muscle, muscle-tendon unit, or at the joint level (Kurokawa et al., 2001; Farris et al., 2016; Aeles et al., 2018). In a study using similar methodologies as Kurokawa et al. (2001, 2003) investigated the medial gastrocnemius muscle-tendon behavior during a counter-movement squat jump, in which one could expect that as this movement does have a SSC at the joint level, the SSC would also be found at the level of the muscle-tendon unit or muscle. The authors, however, found no differences in muscle-tendon unit, muscle, or tendon length changes in medial gastrocnemius compared to the squat jump. In a recent study, we were able to overcome the lack of MTU stretching in a classic squat jump and counter-movement jump and induced a SSC at the level of the medial gastrocnemius muscle-tendon unit by adding a specific pre-hop to the squat jump, effectively changing the behavior of the muscle and tendon of the plantar flexors (Aeles et al., 2018). This resulted in a SSC at the level of the joint, muscle-tendon unit and tendon. However, a SSC of the muscle itself was not found in any of the aforementioned studies on walking, running, and jumping. There are a few studies that did find stretching of the muscle during walking, but this generally occurred when muscle activation was low (Ishikawa et al., 2005; Chleboun et al., 2007; Maharaj et al., 2016). Two other studies have shown stretching of the muscle, both during landing tasks (Werkhausen et al., 2017; Hollville et al., 2019). However, as the main role of the muscle-tendon unit in these tasks was to dissipate energy, there was no further requirement for the muscle to do work after the landing, and a subsequent shortening was thus absent. It appears that a highly active SSC of the lower limbs is much more common at the level of the joints and in the muscle-tendon unit, and tendon and rather rare in the muscle. Because of this, our understanding of the mechanical functioning of the muscle during highly active muscle SSCs *in vivo* remains poor.

Although we lack knowledge on the direct effect of a SSC in the muscle itself, the effect of a tendon SCC on the muscle behavior and performance in humans has been investigated more often, mostly in the plantar flexors (Fukunaga et al., 2001; Lichtwark and Wilson, 2006; Farris and Sawicki, 2012; Aeles et al., 2018). Collectively, these studies have shown that the conditions for the muscle to produce force can be optimized by altering the working length and velocity of the muscle. Another mechanism that allows optimization of the working length and velocity of the muscle is the architectural gearing ratio (architectural gearing ratio) found in pennated muscles. The architectural gearing ratio allows the muscle fascicles to shorten at slower velocities than the longitudinal muscle velocity muscle (Brainerd and Azizi, 2005). Azizi et al. (2008) introduced the concept of a variable gearing mechanism in the muscle, which allows the muscle to automatically increase its architectural gearing ratio at high muscle shortening velocities. It was later found that the muscle also relies on a high architectural gearing ratio during muscle lengthening, which by allowing the fascicles to lengthen at a slower velocity than the whole muscle serves as a protective mechanism by avoiding damage from rapid fascicle lengthening (Azizi and Roberts, 2014). Much of our knowledge on the architectural gearing ratio in muscle is derived from *ex vivo* animal studies under well-controlled, single-mode conditions and the use of an architectural gearing ratio during more complex human *in vivo* movement remains mostly unexplored. Indeed, only very few studies have made attempts at investigating the use of the architectural gearing ratio in humans. Dick and Wakeling (2017) were the first to successfully calculate the architectural gearing ratio at maximal muscle shortening velocity from experimental data in humans and confirmed the variable gearing theory proposed by Azizi et al. (2008) for humans. Other studies have since calculated the architectural gearing ratio during running (Werkhausen et al., 2017) and drop landings (Hollville et al., 2019), yet all of these studies have calculated the architectural gearing ratio as a single value and using different methods. Because of this, it remains unclear whether or not the architectural gearing ratio of a muscle can be tuned within a single movement. In many human movements there are two distinct phases, a phase of long stretching and a phase of fast shortening of the tendon. Because of this, the muscle itself shortens at very different velocities and with different loads during these two phases. From the previous work done on the architectural gearing ratio, it would be expected that the architectural gearing ratio of the muscle is tuned to better fit these different conditions, however, this has never been tested.

In a recent study, we investigated if the preference for one leg over the other for jumping was associated with architectural adaptations of the muscle (Aeles et al., 2017). We found large, unexpected differences in muscle architecture between the two legs in jumping athletes and untrained individuals, but the differences were not related to leg preference for jumping. As the different architectures in this muscle may lead to different dynamic behavior during jumps, and perhaps different tuning of the architectural gearing ratio of the muscle between the two legs, we further explored this in this study.

As such, our aim for this study was to use a unilateral jump with a pre-hop, which was expected to induce an active SSC at the level of the joints, muscle-tendon unit, muscle and tendon of

the medial gastrocnemius, to further explore remaining questions on the muscle and tendon behavior *in vivo*. Our first hypothesis was therefore that the single-leg forward jumping movement we chose for this study would be of high enough loading to induce an active SSC at the level of the ankle joint, medial gastrocnemius muscle-tendon unit, muscle and tendon. We also hypothesized that the architectural gearing ratio of the muscle is tuned differently between phases during which the tendon is slowly lengthening versus when it is rapidly shortening at the end of the movement. More specifically, this means that when the tendon is stretching slowly, the muscle is generally shortening at low velocities but high loads and so we hypothesize that the architectural gearing ratio will be low compared to when the muscle and tendon are shortening at high velocities. We further explored the effect of different architectures between the left and right leg on dynamic differences in the interaction between muscle and tendon.

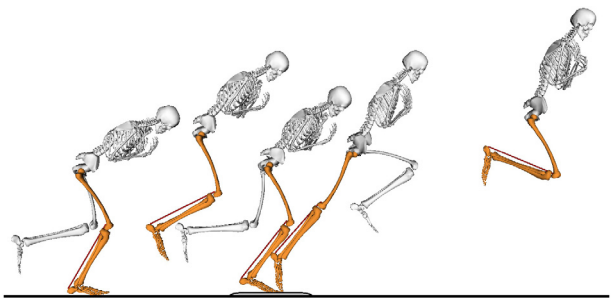

FIGURE 1 | The movement task consisted of a single-leg small forward hop onto a force plate, followed by a maximal-effort forward jump. Only the jumping leg (orange) made contact with the ground during the task. The non-jumping leg (white) is shown only during ground contact for clarity of the figure.

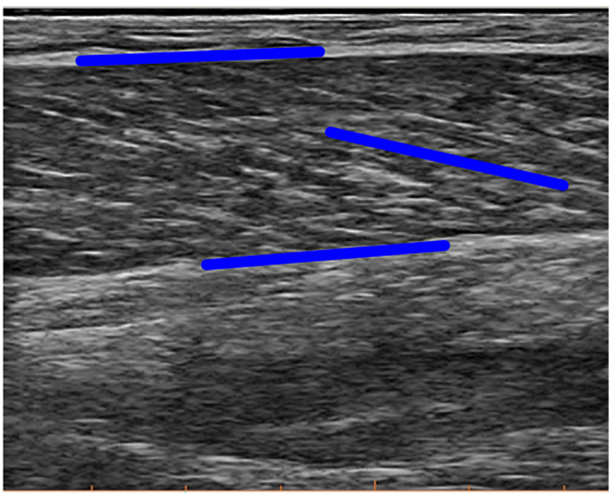

FIGURE 2 | Example image of the ultrasound measurement. Blue lines illustrate tracking of the orientation of both aponeuroses and the fascicle. Note that the blue line in parallel to the fascicle here is not the final fascicle length, rather extrapolation methods were used on the local coordinates of these lines to calculate final fascicle length and pennation angle.

MATERIALS AND METHODS

Participants and Protocol

Nine highly trained jumping athletes (three female, six male, high and long jumpers; body mass: 71.1 ± 5.4 kg; body length: 182.3 ± 6.1 m) participated in this study. All participants were ranked in the top 10 in Belgium in their respective field and were injury free at least 3 months prior to testing, had no chronic lower limb injuries and were active in competition. The preferred leg for jumping for each participant was self-reported at the start of the study and was the same as the take-off leg used in competition for all participants. All participants gave written informed consent and the study was approved by the local ethics committee (Medical Ethical Committee of UZ Leuven, file number: S57477).

After a 15 min warm-up consisting of running at a comfortable speed, squat jumping and countermovement jumping, the athletes performed single-leg forward jumps. To maximize the chance of inducing a SSC in the muscle-tendon unit, muscle, and tendon, the athlete started by performing a small forward hop onto the force plate on one leg, followed by a maximal-effort forward jump on the same leg (see **Figure 1**). The other leg did not make contact with the ground other than to stabilize the body at the start of the small forward hop and at the final landing after the maximal-effort jump. All data was analyzed for the foot-ground contact period on the force plate except for EMG data, which was analyzed throughout the whole movement to assess pre-activation. After two successful trials, the jumps were repeated for the other leg. A successful trial was defined as the foot making contact with the force plate only and clear ultrasound images. For both legs, the jump that had the greatest impulse (see below for calculations) was chosen for further analysis.

Data Acquisition and Analysis

A linear ultrasound transducer (128 elements, 8 MHz, 60 mm field of view, UAB Telemed Lithuania) was attached to the lower leg that was used for the jumps. The transducer was placed over the mid-belly of the medial gastrocnemius muscle and aligned with the orientation of the muscle fascicles to obtain longitudinal images of the fascicles. The transducer was securely fixed on the leg with bandages and medical tape and images were sampled at 60 Hz. Ultrasound image recordings were processed by a single person as described in Aeles et al. (2018). Briefly, for each image in a recording, the superficial and deep aponeurosis and fascicle orientation were tracked using freely available software (UltraTrack, Farris and Lichtwark, 2016), see **Figure 2**. The reliability of the person that processed the images was reported earlier in Aeles et al. (2017) (intra-class correlations > 0.93 and standard error of measurements < 1.0 mm and 0.6° for fascicle lengths and pennation angles, respectively). Fascicle length was calculated as the extrapolated line along the fascicle orientation between the intersection points with the visible aponeuroses. This method

is more robust and reliable when using the aforementioned tracking algorithm and is suitable in this muscle, which has no significant curvature of the fascicles. The muscle was also scanned along its length prior to the ultrasound transducer placement for these dynamic measurements to ensure that there was no significant curvature of either of the aponeuroses at least 2–3 cm more proximal than the location of the transducer. Pennation angles were defined as the angle between this fascicle and the deep aponeurosis. The longitudinal displacement of the muscle was calculated by multiplying the fascicle length with the cosine of the pennation angle. We further use the term longitudinal muscle shortening and longitudinal muscle lengthening when the displacement follows the direction of fascicle shortening or lengthening, respectively. The length changes of the series-elastic element (series-elastic element) were estimated as the difference in the length changes of the muscle-tendon unit and the fascicle, taking into account the pennation angle (Fukunaga et al., 2001). Fascicle and longitudinal muscle velocities were calculated by taking the time derivative of their length changes. The architectural gearing ratio of the muscle was calculated by dividing the longitudinal muscle velocity by the fascicle velocity at each data point. As to only take the AGRs during significant periods of high longitudinal muscle velocities into further analyses, we extracted the architectural gearing ratio values that corresponded to longitudinal muscle shortening at velocities faster than −25 mm/s and longitudinal muscle lengthening at velocities faster than 25 mm/s. This value was chosen based on the fact that we are confident in detecting a minimal absolute length change of 5 mm with the ultrasound technique. Combined with a minimal ground-contact time of roughly 220 ms, we rounded up the value of a minimal detectable velocity of 22.7 to 25 mm/s We then also further split these architectural gearing ratio values into phases during which the series-elastic element was lengthening (long, slow phase) and when it was shortening rapidly (at the end of the movement). Fascicle lengths are used further in the manuscript when referencing to "the muscle," series-elastic element length changes when referencing to "the tendon."

The ultrasound image collection was synchronized with a Vicon motion capture system for 3D motion analyses (Vicon, Oxford Metrics, United Kingdom). 42 reflective markers containing four technical clusters were placed on anatomical landmarks to make a 3D reconstruction of the motion using 10 infrared cameras sampling at 150 Hz. Ground reaction forces were collected with a force plate sampling at 1000 Hz (AMTI, United States). Impulse was chosen as performance parameter and was calculated from the 3D resultant ground reaction force by multiplying the force by time of force application. Marker locations were exported to OpenSim 3.2 (Delp et al., 2007) to scale a full-body musculoskeletal model (Hamner et al., 2010). The scaled models included a muscle-tendon unit (muscle-tendon unit) actuator representing the medial gastrocnemius. A Kalman smoothing algorithm (De Groote et al., 2008) was used to calculate joint angles from the marker coordinates, which also provided us with the joint angular velocities and the length changes of the muscle-tendon unit throughout the motion, taking into account the scaled moment arms as a function of the ankle and knee joint angles. Then, an inverse dynamics analyses was performed in the OpenSim software, using the joint angles and the ground reaction force data. Joint power was calculated from the angular velocities and joint moments and then split into negative (absorption) and positive (generation) phases. From these phases, work for each joint was calculated as the negative and positive work, respectively and net work done by the joint was calculated by subtracting the difference of the positive from the negative work. For some participants and in some joints, the movement ended with power absorption and these data were removed for the joint work calculations as they did not contribute to storage of elastic energy used during the stance phase.

EMG recordings of the medial gastrocnemius were collected from the same leg on which the ultrasound transducer was placed (ZeroWire EMG Aurion, Milano, Italy), sampling at 900 Hz. Raw EMG data signals were first band-pass filtered (20–400 Hz), rectified and then low-pass filtered (10 Hz) using a fourth-order Butterworth filter. Then, for each leg, the resulting EMG signals were normalized to the maximal activation between ground contact and toe-off during the jumps, using a moving average over five data points. To determine the timing of pre-activation before ground contact a threshold of two times the standard deviation during the relaxed standing position was used to define when the muscle was active. Due to technical issues with the EMG recordings for some participants, data from only six participants was analyzed.

Statistical Comparisons

Comparisons between the preferred and non-preferred leg were made on the following parameters: the ground-contact time; the minimal and maximal joint angles, angular velocities, and moments, the power absorption and generation, and the negative, positive, and net work for the ankle, and knee; the peak value of the resultant GRF and the impulse, both normalized to body mass; the pre-activation of the medial gastrocnemius (N = 6); the amount of fascicle shortening and lengthening, pennation angles changes, the amount of longitudinal muscle displacement, and muscle-tendon unit and series-elastic element length changes; the maximal fascicle and aponeurosis displacement velocities; the average architectural gearing ratio during high longitudinal muscle shortening velocity for the whole ground contact phase (rows "All" in **Table 2**), and separated between the phase when the series-elastic element was lengthening and when it was shortening, and the average architectural gearing ratio during high longitudinal muscle lengthening velocity for the same phases as the shortening. Because of the small dataset (N = 9 unless otherwise stated), comparisons between the preferred and non-preferred leg were made using the Wilcoxon signed ranks test. Median values and interquartile ranges between the 75th and the 25th percentiles are reported. The mean values and the standard deviation are also reported for descriptive purposes but were not used for statistical testing. A linear regression analysis was performed on both datasets of architectural gearing ratio as a function of fascicle shortening

or lengthening velocities and the correlation coefficients were calculated. This was done for data of the preferred and non-preferred leg combined (as their was no statistical difference in architectural gearing ratio between the two; $p = 0.570$). Alpha values were set at 0.05. Some parameters had datasets that were too small (e.g., only three participants had longitudinal muscle lengthening at velocities faster than 25 mm/s and thus the architectural gearing ratio during this lengthening was calculated for these three participants only) and were therefore not compared statistically but are discussed in a descriptive manner.

RESULTS

Despite the athletes having a clear preference for one leg over the other for jumping, we found no significant difference between the body mass normalized peak resultant GRF or impulse generated between the preferred and non-preferred leg (**Table 1**). We also found no differences between the preferred and non-preferred leg in any of the minimal or maximal joint angles, maximal angular velocities, maximal body mass normalized moments, maximal power absorption and generation, or total negative, positive or net work done at the ankle or knee joint (**Table 1**).

The medial gastrocnemius was activated prior to ground contact by an average of 0.82 ± 0.57 s in the preferred and by 0.63 ± 0.29 s in the non-preferred leg. There was no statistical difference between the preferred and non-preferred leg (median: 0.79 [0.70 0.91] and 0.74 [0.68 0.81], respectively; $p = 0.313$). The long pre-activation time in both legs prior to ground contact, confirms that the findings here represent active SSCs.

As expected, the movement performed by the participants results in a SSC at the level of the ankle and knee joint, medial gastrocnemius muscle-tendon unit, and series-elastic element (**Figure 3**). However, contrary to our first hypothesis, the muscle fascicles were stretched only notably in the preferred leg of one participant (9 mm, participant 8) and very little or not at all in all other participants (**Figure 4**). In some participants, the muscle fascicles shortened considerably following ground-contact whereas in others they behaved mostly isometrically.

During ground contact, the muscle fascicles shortened on average by 16 ± 9 and 14 ± 6 mm in the preferred and non-preferred leg, respectively (median: 14 [11 19] and 16 [9 18] respectively; $p = 0.496$). This coincided with a pennation angle increase of 13 ± 8° and 14 ± 9°, respectively (median: 11 [9 23] and 11 [7 17], respectively; $p = 0.652$). The fascicle shortening, combined with pennation angle changes caused a longitudinal muscle shortening of 19 ± 10 mm in the preferred leg, but only an average shortening of 14 ± 11 mm in the non-preferred leg, which was statistically lower (median: 17 [15 26] and 14 [10 18], respectively; $p = 0.008$). The muscle-tendon unit was initially stretched on average by 14 ± 5 mm in the preferred leg and 14 ± 6 mm in the non-preferred leg (median: 16 [10 18] and 15 [10 16], respectively; $p = 1.000$) (**Figure 3**). This was followed by a long quasi-isometric phase of the muscle-tendon unit between 20 and 80% of the ground-contact phase. Then, a rapid shortening of the muscle-tendon unit was found with average shortening amplitudes of 35 ± 3 mm in the preferred leg and 35 ± 6 mm in the non-preferred leg (median: 34 [33 37] and 35 [30 39] respectively; $p = 0.910$). The series-elastic element stretched on average by 29 ± 9 mm in the preferred leg and 27 ± 4 mm in the non-preferred leg (median: 30 [23 33] and 25 [24 30] respectively; $p = 0.820$). The stretching phase took up the majority of the ground-contact for the series-elastic element (as shown by the vertical bar in **Figure 3**), with rapid shortening by 34 ± 4 and 33 ± 8 mm in the preferred and non-preferred leg, respectively near the end of the movement (median: 34 [31 36] and 34 [28 38], respectively; $p = 1.000$).

The maximal shortening velocity of the fascicles was not statistically different between the preferred leg and non-preferred leg with values of 211 ± 186 and 191 ± 123 mm/s, respectively (median: 162 [137 204] and 181 [92 225], respectively; $p = 1.000$). The maximal longitudinal muscle shortening velocity was 248 ± 206 compared to 168 ± 68 mm/s for the preferred leg and non-preferred leg, respectively. Despite the large differences, this did not result in a statistically significant difference between the two legs (median: 181 [149 261] and 157 [111 235], respectively; $p = 0.652$). However, this did result in a statistically significant difference between the maximal fascicle shortening velocity and maximal longitudinal muscle shortening velocity in the preferred leg ($p = 0.012$), but not in the non-preferred leg ($p = 0.570$). Maximal stretching velocity of the muscle-tendon unit was 285 ± 106 mm/s in the preferred leg and 277 ± 115 mm/s in the non-preferred leg (median: 337 [202 365] and 270 [214 332], respectively; $p = 0.820$). Maximal shortening velocity of the muscle-tendon unit was 600 ± 74 mm/s in the preferred leg and 617 ± 110 mm/s in the non-preferred leg (median: 593 [524 667] and 589 [545 715], respectively; $p = 0.820$). The maximal stretching velocity of the series-elastic element was 383 ± 230 mm/s in the preferred leg and 383 ± 122 mm/s in the non-preferred leg (median: 341 [276 409] and 364 [285 487], respectively; $p = 0.570$). Maximal shortening velocity of the series-elastic element was 607 ± 109 mm/s in the preferred leg and 611 ± 96 mm/s in the non-preferred leg (median: 596 [525 688] and 592 [543 714], respectively; $p = 1.000$). No statistical differences were found between the preferred and non-preferred leg in any of these parameters. The maximal shortening velocities of the fascicles and the longitudinal muscle were statistically lower than the maximal shortening velocities of the muscle-tendon unit and series-elastic element in both the preferred ($p = 0.008$ for both) and the non-preferred leg ($p = 0.004$ for both).

No differences between the preferred and non-preferred leg were found for the architectural gearing ratio analysis (**Table 2**). During series-elastic element stretching and shortening, respectively, we found phases of longitudinal muscle shortening velocities greater than 25 mm/s in the preferred leg for eight and seven athletes and in the non-preferred leg for nine and eight athletes. In order to compare values only for athletes that had longitudinal muscle shortening velocities greater than 25 mm/s in both phases, the descriptive comparisons

TABLE 1 | Kinetic and kinematic variables for the preferred and non-preferred leg.

		Preferred	Non-preferred	*p*-value
Ground contact time (s)		0.291 [0.282 0.311] (0.295 ± 0.037)	0.313 [0.281 0.328] (0.307 ± 0.034)	0.359
GRF (N/kg)	Peak	27.92 [26.83 29.36] (28.94 ± 3.76)	29.09 [25.30 31.88] (28.98 ± 3.52)	1.000
Impulse (N·s/kg)		0.61 [0.57 0.63] (0.61 ± 0.05)	0.63 [0.60 0.65] (0.63 ± 0.03)	0.203
Peak joint angles (deg)				
Ankle	DF	29 [27 32] (30 ± 6)	32 [29 34] (31 ± 5)	0.652
	PF	−30 [−31 −27] (−29 ± 4)	−29, [−34 −26] (−29 ± 7)	0.910
Knee	Flx	−58 [−61 −56] (−58 ± 6)	−59 [−63 −52] (−57 ± 6)	0.734
	Ext	−9 [−11 −5] (−8 ± 5)	−5 [−11 −4] (−7 ± 3)	0.734
Peak joint angular velocities (deg/s)				
Ankle	DF	397 [347 455] (391 ± 97)	360 [318 482] (395 ± 113)	0.820
	PF	−828 [−921 −777] (−864 ± 109)	−845 [−995 −781] (−884 ± 141)	0.820
Knee	Flx	−249 [−323 −169] (−241 ± 87)	−232 [−310 −162] (−235 ± 81)	0.570
	Ext	607 [575 686] (624 ± 97)	644 [590 698] (617 ± 92)	0.910
Peak joint moments (Nm/kg)				
Ankle	PF	−4.3 [−4.4 −3.9] (−4.3 ± 0.5)	−4.3 [−4.7 −3.9] (−4.3 ± 0.6)	0.821
Knee	Flx	−1.3 [−1.5 −1.1] (−1.4 ± 0.3)	−1.1 [−1.3 −0.9] (−1.2 ± 0.6)	0.164
	Ext	2.9 [2.6 3.2] (2.8 ± 0.5)	2.5 [2.3 2.9] (2.6 ± 0.5)	0.204
Peak joint power (W/kg)				
Ankle	Abs	−13.0 [−17.3 −8.1] (−13.0 ± 5.1)	−12.1 [−14.5 −8.5[(−11.7 ± 3.3)	0.250
	Gen	27.2 [26.4 34.5] (23.0 ± 5.5)	27.2 [23.3 30.2] (28.4 ± 6.0)	0.250
Knee	Abs	−4.9 [−6.0 −4.0] (−5.0 ± 1.9)	−5.1 [−6.5 −4.6] (−4.9 ± 2.2)	0.734
	Gen	10.7 [9.0 13.2] (10.8 ± 3.3)	9.2 [8.6 13.0] (10.6 ± 3.1)	0.570
Joint work (J/kg)				
Ankle	Neg	−1.7 [−2.0 −1.3] (−1.8 ± 0.7)	−1.8 [−2.3 −1.3] (−1.9 ± 0.7)	0.910
	Pos	4.5 [3.9 5.5] (4.8 ± 1.4)	4.3 [3.7 5.0] (4.5 ± 0.9)	0.359
	Net	3.1 [2.3 4.0] (3.0 ± 1.2)	2.4 [2.0 3.6] (2.5 ± 0.7)	0.129
Knee	Neg	−0.5 [−0.7 −0.3] (−0.5 ± 0.2)	−0.6 [−0.8 −0.4] (−0.5 ± 0.3)	0.570
	Pos	2.0 [1.5 2.6] (2.0 ± 0.7)	1.5 [1.3 2.4] (1.9 ± 0.6)	0.301
	Net	1.4 [0.9 1.9] (1.5 ± 0.7)	1.2 [0.9 1.6] (1.3 ± 0.5)	0.203

Values are medians [25% quartile 75% quartile] (means ± SD). GRF, ground reaction force; DF, dorsiflexion, PF, plantar flexion/flexor; Flx, flexion/flexor, Ext, extension/extensor; Abs, absorption; Gen, generation; Neg, negative; Pos, positive. No significant differences between preferred and non-preferred leg were found.

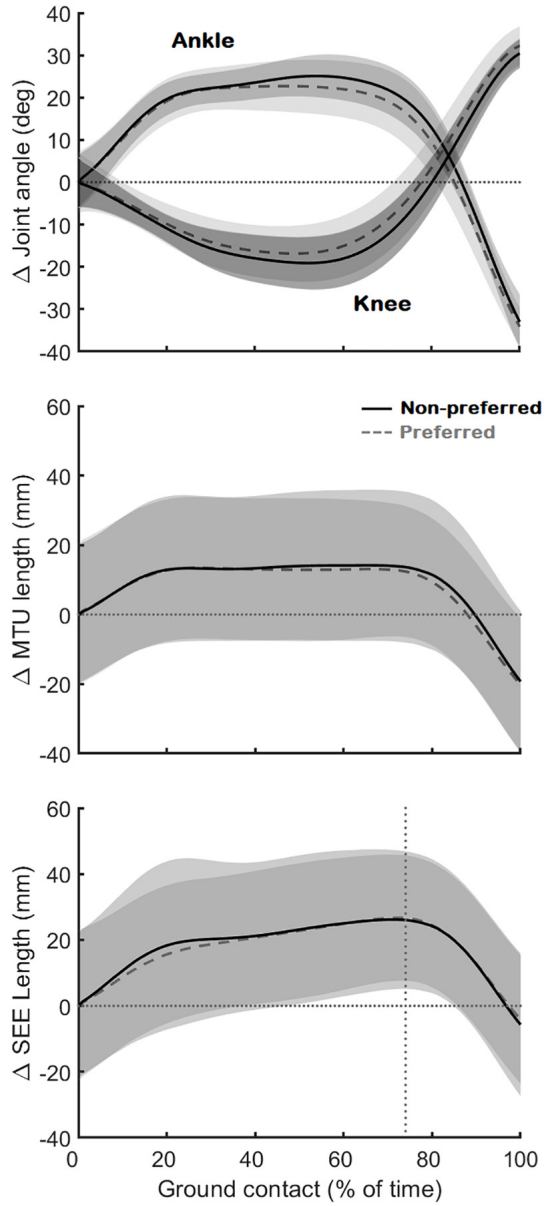

FIGURE 3 | Joint angle changes of the ankle and knee **(Top)**, muscle-tendon unit (MTU) length changes **(Middle)**, and series-elastic element length (SEE) length changes **(Bottom)**. The black continuous line is the average (N = 10) for the preferred leg, the gray dashed line the average (N = 10) for the non-preferred leg. All data is shown as changes relative to the first data point at ground contact (shown as the horizontal dotted lines). The vertical dotted line on the bottom figure shows where the lengthening phase of the series-elastic element stops and the shortening phase begins.

were made for five athletes (**Table 2**, gray panel). There appears to be a trend in which the architectural gearing ratio seems to be greater during series-elastic element lengthening than during series-elastic element shortening. Only three participants had a period of longitudinal muscle lengthening at velocities greater than 25 mm/s, hence the results of only these three participants are shown in **Table 2** (bottom, white panel). Because of the low number of participants for this parameter, the results of these comparisons are presented but not further discussed. This could be a point of interest for future studies. The correlation coefficients for the architectural gearing ratio as a function of fascicle shortening velocity during both longitudinal muscle shortening and lengthening at velocities greater than 25 mm/s were very low (**Figure 5**).

DISCUSSION

In this study, we aimed to explore in detail the muscle-tendon interaction in the medial gastrocnemius during a movement involving a SSC. Contrary to our hypothesis, the SSC did not generally occur in the muscle fascicles, but it did result in a SSC at the level of the joints (i.e., a rapid countermovement), medial gastrocnemius muscle-tendon unit and tendon (measured as series-elastic element). We further investigated whether in a single movement the architectural gearing ratio of a muscle is tuned differently in the phases during which the series-elastic element is stretching versus shortening. We found that when the series-elastic element is stretching, the average architectural gearing ratio is slightly higher than when it is shortening, but interestingly, at instantaneous time points throughout the movement this was not related to the fascicle shortening velocity. We are also the first to compare the muscle-tendon interaction during a dynamic movement between the preferred leg used for jumping and the non-preferred leg. Despite the athletes having a clear preference on which leg to use for jumping, we did not find differences in any kinematic or kinetic parameter, activation of the muscle, or muscle-tendon interaction other than a reduced longitudinal muscle shortening in the non-preferred leg compared to the preferred leg.

Absence of a SSC in the Muscles Fascicles

Our results show that even during high-loading movement tasks, a highly active SSC of the medial gastrocnemius muscle in humans is rare, which is not in agreement with our initial hypothesis (**Figure 4**). This is consistent with previous studies on the medial gastrocnemius muscle during walking, running, and bilateral jumping (Fukunaga et al., 2001; Lichtwark and Wilson, 2006; Farris and Sawicki, 2012; Aeles et al., 2018) and with results from other triceps surae muscles such as the lateral gastrocnemius (Farris et al., 2016) and soleus (Cronin and Finni, 2013; Lai et al., 2015). In a recent study on the muscle-tendon interaction in the vastus lateralis muscle, also no active stretching of the muscle fascicles was found during a squat jump (Nikolaidou et al., 2017). In the study by Nikolaidou et al. (2017), the fascicles did lengthen in the counter-movement jump, however, this occurs prior to activation of the muscle, as can be seen from the EMG data, and is therefore not considered an active SSC. In other studies that have shown stretching of the muscle fascicles in the medial gastrocnemius and soleus, vastus laterlias, and tibialis posterior,

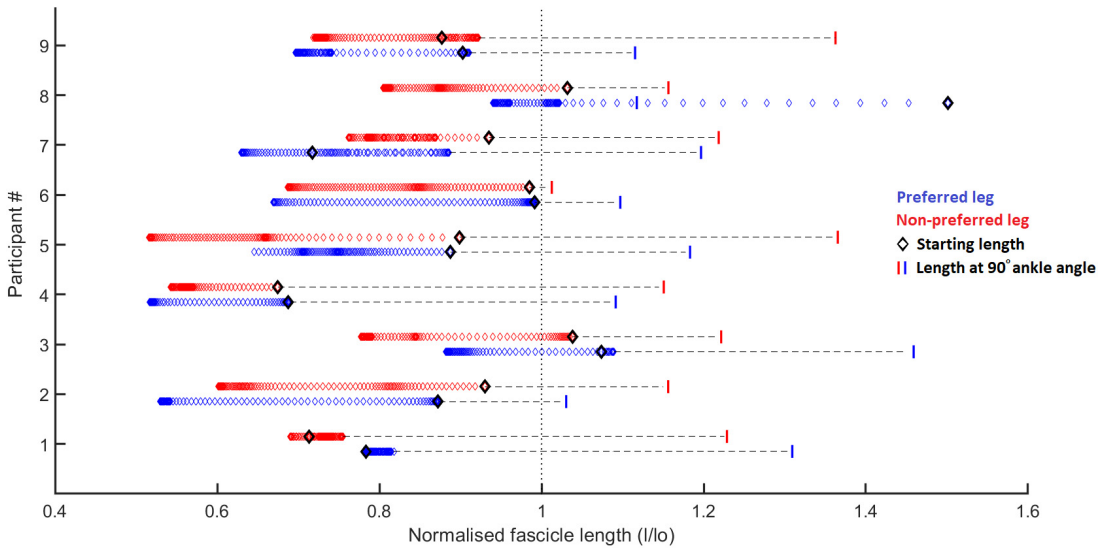

FIGURE 4 | Fascicle length changes normalized to the resting fascicle length [measured at tendon slack length (data from Aeles et al., 2017)] for the preferred (blue) and non-preferred (red) leg for each participant. Each diamond represents a single data point, 1 for every 1% of the stance phase. The black diamond represents the fascicle length at the start of the ground contact phase. The vertical bars represent the fascicle length at a 90° ankle joint angle (in relaxed state, data from Aeles et al., 2017). The figure shows that most participants have little to no stretching of the fascicles following ground contact, other than participant 7 in the preferred leg. It also shows significant shortening of the fascicles in some participants (e.g., participant 2), whereas in others the fascicles behave mostly isometrically (e.g., participant 1). For all participants the fascicles at the end of the ground contact sit at (much) shorter lengths than their slack length (vertical dotted line). Considering that all participants had an ankle angle that is more dorsiflexed than 90° at initial ground contact, it is obvious that there is already considerable shortening of the fascicles (other than the preferred leg in participant 8) prior to ground contact due to pre-activation of the muscle, as shown by the horizontal dashed lines.

TABLE 2 | Architectural gearing ratios during various phases of ground contact for the preferred and non-preferred leg.

			Preferred		Non-preferred
Longitudinal muscle shortening velocity > 25 mm/s	All (p = 0.570)	N = 9	1.22 [1.19 1.30]	N = 9	1.21 [1.15 1.27]
			(1.26 ± 0.20)		(1.22 ± 0.30)
	During series-elastic element lengthening	N = 5	1.25 ± 0.19	N = 5	1.23 ± 0.30
	During series-elastic element shortening	N = 5	1.14 ± 0.10	N = 5	1.13 ± 0.19
Longitudinal muscle lengthening velocity > 25 mm/s	All	N = 3	0.82 ± 0.22	N = 3	1.15 ± 0.38
	During series-elastic element lengthening	N = 1	0.83	N = 1	0.46
	During series-elastic element shortening	N = 1	0.54	N = 1	1.18

Values are medians [25% quartile 75% quartile] (means ± SD) for the top row on which a statistical analysis was performed and means ± SD for all other rows. An architectural gearing ratio > 1 means faster longitudinal muscle velocity than fascicle velocity. To make a fair comparison, for parameters with N lower than 9, only the participants that could be compared between preferred and non-preferred and between series-elastic element shortening and series-elastic element lengthening phases were included, resulting in N = 5 for phases of high longitudinal muscle shortening velocities (gray panel). The p-values in the gray panel are for the comparison between preferred and non-preferred leg. Only three athletes had phases during which the aponeurosis was lengthening at high velocities (white panel). Of these three athletes only one athlete had high longitudinal muscle lengthening velocities during both the series-elastic element lengthening and series-elastic element shortening.

there is a similar trend of very low activation during fascicle stretching (Ishikawa et al., 2005; Chleboun et al., 2007; Maharaj et al., 2016, respectively). This suggests that muscle fascicles do sometimes stretch but never at high activation levels. The contradictory findings in studies in the same muscles (medial gastrocnemius and soleus) and during the same task (walking) warrant further investigation. The loading induced during the ground contact phase in the current study was high as the ankle and knee joint moments and positive work in the ankle were, respectively about 1.8, 1.2, and 3 times higher compared to the bilateral pre-hop squat jump in our previous study (Aeles et al., 2018). However, this did not result in a stretching of the muscle fascicles, other than in the preferred leg of only one participant. We did not find a clear explanation in any of the other data as to why this participant showed lengthening in this one leg, but this could be a noteworthy focus of a future study. The loading induced by this movement was far greater than in the step-down task in the study by Werkhausen et al. (2017) (peak ankle moment of 4.3 Nm/kg in our study versus 1.8 Nm/kg in Werkhausen et al., 2017), who did find an average stretching of about 20 mm for the medial gastrocnemius fascicles, suggesting that the stretching of muscle fascicles is not fully dependent on the loading. In two other studies looking at similar tasks, similar fascicle stretching (23 and 16 mm) was found

(Spanjaard et al., 2007 and Hollville et al., 2019 respectively). This striking difference in muscle-tendon interaction between both the step-down and drop landing tasks and our single-leg jumping movement can be explained by the wide variety of roles played by the elastic tissues in muscle-tendon systems (Roberts and Azizi, 2011). Because the single-leg jump was followed by a maximal forward jump, the potential energy from the initial pre-hop is better stored and recycled later on to power the maximal jump, as dissipating this energy would be wasteful.

Energy Dissipation Versus Energy Recycling

These different roles for the muscle-tendon system are carefully regulated by the nervous system by adapting the timing and magnitude of muscle activation. Comparing the activation of the muscle between the different studies shows that during the step-down and drop landing tasks, the medial gastrocnemius has peak activation at the start of the ground contact and then rapidly declines (Spanjaard et al., 2007; Werkhausen et al., 2017; Hollville et al., 2019). This allows for the muscle fascicles to act quasi-isometrically or even shorten slightly during the initial loading, when the forces rise rapidly, before finally lengthening during the phase of force decay. This initial active shortening prior to the passive lengthening of the muscle fascicles has previously been suggested to attenuate the high lengthening velocities of the muscle-tendon unit to much lower velocities in the muscle fascicles, serving as a protective buffer and reducing muscle damage (Proske and Morgan, 2001; Lieber and Fridén, 2002; Konow et al., 2012). In the single-leg jump, however, the medial gastrocnemius muscle stays active for a much longer period, only decreasing its activation around 80% of the ground-contact phase, allowing for a long period of stretching of the series-elastic element, storing significant amounts of potential energy to be used later in the movement, when both the series-elastic element and muscle-tendon unit are recoiling at high velocities. Combined, our findings suggest that highly active SSCs of the medial gastrocnemius muscle are unlikely to occur in human movement when the main role for the elastic tissues is not to dissipate energy. This may especially be the case in MTUs that have considerable in-series compliance, such as the triceps surae muscles. It is also noteworthy to take into account that the participants in this study were all highly trained jumping athletes. Considering the high forces that are likely acting on the lower limb muscles, it is possible that lesser trained individuals may not be able to avoid fascicle lengthening. This could be an interesting focus point for future studies.

The Effect on the Tendon and Muscle-Tendon Unit

Considering the high loading, it could be expected that the muscle-tendon unit of the medial gastrocnemius would stretch more as compared to other movements, resulting in greater stretching of the series-elastic element and a greater amount of energy storage. However, it is likely that the peak ankle dorsiflexion angle during ground contact is close to the maximal range of motion for this joint, limiting further stretching of the muscle-tendon unit. Extending the knee more would allow for further stretching in the muscle-tendon unit of the medial gastrocnemius, but would come at the cost of less stretching of the MTUs of the knee extensors, which have also been shown to store and release significant amounts of elastic energy in the series-elastic element (Nikolaidou et al., 2017). On the other hand, at ground contact, the ankle was already in a more dorsiflexed position compared to the bilateral pre-hop squat jump while the initial knee joint angle is very similar (Aeles et al., 2018). This would mean that the muscle-tendon unit already starts at a longer length in the single-leg jump upon initial ground contact, potentially causing more total elastic energy to be stored in it. Furthermore, the fact that the muscle fascicles are already at a shorter length at the start of ground contact compared to their length at a similar joint angle in rest (**Figure 4**) suggests that there must already be energy being stored in the series-elastic element. This could explain why both the muscle-tendon unit and series-elastic element also have much higher maximal shortening velocities in the single-leg compared to the bilateral jump (1.3 and 1.6 times for muscle-tendon unit and series-elastic element, respectively). In our study on the pre-hop squat jump we were surprised to find that the net work in the ankle was reduced considerably in the pre-hop squat jump compared to a standard squat jump and we argued that the additional negative work that can be recycled in the former but not in the latter should have

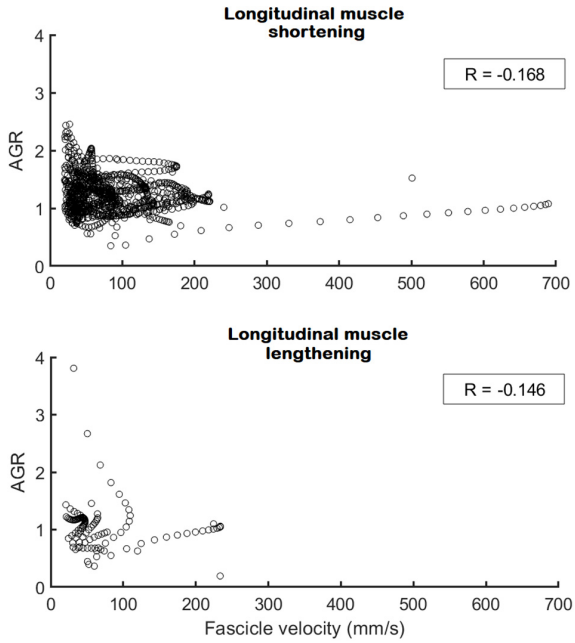

FIGURE 5 | Architectural gearing ratio as a function of fascicle velocity for all participants during longitudinal muscle shortening at velocities > 25 mm/s (N = 9; **Top**) and during longitudinal muscle lengthening at velocities > 25 mm/s (N = 3; **Bottom**). Each circle represents a single data point for both preferred and non-preferred leg data combined. A very low, negative correlation coefficient (in box) was obtained for both datasets. Note that the x-axis on the top panel is fascicle shortening velocity whereas on the bottom panel this is fascicle lengthening velocity.

allowed for more positive work to be done in the ankle during the pre-hop squat jump (Aeles et al., 2018). We suggested that further increasing the positive work done in the ankle may interfere with the correct execution of the jump, as the joint moments need to be balanced (Farris et al., 2016). This limitation may not be applicable to the single-leg forward jump used in the current study, potentially explaining the ability of the ankle to stretch the medial gastrocnemius series-elastic element more and indeed produce much greater positive work and in result have much more and faster recoil shortening of the series-elastic element when the stored energy is released.

The Fine-Tuning of the Architectural Gearing Ratio

The decoupling of the muscle fascicles from the entire muscle-tendon unit allowed the medial gastrocnemius fascicles to shorten at much lower maximal velocities compared to the muscle-tendon unit and series-elastic element. This is similar to what was previously shown in other tasks such as walking, running, and bilateral jumping (Fukunaga et al., 2001; Kurokawa et al., 2001, 2003; Lichtwark and Wilson, 2006; Farris and Sawicki, 2012; Aeles et al., 2018). Despite this, the muscles fascicles still shorten at high velocities compared to walking and running (Lichtwark and Wilson, 2006), yet still at less than one third of their expected maximal shortening velocities (Geyer and Herr, 2010). Our results show that the single-leg jump also has the two distinct phases found in the medial gastrocnemius muscle-tendon interaction in other movements, namely an initial phase of long stretching of the series-elastic element, which usually takes up between 60 and 85% of the ground contact phase, and a rapid shortening of the series-elastic element at the end of the movement. Contrary to our hypothesis, we found a trend for the architectural gearing ratio to be higher during the stretching of the series-elastic element, compared to when the series-elastic element is shortening. However, we noticed that the peak shortening velocity of the fascicles occurred during the stretching phase of the series-elastic element in many of our participants rather than in the shortening phase of the series-elastic element as we expected. Combined, these findings agree with the theory that the muscle is able to tune its architectural gearing ratio based on the demands of the task. This is also in agreement with an earlier study on the architectural gearing ratio measured in humans during cycling (Dick and Wakeling, 2017). However, all aforementioned studies have only reported the architectural gearing ratio during a single instance in time. Yet, if the architectural gearing ratio of a muscle would actually be tuned to the requirements of the task, one would expect the architectural gearing ratio to be relatively constant during a specific task or at least to be highly correlated with the instantaneous velocity of the fascicles. When plotting the architectural gearing ratio as a function of the fascicle shortening velocity at instantaneous time points throughout the whole movement, however, very low correlation coefficients were found when the fascicles were shortening as well as when they were lengthening (**Figure 5**). This finding is in contrast with our expectation that the architectural gearing ratio of the muscle is tuned precisely throughout the movement to accommodate the requirements of the task. Nonetheless, when the fascicles are shortening, the medial gastrocnemius muscle still mostly works at an architectural gearing ratio greater than 1, resulting in greater longitudinal muscle velocities relative to the fascicle velocities. In the preferred leg, this resulted in significantly greater longitudinal muscle shortening velocities relative to the muscle fascicles. The fascicle lengthening velocities reported here are also much lower compared to the values found during dissipation tasks as reported by Werkhausen et al. (2017) and Hollville et al. (2019).

Concluding Remarks on Lack of Bilateral Differences and Limitations

This study was the first to make a bilateral comparison on the muscle-tendon interaction during a dynamic movement. We found no differences between the preferred and non-preferred leg in most of the tested parameters, despite the athletes having a clear preference for which leg to use for jumping. In an earlier study we found high variability in the medial gastrocnemius muscle architecture bilaterally (Aeles et al., 2017). Visual inspection of the fascicle length changes during ground contact from the single-leg jumps (**Figure 3**) also suggests that they behave very similarly in both legs, even regardless of preference. This is interesting because when two fascicles have different resting lengths, but are shortened a similar amount, assuming similar sarcomere lengths, the shorter fascicle would have greater shortening per sarcomere. This would then further result in greater shortening velocities per sarcomere, which would lower the maximal capacity of the sarcomeres to produce force. In theory, this would cause an imbalance in the force generating capacity between both muscles. This imbalance, however, could be compensated for by various mechanisms such as differences in neural drive to the muscle, or other agonistic muscles.

The small sample size in this study is a potential limitation which may affect the interpretation of the statistical findings presented here. However, because of the fairly one-sided findings in both the comparison between preferred and non-preferred leg and in the lack of muscle fascicle stretching in most participants, we suspect this sample represents the specific population. Because of the low numbers we were able to use for the architectural gearing ratio analysis, we would encourage others to perform this analysis on a larger dataset.

CONCLUSION

Although the SSC of muscle is a phenomenon worthy of study, we argue that it only rarely occurs at high activation levels during *in vivo* human movement, at least in muscles that have high in-series compliance such as the medial gastrocnemius. The rare occurrence of highly active SSCs should be considered when discussing the potential effects of mechanisms such as residual force enhancement *in vivo*. Whether or not muscles actively

lengthen during high loading movements is not just of relevance for performance but also in terms of injury. We further conclude that the architectural gearing ratio of the medial gastrocnemius muscle is not precisely tuned and there is high variability between data points within a single movement, and that the medial gastrocnemius muscle-tendon interaction between a preferred and non-preferred leg for jumping is very similar.

DATA AVAILABILITY STATEMENT

The datasets generated for this study are available on request to the corresponding author.

ETHICS STATEMENT

The studies involving human participants were reviewed and approved by the Ethics Committee Research UZ/KU Leuven. The patients/participants provided their written informed consent to participate in this study.

AUTHOR CONTRIBUTIONS

JA was involved in project design, participant recruitment, data analyses, figure creation, and manuscript writing. BV was involved in project design and manuscript writing.

REFERENCES

Aeles, J., Lenchant, S., Vanlommel, L., and Vanwanseele, B. (2017). Bilateral differences in muscle fascicle architecture are not related to the preferred leg in jumping athletes. *Eur. J. Appl. Physiol.* 117, 1453–1461. doi: 10.1007/s00421-017-3638-5

Aeles, J., Lichtwark, G. A., Peeters, D., Delecluse, C., Jonkers, I., and Vanwanseele, B. (2018). The effect of a pre-hop on the muscle-tendon interaction during vertical jumps. *J. Appl. Physiol.* 124, 1203–1211. doi: 10.1152/japplphysiol.00462.2017

Azizi, E., and Roberts, T. J. (2014). Geared up to stretch: pennate muscle behaviour during active lengthening. *J. Exp. Biol.* 217, 376–381. doi: 10.1242/jeb.094383

Azizi, E., Brainerd, E. I., and Roberts, T. J. (2008). Variable gearing in pennate muscles. *Proc. Natl. Acad. Sci. U.S.A.* 105, 1745–1750. doi: 10.1073/pnas.0709212105

Bosco, C., Viitasalo, J. T., Komi, P. V., and Luhtanen, P. (1982). Combined effect of elastic energy and myoelectrical potentiation during stretch-shortening cycle exercise. *Acta Physiol. Scand.* 114, 557–565. doi: 10.1111/j.1748-1716.1982.tb07024.x

Brainerd, E. L., and Azizi, E. (2005). Muscle fiber angle, segment bulging and architectural gear ratio in segmented Musculature. *J. Exp. Biol.* 208, 3249–3261. doi: 10.1242/jeb.01770

Cavagna, G. A., Saibene, F. P., and Margaria, R. (1965). Effect of negative work on the amount of positive work performed by an isolated muscle. *J. Appl. Physiol.* 20, 157–158. doi: 10.1152/jappl.1965.20.1.157

Chleboun, G. S., Busic, A. B., Graham, K. K., and Stuckey, H. A. (2007). Fascicle length change of the human tibialis anterior and vastus lateralis during walking. *J. Orthop. Sports Phys. Ther.* 37, 372–379. doi: 10.2519/jospt.2007.2440

Cronin, N. J., and Finni, T. (2013). Treadmill versus overground and barefoot versus shod comparisons of triceps surae fascicle behaviour in human walking and running. *Gait Posture* 38, 528–533. doi: 10.1016/j.gaitpost.2013.01.027

De Groote, F., De Laet, T., Jonkers, I., and De Schutter, J. (2008). Kalman smoothing improves the estimation of joint kinematics and kinetics in marker-based human gait analysis. *J. Biomech.* 41, 3390–3398. doi: 10.1016/j.jbiomech.2008.09.035

Delp, S. L., Anderson, F. C., Arnold, A. S., Loan, P., Habib, A., John, C. T., et al. (2007). OpenSim: open-source software to create and analyze dynamic simulations of movement. *IEEE Trans. Biomed. Eng.* 54, 1940–1950. doi: 10.1109/tbme.2007.901024

Dick, T. J. M., and Wakeling, J. M. (2017). Shifting gears: dynamic muscle shape changes and force-velocity behavior in the medial gastrocnemius. *J. Appl. Physiol.* 123, 1433–1442. doi: 10.1152/japplphysiol.01050.2016

Farris, D. J., and Lichtwark, G. A. (2016). Ultratrack: software for semi-automated tracking of muscle fascicles in sequences of B-mode ultrasound images. *Comput. Methods Programs Biomed.* 128, 111–118. doi: 10.1016/j.cmpb.2016.02.016

Farris, D. J., and Sawicki, G. S. (2012). Human medial gastrocnemius force-velocity behaviour shifts with locomotion speed and gait. *Proc. Natl. Acad. Sci. U.S.A.* 109, 977–982. doi: 10.1073/pnas.1107972109

Farris, D. J., Lichtwark, G. A., Brown, N. A. T., and Cresswell, A. G. (2016). The role of human ankle plantar flexor muscle-tendon interaction and architecture in maximal vertical jumping examined in vivo. *J. Exp. Biol.* 219, 528–534. doi: 10.1242/jeb.126854

Fukunaga, T., Kubo, K., Kawakami, Y., Fukashiro, S., Kanehisa, H., and Maganaris, C. N. (2001). In vivo behavior of human muscle tendon during walking. *Proc. R. Soc. Lond. B* 268, 229–233.

Geyer, H., and Herr, H. (2010). A muscle-reflex model that encodes principles of legged mechanics produces human walking dynamics and muscle activities. *IEEE Trans. Neural Syst. Rehabil. Eng.* 18, 263–273. doi: 10.1109/TNSRE.2010.2047592

Griffiths, R. I. (1984). *Mechanical properties of an ankle extensor muscle in a freely hopping wallaby*. Ph.D Thesis, Monash University, Clayton, VIC.

Griffiths, R. I. (1987). Ultrasound transit time gives direct measurement of muscle fibre length in vivo. *J. Neurosci. Meth.* 21, 159–165. doi: 10.1016/0165-0270(87)90113-0

Hamner, S. R., Seth, A., and Delp, S. L. (2010). Muscle contributions to propulsion and support during running. *J. Biomech.* 43, 2709–2716. doi: 10.1016/j.jbiomech.2010.06.025

Hollville, E., Nordez, A., Guilhem, G., Lecompte, J., and Rabita, G. (2019). Interactions between fascicles and tendinous tissues in gastrocnemius medialis and vastus lateralis during drop landing. *Scand. J. Med. Sci. Sports* 29, 55–70. doi: 10.1111/sms.13308

Ishikawa, M., Komi, P. V., Grey, M. J., Lepola, V., and Bruggemann, G. P. (2005). Muscle-tendon interactions and elastic energy usage in human walking. *J. Appl. Physiol.* 99, 603–608. doi: 10.1152/japplphysiol.00189.2005

Konow, N., Azizi, E., and Roberts, T. J. (2012). Muscle power attenuation by tendon during energy dissipation. *Proc. R. Soc. B* 279, 1108–1113. doi: 10.1098/rspb.2011.1435

Kurokawa, S., Fukunaga, T., and Fukashiro, S. (2001). Behavior of fascicles and tendinous structures of human gastrocnemius during vertical jumping. *J. Appl. Physiol.* 90, 1349–1358. doi: 10.1152/jappl.2001.90.4.1349

Kurokawa, S., Fukunaga, T., Nagano, A., and Fukashiro, S. (2003). Interaction between fascicles and tendinous structures during counter movement jumping investigated in vivo. *J. Appl. Physiol.* 95, 2306–2314. doi: 10.1152/japplphysiol.00219.2003

Lai, A., Lichtwark, G. A., Schache, A. G., Lin, Y. C., Brown, N. A. T., and Pandy, M. G. (2015). In vivo behavior of the human soleus muscle with increasing walking and running speeds. *J. Appl. Physiol.* 118, 1266–1275. doi: 10.1152/japplphysiol.00128.2015

Lichtwark, G. A., and Wilson, A. M. (2006). Interactions between the human gastrocnemius muscle and the Achilles tendon during incline, level and decline locomotion. *J. Exp. Biol.* 209, 4379–4388. doi: 10.1242/jeb.02434

Lieber, R. L., and Fridén, J. (2002). Mechanisms of muscle injury gleaned from animal models. *Am. J. Phys. Med. Rehabil.* 81, S70–S79.

Maharaj, J. N., Cresswell, A. G., and Lichtwark, G. A. (2016). The mechanical function of the tibialis posterior muscle and its tendon during locomotion. *J. Biomech.* 49, 3238–3243. doi: 10.1016/j.jbiomech.2016.08.006

Nicol, C., Avela, J., and Komi, P. V. (2006). The stretch-shortening cycle, a model to study naturally occurring neuromuscular fatigue. *Sports Med.* 36, 977–999. doi: 10.2165/00007256-200636110-00004

Nikolaidou, M. E., Marzilger, R., Bohm, S., Mersmann, F., and Arampatzis, A. (2017). Operating length and velocity of human M. vastus lateralis fascicles during vertical jumping. *R. Soc. Open Sci.* 4:170185. doi: 10.1098/rsos.170185

Proske, U., and Morgan, D. L. (2001). Muscle damage from eccentric exercise: mechanism, mechanical signs, adaptation and clinical applications. *J. Physiol.* 537, 333–345. doi: 10.1111/j.1469-7793.2001.00333.x

Roberts, T. J., and Azizi, E. (2011). Flexible mechanisms: the diverse roles of biological springs in vertrebrate movement. *J. Exp. Biol.* 214, 353–361. doi: 10.1242/jeb.038588

Seiberl, W., Power, G. A., Herzog, W., and Hahn, D. (2015). The stretch-shortening cycle (SSC) revisited: residual force enhancement contributes to increased performance during fast SSCs of human m. adductor pollicis. *Physiol. Rep.* 3:e12401. doi: 10.14814/phy2.12401

Spanjaard, M., Reeves, N. D., van Dieën, J. H., Baltzopoulos, V., and Maganaris, C. N. (2007). Gastrocnemius muscle fascicle behavior during stair negotiation in humans. *J. Appl. Physiol.* 102, 1618–1623. doi: 10.1152/japplphysiol.00353.2006

Werkhausen, A., Albracht, K., Cronin, N. J., Meier, R., Bojsen-Møller, J., and Seynnes, O. R. (2017). Modulation of muscle–tendon interaction in the human triceps surae during an energy dissipation task. *J. Exp. Biol.* 220, 4141–4149. doi: 10.1242/jeb.164111

Conflict of Interest: The authors declare that the research was conducted in the absence of any commercial or financial relationships that could be construed as a potential conflict of interest.

frontiers in Physiology

ORIGINAL RESEARCH
published: 20 December 2019
doi: 10.3389/fphys.2019.01511

Medial Gastrocnemius Muscle Architecture Is Altered After Exhaustive Stretch-Shortening Cycle Exercise

Adam Kositsky[1]†, Dawson J. Kidgell[2] and Janne Avela[1]*

[1]Biology of Physical Activity, Neuromuscular Research Center, Faculty of Sport and Health Sciences, University of Jyväskylä, Jyväskylä, Finland, [2]Department of Physiotherapy, School of Primary and Allied Health Care, Faculty of Medicine, Nursing and Health Sciences, Monash University, Melbourne, VIC, Australia

OPEN ACCESS

Edited by:
Geoffrey A. Power, University of Guelph, Canada

Reviewed by:
Emiliano Cè, University of Milan, Italy
Nicolas Babault, Université Bourgogne Franche-Comté, France

***Correspondence:**
Adam Kositsky
adam.kositsky@griffithuni.edu.au; akositsky@hotmail.com

†Present address:
Adam Kositsky, School of Allied Health Sciences, Griffith University, Gold Coast, QLD, Australia

Specialty section:
This article was submitted to Exercise Physiology, a section of the journal Frontiers in Physiology

Received: *15 September 2019*
Accepted: *29 November 2019*
Published: *20 December 2019*

Citation:
Kositsky A, Kidgell DJ and Avela J (2019) Medial Gastrocnemius Muscle Architecture Is Altered After Exhaustive Stretch-Shortening Cycle Exercise. Front. Physiol. 10:1511. doi: 10.3389/fphys.2019.01511

Muscle architecture is an important component of muscle function, and recent studies have shown changes in muscle architecture with fatigue. The stretch-shortening cycle is a natural way to study human locomotion, but little is known about how muscle architecture is affected by this type of exercise. This study investigated potential changes in medial gastrocnemius (MG) muscle architecture after exhaustive stretch-shortening cycle exercise. Male athletes (n = 10) performed maximal voluntary contractions (MVC) and maximal drop jump (DJ) tests before and after an exercise task consisting of 100 maximal DJs followed by successive rebound jumping to 70% of the initial maximal height. The exercise task ceased upon failure to jump to 50% of maximal height or volitional fatigue. Muscle architecture of MG was measured using ultrasonography at rest and during MVC, and performance variables were calculated via a force plate and motion analysis. After SSC exercise, MVC (−13.1%; $p = 0.005$; $d_z = 1.30$), rebound jump height (−14.8%, $p = 0.004$; $d_z = 1.32$), and ankle joint stiffness (−26.3%; $p = 0.008$; $d_z = 1.30$) decreased. Ankle joint range of motion (+20.2%; $p = 0.011$; $d_z = 1.09$) and MG muscle-tendon unit length (+12.0%; $p = 0.037$; $d_z = 0.91$) during the braking phase of DJ, the immediate drop-off in impact force (termed peak force reduction) (Δ27.3%; $p = 0.033$; $d_z = 0.86$), and lactate (+9.5 mmol/L; $p < 0.001$; $d_z = 3.58$) increased. Fascicle length increased at rest (+4.9%; $p = 0.013$; $d_z = 1.16$) and during MVC (+6.8%; $p = 0.048$; $d_z = 0.85$). Pennation angle decreased at rest (−6.5%; $p = 0.034$, $d_z = 0.93$) and during MVC (−9.8%; $p = 0.012$; $d_z = 1.35$). No changes in muscle thickness were found at rest (−2.6%; $p = 0.066$; $d_z = 0.77$) or during MVC (−1.6%; $p = 0.204$; $d_z = 0.49$). The greater MG muscle-tendon stretch during the DJ braking phase after exercise indicates that muscle damage likely occurred. The lower peak force reduction and ankle joint stiffness, indicative of decreased active stiffness, suggests activation was likely reduced, causing fascicles to shorten less during MVC.

Keywords: fatigue, ultrasound, fascicle length, pennation, stretch reflex, afferent, force

INTRODUCTION

The architecture of a skeletal muscle describes the structural component that influences its function (Lieber and Fridén, 2000). The force-length relationship and the direction of muscle fiber force transmitted to the line of muscle action are imperative components of muscle mechanics. Muscle architecture can be visualized *in vivo* utilizing B-mode ultrasonography, and this methodology has been used over the past few decades to assess key architecture parameters, i.e., muscle fascicle length (FL) and pennation angle (PA), in various conditions (Franchi et al., 2018).

As fatigue is defined as a reduction in maximal force production resulting from exercise (Taylor and Gandevia, 2008), muscle architecture measures during maximal voluntary contraction (MVC) may reveal important information about muscle function immediately after exercise. Indeed, acute changes in muscle architecture have previously been reported in the human triceps surae after various exercise tasks. In particular, increased FL of medial gastrocnemius (MG) during an active contraction has been observed following repeated maximal isometric (Mitsukawa et al., 2009; Thomas et al., 2015) and eccentric contractions (Guilhem et al., 2016). In contrast, fascicles were shorter after repeated isometric contractions at submaximal levels (Mademli and Arampatzis, 2005). Nonetheless, prolonged exercise appears to have an effect on muscle architecture.

However, the immediate effects on muscle architecture after stretch-shortening cycle (SSC) exercise are less clear. The SSC is a crucial and inherent function that exists in human locomotion, whereby preactivated muscle-tendon units (MTU) lengthen eccentrically prior to concentric shortening (Komi, 2000). Because the SSC sequence occurs in many common activities, such as running and jumping, repetitive SSC exercise better represents naturally occurring fatigue compared to repetitive isolated isometric, concentric, or eccentric tasks (Komi, 2000; Nicol et al., 2006). Although fatiguing SSC exercise has been reported to alter MG (Lidstone et al., 2016; Kubo and Ikebukuro, 2019) and soleus (Ishikawa et al., 2006) muscle architecture, neither study took measures during MVC immediately post-exercise. Further, while there was increased length of soleus fascicles at rest following SSC exercise (Ishikawa et al., 2006), to our knowledge there are no data available regarding fatigue-related changes in resting MG muscle architecture after SSC exercise. Therefore, the purpose of the present study was to investigate the effect of exhaustive SSC exercise on MG muscle architecture at rest and during MVC. Based on the results of previous experiments, it was hypothesized that the exercise task would cause increases in FL and decreases in PA in both conditions. Performance parameters were also measured during MVC and SSC tasks.

MATERIALS AND METHODS

Subjects

Ten male soccer players [mean age = 18.9 ± 0.9 years (all >18 years); mean height = 182.3 ± 6.2 cm; mean body mass = 75.9 ± 6.6 kg] were recruited. Subjects were requested to not perform any strenuous activity beginning 48 h prior to testing. The University of Jyväskylä Ethical Committee, in accordance with the Declaration of Helsinki, approved the study. Each subject was informed of the benefits and risks of the study and provided written consent prior to the commencement of the investigation.

Procedures

At least one week prior to the fatigue protocol, subjects visited the lab for a familiarization session. Subjects were introduced to the sledge apparatus (Aura and Komi, 1986) inclined 24.9° from horizontal and the optimal dropping height for drop jumps (DJs) was determined (Avela et al., 2006). After being instructed to rebound jump as high and as fast as they could, subjects were dropped from 10 cm intervals and the rebound jump height was recorded. Dropping heights were increased until the rebound height no longer improved, and the dropping height with the corresponding highest rebound height was determined to be the optimal dropping height. Subjects were also shown how to perform and practiced MVCs of the plantarflexors on the sledge apparatus.

The second session consisted of the fatigue protocol on the sledge apparatus with MVC and maximal DJ measurements prior to, and ~5 min after, exercise. These post-exercise tests were not completely immediate as lactate and resting muscle architecture measurements were conducted first. Subjects performed a standardized, moderate-intensity warm-up on a cycle ergometer for 10 min (Regueme et al., 2005). Subjects then performed 100 successive maximal bilateral DJs (one DJ every 5 s; controlled with an audible metronome) from the optimal dropping height (Kuitunen et al., 2002; Ishikawa et al., 2006; Dousset et al., 2007), split into 5 sets of 20 with 2 min rest given between sets (Miyama and Nosaka, 2004). Immediately after the 100th maximal DJ, the subjects began continuous submaximal rebounding to a height corresponding to 70% of the initial maximal rebound height (Kuitunen et al., 2002; Ishikawa et al., 2006; Dousset et al., 2007). This was necessary because blood lactate does not accumulate after 100 sledge DJs in athletes (Avela et al., 2006). Rebound jumping continued until either 50% of maximal rebound height could not be attained or volitional fatigue. Subjects were given audible feedback regarding rebound jump height. To maximize fatigue of the triceps surae, subjects were not allowed to contact the force platform with their heels and were instructed to limit their knee angle to a maximum of 90° during ground contact (Regueme et al., 2005). During all jumps, the seat was inclined to 120° and subjects were advised to allow their knees to passively flex freely during the rebound airborne phase to reduce fatigue of the hip and knee extensors (Dousset et al., 2007).

Performance Measures

A rigid, built-in force plate located at the bottom of the sledge apparatus recorded ground reaction force perpendicular to the movement plane of the sledge (Aura and Komi, 1986). Data were sampled at 1,000 Hz using Spike2 software (version 6.17, Cambridge Electronics Design, Cambridge, UK). MVCs were performed with subjects seated in the sledge apparatus. To maximize activation of the plantarflexors, heels were kept off

the force plate by placing the distal, plantar surface of the feet over a footplate. During MVCs, adjustable metal bars held the sledge in a locked position with the knees in full extension and the ankles neutral. Data were taken as an average of 500 ms around the peak value and subtracted by baseline force (average of 500 ms prior to contraction) to exclude each subject's body weight. Subjects were given 2 min rest between trials and the average of two trials was used.

As a performance test, subjects performed maximal bilateral DJs from the optimal dropping height with the same instructions and joint angle restrictions as in the familiarization session and fatigue protocol. Arms were folded across their chest to limit upward propulsion by the upper body. Jump height was recorded by marking the highest position of the sledge's potentiometer and subtracting the subject's relative standing height on the sledge. Upon landing, there is a large impact spike preceding a drop-off in force (Komi, 2000), termed peak force reduction, which was calculated as the difference between the peak impact force and the immediate lowest force level (Avela et al., 1999b). All jumps were recorded from the subject's right side using a high-speed camera (Sony NXCAM, HXR-NX5E, Japan) at 200 frames per second. Reflective markers were placed over the greater trochanter, lateral femoral condyle, lateral malleolus, heel, and base of the fifth metatarsal of the right lower limb. Markers were digitized and processed (Vicon Motus 10.0, Vicon Motion Systems, Oxford, UK) with a 20 Hz low-pass Butterworth filter applied to the raw coordinates. Estimates of MG MTU length were derived from kinematic data using the equation of Hawkins and Hull (1990) and normalized to lower leg length (lateral femoral condyle to lateral malleolus). Videos were synchronized using an LED light that brightened when force increased above baseline levels. Subjects were given 2 min rest between trials and the average of 2–3 trials were used.

The ankle joint moment was estimated using the equation of Kawakami et al. (2002). Briefly, the formula accounts for the perpendicular ground reaction force, the estimated length between the center of the ankle joint (center of the lateral malleolus) and the ball of the foot, and the ankle joint angle at the lowest point (transition from braking to propulsion phase). Ankle joint stiffness was calculated as the change in ankle joint moment divided by the change in ankle joint angle during the braking (eccentric) phase (Kuitunen et al., 2002; Kubo and Ikebukuro, 2019).

Fingertips were cleansed with sanitizing alcohol before blood samples were drawn, and lactate was analyzed instantly using an automated device (Lactate Scout, SensLab GmbH, Germany). This analysis was conducted prior to warm-up and immediately upon completion of the fatiguing task.

Muscle Architecture

Real-time B-mode ultrasonography (SSD-α10, Aloka, Japan) recorded longitudinal images of MG (**Figure 1**). The imaging location was determined by scanning the muscle belly for the thickest region where fascicles could be clearly seen from superficial to deep aponeurosis. A 7.5 MHz transducer (scanning length: 60 mm) was longitudinally attached over the skin of the right leg using a custom-made foam holder and elastic bandages. Acoustic coupling gel was applied between the transducer surface and skin. Resting images were taken with the subjects resting prone on a plinth with the ankle neutral. Images were obtained at 94 Hz and for MVCs synchronized with an electronic pulse on the force recordings that signaled video onset. FL was determined as the length of an ultrasonic echo, parallel to the muscle fascicles, between superficial and deep aponeuroses (Fukunaga et al., 1997) and extrapolated where necessary (Thomas et al., 2015; Guilhem et al., 2016). PA was measured as the angle between the fascicle and deep aponeurosis. The vertical distance between superficial and deep aponeuroses, defined as muscle thickness (MT), was averaged over three locations (left, center, right) of each image. Because MG images taken at rest have previously been established to be reliable (Kwah et al., 2013), FL and PA were taken as the average of three separate fascicles from a single image. For PA and MT during MVC, a still image was taken from the absolute peak force from the trials used in MVC force data. Data from 2–3 fascicles from two images and videos were averaged. Using a reliable, automated fascicle tracking algorithm (Matlab version R2016b, The MathWorks Inc., Massachusetts, USA) (Cronin et al., 2011), active FL was averaged over the synchronized and corresponding 500 ms window from trials that were used for peak MVC force analysis. All data were manually checked and corrected if necessary. For single images, open-source computer software (ImageJ 1.51h, National Institutes of Health, USA) was used.

Statistical Analysis

Statistical analyses were performed on absolute values using IBM SPSS Statistics 25 (SPSS Inc., Chicago, USA). A

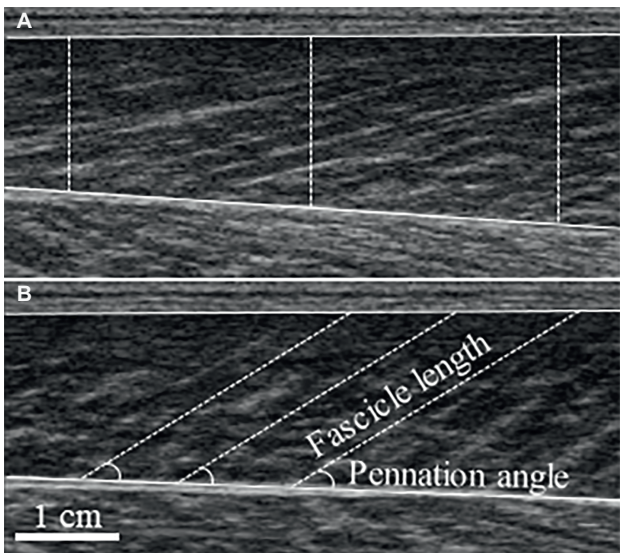

FIGURE 1 | Typical ultrasound images of the medial gastrocnemius taken at rest **(A)** and during maximal voluntary contraction **(B)**. Measurement of muscle thickness is depicted by dashed vertical lines superimposed on the resting image, with fascicle length and pennation angle superimposed on the maximal voluntary contraction image.

Shapiro-Wilk test was performed to assess normal distribution. Two-tailed paired-sampled *t*-tests were used to assess differences from baseline measurements. As PA data during MVC were not normally distributed, a Wilcoxon signed-rank test was conducted instead. Statistical significance was set at $p < 0.05$ and confidence intervals at 95%. Cohen's d_z effect sizes (within-subjects design) were calculated from absolute values (Lakens, 2013) and interpreted as small ≥0.20, medium ≥0.50, and large ≥0.80.

One subject was excluded from all data as his post MVC value was considerably increased (~17%). It is possible that the optimal dropping height was determined incorrectly, inducing some facilitatory responses (Nicol et al., 2006). A second subject was excluded from ultrasound data due to errors in the recording. For a third subject, the braking phase could not be synchronized with the force signal during post-exercise DJ testing; thus, ankle joint stiffness could not be calculated, and he was excluded from this parameter. Finally, the reflective marker over the greater trochanter could not be accurately tracked for a fourth subject during the pre-exercise DJ trials. Therefore, knee joint range of motion and MG MTU length could not be determined, and he was excluded from these parameters. This resulted in $n = 8$ for the ultrasound, ankle joint stiffness, knee joint range of motion, and MG MTU length measures, and $n = 9$ for all other variables.

RESULTS

Performance parameters are summarized in **Table 1** and demonstrate that fatigue was clearly induced. After exercise, significant reductions were shown in MVC (−13.1%; $p = 0.005$; $d_z = 1.30$), rebound jump height (−14.8%, $p = 0.004$; $d_z = 1.32$), and ankle joint stiffness (−26.3%; $p = 0.008$; $d_z = 1.30$). Peak force reduction (Δ27.3%; $p = 0.033$; $d_z = 0.86$) and lactate (mean difference: +9.5 mmol/L; $p < 0.001$; $d_z = 3.58$) were significantly increased. During the maximal DJ test after exercise, only the change in ankle joint range of motion during the braking phase was significantly different (+20.2%; $p = 0.011$; $d_z = 1.09$). The change in ankle joint range of motion during the propulsion phase (+2.3%; $p = 0.459$; $d_z = 0.26$), and the change in knee joint range of motion during the braking (+2.1%; $p = 0.647$; $d_z = 0.17$) and propulsion (−3.9%; $p = 0.097$; $d_z = 0.68$) phases were not significantly different. This resulted in a significant difference in MG MTU length change during the braking (+12.0%; $p = 0.037$; $d_z = 0.91$), but not the propulsion (−0.6%; $p = 0.826$; $d_z = 0.08$), phase after exercise.

Significant changes in muscle architecture were apparent post-exercise. FL was significantly longer at rest (+4.9%; $p = 0.013$; $d_z = 1.16$) and during MVC (+6.8%; $p = 0.048$; $d_z = 0.85$) (**Table 2**). Significant decreases were found for PA in both resting (−6.5%; $p = 0.034$, $d_z = 0.93$) and MVC (−9.8%; $p = 0.012$; $d_z = 1.35$) conditions (**Table 2**). There was no change in MT at rest (−2.6%; $p = 0.066$; $d_z = 0.77$) or during MVC (−1.6%; $p = 0.204$; $d_z = 0.49$).

DISCUSSION

The purpose of the study was to investigate changes in MG muscle architecture after exhaustive SSC exercise on a sledge apparatus. The results show increased FL and decreased PA with large effect sizes. Further, the changes in FL (rest: +4.9%; MVC: +6.8%) and PA (rest: −6.5%; MVC: −9.8%) were greater than the intra-session minimal detectable changes in gastrocnemius FL (4.8%) and PA (1.8%), as reported by Cè et al. (2015). There were no significant differences in MT either at rest or MVC. Additionally, the exercise task induced significant decrements to MVC and DJ performance.

Muscle Architecture Changes at Rest

The increased range of motion at the ankle, but not knee, joint during DJ after exercise resulted in a greater stretch of the MG MTU during the braking phase. Because Achilles tendon mechanical properties are typically unchanged after prolonged SSC exercise (Peltonen et al., 2010, 2012; Lichtwark et al., 2013; Kubo and Ikebukuro, 2019), this likely resulted in changes at the muscle fascicle level. In non-fatigued conditions, MG fascicles generally shorten before operating quasi-isometrically or minimally stretching during DJs from the optimal dropping height, but undergo a larger stretch during DJs from heights greater than optimal (Ishikawa et al., 2005; Sousa et al., 2007). Indeed, Kubo and Ikebukuro (2019) have recently reported a large reduction in the amount of MG fascicle shortening during the braking phase of ankle-joint only DJs after repeated hopping. In particular, at group level the fascicles showed an initial stretch immediately after ground contact (Figure 1B in Kubo and Ikebukuro, 2019), demonstrating potential for fascicles to be exposed to greater strain as the exercise protocol proceeded. Greater fascicle strain as the exercise task progressed would have led to muscle damage (Lieber and Fridén, 1993; Peñailillo et al., 2015) that has previously been reported after similar fatigue protocols (Miyama and Nosaka, 2004; Ishikawa et al., 2006; Dousset et al., 2007). Damage to the non-contractile elements has been attributed to the increase in resting soleus fascicle length immediately after a similar SSC protocol (Ishikawa et al., 2006). While we did not find increases in MT, a measure that is associated with muscle damage, increases in MT do not always occur immediately after muscle damaging SSC exercise (Ishikawa et al., 2006; Dousset et al., 2007). Therefore, intramuscular pressure likely did not immediately change, and thus the resting pennation angle became smaller owing to space constraints within the muscle. Further, although muscle damage has recently been associated with increased passive stiffness (Lacourpaille et al., 2017), due to the constraints imposed by our experimental set-up, we were only able to test a surrogate of active stiffness (explained in the section "Limitations"). Nonetheless, longer MG fascicles at rest as a result of muscle damage is supported by a previous report of increased resting FL of soleus, in combination with greater passive stiffness, immediately post-exhaustive, muscle damaging SSC exercise (Ishikawa et al., 2006). Future studies should investigate the relationship of resting FL changes with changes in passive stiffness measures (e.g., shear modulus, passive torque) and muscle damage.

TABLE 1 | Performance parameters before and after exhaustive exercise.

	Pre	Post
Maximal voluntary contraction (N)	1375.5(328.9)	1195.7(322.8)**
Rebound jump height (cm)	79.5(11.1)	67.7(11.6)**
Peak force reduction (N)	−746.3(201.8)	−949.7(253.0)*
Ankle joint stiffness (Nm/°)	7.36(1.98)	5.42(1.52)**
Ankle joint ROM braking phase (°)	38.6(8.3)	46.4(8.9)*
Ankle joint ROM propulsion phase (°)	55.8(8.3)	57.1(7.9)
Knee joint ROM braking phase (°)	62.7(13.3)	64.0(12.4)
Knee joint ROM propulsion phase (°)	88.1(6.1)	84.6(9.2)
MG MTU length change braking phase (mm)	52.6(8.9)	58.9(9.2)*
MG MTU length change propulsion phase (mm)	−74.1(11.3)	−73.6(10.7)
Lactate (mmol/L)	1.8(0.3)	11.3(2.7)***

*(p < 0.05); **(p ≤ 0.01); ***(p < 0.001) from pre-exercise measures. MG, Medial gastrocnemius; MTU, Muscle-tendon unit; ROM, Range of motion.
Joint angle changes are in absolute values. For MTU length changes, positive and negative values refer to lengthening and shortening, respectively.
Means with standard deviations in parentheses.

TABLE 2 | Muscle architecture measures at rest and during maximal voluntary contraction (MVC) before and after exhaustive exercise.

	Rest		MVC	
	Pre	Post	Pre	Post
Fascicle length (mm)	51.7 ± 7.0	54.3 ± 7.5*	26.2 ± 2.1	28.0 ± 4.1*
Pennation angle (°)	14.3 ± 2.2	13.4 ± 2.8*	31.9 ± 2.7	28.8 ± 4.8*
Muscle thickness (mm)	14.7 ± 1.4	14.4 ± 1.3	14.9 ± 1.0	14.7 ± 1.2

*(p < 0.05) from pre-exercise measures.
Means with standard deviations in parentheses.

Muscle Architecture Changes During Maximal Voluntary Contraction

Whereas passive stiffness may have increased, active stiffness likely decreased, as evidenced by reduced joint stiffness (Kuitunen et al., 2002; Kubo and Ikebukuro, 2019), greater peak force reduction (Avela et al., 1999b), and MVC output (Morel et al., 2019), all of which were found in the current study. Myoelectric activity, which is a major factor in active stiffness (Aura and Komi, 1986), has previously been shown to be decreased during MVC and maximal DJs after exhaustive SSC exercise (Avela et al., 1999b; Kuitunen et al., 2002; Ishikawa et al., 2006; Dousset et al., 2007). Reduced activation leads to fascicles being longer during contraction by way of less fascicle shortening (Avela et al., 2004; Bennett et al., 2014), which was not directly measured in the current study (explained in the section "Limitations"). Further, as fascicles shorten during contraction, the insertion points on the superficial and deep aponeuroses are pulled closer together, increasing pennation angle (Narici et al., 1996). Decreased activation would result in fascicle insertions being pulled together less, in turn causing less pennation change and thus a smaller overall pennation angle (Narici et al., 1996; Manal et al., 2008), which we did observe.

Although this could explain the reduction in fascicle shortening reported by Thomas et al. (2015), we, however, do not agree with those authors' suggestion that longer fascicles would be a countermeasure from the central nervous system in an attempt to maintain optimal force in a fatigued state (Thomas et al., 2015). Increased FL of MG after fatigue has previously been reported to have an inverse relationship with torque, whereby subjects with greater FL had lower plantarflexion torque during MVC (Mitsukawa et al., 2009). This negative correlation may be because the longer fascicles are on the descending limb of the force-length relationship; however, this would clearly be detrimental for force production and not a strategy used by the central nervous system to preserve force in a fatigued state. Rather, Mitsukawa et al. (2009) also reported a decrease in electromyography amplitude concomitantly with increased MG FL as fatigue progressed. This supports a reduced muscle activation with fatigue resulting in less fascicle shortening during MVC.

As the Ia afferent system contributes to the active stiffness component and the impairment of the short-latency reflex (SLR) after exhaustive SSC is well established (Nicol et al., 2006), we cannot exclude the potential role that the intrafusal muscle fibers (i.e., Ia afferents), which are known to be activated and contribute to voluntary isometric contractions (Vallbo et al., 1979; Macefield et al., 1993), may have on this reduced fascicle shortening. As fatigue progresses, the discharge of muscle spindles decreases, reducing the output of alpha motoneurones during isometric contractions (Bongiovanni and Hagbarth, 1990; Macefield et al., 1991). A reduction in spindle support to alpha motoneurones would reduce activation level and force production and thus fascicles would shorten less during MVC. Although Day et al. (2017) found tibialis anterior FL and muscle spindle firing rate to follow the same pattern during passive, slow ankle rotations, and spindle length is largest when muscle length is also greatest (Figure 3 in Hoffer et al., 1989), spindle feedback rather than spindle lengthening appears to be affected by fatigue (Bongiovanni and Hagbarth, 1990; Macefield et al., 1991; Avela et al., 1999b). In that case, muscle spindles may be increased in length yet less responsive, dissociating the link between muscle FL and spindle discharge. Future studies should confirm this and additionally investigate the relationship between the amount of depressed SLR sensitivity and FL changes, as measuring FL could be a simpler way of determining reflex impairment in a fatigued state.

Contrary to our findings, Mademli and Arampatzis (2005) reported decreased FL of MG after a submaximal MVC fatiguing task. However, the exercise task was a sustained isometric contraction at 40% of MVC (Mademli and Arampatzis, 2005), an intensity likely too low to induce muscle damage. Further, Mademli and Arampatzis (2005) also reported increased MG myoelectric activity as fatigue progressed, even after tendon creep occurred, suggesting that there was at least some increase in muscle activation at the end of the exercise that could contribute to greater fascicle shortening. Thus, changes in muscle architecture are likely different depending on if the fatiguing task was of maximal or submaximal intensity.

Implications for Performance

Ankle joint angle during the eccentric, braking phase is the denominator in the equation for ankle joint stiffness (Kuitunen et al., 2002; Kubo and Ikebukuro, 2019). Therefore, a greater change in ankle joint range of motion, as found in the current study, is also shown by a decrease in ankle joint stiffness, which needs to be high for efficient SSC performance (Hoffrén et al., 2007; Yoon et al., 2007). Indeed, the reduction in ankle joint stiffness during DJs after fatiguing hops was recently shown to be strongly related to the increase in ankle joint angle ($r = -0.892$), but not peak ankle moment ($r = 0.318$), which was unchanged (Kubo and Ikebukuro, 2019). In the current study, rebound jump height and ankle joint stiffness were reduced after exercise, suggesting that there is an optimal range of ankle joint motion during the eccentric, braking phase of SSC tasks that allows for maximizing SSC performance. Furthermore, the presence of high amounts of lactate post-exercise clearly suggests metabolic fatigue occurred. Because chemical factors are not always the main cause of the impaired SLR (Avela et al., 1999a), we did not specifically measure peripheral fatigue; however, metabolic fatigue stimulates the group III and IV afferents (Garland and Kaufman, 1995; Taylor and Gandevia, 2008). These small-diameter afferents can increase presynaptic inhibition of the Ia fibers (Bigland-Ritchie et al., 1986; Nicol et al., 2006), decreasing the contribution of the SLR to active stiffness during DJs and further hampering intrafusal fiber contribution to MVC. Therefore, maintaining active stiffness components appears to be essential for both SSC and MVC performance.

LIMITATIONS

Not using electromyography to directly measure myoelectric activity and the SLR was a limitation in the present study; however, the decrements in performance parameters are comparable with those of previous reports using near-identical fatiguing protocols and impaired muscle activation and SLR function as a result of exhaustive jumps is clearly established (Nicol et al., 2006). Furthermore, although tendon slack length has been suggested to affect muscle architecture measurements (Aeles et al., 2017), the pre-post within-subjects study design likely negated these effects as Achilles tendon mechanical properties generally do not change after SSC exercise (Peltonen et al., 2010, 2012; Lichtwark et al., 2013; Kubo and Ikebukuro, 2019). Although a recent study demonstrated decreased Achilles tendon stiffness after a prolonged run at submaximal speed (Fletcher and MacIntosh, 2018), this would reduce the tension on the muscle fascicles, potentially shortening rather than lengthening them. Therefore, although tendon properties were unmeasured, they would be unlikely to explain the changes in muscle architecture in the current study. Additionally, FL at rest (prone) and during MVC (on the sledge) was measured in two different positions, which was necessary as the study set-up did not allow for the use of an isokinetic dynamometer. As subjects were "resting" on the sledge against body weight, we chose not to measure FL immediately prior to MVC. As such, comparing the changes from rest to MVC in two different positions could have led to errors when determining the amount of fascicle shortening and muscle bulging and thus were not reported.

CONCLUSION

In summary, this study investigated the effects of exhaustive SSC exercise on MG muscle architecture, demonstrating increased FL, decreased PA, and no changes in MT both at rest and during MVC. The changes at rest are likely due to exercise-induced muscle damage and the changes during MVC are seemingly a result of reduced activation. Additionally, there appears to be an optimal range of ankle joint range of motion that allows for maximizing DJ rebound height. These results have important implications for better describing how human muscle adapts to fatigue and how SSC performance is optimized.

DATA AVAILABILITY STATEMENT

The raw data supporting the conclusions of this article will be made available by the authors upon reasonable request.

ETHICS STATEMENT

This study involving human participants was reviewed and approved by the University of Jyväskylä Ethical Committee. The subjects provided their written informed consent to participate in this study.

AUTHOR CONTRIBUTIONS

AK and JA conceived and designed the research. AK conducted experiments, analyzed and interpreted data, and wrote the initial manuscript draft. DK and JA assisted in data interpretation and manuscript revisal. All authors read and approved the final manuscript.

REFERENCES

Aeles, J., Lenchant, S., Vanlommel, L., and Vanwanseele, B. (2017). Bilateral differences in muscle fascicle architecture are not related to the preferred leg in jumping athletes. *Eur. J. Appl. Physiol.* 117, 1453–1461. doi: 10.1007/s00421-017-3638-5

Aura, O., and Komi, P. V. (1986). Effects of prestretch intensity on mechanical efficiency of positive work and on elastic behavior of skeletal muscle in stretch-shortening cycle exercise. *Int. J. Sports Med.* 7, 137–143. doi: 10.1055/s-2008-1025751

Avela, J., Finni, J., and Komi, P. V. (2006). Excitability of the soleus reflex arc during intensive stretch-shortening cycle exercise in two power-trained athlete groups. *Eur. J. Appl. Physiol.* 97, 486–493. doi: 10.1007/s00421-006-0209-6

Avela, J., Finni, T., Liikavainio, T., Niemelä, E., and Komi, P. V. (2004). Neural and mechanical responses of the triceps surae muscle group after 1 h of

repeated fast passive stretches. *J. Appl. Physiol.* 96, 2325–2332. doi: 10.1152/japplphysiol.01010.2003

Avela, J., Kyröläinen, H., and Komi, P. V. (1999a). Altered reflex sensitivity after repeated and prolonged passive muscle stretching. *J. Appl. Physiol.* 86, 1283–1291. doi: 10.1152/jappl.1999.86.4.1283

Avela, J., Kyröläinen, H., Komi, P. V., and Rama, D. (1999b). Reduced reflex sensitivity persists several days after long-lasting stretch-shortening cycle exercise. *J. Appl. Physiol.* 86, 1292–1300. doi: 10.1152/jappl.1999.86.4.1292

Bennett, H. J., Rider, P. M., Domire, Z. J., DeVita, P., and Kulas, A. S. (2014). Heterogeneous fascicle behavior within the biceps femoris long head at different muscle activation levels. *J. Biomech.* 47, 3050–3055. doi: 10.1016/j.jbiomech.2014.06.032

Bigland-Ritchie, B. R., Dawson, N. J., Johansson, R. S., and Lippold, O. C. (1986). Reflex origin for the slowing of motoneurone firing rates in fatigue of human voluntary contractions. *J. Physiol.* 379, 451–459. doi: 10.1113/jphysiol.1986.sp016263

Bongiovanni, L. G., and Hagbarth, K. E. (1990). Tonic vibration reflexes elicited during fatigue from maximal voluntary contractions in man. *J. Physiol.* 423, 1–14. doi: 10.1113/jphysiol.1990.sp018007

Cè, E., Longo, S., Rampichini, S., Devoto, M., Limonta, E., Venturelli, M., et al. (2015). Stretch-induced changes in tension generation process and stiffness are not accompanied by alterations in muscle architecture of the middle and distal portions of the two gastrocnemii. *J. Electromyogr. Kinesiol.* 25, 469–478. doi: 10.1016/j.jelekin.2015.03.001

Cronin, N. J., Carty, C. P., Barrett, R. S., and Lichtwark, G. (2011). Automatic tracking of medial gastrocnemius fascicle length during human locomotion. *J. Appl. Physiol.* 111, 1491–1496. doi: 10.1152/japplphysiol.00530.2011

Day, J., Bent, L. R., Birznieks, I., Macefield, V. G., and Cresswell, A. G. (2017). Muscle spindles in human tibialis anterior encode muscle fascicle length changes. *J. Neurophysiol.* 117, 1489–1498. doi: 10.1152/jn.00374.2016

Dousset, E., Avela, J., Ishikawa, M., Kallio, J., Kuitunen, S., Kyröläinen, H., et al. (2007). Bimodal recovery pattern in human skeletal muscle induced by exhaustive stretch-shortening cycle exercise. *Med. Sci. Sports Exerc.* 39, 453–460. doi: 10.1249/mss.0b013e31802dd74e

Fletcher, J. R., and MacIntosh, B. R. (2018). Changes in Achilles tendon stiffness and energy cost following a prolonged run in trained distance runners. *PLoS One* 13:e0202026. doi: 10.1371/journal.pone.0202026

Franchi, M. V., Raiteri, B. J., Longo, S., Sinha, S., Narici, M. V., and Csapo, R. (2018). Muscle architecture assessment: strengths, shortcomings and new frontiers of in vivo imaging techniques. *Ultrasound Med. Biol.* 44, 2492–2504. doi: 10.1016/j.ultrasmedbio.2018.07.010

Fukunaga, T., Kawakami, Y., Kuno, S., Funato, K., and Fukashiro, S. (1997). Muscle architecture and function in humans. *J. Biomech.* 30, 457–463. doi: 10.1016/S0021-9290(96)00171-6

Garland, S. J., and Kaufman, M. P. (1995). Role of muscle afferents in the inhibition of motoneurons during fatigue. *Adv. Exp. Med. Biol.* 384, 271–278. doi: 10.1007/978-1-4899-1016-5_21

Guilhem, G., Doguet, V., Hauraix, H., Lacourpaille, L., Jubeau, M., Nordez, A., et al. (2016). Muscle force loss and soreness subsequent to maximal eccentric contractions depend on the amount of fascicle strain in vivo. *Acta Physiol.* 217, 152–163. doi: 10.1111/apha.12654

Hawkins, D., and Hull, M. L. (1990). A method for determining lower extremity muscle-tendon lengths during flexion/extension movements. *J. Biomech.* 23, 487–494. doi: 10.1016/0021-9290(90)90304-L

Hoffer, J. A., Caputi, A. A., Pose, I. E., and Griffiths, R. I. (1989). Roles of muscle activity and load on the relationship between muscle spindle length and whole muscle length in the freely walking cat. *Prog. Brain Res.* 80, 75–85. doi: 10.1016/S0079-6123(08)62201-3

Hoffrén, M., Ishikawa, M., and Komi, P. V. (2007). Age-related neuromuscular function during drop jumps. *J. Appl. Physiol.* 103, 1276–1283. doi: 10.1152/japplphysiol.00430.2007

Ishikawa, M., Dousset, E., Avela, J., Kyröläinen, H., Kallio, J., Linnamo, V., et al. (2006). Changes in the soleus muscle architecture after exhausting stretch-shortening cycle exercise in humans. *Eur. J. Appl. Physiol.* 97, 298–306. doi: 10.1007/s00421-006-0180-2

Ishikawa, M., Niemelä, E., and Komi, P. V. (2005). Interaction between fascicle and tendinous tissues in short-contact stretch-shortening cycle exercise with varying eccentric intensities. *J. Appl. Physiol.* 99, 217–223. doi: 10.1152/japplphysiol.01352.2004

Kawakami, Y., Muraoka, T., Ito, S., Kanehisa, H., and Fukunaga, T. (2002). In vivo muscle fibre behaviour during counter-movement exercise in humans reveals a significant role for tendon elasticity. *J. Physiol.* 540, 635–646. doi: 10.1113/jphysiol.2001.013459

Komi, P. V. (2000). Stretch-shortening cycle: a powerful model to study normal and fatigued muscle. *J. Biomech.* 33, 1197–1206. doi: 10.1016/S0021-9290(00)00064-6

Kubo, K., and Ikebukuro, T. (2019). Changes in joint, muscle, and tendon stiffness following repeated hopping exercise. *Physiol. Rep.* 7:e14237. doi: 10.14814/phy2.14237

Kuitunen, S., Avela, J., Kyröläinen, H., Nicol, C., and Komi, P. V. (2002). Acute and prolonged reduction in joint stiffness in humans after exhausting stretch-shortening cycle exercise. *Eur. J. Appl. Physiol.* 88, 107–116. doi: 10.1007/s00421-002-0669-2

Kwah, L. K., Pinto, R. Z., Diong, J., and Herbert, R. D. (2013). Reliability and validity of ultrasound measurements of muscle fascicle length and pennation in humans: a systematic review. *J. Appl. Physiol.* 114, 761–769. doi: 10.1152/japplphysiol.01430.2011

Lacourpaille, L., Nordez, A., Hug, F., Doguet, V., Andrade, R., and Guilhem, G. (2017). Early detection of exercise-induced muscle damage using elastography. *Eur. J. Appl. Physiol.* 117, 2047–2056. doi: 10.1007/s00421-017-3695-9

Lakens, D. (2013). Calculating and reporting effect sizes to facilitate cumulative science: a practical primer for t-tests and ANOVAs. *Front. Psychol.* 4:863. doi: 10.3389/fpsyg.2013.00863

Lichtwark, G. A., Cresswell, A. G., and Newsham-West, R. J. (2013). Effects of running on human Achilles tendon length-tension properties in the free and gastrocnemius components. *J. Exp. Biol.* 216, 4388–4394. doi: 10.1242/jeb.094219

Lidstone, D. E., van Werkhoven, H., Stewart, J. A., Gurchiek, R., Burris, M., Rice, P., et al. (2016). Medial gastrocnemius muscle-tendon interaction and architecture change during exhaustive hopping exercise. *J. Electromyogr. Kinesiol.* 30, 89–97. doi: 10.1016/j.jelekin.2016.06.006

Lieber, R. L., and Fridén, J. (1993). Muscle damage is not a function of muscle force but active muscle strain. *J. Appl. Physiol.* 74, 520–526. doi: 10.1152/jappl.1993.74.2.520

Lieber, R. L., and Fridén, J. (2000). Functional and clinical significance of skeletal muscle architecture. *Muscle Nerve* 23, 1647–1666. doi: 10.1002/1097-4598(200011)23:11<1647::AID-MUS1>3.0.CO;2-M

Macefield, V. G., Gandevia, S. C., Bigland-Ritchie, B., Gorman, R. B., and Burke, D. (1993). The firing rates of human motoneurones voluntarily activated in the absence of muscle afferent feedback. *J. Physiol.* 471, 429–443. doi: 10.1113/jphysiol.1993.sp019908

Macefield, G., Hagbarth, K. E., Gorman, R., Gandevia, S. C., and Burke, D. (1991). Decline in spindle support to alpha-motoneurones during sustained voluntary contractions. *J. Physiol.* 440, 497–512. doi: 10.1113/jphysiol.1991.sp018721

Mademli, L., and Arampatzis, A. (2005). Behaviour of the human gastrocnemius muscle architecture during submaximal isometric fatigue. *Eur. J. Appl. Physiol.* 94, 611–617. doi: 10.1007/s00421-005-1366-8

Manal, K., Roberts, D. P., and Buchanan, T. S. (2008). Can pennation angles be predicted from EMGs for the primary ankle plantar and dorsiflexors during isometric contractions? *J. Biomech.* 41, 2492–2497. doi: 10.1016/j.jbiomech.2008.05.005

Mitsukawa, N., Sugisaki, N., Kanehisa, H., Fukunaga, T., and Kawakami, Y. (2009). Fatigue-related changes in fascicle-tendon geometry over repeated contractions: difference between synergist muscles. *Muscle Nerve* 40, 395–401. doi: 10.1002/mus.21303

Miyama, M., and Nosaka, K. (2004). Influence of surface on muscle damage and soreness induced by consecutive drop jumps. *J. Strength Cond. Res.* 18, 206–211. doi: 10.1519/R-13353.1

Morel, B., Hug, F., Nordez, A., Pournot, H., Besson, T., Mathevon, L., et al. (2019). Reduced active muscle stiffness after intermittent submaximal isometric contractions. *Med. Sci. Sports Exerc.* 51, 2603–2609. doi: 10.1249/MSS.0000000000002080

Narici, M. V., Binzoni, T., Hiltbrand, E., Fasel, J., Terrier, F., and Cerretelli, P. (1996). In vivo human gastrocnemius architecture with changing joint angle at rest and during graded isometric contraction. *J. Physiol.* 496, 287–297. doi: 10.1113/jphysiol.1996.sp021685

Nicol, C., Avela, J., and Komi, P. V. (2006). The stretch-shortening cycle: a model to study naturally occurring neuromuscular fatigue. *Sports Med.* 36, 977–999. doi: 10.2165/00007256-200636110-00004

Peltonen, J., Cronin, N. J., Avela, J., and Finni, T. (2010). In vivo mechanical response of human Achilles tendon to a single bout of hopping exercise. *J. Exp. Biol.* 213, 1259–1265. doi: 10.1242/jeb.033514

Peltonen, J., Cronin, N. J., Stenroth, L., Finni, T., and Avela, J. (2012). Achilles tendon stiffness is unchanged one hour after a marathon. *J. Exp. Biol.* 215, 3665–3671. doi: 10.1242/jeb.068874

Peñailillo, L., Blazevich, A. J., and Nosaka, K. (2015). Muscle fascicle behavior during eccentric cycling and its relation to muscle soreness. *Med. Sci. Sports Exerc.* 47, 708–717. doi: 10.1249/MSS.0000000000000473

Regueme, S. C., Nicol, C., Barthèlemy, J., and Grélot, L. (2005). Acute and delayed neuromuscular adjustments of the triceps surae muscle group to exhaustive stretch-shortening cycle fatigue. *Eur. J. Appl. Physiol.* 93, 398–410. doi: 10.1007/s00421-004-1221-3

Sousa, F., Ishikawa, M., Vilas-Boas, J. P., and Komi, P. V. (2007). Intensity- and muscle-specific fascicle behavior during human drop jumps. *J. Appl. Physiol.* 102, 382–389. doi: 10.1152/japplphysiol.00274.2006

Taylor, J. L., and Gandevia, S. C. (2008). A comparison of central aspects of fatigue in submaximal and maximal voluntary contractions. *J. Appl. Physiol.* 104, 542–550. doi: 10.1152/japplphysiol.01053.2007

Thomas, N. M., Dewhurst, S., and Bampouras, T. M. (2015). Homogeneity of fascicle architecture following repeated contractions in the human gastrocnemius medialis. *J. Electromyogr. Kinesiol.* 25, 870–875. doi: 10.1016/j.jelekin.2015.08.007

Vallbo, Å. B., Hagbarth, K. E., Torebjörk, H. E., and Wallin, B. G. (1979). Somatosensory, proprioceptive, and sympathetic activity in human peripheral nerves. *Physiol. Rev.* 59, 919–957. doi: 10.1152/physrev.1979.59.4.919

Yoon, S. J., Tauchi, K., and Takamatsu, K. (2007). Effect of ankle joint stiffness during eccentric phase in rebound jumps on ankle joint torque at midpoint. *Int. J. Sports Med.* 28, 66–71. doi: 10.1055/s-2006-923903

Conflict of Interest: The authors declare that the research was conducted in the absence of any commercial or financial relationships that could be construed as a potential conflict of interest.

frontiers in Physiology

ORIGINAL RESEARCH
published: 17 March 2020
doi: 10.3389/fphys.2020.00231

Countermovement Jump Training Is More Effective Than Drop Jump Training in Enhancing Jump Height in Non-professional Female Volleyball Players

Jan Ruffieux[1], Michael Wälchli[1], Kyung-Min Kim[2] and Wolfgang Taube[1]*

[1] Department of Neurosciences and Movement Sciences, Université de Fribourg, Fribourg, Switzerland, [2] Department of Kinesiology and Sport Sciences, University of Miami, Coral Gables, FL, United States

The aim of the present study was to compare the effects of countermovement jump (CMJ) and drop jump (DJ) training on the volleyball-specific jumping ability of non-professional female volleyball players. For that purpose, 26 female volleyball players (15–32 years) were assigned to either a CMJ (20.4 ± 3.1 years, 171.0 ± 3.0 cm) or a DJ training group (22.0 ± 4.4 years, 168.2 ± 5.0 cm), which performed a six-week jump training (two sessions per week, 60 jumps per session). Each group performed 20% of the jumps in the jump type of the other group in order to minimize the influence of enhanced motor coordination on the differences between groups regarding the improvements of jump performance. Before and after the training, jump height was assessed in four jump types, including the trained and volleyball-specific jump types. Although both training forms substantially improved jump height, the CMJ training was significantly more effective in all jump types (17 vs. 7% on average; $p < 0.001$). This suggests that, at least for non-professional female volleyball players and a training duration of six weeks, training with a high percentage of CMJs is more effective than one with a high percentage of DJs. We hypothesize that this might be related to the slower stretch-shortening cycle during CMJs, which seems to be more specific for these players and tasks. These findings should support volleyball coaches in designing optimal jump trainings.

Keywords: stretch-shortening cycle, CMJ, DJ, jump performance, volleyball

OPEN ACCESS

Edited by:
Tobias Siebert,
University of Stuttgart, Germany

Reviewed by:
Lars Donath,
German Sport University Cologne, Germany
Falk Mersmann,
Humboldt University of Berlin, Germany

****Correspondence:***
Jan Ruffieux
jan.ruffieux@unifr.ch

Specialty section:
This article was submitted to Exercise Physiology, a section of the journal Frontiers in Physiology

Received: *03 December 2019*
Accepted: *28 February 2020*
Published: *17 March 2020*

Citation:
Ruffieux J, Wälchli M, Kim K-M and Taube W (2020) Countermovement Jump Training Is More Effective Than Drop Jump Training in Enhancing Jump Height in Non-professional Female Volleyball Players. Front. Physiol. 11:231. doi: 10.3389/fphys.2020.00231

INTRODUCTION

In volleyball, a player's maximal height above the net is a key determinant for successful attacking and blocking, and thus, for performance. The critical factors for this maximal height are anthropometric characteristics (body height and arm length) and vertical jumping ability. While the former cannot be modified, an athlete's jumping ability can be significantly improved through training. Volleyball coaches, therefore, seek for the most effective and most efficient exercises to improve their players' jumping ability.

The most common jump types in volleyball, i.e., for attacking and for blocking, can be classified as countermovement jumps (CMJs). More precisely, the block jump often resembles a "shortened version" of a CMJ due to time constraints, which prevent the players from performing a classic CMJ (Sattler et al., 2012). The attack jump on the other hand, which is performed with a run-up, can be regarded as a combination of a drop jump (DJ) and a CMJ (Sattler et al., 2012). CMJs and DJs are stretch-shortening cycle (SSC) movements, which involve a high-intensity eccentric contraction immediately before a rapid concentric contraction (Komi and Bosco, 1978; Van Hooren and Zolotarjova, 2017). Thus, in order to maximize performance in these jumps, it is important to quickly switch from yielding work to overcoming work and to rapidly develop maximal forces during the concentric phase (Bosco et al., 1981; Bobbert, 1990). Therefore, exercises aimed at improving jump performance in volleyball must target these reactive and explosive abilities of the neuromuscular system.

The most obvious training method to improve jump height is to perform jumps. This method is also referred to as plyometric training or plyometrics. Compared to other training methods often applied for improving jump performance, such as resistance training or weight lifting, jumps can be practiced everywhere and without any equipment. Furthermore, jumps represent the most specific training method. Not surprisingly, CMJ training has been shown to improve jump performance (Holcomb et al., 1996; Gehri et al., 1998). Another exercise for improving jumping ability, which has often been advised and which is often used by coaches, are DJs. DJs involve jumping or dropping from a raised platform and performing a vertical jump immediately after landing. The development of this method is ascribed to the Russian athletics coach Yuri Verhoshanski (Bobbert, 1990). For his "depth jumps," Verhoshanski used drop heights of 0.75 and 1.1 m (Verhoshanski, 1967). For him, this so-called "shock" method should be incorporated only "in the later stages of a program over many years of specialized strength preparation" (Bobbert, 1990, p. 10). Because of the success of Verhoshanski's athletes, coaches and scientists around the world adopted the idea of depth or drop jumping as an effective training method and started to develop it. Today, DJs – mainly with lower drop heights of around 20–50 cm – are integrated in strength and conditioning programs by coaches on all levels.

It has been suggested that in order to enhance jump performance, the capacity of individual muscles to release energy (i.e., power output) must be increased (Bobbert, 1990). According to Bobbert (1990), this can be achieved with exercises that come as close as possible to the target exercise (in our case volleyball jumps) with regard to the characteristics of the movement (specificity) but during which the muscles produce a greater mechanical output (larger forces and power output) than during the target exercises (so-called training overload; Bobbert, 1990). The mechanical output of a muscle during a concentric contraction can be enhanced by prestretch (potentiation; Bosco et al., 1981; Bobbert, 1990). This potentiation effect depends on the speed of prestretch and the delay between the prestretch and the concentric phase (Bosco et al., 1981). The increased negative speed during a DJ compared to a CMJ increases the speed of prestretch of the knee extensors and the plantar flexors and decreases the delay between the prestretch and the concentric phase (Bobbert et al., 1987), leading to a greater mechanical output during the push-off phase, which is believed to stimulate a more effective utilization of the SSC (Bobbert, 1990; Moran and Wallace, 2007). Thus, DJs seem to meet these requirements of being specific and inducing training overload. In line with this, numerous studies have shown that DJ training can significantly improve vertical jumping ability (for reviews, see Bobbert, 1990; Markovic, 2007).

Very few studies, however, have compared the effect of DJ to that of CMJ training on CMJ or volleyball-specific jump performance and they suggest that the two methods are equally effective (Clutch et al., 1983; Holcomb et al., 1996; Gehri et al., 1998). Improvements in jump height can be the consequence of both improvements in the capacity of muscles to release energy (peripheral mechanisms) and intra- and intermuscular coordination (central mechanisms; Bobbert, 1990). It could be argued that the similar effects of the two training methods on CMJ performance in previous studies (which compared pure CMJ training to pure DJ training) could be explained by a greater effect of the DJ training on the capacity of muscles to release energy (see above), which was compensated for by more specific neural adaptations in the CMJ groups. It has been shown that different forms of strength training lead to task-specific neural adaptations (Giboin et al., 2018). Therefore, the aim of the present study was to compare the effects of CMJ and DJ training on (volleyball-specific) jump performance while trying to minimize the influence of enhanced motor coordination on the differences between groups regarding the improvements of jump performance. To this end, we compared a CMJ with a DJ training group with each group completing 20% of the jumps in the other form (i.e., the CMJ training group performed 80% CMJs and 20% DJs while the DJ training group performed 80% DJs and 20% CMJs). We expected that the 80% DJs would allow the DJ group to benefit to a great extent from the greater mechanical output during this jump type, while the 20% CMJs would be sufficient to induce task-specific motor coordination improvements in the CMJ. Therefore, we hypothesized that the proposed DJ training would be more effective in improving overall vertical jumping ability.

MATERIALS AND METHODS

Participants

Thirty-three female volleyball players (15–32 years) of three different teams participated in the study. All teams play on a regional level and practice at least two times per week. All players were experienced with jump and plyometric training (4–15 years) but had no history of a long-term specialized jump and resistance training. The participants were assigned to either a CMJ or a DJ training group, which were matched for jump height at the pre-test, age, and team affiliation. Seven participants had to be excluded from the study due to injuries unrelated to the intervention ($n = 2$) or because they attended less than 80% of the training sessions ($n = 5$). Thus, 13 participants were included

in the analysis for the CMJ (20.4 ± 3.1 years, 171.0 ± 3.0 cm) and 13 participants for the DJ training group (22.0 ± 4.4 years, 168.2 ± 5.0 cm). Written informed consent was obtained from all participants, and from a parent for underage participants, prior to participation. The study was approved by the local ethics committee and was in accordance with the latest version of the Declaration of Helsinki.

Study Design

This training study consisted of a six-week jump training. In pre- and post-measurements, jump performance was assessed in four different jump types. During the training, the participants mainly performed either CMJs or DJs, according to their group. The jump types as well as the measurements and the training are described in detail below.

Measurements

Before and after training, jump performance was assessed in four different jump types: (a) CMJ with the hands akimbo, (b) CMJ with arm swing (which is similar to a block jump in volleyball), (c) CMJ with run-up and arm swing (identical to an attack jump in volleyball), and (d) DJ with arm swing with a drop height of 37 cm. Jump heights were calculated from flight times, which we measured with an OptoGait system (Microgate Srl, Bolzano, Italy). A very high degree of validity and reliability has been demonstrated for both the tested jump types and the measuring instrument used (Carroll et al., 2019; Glatthorn et al., 2011; Sattler et al., 2012). In addition, ground contact times were recorded for the DJs. Five jumps were recorded in each jump type, resulting in a total number of 20 jumps. The low number of jumps should prevent effects of fatigue. The order of the jump types was randomized between participants. For all jumps, the participants were instructed to jump as high as possible. No instructions were given regarding the range of motion or ground contact time. They received feedback about their jump height after each jump. Before each measurement session, the participants performed a standardized specific warm-up, which also included the four jump types assessed during the measurements.

Training

The training lasted six weeks, with two sessions per week. This corresponds to a typical volume of a pre-season athletic training during summer for players of this level. The jump training was performed at the beginning of the regular training sessions of the teams and was led by an experimenter. The actual jump training was always preceded by the same standardized warm-up that was conducted before the measurements. Each participant performed 60 jumps per session, which were grouped in blocks of three jumps with 3–5 s rest in between jumps and 30 s in between blocks. Five blocks constituted one series and one session comprised four series with 2 min rest between series. According to their group, the participants performed either CMJs (with arm swing but without run-up) or DJs (with arm swing, drop height of 37 cm).

However, each group performed one block per series (i.e., 20% of the jumps) in the jump type of the other group. With this we wanted to reduce the influence of task-specific improvements in motor coordination on the differences between groups regarding the improvements of jump performance. The participants were encouraged to perform each jump maximally. In order to maximize their motivation, the jump height was fed back to the participants in one of six jumps on average.

Statistical Analyses

For each participant, jump type, and time point, the best of the five trials was used for statistical analysis. We performed a linear mixed effects analysis of the effect of the two training modalities on jump height. As fixed effects, we entered group, time point, and jump type and all interaction terms into the model. As random effects, we had intercepts for subjects and by-subject random slopes for the effects of group and time point. A similar analysis was performed on the ground contact times during the DJs with group, time point, and the interaction term as fixed effects and intercepts for subjects as random effects. Visual inspection of residual plots did not reveal any obvious violations of the homoscedasticity or normality assumptions. The significance of the fixed effects was tested using Kenward–Roger's *F*-test with an alpha level of 0.05. The analyses were performed using R (R Core Team, 2018) and the *lmerTest* package (Kuznetsova et al., 2017).

RESULTS

Table 1 shows the group mean jump heights before and after training in the four jump types. The percent improvements of the two groups in the four jump types are illustrated in **Figure 1**. Averaged over the four jump types, the CMJ training group improved jump height by 16.7 ± 9.2%, the DJ training group by 7.3 ± 5.4%. The statistical analysis showed that this group difference was significant, as indicated by the significant interaction of group and time point, $F(1,24) = 22.05$, $p < 0.001$, $\eta_p^2 = 0.48$ (see **Figure 2**). The three-way interaction (i.e., group × time point × jump type) was not significant

TABLE 1 | Jump heights (in cm) before (Pre) and after (Post) training in the four jump types for the countermovement jump (CMJ) and the drop jump (DJ) training groups.

	CMJ training group	DJ training group
CMJ		
Pre	28.8 ± 4.5	29.2 ± 3.8
Post	32.7 ± 4.0	31.4 ± 3.5
CMJ w/arm swing		
Pre	32.7 ± 4.7	33.8 ± 3.4
Post	37.8 ± 4.1	35.9 ± 4.8
CMJ w/run-up		
Pre	38.7 ± 5.2	38.8 ± 5.2
Post	44.9 ± 4.5	40.9 ± 4.7
DJ w/arm swing		
Pre	33.4 ± 5.1	34.6 ± 4.3
Post	39.7 ± 4.7	37.8 ± 4.1

Values represent the mean ± standard deviation.

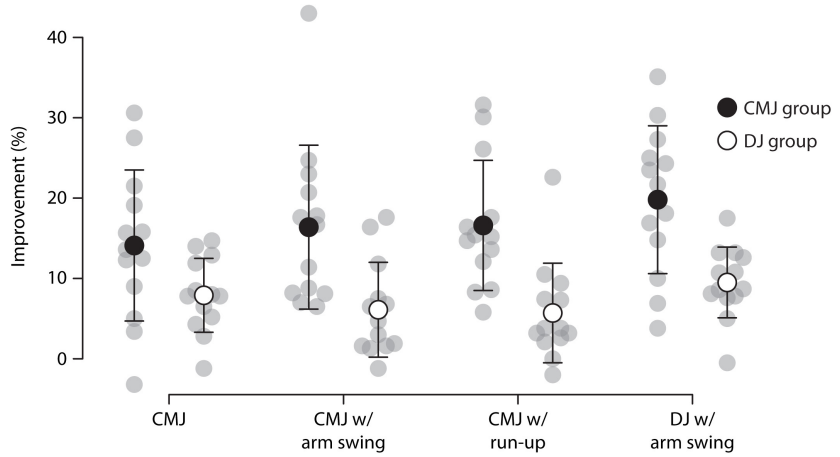

FIGURE 1 | Percent improvement for the countermovement jump (CMJ; filled circles) and the drop jump (DJ; open circles) training groups in the four jump types. Gray circles represent the individual participants. Error bars represent the standard deviation.

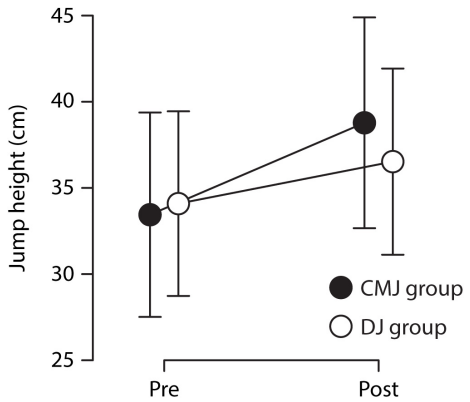

FIGURE 2 | Mean jump heights (over all jump types) for the countermovement jump (CMJ) and the drop jump (DJ) training groups before (Pre) and after (Post) training. Statistical analysis showed that the improvement was significantly greater in the CMJ training group ($p < 0.001$). Error bars represent the standard deviation.

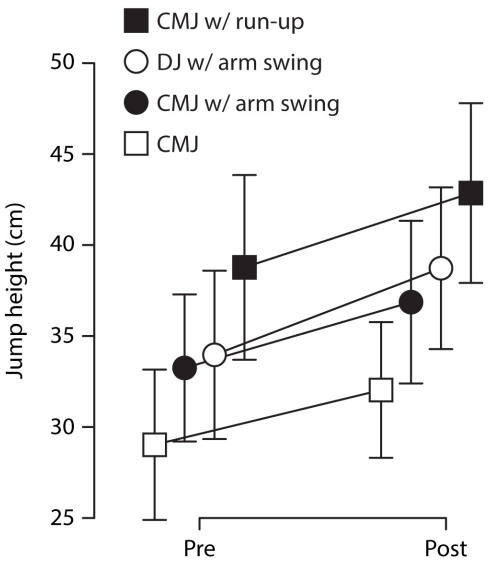

FIGURE 3 | Mean jump heights (over both groups) in the four jump types before (Pre) and after (Post) training. Statistical analysis showed that jump height ($p < 0.001$) and improvements ($p = 0.002$) differed between jump types, with the greatest jump heights in the countermovement jump (CMJ) with run-up and the greatest improvements in the drop jump (DJ). Circles represent the jump types that were practiced. Error bars represent the standard deviation.

($p = 0.064$), indicating that the CMJ training group improved more than the DJ training group in all jump types. The effect of time point, $F(1,24) = 152.35$, $p < 0.001$, $\eta_p^2 = 0.86$, indicates significant overall training improvements. The analysis further revealed an effect of jump type, $F(3,22) = 209.04$, $p < 0.001$, $\eta_p^2 = 0.97$, and an interaction of jump type and time point, $F(3,72) = 5.33$, $p = 0.002$, $\eta_p^2 = 0.18$, suggesting that absolute jump heights and improvements were different between jump types, with the greatest jump heights in the CMJ with run-up and the greatest improvements in the DJ (see **Figure 3**).

After removal of one outlier in the CMJ group, the ground contact times during the DJs were 339 ± 71 ms before and 380 ± 79 ms after the training in the CMJ group and 317 ± 73 ms and 318 ± 48 ms, respectively, in the DJ group. The statistical analysis showed no significant effect of group or time point (all $p > 0.082$).

DISCUSSION

The six-week jump training led to a substantial increase in jump height in both groups. However, against our hypothesis, training with 80% CMJs led to significantly greater improvements (16.7% on average) than training with 80% DJs (7.3% on average), in all jump types. The largest group differences were found for the CMJ with run-up and the CMJ with arm swing, which can be compared with an attack or block jump in volleyball,

respectively. In these jumps, the CMJ group was able to increase their maximum jump height by 6.1 and 5.1 cm, respectively, – a difference that can have a big impact on the performance in the game. In contrast, the DJ group increased jump height in these jumps by 2.1 cm. Thus, training has led to major, volleyball-specific improvements, especially in the CMJ group.

CMJ vs. DJ Training

The question then arises as to why CMJ training was so much more effective than DJ training in the present study. As mentioned in the introduction, jump performance can be improved by both peripheral and central adaptations. Although the present study design does not allow a distinction between the two, the fact that the CMJ group was able to make greater progress than the DJ group even in the DJs suggests, at first glance, that the group differences are not (only) due to greater central but (also) to greater peripheral adaptations. However, if we look at the ground contact times during the DJs, we see that they were rather long (>300 ms) in both groups and tended to become even longer through training in the CMJ group (although not statistically significant). The players obviously performed so-called "countermovement" DJs and not "bounce" DJs (Marshall and Moran, 2013). Thus, it is conceivable that the CMJ group was able to improve DJ performance more because they learned to extend ground contact time in order to develop greater impulse. A similar observation was made in a study comparing the effect of a DJ training with a fixed drop height of 30 cm to that of a training with varying (greater) drop heights (30, 50, and 75 cm; Taube et al., 2012). Training with the greater drop heights resulted in longer ground contact times combined with an increased DJ height, while training with a drop height of 30 cm reduced ground contact time without a significant change in jump height (Taube et al., 2012). From this point of view, the greater increase in performance of the CMJ group in the DJ could, nevertheless, be attributed, to some extent, to central adaptations. Considering the long ground contact times during the DJs, we are talking about rather slow SSCs here, which are even longer for the CMJ forms. From this perspective, the CMJ was closer to the target forms (both CMJ forms and DJ) for the population of this study and the CMJ training thus led to more specific central adaptations. This would be in line with the training specificity principle (Giboin et al., 2018).

A second possible explanation for the different progress of the two groups concerns muscular activation. Since the participants were more familiar with the CMJ, it is conceivable that they had deficits in motor coordination in the DJ compared to the CMJ at the beginning of the training. The fact that both groups improved most in the DJ also indicates this. This could have led to a greater activation deficit during the DJs than during the CMJs. Thus, a larger percentage of muscle volume would have been active and loaded in the CMJ group, at least during the first weeks of training. This reasoning would argue for larger peripheral adaptations in the CMJ group. In most previous studies that compared DJ to CMJ training, training interventions were usually longer (Bobbert, 1990; Markovic, 2007), which could have compensated for differences in the activation deficit at the beginning of training. This could explain the differences between our results and those of previous studies, which could not find any differences in the training effect between CMJ and DJ training. However, this is speculative and cannot be answered by the present study as no recordings of muscle activity were made.

Limitations

The above considerations lead us to a first limitation of this study, the target population. The participants of this study had some experience with jump training, but were non-professional players with no history of a long-term specialized jump and resistance training. It is conceivable that players with a higher technical and physical starting level could benefit more from DJ training than the sample of this study. Furthermore, we cannot say to what extent our findings can be transferred to male players.

A second point that needs to be discussed is the training protocol. Both groups performed 20% of the jumps in the other jump type. We chose this design in order to minimize the influence of enhanced motor coordination on the differences between groups regarding the improvements of jump performance. Although, from our point of view, this design is a strength of this study, the present data does not allow us to say whether a training regimen with CMJs only or with a higher percentage of DJs would be even more beneficial. Despite the relatively low percentage of 20% DJs in the CMJ group, we have to consider the possibility that these DJs were critical to training success, at least for performance in the DJ. Nevertheless, the findings suggest that a training regimen with a high percentage of CMJs is more effective than one with a high percentage of DJs. Already Verhoshanski did not suggest performing DJs exclusively but rather that drop jumping is just one of the exercises incorporated in a training program (Verhoshanski, 1967). Our results suggest that an optimal percentage of DJs could be rather low for volleyball players of this level. Furthermore, as mentioned above, the design does not allow a distinction to be made between peripheral and central adaptations.

A last point we would like to mention is the drop height. The drop height of 37 cm we used is within the range that is commonly used for DJ training. However, we cannot exclude the possibility that this drop height was not optimal for each participant and that a different height would have led to different adaptations. Following the discussion above, one can imagine that a greater drop height would have led to longer ground contact times and thus to greater improvements in the DJ group. Thus, further studies are needed in order to refine and extend our findings.

CONCLUSION

The aim of the present study was to compare the effects of CMJ and DJ training on the volleyball-specific jumping ability of non-professional female volleyball players. Although both training forms substantially improved jump height, the CMJ training was significantly more effective. This suggests that, at least for non-professional female volleyball players and a training duration of six weeks, training with a high percentage

of CMJs is more effective than one with a high percentage of DJs. We hypothesize that this might be related to the slower SSC during CMJs, which seems to be more specific for these players and tasks. These findings should support volleyball coaches in designing optimal jump trainings.

DATA AVAILABILITY STATEMENT

The raw data supporting the conclusions of this article will be made available by the authors, without undue reservation, to any qualified researcher.

ETHICS STATEMENT

The studies involving human participants were reviewed and approved by Commission d'éthique de recherche du Canton de Fribourg. Written informed consent to participate in this study was provided by the participants' legal guardian/next of kin.

AUTHOR CONTRIBUTIONS

All authors contributed to the conceptualization and the design of the study, critically revised the work for important intellectual content, and approved the final manuscript. JR performed the experiments, analyzed the data, and prepared the manuscript.

ACKNOWLEDGMENTS

The authors would like to thank Serge Andrey and Christian Cotting for their help in data collection and supervision of the training sessions.

REFERENCES

Bobbert, M. F. (1990). Drop jumping as a training method for jumping ability. *Sports Med.* 9, 7–22. doi: 10.2165/00007256-199009010-00002

Bobbert, M. F., Huijing, P. A., and van Ingen Schenau, G. J. (1987). Drop jumping. I. The influence of jumping technique on the biomechanics of jumping. *Med. Sci. Sports Exerc.* 19, 332–338.

Bosco, C., Komi, P. V., and Ito, A. (1981). Prestretch potentiation of human skeletal muscle during ballistic movement. *Acta Physiol. Scand.* 111, 135–140. doi: 10.1111/j.1748-1716.1981.tb06716.x

Carroll, K. M., Wagle, J. P., Sole, C. J., and Stone, M. H. (2019). Intrasession and intersession reliability of countermovement jump testing in division-I volleyball athletes. *J. Strength Cond. Res.* 33, 2932–2935. doi: 10.1519/JSC.0000000000003353

Clutch, D., Wilton, M., McGown, C., and Bryce, G. R. (1983). The effect of depth jumps and weight training on leg strength and vertical jump. *Res. Quar. Exerc. Sport* 54, 5–10. doi: 10.1080/02701367.1983.10605265

Gehri, D. J., Ricard, M. D., Kleiner, D. M., and Kirkendall, D. T. (1998). A comparison of plyometric training techniques for improving vertical jump ability and energy production. *J. Strength Cond. Res.* 12, 85–89. doi: 10.1519/00124278-199805000-00005

Giboin, L. S., Weiss, B., Thomas, F., and Gruber, M. (2018). Neuroplasticity following short-term strength training occurs at supraspinal level and is specific for the trained task. *Acta Physiol.* 222:e12998. doi: 10.1111/apha.12998

Glatthorn, J. F., Gouge, S., Nussbaumer, S., Stauffacher, S., Impellizzeri, F. M., and Maffiuletti, N. A. (2011). Validity and reliability of Optojump photoelectric cells for estimating vertical jump height. *J. Strength Cond. Res.* 25, 556–560. doi: 10.1519/JSC.0b013e3181ccb18d

Holcomb, W. R., Lander, J. E., Rutland, R. M., and Wilson, G. D. (1996). The effectiveness of a modified plyometric program on power and the vertical jump. *J. Strength Cond. Res.* 10, 89–92. doi: 10.1519/00124278-199605000-00005

Komi, P. V., and Bosco, C. (1978). Utilization of stored elastic energy in leg extensor muscles by men and women. *Med. Sci. Sports* 10, 261–265.

Kuznetsova, A., Brockhoff, P. B., and Christensen, R. H. B. (2017). lmerTest package: tests in linear mixed effects models. *J. Stat. Softw.* 82, 1–26.

Markovic, G. (2007). Does plyometric training improve vertical jump height? A meta-analytical review. *Br. J. Sports Med.* 41, 349–355. doi: 10.1136/bjsm.2007.035113

Marshall, B. M., and Moran, K. A. (2013). Which drop jump technique is most effective at enhancing countermovement jump ability, "countermovement" drop jump or "bounce" drop jump? *J. Sports Sci.* 31, 1368–1374. doi: 10.1080/02640414.2013.789921

Moran, K. A., and Wallace, E. S. (2007). Eccentric loading and range of knee joint motion effects on performance enhancement in vertical jumping. *Hum. Mov. Sci.* 26, 824–840. doi: 10.1016/j.humov.2007.05.001

R Core Team (2018). *R: A Language, and Environment for Statistical Computing*. Vienna: R Foundation for Statistical Computing.

Sattler, T., Sekulic, D., Hadzic, V., Uljevic, O., and Dervisevic, E. (2012). Vertical jumping tests in volleyball: reliability, validity, and playing-position specifics. *J. Strength Cond. Res.* 26, 1532–1538. doi: 10.1519/JSC.0b013e318234e838

Taube, W., Leukel, C., Lauber, B., and Gollhofer, A. (2012). The drop height determines neuromuscular adaptations and changes in jump performance in stretch-shortening cycle training. *Scand J. Med. Sci. Sports* 22, 671–683. doi: 10.1111/j.1600-0838.2011.01293.x

Van Hooren, B., and Zolotarjova, J. (2017). The difference between countermovement and squat jump performances: a review of underlying mechanisms with practical applications. *J. Strength Cond. Res.* 31, 2011–2020. doi: 10.1519/JSC.0000000000001913

Verhoshanski, Y. (1967). Are depth jumps useful? *Track Field* 12, 75–78.

Conflict of Interest: The authors declare that the research was conducted in the absence of any commercial or financial relationships that could be construed as a potential conflict of interest.

frontiers in Physiology

ORIGINAL RESEARCH
published: 17 June 2020
doi: 10.3389/fphys.2020.00521

10% Higher Rowing Power Outputs After Flexion-Extension-Cycle Compared to an Isolated Concentric Contraction in Sub-Elite Rowers

Steffen Held[1]*, *Tobias Siebert*[2] and *Lars Donath*[1]

[1] Department of Intervention Research in Exercise Training, German Sport University Cologne, Cologne, Germany,
[2] Department of Motion and Exercise Science, University of Stuttgart, Stuttgart, Germany

The resulting muscular performance is considered notably higher during a stretch shortening cycle (SSC) compared to an isolated concentric contraction. Thus, the present study examined the occurrence and magnitude of rowing performance enhancement after a flexion–extension cycle (FEC) of the legs compared to both concentric contractions only and isometric pre-contraction. Therefore, 31 sub-elite male rowers (age: 25 ± 6 years, height: 1.90 ± 0.02 m, weight: 91 ± 10 kg, weekly training volume: 11.4 ± 5.3 h/week, rowing experience: 7.1 ± 2.7 years) randomly completed (a) isolated concentric rowing strokes (DRIVE), (b) single FEC-type rowing strokes (SLIDE-DRIVE), and (c) rowing strokes with an isometric pre-contraction (ISO-DRIVE). The resulting rowing power (P_{row}), leg power (P_{leg}), and work per stroke (WPS) were recorded using motion-capturing, force, and rotation sensors. Comparison of DRIVE and SLIDE-DRIVE revealed significantly ($p < 0.05$) higher P_{row} (+11.8 ± 14.0%), P_{leg} (+19.6 ± 26.7%), and WPS (+9.9 ± 10.5%) during SLIDE-DRIVE. Compared to ISO-DRIVE, P_{leg} (+9.8 ± 26.6%) and WPS (+6.1 ± 6.7%) are again significantly ($p < 0.05$) higher for SLIDE-DRIVE. In conclusion, notably higher work and power outputs (compared to an isolated concentric contraction) during FEC rowing referred to an underlying SSC. Future ultrasound studies should elucidate whether a real SSC on the muscle tendon unit level account for these performance enhancements.

Keywords: SSC, ergometer, motion capture, concentric, eccentric, force enhancement, muscle, potentiation

OPEN ACCESS

Edited by:
François Billaut,
Laval University, Canada

Reviewed by:
Janne Avela,
University of Jyvaskyla, Finland
Stefanos Volianitis,
Aalborg University, Denmark

***Correspondence:**
Steffen Held
s.held@dshs-koeln.de

Specialty section:
This article was submitted to Exercise Physiology, a section of the journal Frontiers in Physiology

Received: *20 February 2020*
Accepted: *28 April 2020*
Published: *17 June 2020*

Citation:
Held S, Siebert T and Donath L (2020) 10% Higher Rowing Power Outputs After Flexion-Extension-Cycle Compared to an Isolated Concentric Contraction in Sub-Elite Rowers. Front. Physiol. 11:521. doi: 10.3389/fphys.2020.00521

INTRODUCTION

The sequence of stretching and subsequent contraction of a muscle tenon unit (MTU) is considered a stretching shortening cycle (SSC) (Komi, 2003). The resulting muscular force, work, and power during an SSC enable up to 50% higher power output values compared to isolated concentric contractions (Cavagna et al., 1968; Bosco et al., 1987; Gregor et al., 1988). Increased muscular efficiency and decreased metabolic costs have been discussed to account for these findings (Dawson and Taylor, 1973; Aura and Komi, 1986). The increased muscle performance during SSC is, however, still not completely understood (Seiberl et al., 2015). The power enhancement during an SSC can be mainly attributed to (a) the storage and release of elastic energy (Kubo et al., 1999;

Bojsen-Møller et al., 2005), (b) stretch-induced contractility enhancement (Rode et al., 2009; Seiberl et al., 2015), and (c) reflex activity and time-to-peak force (Schenau et al., 1997a,b).

In this regard, the rowing cycle can be classified into a propulsive phase (drive, see **Figure 1D**) and a gliding phase (slide, see **Figure 1B**). During one rowing cycle, the legs are firstly undergoing a flexion (slide) followed by an extension pattern (drive). This flexion–extension cycle (FEC) movement can be performed in rowing as fast as in countermovement jumps (Held et al., 2019, 2020). The leg extensor muscle activity (rectus femoris, vastus medialis, and vastus lateralis) during the late slide phase prior to the onset of a new rowing stroke was detected (Janshen et al., 2009; Guével et al., 2011; Turpin et al., 2011; Fleming et al., 2014; Shaharudin et al., 2014; Held et al., 2020). Accordingly, the combination of flexion (slide) and extension (drive) of legs (potentially corresponding to a stretching and contraction of leg extensor muscles) in rowing can be defined as a FEC.

As more than 90% of the annual rowing training is completed at low stroke rates (Steinacker, 1993; Guellich et al., 2009; Bourgois et al., 2014), aspects of reactive forces are rarely considered in rowing training (Held et al., 2019, 2020). These low stroke rates (about 18 spm) are characterized by approximately four times the duration of the slide phase during a 2,000-m rowing competition (about 36 spm or higher) (Kleshnev, 2016; Held et al., 2019) and showed no leg extensor muscle (vastus medialis) activity during the late slide phase prior to the onset of a new rowing stroke (Held et al., 2020). This imbalance between training and competition requirements seems unsuitable due to the force–velocity relation of the muscle (van Soest and Casius, 2000) and the SSC (Komi, 2003).

Against this background, the present study was conceptualized and conducted in order to elucidate whether rowing enables force, work, and power enhancement (as described above) during FEC-type rowing compared to isolated concentric muscle actions (drive phase only, **Figures 1C,D**) comparable to those expected in SSC. The underlying design was based on the assumption that training a sport-specific muscle action is required and has been repeatedly emphasized (Gollhofer et al., 1987; Komi, 2003; Nicol et al., 2006). Therefore, we aimed at investigating the occurrence and magnitude of force, work, and power outputs during FEC-type rowing compared to isolated concentric rowing and concentric rowing with isometric precontraction on the rowing ergometer. We assume that the general force, work, and power enhancement of FEC-type rowing are crucial and meaningful. Finally, the resulting data would have an impact on the conceptualization of rowing-specific testing and training by paying more attention to reactive force abilities.

MATERIALS AND METHODS

Participants

Thirty-one sub-elite male rowers (age: 25 ± 6 years, height: 1.90 ± 0.04 m, weight: 91 ± 10 kg, 2,000-m ergometer Time Trial mean power: 374 ± 74 W, weekly training volume: 11.4 ± 5.3 h/week, rowing experience: 7.1 ± 2.7 years) were enrolled in this randomized controlled crossover trial. The inclusion criteria were as follows: at least 5 years of rowing competition experience and at least rowers on the national level with no health complaints and impairments. After providing all relevant study information, informed consent was requested from all athletes prior to the start of the study. The study protocol complied with the Declaration of Helsinki and has been previously approved by the local ethical committee (001/2019), fulfilling the international ethical standards (Harriss and Atkinson, 2015).

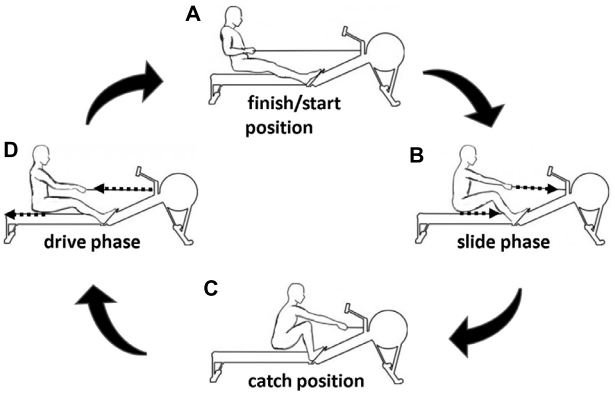

FIGURE 1 | Exemplary representation of a rowing cycle separated into different phases: slide **(B)** and drive **(D)** phase. The finish/start **(A)** and catch **(C)** position are the turning points of the extension and flexion phase, respectively.

Study Design

After a standardized 15-min warm-up program (10-min rowing at a low intensity/heart rate, which corresponds to a blood lactate concentration <2 mmol/L and about three practice trials), the participants performed five isolated concentric rowing strokes (DRIVE, see **Figures 1C** to **1A**), five single rowing strokes with isometric precontraction (ISO-DRIVE, see **Figures 1C** to **1A**), and five single FEC-type rowing strokes (SLIDE-DRIVE, see **Figure 1**) in a randomized order. Since the DRIVE measurement was started with non-activated muscle, the muscle was already pre-activated in the SLIDE-DRIVE-measurement at the beginning of the concentric phase (Janshen et al., 2009; Guével et al., 2011; Turpin et al., 2011; Fleming et al., 2014; Shaharudin et al., 2014; Held et al., 2020). Accordingly, measurements with an isometric precontraction (ISO-DRIVE) were additionally performed in order to observe the different starting conditions of the DRIVE and SLIDE-DRIVE trials. The DRIVE measurements started at the catch position (see **Figure 1C**) and consisted only of the drive phase (see **Figure 1D**) until the finish position (see **Figure 1A**). During the ISO-DRIVE measurements, an additional 3-s-lasting isometric precontraction was performed with maximal efforts. Thereby, the rowing handle was fixed at the catch position (see **Figure 1C**) using a hook, which was released upon the start signal. The SLIDE-DRIVE measurements comprise a full rowing cycle (slide and drive phase; see **Figure 1**), starting at

the finish position. The participants received the instructions to generate maximum power for each measurement trial. The mean values of the three rowing strokes with the highest power outputs (of the five attempts) for each rowing condition were included into further analyses. Between all rowing strokes, a break of 2 min was guaranteed. The flywheel of the rowing ergometer was still standing at the start of the drive phase during all rowing conditions (DRIVE, ISO-DRIVE, and SLIDE-DRIVE). A complete familiarization session (consisting of 10 DRIVE, ISO-DRIVE, and SLIDE-DRIVE rowing strokes) was completed 1 week before the measurement, and the athletes were asked to refrain from any strenuous activity 24 h prior to each assessment condition.

Data Collection

All tests were performed on a wind-braked rowing ergometer (Concept2/Type D, Morrisville, NC, United States). The ergometer was additionally equipped with the FES Ruderergo-System [Institut für Forschung und Entwicklung von Sportgeräten (FES), Berlin, Germany] using a load cell for handle force (F_{drive}) measurement (Type KM26z; ME-Meßsysteme GmbH, Hennigsdorf, Germany) placed between the chain and the handlebar. Therewith, precise measurements of mechanical power were enabled. Since the load cell was placed between the chain and the handlebar, the forces of each isometric precontraction cannot be detected. As there is no handlebar movement during this isometric precontraction, no mechanical power output was generated during this phase. Accordingly, the used setup is considered suitable for the investigation of power outputs during all dynamic rowing conditions (Treff et al., 2018). An incremental encoder (ERN 1020/250 01-03; Heidenhain, Traunreut, Germany) was placed on the rotation axis of the flywheel to measure the displacement of the handlebar. The error of measurement of the FES setup was equal to or smaller than 1.5% (Treff et al., 2018). In addition to the kinematic assessment, a motion capturing system was employed (Rienks et al., 2020): The entire measurement was video-captured using 120 fps. The employed camera (Type Hero 5, GoPro, San Mateo, CA, United States) was placed in the middle of the rowing ergometer (90°-angled distance 3 m, height 0.5 m). The seat and handle positions (marked with luminous markers) were captured using a motion-capture software (Tracker, open-source physics, Boston, MA, United States). For the calibration of the motion-capturing system, a coordinate system including proper scaling was defined: In this context, a known length (1-m scale, marked on the seat track of the rowing ergometer) was marked in the video with the help of the motion-capturing software. This calibration scale was located at the same level (distance to the camera) as the handle and seat movement. In addition, the reference coordinate was uniformly placed in the axis of the rotation of the flywheel. The accuracy of the method was five pixels, which corresponds to less than 0.01 m at the current setup (Suleder, 2010). This accuracy was confirmed by comparing the handle displacement data of the FES setup (error of measurement <2%) with the motion-capturing data. Based on this motion-capturing, the length of the seat motion (L_{slide}) was recorded. Then, the speed of the seat (corresponding to leg extension or shortening velocity, vleg) was subsequently determined as the derivation of (time-dependent) seat position. Mechanical work per stroke (WPS) and mechanical rowing power (P_{row}) were calculated based on the data of the FES Ruderergo System. In addition, the maximum force during the drive (F_{max}), the force at the catch position (F_0), the drive time (T_{drive}), the length of the drive (L_{drive}), and the handle speed during the drive (v_{drive}) were determined. Rowing power (P_{row}) was calculated by multiplying the handle force $F_{drive}(t)$ by velocity v_{drive} (t) (Fukunaga et al., 1986; Dal-Monte and Komo, 1989; Zatsiorsky and Yakunin, 1991). The proportion of leg power (P_{leg}) on the total P_{row} was further determined based on multiplying $F_{drive}(t)$ by leg (seat) movement speed $v_{leg}(t)$ (Kleshnev, 2016; Held et al., 2019). Based on the current measurements, DRIVE ($r = 0.998$, $p < 0.001$), ISO-DRIVE ($r = 0.970$, $p < 0.001$), and SLIDE ($r = 0.994$, $p < 0.001$) showed exclusively high split-half-reliability values.

Statistics

Statistical analyses were performed using a statistic software package (IBM SPSS Statistics, Version 25.0, Armonk, NY, United States). All data are presented as group mean with standard deviation. All data were checked for normal distribution and variance homogeneity using the Kolmogorov–Smirnov and Levene tests, respectively. Separate repeated measurement analysis of variance (rANOVA) was applied for the different rowing conditions (DRIVE, ISO-DRIVE, and SLIDE-DRIVE) using P_{row}, WPS, F_{max}, F_0, $F_{drive}(t)$, T_{drive}, L_{drive}, v_{drive}, L_{slide}, and P_{leg} as within-subject variables. In case of significant interaction effects, Bonferroni *post hoc* tests were subsequently computed for pairwise comparisons. To estimate the overall time and interaction effect sizes, η_p^2 were calculated with $\eta_p^2 \geq 0.01$ indicating small, $\geq$0.059 medium, and $\geq$0.138 large effects (Cohen, 1988). Standardized mean group differences as a measure of pairwise effect size estimation were also calculated (SMD, trivial: $d < 0.2$, small: $0.2 \leq d < 0.5$, moderate: $0.5 \leq d < 0.8$, large $d \geq 0.8$) (Cohen, 1988). Moreover, a p-value below 0.05 was considered statistically significant.

RESULTS

Handle Forces as a Function of Handle Length and Speed

Figure 2A shows the averaged force–distance graphs for the DRIVE, ISO-DRIVE, and SLIDE-DRIVE conditions. In the catch position (L_{drive} = 0%) the SLIDE-DRIVE and ISO-DRIVE forces (F_0) were obviously higher than the DRIVE force ($p < 0.001$, $\eta_p^2 > 0.138$) due to muscle preactivation. It is clearly visible that SLIDE-DRIVE forces $F_{drive}(t)$ are higher ($p < 0.001$, $\eta_p^2 = 0.398$) than DRIVE forces during almost the total rowing stroke (T_{drive}). The averaged force–speed graphs of the DRIVE, ISO-DRIVE, and SLIDE-DRIVE measurements for the entire sample are displayed in **Figure 2B**. From visual inspection, the loop area (P_{row}) increases from DRIVE to ISO-DRIVE to SLIDE-DRIVE, which is also confirmed by the following rANOVA results.

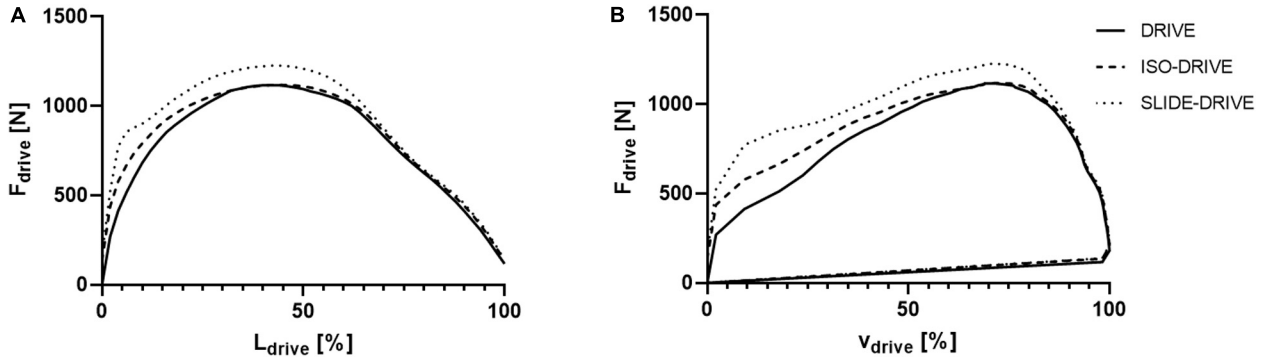

FIGURE 2 | Representation of the average handle force (F_{drive}) as a function of handle pathway length (length of drive: L_{drive}; **A**) and as a function of handle speed during drive (v_{drive}; **B**) for the concentric (DRIVE), isometric precontraction (ISO-DRIVE), and FEC type (SLIDE-DRIVE) rowing trials. The force length and force–speed graph are normalized to the length of the drive.

Power, Work, and Force

The rANOVA yielded significant interaction effects ($0.01 < p < 0.001$; $0.214 < \eta_p^2 < 0.331$) for the rowing conditions (DRIVE, ISO-DRIVE, SLIDE-DRIVE) regarding all parameters (P_{row}, P_{leg}, WPS, F_{max}, L_{drive}, L_{slide}, and v_{drive}), except for T_{drive} ($p = 0.351$; $\eta_p^2 = 0.072$). Subsequent pairwise *post hoc* testing showed a significant ($p < 0.05$) increase of P_{row} (see **Figure 3A**; +11.8 ± 14.0%, SMD = 0.290), P_{leg} (see **Figure 3B**; +19.6 ± 26.7%, SMD = 0.429), WPS (see **Figure 3C**; +9.9 ± 10.5%, SMD = 0.534), F_{max} (see **Figure 3D**; +4.4 ± 7.0%, SMD = 0.260), L_{drive} (+6.3 ± 4.8%, SMD = 0.552), and v_{drive} (+7.6 ± 6.0%, SMD = 0.889) between DRIVE and SLIDE-DRIVE measurements. Between ISO-DRIVE and SLIDE-DRIVE measurements, the *post hoc* tests show only significant ($p < 0.05$) increases in WPS (see **Figure 3C**; +6.1 ± 6.7%, SMD = 0.307), F_{max} (see **Figure 3D**; +5.0 ± 4.8%, SMD = 0.287), L_{drive} (+3.2 ± 5.2%, SMD = 0.210), and v_{drive} (+4.2 ± 4.0%, SMD = 0.587). In contrast, the *post hoc* tests show no significant ($p > 0.05$, SMD < 0.448) differences between DRIVE- and ISO-DRIVE measurements for all variables (P_{row}, P_{leg}, WPS, F_{max}, L_{drive}, L_{slide}, and v_{drive}). The descriptive data, the resulting effects of ANOVA, and the percentage increases for the DRIVE, ISO-DRIVE, and SLIDE-DRIVE measurements are presented in **Supplementary Table S1**.

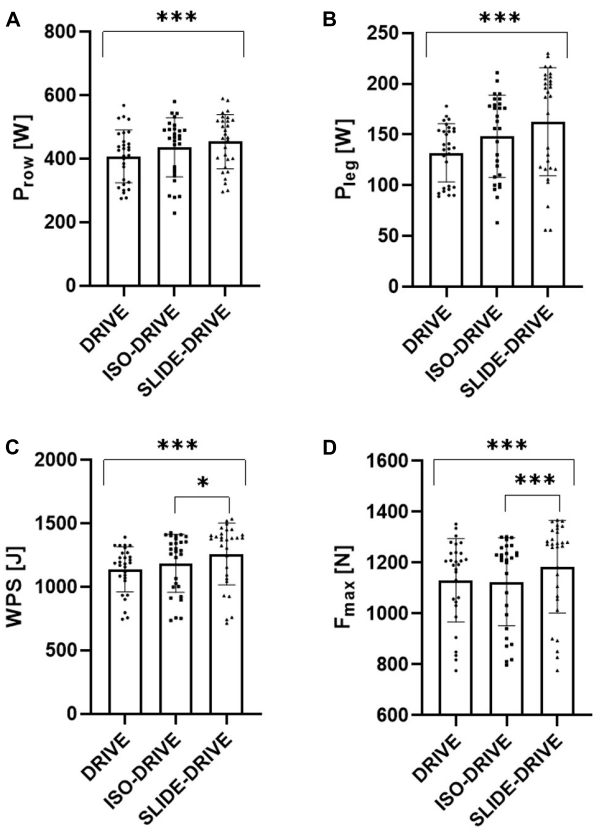

FIGURE 3 | Representation of rowing power (P_{row}, **A**), leg power (P_{leg}, **B**), work per stroke (WPS, **C**), and maximum force (F_{max}, **D**) results of the concentric (DRIVE), isometric precontraction (ISO-DRIVE), and FEC type (SLIDE-DRIVE) rowing trials (mean ± standard deviation). In addition, the significances of the post-hoc tests were presented (***$p < 0.001$; *$p < 0.05$).

DISCUSSION

The present randomized controlled crossover trial aimed at investigating whether maximum handle forces, WPS, P_{row}, and P_{leg} differ depending on the applied rowing movement pattern. We intended to elucidate whether a flexion–extension cycle (FEC) leads to notably higher power outputs compared to a pure concentric movement. Therefore, single (purely) concentric rowing strokes (DRIVE, see **Figures 1C** to **1A**), single FEC-type rowing strokes (SLIDE-DRIVE, see **Figure 1**), and rowing strokes with isometric precontraction (ISO-DRIVE, see **Figures 1C** to **1A**) have been examined. Compared to purely concentric rowing (DRIVE), remarkably higher WPS, P_{row}, and P_{leg} have been observed during ISO-DRIVE and SLIDE-DRIVE measurements (see **Figure 3**). Compared to ISO-DRIVE, these increases (from DRIVE to ISO-DRIVE) in P_{row}, P_{leg}, and WPS remain statistically insignificant (see **Figure 3**). A tendency

toward higher values during ISO-DRIVE can be, however, partly explained by the following assumptions: In general, muscle activity and performance are higher (in particular) at the beginning of a concentric movement when preceded by an isometric precontraction (compared to purely concentric contractions) (Svantesson et al., 1994). Despite the fact that we did not measure muscle activity, we assume higher muscle activations at the beginning of a rowing stroke during the ISO-DRIVE condition, compared to almost non-activated muscles in the DRIVE condition, which results in higher handle forces at the start of the rowing stroke. The SLIDE-DRIVE measurement revealed a significantly and notably higher maximum handle force (compared to DRIVE). Consequently, muscular P_{row}, P_{leg}, and WPS during FEC-type rowing (SLIDE-DRIVE) elicited between 10 and 20% higher values compared to isolated concentric (DRIVE) rowing strokes. These results are in line with earlier findings pointing to performance (force, work, and power) enhancements within an SSC in isolated muscle preparations with constant electrical stimulation (Cavagna et al., 1968), in animal experiments with natural and variable muscle activation (Gregor et al., 1988), and during maximal voluntary SSC actions of human muscles (Cavagna et al., 1968; Aura and Komi, 1986; Bosco et al., 1987). Overall, the present study revealed that rowing showed similar performance enhancements like other reactive (SSC) sports movements: A vertical jump preceded by a countermovement (SSC) will increase vertical displacement above a squat jump (concentric only) (Bosco et al., 1987; Bobbert et al., 1996; Bobbert and Casius, 2005). Similarly, a windup movement in throwing (SSC) resulted in an increased power output (Newton et al., 1997). Consequently, the rowing cycle behaves like other SSC (sports) movement. Although we cannot clearly presume a real SSC without ultrasound verification, this increase in P_{row} and forces due to a potential SSC has been frequently linked to the storage and release of elastic energy (Kubo et al., 1999; Bojsen-Møller et al., 2005), stretch-induced contractility enhancement (Rode et al., 2009; Seiberl et al., 2015), reflex activity, and time-to-peak force (Schenau et al., 1997a,b). Since muscle reflexes and preactivation in rowing have been ruled out in a previous (surface) electromyographic (sEMG) study (Held et al., 2020), the storage (and delivery) of elastic energy (induced by muscle activation during the eccentric phase) and the stretch-induced increase in contractility during the concentric phase are most likely relevant contributors to the observed performance enhancement in rowing. In the context of rowing, it should be noted that in addition to P_{row}, P_{leg}, and WPS, also the total stroke length (L_{drive}) increased from DRIVE to SLIDE-DRIVE. This could be an indication of a changed rowing strategy. Since the amount of leg movement (L_{slide}) does not change between all conditions (DRIVE, ISO-DRIVE, SLIDE-DRIVE), the FEC seems to be unaffected. Nevertheless, the aspect of different stroke lengths for DRIVE, ISO-DRIVE, and SLIDE-DRIVE should be considered in further research.

Investigations revealed that force, work, and power increase during an SSC of up to 50% compared to isolated concentric contractions (Cavagna et al., 1968; Gregor et al., 1988); the observed performance (work and power) increase (about 10–20%) of flexion–extension contractions rowing is comparatively low. In contrast, jump-specific SSC showed a performance increase in the countermovement jumps compared to squat jumps of 18–30% (Bosco et al., 1987; Bobbert et al., 1996; Bobbert and Casius, 2005), which is closer to the observed performance enhancement in rowing. In this context, the maximum kinetic energy during a rowing slide is 60 ± 20% of the (maximum) potential energy for a (drop) jump (Held et al., 2020). As a consequence, the potential energy to be stored during rowing is notably lesser than in (drop) jumps. These differences may be key reasons for a smaller power enhancement during SLIDE-DRIVE rowing compared to jumping. Moreover, five subjects (equivalent to 13.5% of the entire sample) showed lower work and power outputs during the SLIDE-DRIVE measurement (compared to DRIVE and ISO-DRIVE measurements). These few poor responders might exhibit a deficiency of reactive force capabilities (motions in SSC). In general, numerous studies showed (Stojanović et al., 2017; Berton et al., 2018) that SSC performance can be increased mainly by reactive force capabilities, induced by adequate training (e.g., plyometrics). In the context of plyometric training in rowing, contradictory research results, however, exist: While one intervention study (n = 18, 4 weeks) revealed rowingspecific performance improvements through plyometric training (Egan-Shuttler et al., 2017), another intervention study (n = 24, 9 weeks) observed no rowing-specific performance improvements (Kramer et al., 1993). These contradictory findings might partly be explained by methodological issues. It has been recently shown that examinations of sEMG-activity of selected leg muscles (*m. vastus medialis* and *m. gastrocnemius medialis*) during single scull rowing showed no preactivation and no reflex activity, which implicate that any forms of muscle action in the fast SSC domain (e.g., induced during drop jump) do not reflect discipline-specific muscle actions and could hamper rowing performance enhancement during training and competitions (Held et al., 2020). Moreover, both studies did not differentiate participants due to their reactive force capabilities. However, since the effects of plyometric training were not covered by the current study, these conclusions remain speculative. Accordingly, further research on the effect of plyometric training in rowers with a deficit in the field of reactive force capabilities and the application of slow SSC exercises is needed.

The main limitation of the present study is that no SSC of the fascicle has yet been detected or investigated in rowing. However, the following four aspects suggest SSC mechanisms in rowing: (a) The sequence of flexion and extension (of the legs) during one rowing cycle, (b) the kinematic observations that this FEC movement can be performed in rowing as fast as in countermovement jumps (Held et al., 2019, 2020), (c) the muscle activity during the late slide phase prior to the onset of a new rowing stroke (Janshen et al., 2009; Guével et al., 2011; Turpin et al., 2011; Fleming et al., 2014; Shaharudin et al., 2014; Held et al., 2020), and (d) the confirmation of the SSC typical performance enhancement during FEC-type rowing. Altogether, future research should precisely determine whether the muscle fasciae complete an SSC during rowing and investigate the verification of the SSC in rowing. In this context, sEMG, goniometer, and ultrasound measurements of the fascicle's operating length and velocity as well as the activation of a leg

extensor muscle during rowing are currently in preparation. Additionally, further research is needed on the extent to which the storage (and delivery) of elastic energy (induced by muscle preactivation during the eccentric phase) (Kubo et al., 1999; Bojsen-Møller et al., 2005) and the stretch-induced increase in contractility during the concentric phase (Rode et al., 2009; Seiberl et al., 2015) contribute to performance enhancement during FEC-type rowing. One methodological limitation of the current study is that the accuracy of the motion-capturing method depends on the examiner (Suleder, 2010). To increase the accuracy, markers were additionally used in order to identify the handle and seat position, and the handle motion takes place on the same level (distance to the camera) as the seat motion. In addition, the accuracy of the motion-capturing system was compared with the handle displacement data of the FES setup (error of measurement <2%). Accordingly, the accuracy of the motion-capture method can be considered as appropriate in the current study. The rowing and P_{leg} determination in the current paper was based on the handle force and the handle pathway (Fukunaga et al., 1986; Dal-Monte and Komo, 1989; Zatsiorsky and Yakunin, 1991). Since the rower applies power at the handle and the foot stretcher, stretcher force is useful for the P_{row} determination (Kleshnev, 2016). Nevertheless, conclusions can also be drawn without the stretcher force, as the calculated P_{row} is the only propulsive energy source of the rower-boat system (Kleshnev, 2016). In this context, the proportion of P_{leg} on the total P_{row} was further determined based on the handle force and the leg (seat) movement speed (Kleshnev, 2016; Held et al., 2019). However, there is some movement of the hips relative to the seat, resulting in small leg speed deviations. Overall, this error can be classified as minimal because the extent of the hip movement (relative to the seat) is negligible (<2% of the total seat movement amplitude) (Held et al., 2019).

In conclusion, the current research clearly showed that an FEC led to notably higher handle force, WPS, P_{row}, and P_{leg} outputs compared to isolated concentric rowing movement. These findings are in line with the general force, work, and power enhancement in an SSC (Cavagna et al., 1968; Bosco et al., 1987; Gregor et al., 1988). Taking the observed sEMG activity during the late slide phase prior to the onset of a new rowing stroke into account (Janshen et al., 2009; Guével et al., 2011; Turpin et al., 2011; Fleming et al., 2014; Shaharudin et al., 2014; Held et al., 2020), the current results deliver meaningful insights into force enhancement enabling an adequate FEC during rowing patterns. Future ultrasound studies should investigate the occurrence and magnitude of potential SSC in rowing.

DATA AVAILABILITY STATEMENT

All datasets generated for this study are included in the article/**Supplementary Material**.

ETHICS STATEMENT

The studies involving human participants were reviewed and approved by the Ethikkommission – Deutsche Sport Hochschule Köln. The patients/participants provided their written informed consent to participate in this study.

AUTHOR CONTRIBUTIONS

SH, TS, and LD have planned the study and together developed the final manuscript. SH conducted the study.

FUNDING

This work was partially supported by the Deutsche Forschungsgemeinschaft (DFG) under grant SI841/15-1.

SUPPLEMENTARY MATERIAL

The Supplementary Material for this article can be found online at: https://www.frontiersin.org/articles/10.3389/fphys.2020.00521/full#supplementary-material

REFERENCES

Aura, O., and Komi, P. V. (1986). The mechanical efficiency of locomotion in men and women with special emphasis on stretch-shortening cycle exercises. *Eur. J. Appl. Physiol. Occup. Physiol.* 55, 37–43. doi: 10.1007/bf00422890

Berton, R., Lixandrão, M. E., Pinto e Silva, C. M., and Tricoli, V. (2018). Effects of weightlifting exercise, traditional resistance and plyometric training on countermovement jump performance: a meta-analysis. *J. Sports Sci.* 36, 2038–2044. doi: 10.1080/02640414.2018.1434746

Bobbert, M. F., and Casius, L. J. R. (2005). Is the effect of a countermovement on jump height due to active state development? *Med. Sci. Sports Exerc.* 37, 440–446. doi: 10.1249/01.MSS.0000155389.34538.97

Bobbert, M. F., Gerritsen, K. G. M., Litjens, M. C. A., and Van Soest, A. J. (1996). Why is countermovement jump height greater than squat jump height? *Med. Sci. Sports Exerc.* 28, 1402–1412. doi: 10.1097/00005768-199611000-00009

Bojsen-Møller, J., Magnusson, S. P., Rasmussen, L. R., Kjaer, M., and Aagaard, P. (2005). Muscle performance during maximal isometric and dynamic contractions is influenced by the stiffness of the tendinous structures. *J. Appl. Physiol.* 99, 986–994. doi: 10.1152/japplphysiol.01305.2004

Bosco, C., Montanari, G., Ribacchi, R., Giovenali, P., Latteri, F., Iachelli, G., et al. (1987). Relationship between the efficiency of muscular work during jumping and the energetics of running. *Eur. J. Appl. Physiol. Occup. Physiol.* 56, 138–143. doi: 10.1007/bf00640636

Bourgois, J., Steyaert, A., and Boone, J. (2014). Physiological and anthropometric progression in an international oarsman: a 15-Year case study. *Int. J. Sports Physiol. Perform.* 9, 723–726. doi: 10.1123/ijspp.2013-0267

Cavagna, G. A., Dusman, B., and Margaria, R. (1968). Positive work done by a previously stretched muscle. *J. Appl. Physiol.* 24, 21–32. doi: 10.1152/jappl.1968.24.1.21

Cohen, J. (1988). *Statistical Power Analysis for the Behavioral Sciences*. Hillside: Lawrence Earlbaum Associates.

Dal-Monte, A., and Komo, A. (1989). "Rowing and sculling mechanics," in *Biomechanics of Sport*, ed. P. McGinnis (Boca Raton: Vaughan, C), 53–119.

Dawson, T., and Taylor, R. (1973). Energetic Cost of Locomotion in Kangaroos. *Nature* 246, 313–314. doi: 10.1038/246313a0

Egan-Shuttler, J. D., Edmonds, R., Eddy, C., O'Neill, V., and Ives, S. J. (2017). The effect of concurrent plyometric training versus submaximal aerobic cycling on rowing economy, peak power, and performance in male high school rowers. *Sports Med. Open* 3:7. doi: 10.1186/s40798-017-0075-2

Fleming, N., Donne, B., and Mahony, N. (2014). A comparison of electromyography and stroke kinematics during ergometer and on-water rowing. *J. Sports Sci.* 32, 1127–1138. doi: 10.1080/02640414.2014.886128

Fukunaga, T., Matsuo, A., Yamamoto, K., and Asami, T. (1986). Mechanical efficiency in rowing. *Eur. J. Appl. Physiol. Occup. Physiol.* 55, 471–475. doi: 10.1007/bf00421639

Gollhofer, A., Komi, P., Miyashita, M., and Aura, O. (1987). Fatigue during stretch-shortening cycle exercises: changes in mechanical performance of human skeletal muscle. *Int. J. Sports Med.* 08, 71–78. doi: 10.1055/s-2008-1025644

Gregor, R. J., Roy, R. R., Whiting, W. C., Lovely, R. G., Hodgson, J. A., and Edgerton, V. R. (1988). Mechanical output of the cat soleus during treadmill locomotion: in vivo vs in situ characteristics. *J. Biomech.* 21, 721–732. doi: 10.1016/0021-9290(88)90281-3

Guellich, A., Seiler, S., and Emrich, E. (2009). Training methods and intensity distribution of young world-class rowers. *Int. J. Sports Physiol. Perform.* 4, 448–460. doi: 10.1123/ijspp.4.4.448

Guével, A., Boyas, S., Guihard, V., Cornu, C., Hug, F., and Nordez, A. (2011). Thigh muscle activities in elite rowers during on-water rowing. *Int. J. Sports Med.* 32, 109–116. doi: 10.1055/s-0030-1268412

Harriss, D., and Atkinson, G. (2015). Ethical Standards in Sport and Exercise Science Research: 2016 Update. *Int. J. Sports Med.* 36, 1121–1124. doi: 10.1055/s-0035-1565186

Held, S., Siebert, T., and Donath, L. (2019). Changes in mechanical power output in rowing by varying stroke rate and gearing. *Eur. J. Sport Sci.* 1–9. doi: 10.1080/17461391.2019.1628308

Held, S., Siebert, T., and Donath, L. (2020). Electromyographic activity profiles of the vastus medialis and gastrocnemius during single scull rowing in the field reflect short stretch-shortening-cycles: potential impact on training. *Sci. Rep.*

Janshen, L., Mattes, K., and Tidow, G. (2009). Muscular coordination of the lower extremities of oarsmen during ergometer rowing. *J. Appl. Biomech.* 25, 156–164. doi: 10.1123/jab.25.2.156

Kleshnev, V. (2016). *The Biomechanics of Rowing*. London: Crowood Press.

Komi, P. V. (2003). "Stretch-Shortening Cycle," in *Strength and Power in Sport*, ed. P. V. Komi (Oxford: Blackwell Science Publication), 184–204.

Kramer, J., Morrow, A., and Leger, A. (1993). Changes in rowing Ergometer, weight lifting, vertical jump and isokinetic performance in response to standard and standard plus plyometric training programs. *Int. J. Sports Med.* 14, 449–454. doi: 10.1055/s-2007-1021209

Kubo, K., Kawakami, Y., and Fukunaga, T. (1999). Influence of elastic properties of tendon structures on jump performance in humans. *J. Appl. Physiol.* 87, 2090–2096. doi: 10.1152/jappl.1999.87.6.2090

Newton, R. U., Murphy, A. J., Humphries, B. J., Wilson, G. J., Kraemer, W. J., and Häkkinen, K. (1997). Influence of load and stretch shortening cycle on the kinematics, kinetics and muscle activation that occurs during explosive upper-body movements. *Eur. J. Appl. Physiol. Occup. Physiol.* 75, 333–342. doi: 10.1007/s004210050169

Nicol, C., Avela, J., and Komi, P. V. (2006). The stretch-shortening cycle. *Sports Med.* 36, 977–999. doi: 10.2165/00007256-200636110-00004

Rienks, N., de Widt, W. J., van den Broek, T., and Brinkman, J. (2020). *Row Analysis - Analyze Stroke, Benchmark, Row Faster!*. Available online at: http://www.rowanalysis.eu/en/ (accessed January 26, 2020).

Rode, C., Siebert, T., and Blickhan, R. (2009). Titin-induced force enhancement and force depression: A 'sticky-spring' mechanism in muscle contractions? *J. Theor. Biol.* 259, 350–360. doi: 10.1016/j.jtbi.2009.03.015

Schenau, G. J., van, I., Bobbert, M. F., and de Haan, A. (1997a). Does elastic energy enhance work and efficiency in the stretch-shortening cycle? *J. Appl. Biomech.* 13, 389–415. doi: 10.1123/jab.13.4.389

Schenau, G. J., van, I., Bobbert, M. F., and de Haan, A. (1997b). Mechanics and Energetics of the stretch-shortening cycle: a stimulating discussion. *J. Appl. Biomech.* 13, 484–496. doi: 10.1123/jab.13.4.484

Seiberl, W., Power, G. A., Herzog, W., and Hahn, D. (2015). The stretch-shortening cycle (SSC) revisited: residual force enhancement contributes to increased performance during fast SSCs of human m. adductor pollicis. *Physiol. Rep.* 3:e12401. doi: 10.14814/phy2.12401

Shaharudin, S., Zanotto, D., and Agrawal, S. (2014). Muscle synergy during wingate anaerobic rowing test of collegiate rowers and untrained subjects. *Int. J. Sports Sci.* 4, 165–172.

Steinacker, J. M. (1993). Physiological aspects of training in rowing. *Int. J. Sports Med.* 14(Suppl. 1), S3–S10.

Stojanović, E., Ristić, V., McMaster, D. T., and Milanović, Z. (2017). Effect of plyometric training on vertical jump performance in female athletes: a systematic review and meta-analysis. *Sports Med.* 47, 975–986. doi: 10.1007/s40279-016-0634-6

Suleder, M. (2010). *Videoanalyse und Physikunterricht*. Berlin: Aulis Verlag.

Svantesson, U., Grimby, G., and Thomeé, R. (1994). Potentiation of concentric plantar flexion torque following eccentric and isometric muscle actions. *Acta Physiol. Scand.* 152, 287–293. doi: 10.1111/j.1748-1716.1994.tb09808.x

Treff, G., Winkert, K., Machus, K., and Steinacker, J. M. (2018). Computer-aided stroke-by-stroke visualization of actual and target power allows for continuously increasing ramp tests on wind-braked rowing Ergometers. *Int. J. Sports Physiol. Perform.* 13, 729–734. doi: 10.1123/ijspp.2016-0716

Turpin, N. A., Guével, A., Durand, S., and Hug, F. (2011). Effect of power output on muscle coordination during rowing. *Eur. J. Appl. Physiol.* 111, 3017–3029. doi: 10.1007/s00421-011-1928-x

van Soest, A. J., and Casius, L. J. (2000). Which factors determine the optimal pedaling rate in sprint cycling? *Med. Sci. Sports Exerc.* 32, 1927–1934. doi: 10.1097/00005768-200011000-00017

Zatsiorsky, V. M., and Yakunin, N. (1991). Mechanics and biomechanics of rowing: a review. *Int. J. Sport Biomech.* 7, 229–281. doi: 10.1123/ijsb.7.3.229

Conflict of Interest: The authors declare that the research was conducted in the absence of any commercial or financial relationships that could be construed as a potential conflict of interest.

frontiers in Physiology

ORIGINAL RESEARCH
published: 28 July 2020
doi: 10.3389/fphys.2020.00921

Cross-Bridges and Sarcomeric Non-cross-bridge Structures Contribute to Increased Work in Stretch-Shortening Cycles

André Tomalka[1], Sven Weidner[1], Daniel Hahn[2,3], Wolfgang Seiberl[4] and Tobias Siebert[1†]*

[1] Department of Motion and Exercise Science, University of Stuttgart, Stuttgart, Germany, [2] Human Movement Science, Faculty of Sports Science, Ruhr University Bochum, Bochum, Germany, [3] School of Human Movement and Nutrition Sciences, University of Queensland, Brisbane, QLD, Australia, [4] Human Movement Science, Bundeswehr University Munich, Munich, Germany

OPEN ACCESS

Edited by:
P. Bryant Chase, Florida State University, United States

Reviewed by:
Henk Granzier, University of Arizona, United States
Bertrand C. W. Tanner, Washington State University, United States

***Correspondence:**
André Tomalka
andre.tomalka@inspo.uni-stuttgart.de

†Present address:
Tobias Siebert, Stuttgart Center for Simulation Science, University of Stuttgart, Stuttgart, Germany

Specialty section:
This article was submitted to Striated Muscle Physiology, a section of the journal Frontiers in Physiology

Received: *06 April 2020*
Accepted: *09 July 2020*
Published: *28 July 2020*

Citation:
Tomalka A, Weidner S, Hahn D, Seiberl W and Siebert T (2020) Cross-Bridges and Sarcomeric Non-cross-bridge Structures Contribute to Increased Work in Stretch-Shortening Cycles. Front. Physiol. 11:921. doi: 10.3389/fphys.2020.00921

Stretch-shortening cycles (SSCs) refer to the muscle action when an active muscle stretch is immediately followed by active muscle shortening. This combination of eccentric and concentric contractions is the most important type of daily muscle action and plays a significant role in natural locomotion such as walking, running or jumping. SSCs are used in human and animal movements especially when a high movement speed or economy is required. A key feature of SSCs is the increase in muscular force and work during the concentric phase of a SSC by more than 50% compared with concentric muscle actions without prior stretch (SSC-effect). This improved muscle capability is related to various mechanisms, including pre-activation, stretch-reflex responses and elastic recoil from serial elastic tissues. Moreover, it is assumed that a significant contribution to enhanced muscle capability lies in the sarcomeres itself. Thus, we investigated the force output and work produced by single skinned fibers of rat soleus muscles during and after ramp contractions at a constant velocity. Shortening, lengthening, and SSCs were performed under physiological boundary conditions with 85% of the maximum shortening velocity and stretch-shortening magnitudes of 18% of the optimum muscle length. The different contributions of cross-bridge (XB) and non-cross-bridge (non-XB) structures to the total muscle force were identified by using Blebbistatin. The experiments revealed three main results: (*i*) partial detachment of XBs during the eccentric phase of a SSC, (*ii*) significantly enhanced forces and mechanical work during the concentric phase of SSCs compared with shortening contractions with and without XB-inhibition, and (*iii*) no residual force depression after SSCs. The results obtained by administering Blebbistatin propose a titin-actin interaction that depends on XB-binding or active XB-based force production. The findings of this study further suggest that enhanced forces generated during the active lengthening phase of SSCs persist during the subsequent shortening phase, thereby contributing to enhanced

work. Accordingly, our data support the hypothesis that sarcomeric mechanisms related to residual force enhancement also contribute to the SSC-effect. The preload of the titin molecule, acting as molecular spring, might be part of that mechanism by increasing the mechanical efficiency of work during physiological SSCs.

Keywords: contractile behavior, cross-bridge inhibitor, work expenditure, muscle stretch, muscle shortening, history-effects, rFE, rFD

INTRODUCTION

Residual force depression (rFD) following active muscle shortening and residual force enhancement (rFE) following active muscle stretch (Abbott and Aubert, 1952) are fundamentally accepted mechanical properties of skeletal muscle (Rassier, 2017). These phenomena have been consistently investigated across all structural levels of muscle from *in vitro* single sarcomeres (Joumaa et al., 2008a) to *in vivo* human multi-joint-contractions (Seiberl et al., 2015a; Chen et al., 2019) [for recent reviews, see Herzog et al., 2016; Rassier, 2017; for further information of the potential mechanisms of r(FD) and r(FE), see Appendix, **Supplementary Text S1**].

However, stretch-hold (referring to rFE) or shortening-hold (referring to rFD) movements have no real everyday significance. On the contrary, SSCs — eccentric muscle action immediately followed by concentric muscle action — play a significant role in natural locomotion. SSCs represent an essential part of fundamental cyclic movement patterns such as walking, running or jumping (Komi, 2000). Typically, under physiological conditions, a SSC is a rather fast type of contraction during rapid movements (due to short ground contact times of the legs) (Bobbert et al., 1986; van Ingen Schenau et al., 1997; Komi, 2000), while the muscles operating range covers the ascending limb and the plateau-region of their force-length-relation (Burkholder and Lieber, 2001; Kurokawa et al., 2003). An essential feature of the SSC is that the muscular force and work during the concentric phase can be increased by more than 50% compared with concentric muscle actions without preceding stretch (Cavagna et al., 1968; Bosco et al., 1987; Gregor et al., 1988). This SSC-effect (increased muscular capability) is associated with enhanced efficiency accompanied by reduced metabolic energy consumption (Cavagna et al., 1968; Joumaa and Herzog, 2013). However, despite clear evidence concerning increased SSC-effects in various experimental human and animal studies on different structural levels (*in vitro, in situ, in vivo*), the underlying mechanisms remain controversial. This dispute is because none of the currently accepted mechanisms (such as preactivation, stretch-reflex responses, and elastic recoil from serial elastic tissues) can entirely explain the enhanced force response and the increased mechanical work output during SSCs (van Ingen Schenau et al., 1997; Cormie et al., 2011; Seiberl et al., 2015b). Since it was shown early that SSCs provoke increased force/work output in isolated muscle tissue preparations with essentially no tendon, the phenomenon was revisited with approaches designed to identify mechanisms not related to reflex activity or elastic energy recoil, but thought to lie within the sarcomere itself (Cavagna et al., 1968; Seiberl et al., 2015b). This assumption is supported by recent findings, which have shown SSC-effects even on the fiber level (i.e., without serial-elastic components such as the tendon and aponeurosis) (Fukutani and Herzog, 2019).

A potential mechanism to explain the SSC-effect within the sarcomere might be based on different myosin states. Recent X-ray diffraction studies on actively contracting fibers from striated skeletal muscle (Haselgrove, 1975; Linari et al., 2015; Fusi et al., 2016) suggest that the myosin filament can exist in one of two possible states: a relaxed state (OFF) and an activated state (ON). The force response upon muscle stretching, which occurs during the eccentric phase of a SSC, might be affected by the mechanosensitive contributions of XB activation and binding from the myosin OFF into the myosin ON state with stretch (Linari et al., 2015; Fusi et al., 2016; Brunello et al., 2020). Current findings suggest that this regulatory mechanism of thick filament mechano-sensing in striated muscles acts independently of the well-known thin filament-mediated calcium-signaling pathway (Fusi et al., 2016).

Furthermore, there is extensive evidence that the semi-active protein titin (Maruyama et al., 1976) mediates the phenomena of enhanced force response during and following stretch contractions [(r)FE] in skeletal muscle (Tomalka et al., 2017; Herzog, 2018; Freundt and Linke, 2019). Various model approaches (Rode et al., 2009; Nishikawa et al., 2012; Schappacher-Tilp et al., 2015) have been proposed that explain rFE in skeletal muscle and these model approaches are supported by experimental evidence for titin-actin interactions upon muscle activation (Nagy, 2004; Bianco et al., 2007; Dutta et al., 2018; Li et al., 2018; Tahir et al., 2020). Recent studies (Fukutani et al., 2017; Fukutani and Herzog, 2019) suggested that increased rFE is positively related to an increase in force/work during SSCs. These results come from *in vitro* muscle fiber experiments under limited conditions (very slow contraction velocities while the fibers operate mostly on the descending limb of the force-length-relation). There also exist contradictory *in situ* investigations on cat soleus (slow contraction velocities at the ascending limb of the force-length-relation), showing that the effect of rFE disappears as soon as the muscle actively shortens during SSCs (Lee et al.,

Abbreviations: ATP, adenosine 5′ triphosphate disodium salt hydrate; BDM, 2,3-butanedione monoxime; Ca^{2+}, calcium; CK, creatine phosphokinase; CP, creatine phosphate; E-64, *trans*-epoxysuccinyl-L-leucylamido(4-guanidino)butane; EGTA, ethylene glycol-bis(2-aminoethylether)-*N*,*N*,*N*′,*N*′-tetraacetic acid; F/F_0, maximum isometric muscle force; GLH, glutathione; HDTA, 1,6-diaminohexane-*N*,*N*,*N*′,*N*′-tetraacetic acid; *h*, height; IMID, imidazole; KOH, potassium hydroxide; KP, potassium propionate; L/L_0, optimum muscle fiber length associated with F/F_0; non-XB, non-cross-bridge; PMSF, phenylmethanesulfonyl fluoride; rFD, residual force depression; rFE, residual force enhancement; SSC, stretch-shortening cycle; TES, *N*-[tris(hydroxymethyl)methyl]-2-aminoethanesulfonic acid; v/v, volume/volume; v_{max}, maximal shortening velocity; *w*, width; w/w, weight/volume; XB, cross-bridge.

2001). Hence, it is still controversial whether and to what extent rFE and rFD abolish each other during SSCs. Furthermore, the contribution of non-XB structures (as e.g., titin) to a potential SSC-effect in SSCs has to be examined.

This study aims to provide a systematic analysis of mechanical and contractile properties contributing to the increased force/work output in the shortening phase of SSCs compared to active shortening contractions without preceding stretch. To characterize the contribution of XB and non-XB structures to force/work production, we also performed experiments using the actomyosin inhibitor Blebbistatin. To achieve these goals, we performed *in vitro* isokinetic ramp experiments on single skinned skeletal muscle fibers obtained from the m. soleus of adult rats. Lengthening, shortening and SSC perturbations were conducted in the physiological range (along the ascending limb to the plateau region) of the force-length-relation and at fast contraction velocities of the soleus. The soleus muscle is an integral part of the triceps surae of the lower limb, operates as plantarflexor of the lower ankle joint and is mainly involved in SSCs during cyclic terrestrial locomotion of vertebrates.

MATERIALS AND METHODS

Preparation, Handling and Experimental Set-Up

Muscle preparation, storage and activation techniques for permeabilized single muscle fibers were in line with Tomalka et al., 2017, 2019. Briefly, muscle fibers were extracted from seven freshly killed male Wistar rats (3–7 months, 425–500 g, cage-sedentary, 12 h:12 h light: dark cycle, housing-temperature: 22°C). The muscle fibers were obtained from soleus muscles from the left hind limbs. The Soleus is a predominantly slow-twitch skeletal muscle with a fiber type distribution of approximately 96% of type 1 fibers (Soukup et al., 2002). The skeletal muscle fibers from rats used for this study have been provided by another animal study that was approved according to the regulations of the German animal protection law (Tierschutzgesetz, §4 (3); Permit Number: 35-9185.81/0491). The applicants of the approved animal study had no objection against the extraction of muscle fibers from dead rats. The extraction of muscle fibers did not impair their results.

Fiber bundles were permeabilized at 4°C in a skinning solution (see section "Solutions"). Afterward, the demembranated fiber bundles were pinned at both ends — at approximately optimal *in vivo* sarcomere length — to a silicone elastomer surface. Subsequently, the fiber bundles were stored at −20°C in a storage solution (skinning solution made up in 50% glycerol) (see section "Solutions") and used within 6 weeks. On the day of the experiments, small segments of the skinned fiber bundles were dissected under a stereomicroscope (Leica A60) and used to prepare several single muscle fibers (1.0–1.5 mm long) in a petri dish filled with storage solution positioned on a customized temperature-controlled stage at 4–6°C. After that, the fiber ends were loosely clamped by aluminum foil 'T-clips' (Institute of Applied Physics, Ultrafast Optics, Jena, Germany). Afterward, the fibers were treated with relaxing solution (see section "Solutions") containing Triton X-100 (1% v/v) for 1–2 min at 4°C to ensure complete removal of internal membranes without affecting the contractile apparatus (Fryer et al., 1995; Linari et al., 2007). The fibers were either used immediately or stored overnight at −20°C in a storage solution. On the day of the experiments, the isolated muscle fiber was transferred to an experimental chamber (802D, Aurora Scientific, Canada) containing a relaxing solution. The clips of the fiber were attached to a force transducer (403a, Aurora Scientific, Canada) and a high-speed length controller (322 C-I, Aurora Scientific, Canada). Afterward, the fiber width (w) and height (h) were measured in approximately 0.1 mm intervals over the entire length with a 10× dry-objective (NA 0.30, Nikon) and a 10× eyepiece. The fiber cross-sectional area was determined assuming an elliptical cross-section of single muscle fibers ($\pi hw/4$) and was 4920 ± 1139 μm^2. For visualization of the striation pattern and accurate, dynamic tracking of sarcomere length changes, a high-speed camera system (901B, Aurora Scientific, Canada) was used in combination with a 20 × ELWD dry-objective (NA 0.40, Nikon) and an accessory lens (2.5×, Nikon).

Experimental Protocol

Each fiber was activated by calcium diffusion in the presence of ATP. The fiber was immersed in preactivating solution (see section "Solutions") for 60 s for equilibration and afterward in an activating solution (pCa 4.5). This offered maximal activation that was characterized by a continuous rise in force until a plateau was reached (defined as a change in the force of less than 1% over a period of 5 s, achieved approx. 25 s after activation). Then, the ramp perturbations were applied to the fiber. Subsequently, fibers were immersed in relaxing solution for 420 s. Within this time interval of 420 s, a 'cycling-protocol' by Brenner (1983) was used to conserve the structural, functional and mechanical properties in maximally activated fibers over an extended period of time as well as to reduce sarcomere inhomogeneities. According to Tomalka et al. (2017), the following criteria were applied to discard fibers from the analysis: (1) isometric force in reference contractions was decreased by more than 10%; (2) abnormal behavior of force-traces, evidenced by artifacts, oscillations, or abrupt flattening was noted; and (3) lesions, ruptures or fiber contortion were identified visually.

Isokinetic ramp perturbations comprised a set of repeated experiments. The control experiments (**Figure 1**) were designed to investigate the dynamic and static force response during and after isokinetic ramp perturbations. The Blebbistatin experiments are a repeat of the control experiments and involved the separation of the XB-contributions and non-XB-contributions to force production during and after isokinetic ramp perturbations (**Figure 1**).

During the isokinetic ramp perturbations (control condition without XB-inhibition), single skinned muscle fibers (n = 16) were subjected to three different experiments, each consisting of an isometric phase, then a ramp transient, then an isometric phase (**Figure 2**). (*i*) For the SSC experiments (**Figure 2**, solid blue line), fibers were isometrically activated at 0.82 L_0 (corresponding to ∼2.0 μm sarcomere length), stretched to optimum muscle

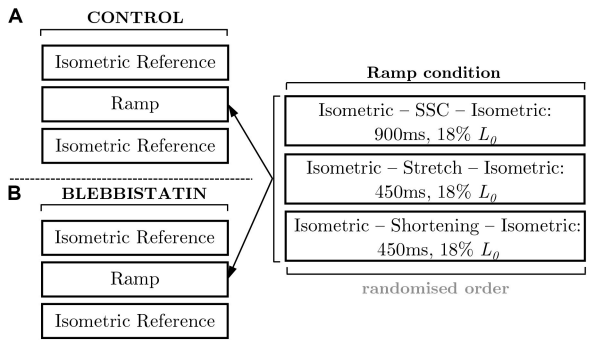

FIGURE 1 | Schematic of the experimental protocol. The left panels illustrate the fixed protocol of muscle contractions consisting of isometric reference contractions and isokinetic ramp perturbations, for **(A)** control and **(B)** Blebbistatin experiments. The isometric reference measurements were performed in a randomized order at 0.82 L_0 and 1.0 L_0. The examination of varying ramp conditions followed a pseudorandomized block design (right panel). The applied stretch-shortening time periods correspond to a maximum shortening velocity (v_{max}) of 85% for all ramp conditions. The stretch-shortening magnitudes are normalized to the optimum muscle length (L_0). SSC stands for stretch-shortening-cycle.

length 1.0 L_0 (∼2.5 μm sarcomere length) in 450 ms, and then immediately shortened to 0.82 L_0 in 450 ms. (*ii*) For the active stretch trial (**Figure 2**, solid purple line), the fibers were isometrically activated at 0.82 L_0 and lengthened to 1.0 L_0 in 450 ms. (*iii*) For the active shortening trial (**Figure 2**, solid yellow line), fibers were isometrically activated at 1.0 L_0 and then shortened to corresponding end length of 0.82 L_0 in 450 ms. Due to consistency and simplification purposes, the following terms are used for the three different experiments: (*i*) SSC, (*ii*) stretch and (*iii*) shortening (**Figure 2**). For the investigation of individual isometric force responses following isokinetic ramp perturbations (rFE/rFD), the steady-state isometric contractions were sustained for 34.5 s at the final lengths (**Figure 2**, second half). To calculate rFE/rFD, we measured the average difference between the redeveloped and the corresponding isometric steady-state force at the same length — within a time interval of 5 s (28 s after the end of each ramp length change or cycle, cf. vertical lines of **Figure 2**).

The Blebbistatin experiments (n = 16) repeated the isokinetic ramps of the control experiments but in the presence of 20 μmol l^{-1} Blebbistatin in all solutions (see section "Solutions"). This photosensitive chemical is a selective inhibitor that blocks the force-generating transition of the bound actomyosin complex and causes myosin heads to bind to actin without exerting any force (Iwamoto, 2018). Blebbistatin does not affect titin mobility (Shalabi et al., 2017). The muscle fibers were treated with Blebbistatin in relaxation solution (pCa 9.0) for approximately 30 min in the dark. Throughout the experiments, the microscope room was maintained dark and a red-light filter (650 nm) was placed over the light source to prevent the breakdown of Blebbistatin when exposed to wavelengths between 365 and 490 nm (Kolega, 2004; Cornachione and Rassier, 2012).

All trials were performed at a constant velocity of 85% of the maximum shortening velocity (v_{max}).

The v_{max} was defined as 0.48 L_0 s^{-1}, an average value (0.48 ± 0.13 L_0 s^{-1}; n = 4) of maximum unloaded shortening velocity of soleus muscle fibers from adult male Wistar rats. The individual v_{max}-values were calculated based on own experimental data from isotonic contractions against forces in the range of 0.1 F_0 to 0.9 F_0. For the determination of force degradation, isometric reference contractions at L_0 were performed before and after each ramp contraction. In ramp experiments (control), the isometric force in successive activations decreased at an average rate of around 3.3% per activation. The order of the ramp protocol was randomized. All experiments were conducted at a constant temperature of 12°C ± 0.1°C. At this temperature, the fibers proved very stable and able to withstand active ramp protocols over an extended period of time as well as prolonged activations (Ranatunga, 1982, 1984; Bottinelli et al., 1996; Tomalka et al., 2017).

Solutions

The relaxing solution contained (in mM) 100 TES, 7.7 $MgCl_2$, 5.44 Na_2ATP, 25 EGTA, 19.11 Na_2CP, 10 GLH (pCa 9.0). The preactivating solution contained (in mM) 100 TES, 6.93 $MgCl_2$, 5.45 Na_2ATP, 0.1 EGTA, 19.49 Na_2CP, 10 GLH, 24.9 HDTA. The activating solution contained (in mM) 100 TES, 6.76 $MgCl_2$, 5.46 Na_2ATP, 19.49 Na_2CP, 10 GLH, 25 CaEGTA (pCa 4.5). The skinning solution contained (in mM) 170 potassium propionate, 2.5 $MgCl_2$, 2.5 Na_2ATP, 5 EGTA, 10 IMID, 0.2 PMSF. The storage solution is the same as the skinning solution, except for the presence of 10 mM GLH and 50% glycerol (v/v). Cysteine and cysteine/serine protease inhibitors [*trans*-epoxysuccinyl-L-leucylamido-(4-guanidino) butane, E-64, 10 mM; leupeptin, 20 μg ml^{-1}] were added to all solutions to preserve lattice proteins and thus sarcomere homogeneity (Linari et al., 2007; Tomalka et al., 2017). pH (adjusted with KOH) was 7.1 at 12°C. 450 U ml^{-1} of CK was added to all solutions, except for skinning and storage solutions. CK was obtained from Roche (Mannheim, Germany) and Blebbistatin was from Enzo Life Sciences Inc., NY, United States); all other chemicals from Sigma (St Louis, MO, United States).

Data Processing and Statistics

Data were collected at 1 kHz. For data acquisition, real-time software (600A, Aurora Scientific, Canada) was used. For data analysis, a custom-written MATLAB (MathWorks, Natick, MA, United States) program was utilized. Unless stated otherwise, forces were expressed in absolute values (mN) and kilopascals (kPa) or normalized to the individual maximal muscle force (F/F_0). The average active isometric force at optimum muscle length L_0 was 0.31 ± 0.09 mN, this force corresponds to relative average stress values, normalized to the cross-sectional area, of 61.10 ± 10.93 kPa. Fiber lengths were expressed relative to the optimum fiber length (L/L_0), while the mean L_0 was 0.80 ± 0.10 mm. Sarcomere lengths were shown in absolute values (μm). Mechanical work was calculated as the line integral of the changing force over the entire shortening distance for both, the active shortening condition and the SSC condition are expressed in normalized values ($\int \frac{F}{F_0} \Delta \frac{L}{L_0}$). All

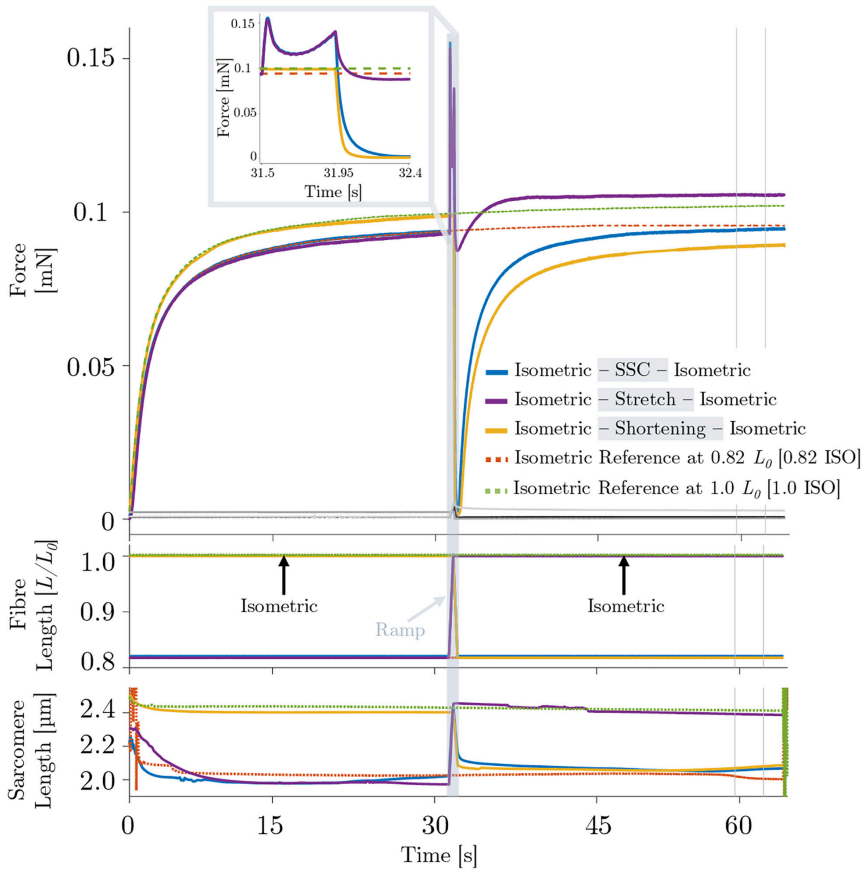

FIGURE 2 | Representative force–time (upper graph), length–time (middle graph) and sarcomere length–time traces (lower graph) of a permeabilized single fiber segment from a rat soleus muscle (n = 1, raw, unfiltered data) at 12°C experimental temperature of the control experiment. The solid blue line indicates the stretch-shortening cycle (SSC), the solid purple line shows the stretch condition and the yellow solid line shows the shortening condition. The black line shows the passive SSC, the bright gray line the passive stretch and the dark gray line shows the passive shortening condition. Each of these experiments consists of an isometric phase, then a ramp transient, then an isometric phase. The red dashed line indicates the isometric reference contraction at 0.82 L_0 (0.82 ISO), and the green dashed line shows the isometric reference contraction at optimum fiber length 1.0 L_0 (1.0 ISO). After maximal isometric activation (pCa 4.5) until a plateau (defined as a change in the force of less than 1% for 5 s) was reached, isokinetic ramp perturbations have been applied to the tissue preparation (ramp initiation at t = 31.5 s). The force is shown in absolute values (mN). The fiber length is normalized to optimum muscle fiber length (L/L_0). The sarcomere length is recorded at maximal activation and is shown in µm. All ramp experiments have been conducted at a constant stretch/shortening amplitude of 0.18 L/L_0 within a constant amount of time (450 ms), respectively. The shaded rectangle indicates the period of the active stretch-shortening cycle (SSC) while the fiber segment is lengthened from 0.82L_0 to 1.0L_0 and immediately shortened to 0.82L_0. The two vertical lines indicate the calculation period for rFE/rFD. Inset: enlarged view of the force response during an active SSC. For reasons of clarity, the passive traces have not been shown in the shaded rectangle or as part of the figure legend.

data are presented as mean ± standard deviation (s.d.) unless stated otherwise. Parameters were tested for normal distribution using the Shapiro-Wilk Test. All data were normally distributed ($p > 0.665$). To test whether the steady-state isometric forces and sarcomere lengths differ between the different conditions ending at 0.82 L_0 (SSC, shortening and isometric reference at 0.82 L_0) an repeated-measures ANOVA was calculated. In case that the ANOVA demonstrated significant main effects, *post hoc* analyses were performed using the student's t-test with Bonferroni correction. To determine significant differences in forces or sarcomere length when comparing the two conditions ending at 1.0 L_0 (stretch and isometric reference at 1.0 L_0), a student's t-test was used. The statistical tests were likewise performed for both the control experiments and the Blebbistatin experiments. The level of significance was set at $p < 0.05$. Statistical analyses were realized using SPSS 25 (IBM Corp., Armonk, NY, United States). The effect sizes of Cohen's d were calculated as $d = \frac{M_1 - M_2}{S_{pooled}}$, where M is the mean and $S_{pooled} = \sqrt{\frac{SD_1^2 + SD_2^2}{2}}$ (Cohen, 1988). The effect sizes were classified as small (d = 0.2), medium (d = 0.5) and large (d = 0.8) (Cohen, 1988).

RESULTS

Isometric Force Development After Isokinetic Ramp Contractions

Figure 2 provides a representative overview of the forces produced by an isolated muscle fiber preparation during the

different isokinetic ramps and the isometric conditions. For statistical comparison of the different contraction conditions, individual and mean isometric steady-state forces obtained 57.5–62.5 s after the start of each activation are shown in **Figure 3A**. Forces were significantly smaller ($p \leq 0.001$, $d = 0.98$, **Table 1**) for the shortening condition [yellow circles, **Figures 3A** (a,b)] compared with the actively isometric reference contraction at corresponding end length of 0.82 L_0 [0.82 ISO, red circles of **Figures 3A** (a,c)]. For the SSC condition [blue circles, **Figures 3A** (b,c)], isometric forces were not statistically different (*ns*) ($p = 0.278$, $d = 0.15$; **Table 1**) compared with 0.82 ISO. The comparison of active shortening and SSC revealed significantly larger ($p = 0.002$, $d = 0.77$) forces for the SSC condition [cf. **Table 1** and **Figure 3A** (b)].

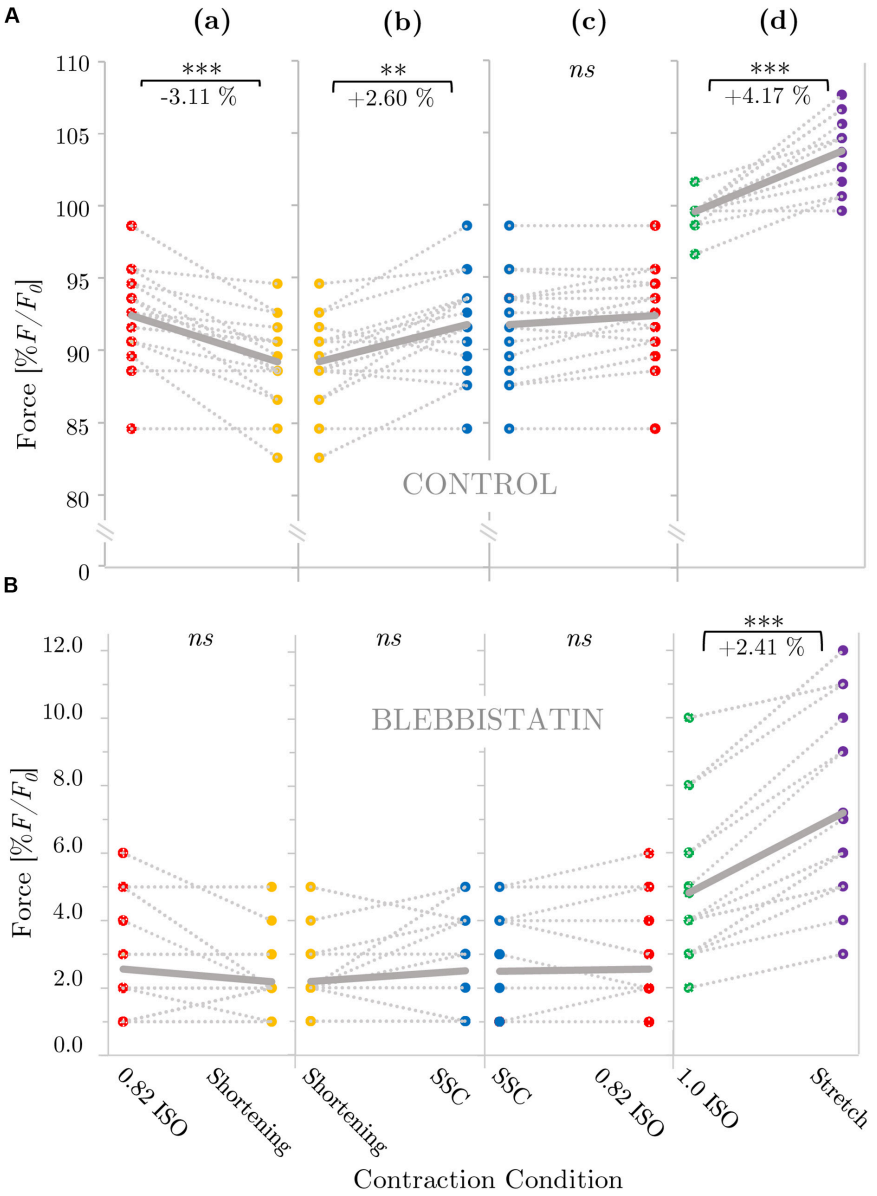

FIGURE 3 | Influence of varying ramp experiments on force for **(A)** control and **(B)** Blebbistatin experiments. The gray dotted lines of the scatterplots shown in panels **(a–d)** indicate the individual paired data values and gray solid lines indicate the mean values ($n = 16$ fibers from seven rats). Two fibers per animal (median) were examined, except for one animal from which one fiber was examined and three animals from which three fibers were examined. Mean forces are normalized to the forces obtained during actively isometric reference contractions at corresponding end lengths (0.82 L_0 [0.82 ISO; red circles] for active shortening [yellow circles] and stretch-shortening [SSC; blue circles] conditions, respectively, and 1.0 L_0 [1.0 ISO; green circles] for active stretch [purple circles] conditions). **(B)** Statistical analyses are based on muscle fiber experiments in the presence of Blebbistatin. Forces are calculated 28–33 s after the end of each ramp and they are expressed in percentage of maximum isometric force (% F/F_0). Brackets and asterisks (*) mark differences in force after varying ramp conditions in the intergroup comparison. Significance levels are marked as follows: *$p < 0.05$, **$p < 0.01$, and ***$p < 0.001$. *ns* means not significant.

TABLE 1 | Pairwise comparisons of isometric steady-state forces obtained during the control experiments.

Control						
$\Delta F/F_0$	Pairwise comparisons $\Delta F/F_0$ [%]				*n*	*p*-values
	Mean differences	s.d.	95% confidence interval of the difference			
			Lower	Upper		
0.82 ISO - shortening	−3.11	2.56	0.77	5.44	16	<0.001
0.82 ISO - SSC	−0.51	1.31	−0.68	1.71	16	0.278
Shortening - SSC	2.60	2.61	−4.98	−0.21	16	0.002
1.0 ISO - stretch	4.17	2.17	−5.32	−3.00	16	<0.001

Force values ± s.d. are normalized to the forces obtained during actively isometric reference contractions at corresponding end lengths (0.82 L_0 [0.82 ISO] for active shortening and stretch-shortening [SSC] conditions, respectively and 1.0 L_0 [1.0 ISO] for active stretch conditions). Forces are calculated 28–33 s after the end of each ramp and differences ($\Delta F/F_0$) are expressed in percentage (%). ns means not significant ($p < 0.05$). n is the number of samples.

For the stretch condition [purple circles, **Figure 3A** (d)], mean isometric steady-state forces were significantly larger ($p \leq 0.001$, $d = 2.39$; **Table 1**) compared with the corresponding isometric reference contraction at 1.0 L_0 [1.0 ISO, green circles of **Figure 3A** (d)].

The corresponding sarcomere lengths for the SSC condition (2.02 ± 0.05 μm, blue line, **Figure 2**) were not statistically different (*ns*) ($p = 0.238$, $d = 0.329$) compared with 0.82 ISO (2.00 ± 0.07 μm, red dashed line, **Figure 2**) and compared with the shortening condition (2.03 ± 0.06 μm, $p = 0.254$, $d = 0.181$). For the stretch condition (2.39 ± 0.05 μm, purple line, **Figure 2**), the sarcomere lengths were not statistically different (*ns*) ($p = 0.051$, $d = 0.340$) compared with 1.0 ISO (2.38 ± 0.04 μm, green dashed line of **Figure 2**).

Effects of Shortening and SSC on Mechanical Work

Mechanical work was significantly larger for the SSC condition (black circles of **Figure 4A**) compared with the active shortening condition (white circles of **Figure 4A**) ($p \leq 0.001$, $d = 3.31$). **Figure 5A** shows the distinct force responses and work (colored areas under the curves) during the shortening phase of the SSC condition and the shortening condition, respectively. While both conditions were subjected to the same amount of shortening (0.18 L_0), mechanical work increased by 114% when shortening was preceded by a stretch (SSC condition) (**Figure 4A**).

Effects of XB-Inhibition on Force Generation and Mechanical Work

Steady-State Isometric Force

A representative example of the forces produced by an isolated muscle fiber preparation during the different isokinetic ramps and the isometric conditions in the presence of Blebbistatin is shown in **Figure 6**. Blebbistatin successfully inhibited active isometric muscle force and led to marginal levels of XB-based force production [about 5% F_0 at optimal muscle length 1.0 L_0; cf. **Figure 3B** (d)]. Mean isometric forces after the end of the isokinetic ramps revealed no significant differences for the active shortening condition [yellow circles of **Figure 3B** (a)] compared with 0.82 ISO [red circles of **Figure 3B** (a)] ($p = 0.086$, $d = 0.44$; cf. **Table 2**). For the SSC condition [blue circles of **Figures 3B** (b,c)], no statistically significant differences were found compared with 0.82 ISO ($p = 0.686$, $d = 0.06$; cf. **Table 2**) and compared with the shortening condition ($p = 0.236$, $d = 0.38$) [cf. **Figures 3B** (b,c)]. Comparison of 1.0 ISO and active stretch conditions [green vs. purple circles of **Figure 3B** (d)] revealed statistically greater forces ($p \leq 0.001$, $d = 0.91$) for the stretch condition (cf. **Table 2**).

The corresponding sarcomere lengths were not statistically different (*ns*) ($p = 0.062$, $d = 0.392$) for the SSC condition (2.13 ± 0.03 μm, blue line, **Figure 6**) compared with 0.82 ISO (2.12 ± 0.02 μm, red dashed line, **Figure 6**) and compared with the shortening condition (2.13 ± 0.04 μm, $p = 0.654$, $d = 000$). For the stretch condition (2.50 ± 0.02 μm, purple line, **Figure 6**), sarcomere lengths were not statistically different (*ns*) ($p = 0.116$, $d = 0.632$) compared with 1.0 ISO (2.49 ± 0.01 μm, green dashed line of **Figure 6**).

Effects of Shortening and SSC on Mechanical Work by Blebbistatin

Mechanical work was significantly higher for the SSC condition (black circles of **Figure 4B**) compared with the active shortening condition (white circles of **Figure 4B**) ($p \leq 0.001$, $d = 2.68$). **Figure 5B** shows the distinct force responses and work (colored areas under the curves) during the shortening phase of the SSC condition and the shortening condition, respectively. Mechanical work increased by 367% for the SSC condition compared with shortening in the presence of Blebbistatin (cf. **Figure 4B**).

Force-Kinetics During Isokinetic Ramp Perturbations

Comparing the active stretch during SSCs and stretch of the control condition without XB-inhibition (cf. **Figure 2** inset, first half) with the active stretch during SSCs and stretch of the Blebbistatin condition with XB-inhibition (cf. **Figure 6** inset, first half) revealed some distinct differences.

Without XB-inhibition, the muscle force increased steeply in the early phase of stretching. Then, up to about half of the stretching time, the force rapidly decreased with further stretching until it recovered by the end of the stretch (**Figure 2** inset, first half). In the presence of Blebbistatin, the force response during the entire active stretch period is characterized by a progressive rise in force (**Figure 6** inset, first half).

DISCUSSION

To the best of our knowledge, this study presents the first *in vitro* investigation of muscle fiber force/work production in physiologically relevant SSC conditions (a fast SSC along

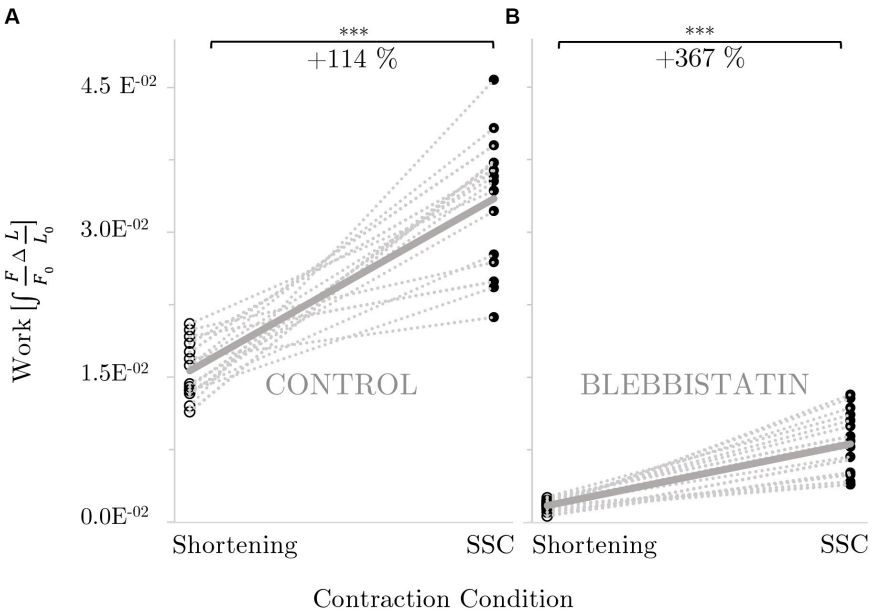

FIGURE 4 | Influence of active shortening and SSC on work for **(A)** control and **(B)** Blebbistatin experiments. The gray dotted lines indicate the individual paired data values and the gray solid line indicates the mean value (n = 16). Work is shown in normalized values ($\int \frac{F}{F0} \Delta \frac{L}{L0}$). Brackets and asterisks (*) mark differences in work obtained during active shortening [white circles] compared with stretch-shortening [SSC; black circles] conditions in the intergroup comparison. **(B)** Statistical analysis is based on muscle fiber experiments in the presence of Blebbistatin. Significance levels are marked as follows: $^{*}p < 0.05$, $^{**}p < 0.01$, and $^{***}p < 0.001$. *ns* means not significant.

the ascending limb to the plateau region of the force-length-relation). To separate XB (contractile component) and non-XB (structural proteins such as titin) contributions to total muscle force in skinned muscle fibers, we used the actomyosin inhibitor Blebbistatin. Our experiments reveal three main results: (*i*) during the stretch phase of the SSC and stretch conditions, a substantial decline follows an initial steep increase in force until the force recovers more slowly — compared to the initial rise in force — up to the end of the stretch (**Figure 2** inset, first half). Further, (*ii*) force output and work during shortening were significantly enhanced for SSCs compared with active shortening conditions (**Figure 4A**). (*iii*) No rFD was observed following SSCs compared with significant rFD following active shortening conditions [cf. blue vs. yellow line of **Figures 2**, **3A** (b,c)].

Isometric Forces Following Ramp Perturbations (Steady-State Phase)-Comparison to Other Studies

The steady-state isometric force following stretch was 4.2% higher (rFE), and the isometric steady-state force following active shortening was 3.1% smaller (rFD), relative to the corresponding isometric reference at the same fiber length (**Table 1**). Similar increases and decreases in force were observed in previous studies which used soleus fibers of the rat (Campbell and Moss, 2002), lumbrical muscles fibers of the frog (Bullimore et al., 2008), soleus muscles of the cat (Herzog and Leonard, 2000; Bullimore et al., 2007) as well as muscles from the hind limb of the rabbit (soleus, gastrocnemius, and plantaris) (Siebert et al., 2015).

There was no difference between the isometric reference force and the corresponding force in the steady-state phase following SSCs [**Figure 3A** (c)]. This result suggests that FE generated during the active lengthening phase of SSCs persisted during the subsequent shortening phase, thereby counteracting shortening-induced rFD when the shortening was preceded by stretching (SSC).

Also, the steady-state force after the SSCs was significantly higher by 2.6%, compared with the steady-state force after active shortening with the same magnitudes of shortening [**Table 1** and **Figure 3A** (b)]. A similar increase in force was observed in a previous *in vitro* study using skinned soleus fibers of the rabbit (Fukutani and Herzog, 2019). Our results also agree with *in vivo* findings using muscles of the human plantar flexor and human adductor pollicis showing increased forces after SSCs compared with active shortening (Seiberl et al., 2015b; Hahn and Riedel, 2018).

Influence of Contraction Velocity on XB-Dynamics During Stretch (Transient Phase)

Muscle fiber kinetics during the stretch phase of SSCs and active stretches were characterized by two consecutive peaks with a relatively compliant transient phase in between (cf. **Figure 2** inset, first half). This distinct behavior has been referred to muscle 'slippage' or 'give,' in which the force redevelops more slowly after an internal 'give' (Katz, 1939; Flitney and Hirst, 1978; Griffiths et al., 1980; Choi and Widrick, 2010). It has been attributed to (partial) XB-detachment under strain when

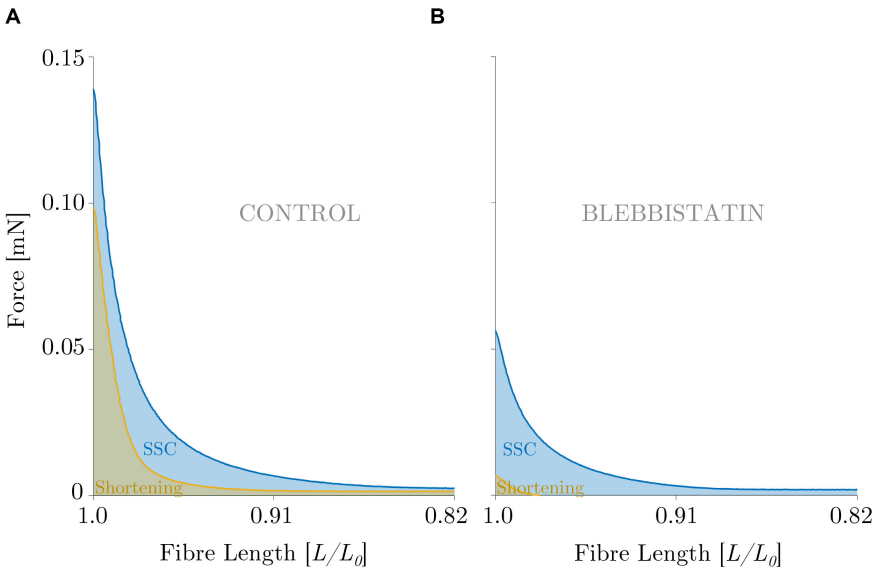

FIGURE 5 | Direct visual comparison of mechanical work output obtained during the **(A)** control and the **(B)** Blebbistatin experiments. Representative force-length trace of a permeabilized single fiber segment from a rat soleus muscle (n = 1, raw data). Mechanical work was determined for a period of 450 ms during the shortening phase from the onset of release until the end of release using numerical integration of force with respect to length. The solid blue line indicates the shorting phase of the SSC, and the solid yellow line shows the active shortening condition. The blue and the brown shaded areas represent the line integrals for the SSC and shortening condition, respectively. The force is shown in mN and the fiber length is normalized to the optimum fiber length (L/L_0). **(A)** The 'CONTROL' condition refers to the experiments without XB-inhibition, **(B)** 'BLEBBISTATIN' refers to the experiments with XB-inhibition.

stretching velocities exceed a given threshold (Huxley, 1969; Sugi, 1972). This indicates that the peak force (referred to the first peak, cf. **Figure 2** inset, first half) represents the force at which XBs are forcibly detached by the stretch (Bagni et al., 2005).

Under physiological conditions — e.g., during fast jumps or sprinting — the human soleus performs fast SSCs (<250 ms ground contact time) at moderate to high contraction velocities (at about 85% v_{max}, equivalent to around 6 FL/s) (Ranatunga, 1984; Bobbert et al., 1986; Widrick et al., 1997; Komi, 2002; Fukashiro et al., 2006). By that, the human soleus' operating range covers the ascending limb and the plateau-region of the force-length-relation (Burkholder and Lieber, 2001; Kurokawa et al., 2003). Our results indicate that at a high contraction velocity (as carried out in this study) XB-dynamics are altered compared with slow and moderate contraction velocities. This assumption is further based on an inherent muscle property which is attributed to short-range stiffness. Short-range stiffness is associated with a slightly damped stiffness with which active muscles resist small, rapid changes in length (Rack and Westbury, 1974; Campbell and Lakie, 1998). It is seen as the deformation of existing cross-bridges without compelling breakdown or reformation (Morgan, 1977). The initial steep linear rise in force upon active muscle stretching for extensions of 327–375 μm (equivalent to 1.16–1.34% L_0) is followed by a negative force slope (**Figure 2**, inset). This transition phase resembles the 'give' termed S2 by Flitney and Hirst (1978) in frog muscle experiments. When the displacement of the filaments in the axial direction exceeds 11–12 nm, the XBs are forcibly detached and sarcomeres are no longer able to resist the rise in force upon active muscle stretching (Flitney and Hirst, 1978). Hence, only a fraction of attached XBs contributes to the total force response during the stretching phase of fast stretches and SSCs, while the other fraction of XBs becomes detached. Thus, short-range stiffness associated with 'slippage' – resulting in altered XB-dynamics – might have an impact on the magnitude of (r)FE (Fukutani et al., 2019).

Nevertheless, for stretch and SSCs starting from 0.82 L_0, mean forces of 1.25 F/F_0 were observed at the end of the stretch where fibers were at the plateau region of the force-length-relation. These force magnitudes exceeded the maximum active forces produced by XBs at these lengths according to the sliding filament and XB-theories. It has been suggested that force enhancement may be caused by the engagement of titin during active muscle stretching (Rode et al., 2009; Edman, 2012; Tomalka et al., 2017; Herzog, 2018). Forces during the stretch exceeding F_0 (**Figure 2**) are in line with findings by Tomalka et al. (2017) in skinned EDL muscle preparations. They observed maximum forces up to 2.5 F/F_0 on the descending limb of the force-length-relation during stretching with constant stretch amplitudes of 0.45 L_0 at a given velocity of 10% v_{max}. Comparable results can be expected for the soleus when tested under equal experimental conditions.

Mechanical Work Output in SSCs vs. Active Shortening (Shortening Phase)

We examined the increase in mechanical work in SSCs compared with active shortening conditions.

The results of this study reveal greater work performed during shortening with preceding stretch (SSC) compared with shortening without preceding stretch (**Figure 4A**). Several factors may explain this increased work production, as they

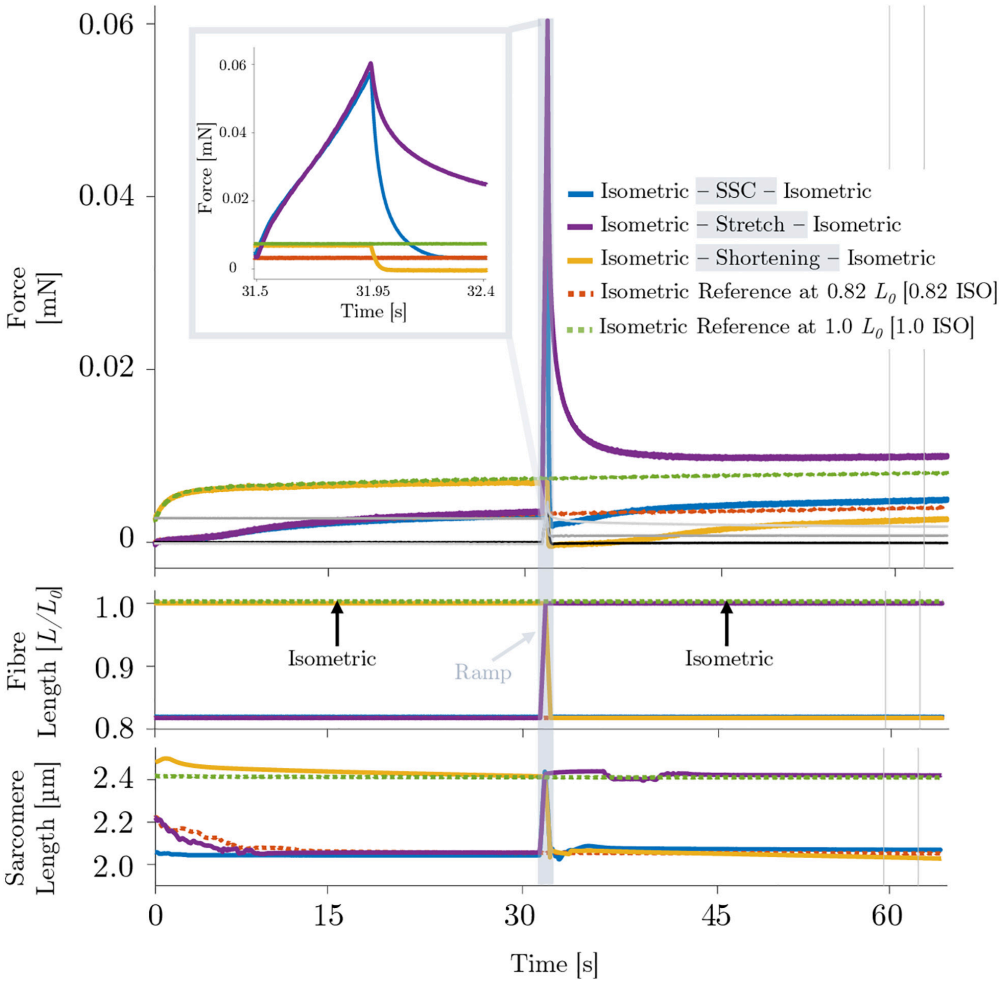

FIGURE 6 | Representative force–time (upper graph), fiber length–time (middle graph) and sarcomere length–time traces of different isokinetic ramp perturbations (SSC, shortening, stretch) applied to a permeabilized single fiber segment from a rat soleus muscle (n = 1) of the Blebbistatin experiment. The actomyosin inhibitor Blebbistatin (20 µmol l^{-1}) leads to marginal active isometric muscle force levels. Inset: enlarged view of the force response during an active SSC. For reasons of clarity, the passive traces have not been shown in the shaded rectangle or as part of the figure legend.

are: (*a*) increased elastic energy in the attached XBs, (*b*) contribution of active XB-forces, and (*c*) engagement of the giant filamentous structure titin.

When an activated muscle fiber is stretched, the attached XBs are also stretched and generate greater force (Huxley, 1957). It is assumed that elastic energy stored in elongated XBs, the myofilaments (Huxley et al., 1994; Wakabayashi et al., 1994) and crosslinking structures as the Z-disk (Luther, 2009; Burgoyne et al., 2015) may contribute to increased force and work during the stretch (Tomalka et al., 2017). As previously shown, peak forces at the end of an active stretch are higher for fast stretching velocities compared with slow stretching velocities (Edman et al., 1978; Sugi and Tsuchiya, 1988; Lombardi and Piazzesi, 1990). Consequently, the higher the stretching velocity, the higher the magnitude of elastic energy stored in XBs (Fukutani et al., 2017). Although fast stretching rates of 85% v_{max} (as carried out in this study) lead to, at least partial, detachment of bound XBs ('slippage,' cf. section "Influence of Contraction Velocity on XB-Dynamics During Stretch (Transient Phase)"), the reattachment of detached XBs is also very rapid (Lombardi and Piazzesi, 1990). Consequently, it can be speculated that elastic energy stored in XBs (due to the alteration of the XB-cycle) during stretching might contribute to the SSC-effect — albeit to a small fraction.

However, work in the shortening phase of the SSC condition was about twice as high than in the active shortening condition (**Figures 4A**, **5A**). Consequently, factors other than altered XB-dynamics must have contributed to enhanced work output in SSCs.

Titin is known to be a significant contributor to the enhanced/depressed force response [(r)FE/(r)FD] during active stretch/shortening contractions (Rode et al., 2009; Leonard and Herzog, 2010; Joumaa et al., 2017; Dutta et al., 2018). Active muscle lengthening leads to increased steady-state isometric forces after stretch (rFE) (**Figure 2**). rFE is long-lasting and highly correlated with the force at the end of active muscle stretching

TABLE 2 | Pairwise comparisons of isometric steady-state forces obtained during the Blebbistatin experiments.

Blebbistatin						
$\Delta F/F_0$	**Pairwise comparisons Δ F/F_0 [%]**				***n***	***p*-values**
	Mean differences	**s.d.**	**95% confidence interval of the difference**			
			Lower	**Upper**		
0.82 ISO - shortening	−0.53	0.96	−0.35	1.41	16	0.086
0.82 ISO - SSC	−0.13	0.53	−0.36	0.62	16	0.686
Shortening - SSC	0.40	0.96	−1.28	0.48	16	0.236
1.0 ISO - stretch	2.41	1.12	−2.80	−1.82	16	<0.001

Force values ± s.d. are normalized to the forces obtained during actively isometric reference contractions at corresponding end lengths (0.82 L_0 [0.82 ISO] for active shortening and stretch-shortening [SSC] conditions, respectively, and 1.0 L_0 [1.0 ISO] for active stretch conditions). Statistical analyses are based on experiments in the presence of Blebbistatin. Forces are calculated 28–33 s after the end of each ramp and differences ($\Delta F/F_0$) are expressed in percentage (%). ns means not significant ($p < 0.05$). n is the number of samples.

(Noble, 1992; Bullimore et al., 2007). The findings of our study suggest that rFE generated during the active lengthening phase of SSCs persisted during the subsequent shortening phase, thereby contributing to the increased force output and work production (Seiberl et al., 2015b). Thus, we suggest that SSC-effects are likely related to rFE, which is in accordance to previous findings (Seiberl et al., 2015b; Fukutani et al., 2017; Fortuna et al., 2018; Hahn and Riedel, 2018; Fukutani and Herzog, 2019).

Chemical XB-Inhibition by Blebbistatin

Isometric Forces Following Ramp Perturbations

The explanations for the SSC-effect given above are supported by the investigations of XB-contributions and non-XB-contributions to total muscle force (Blebbistatin condition) under different contraction conditions (SSC, shortening, stretch). The isometric steady-state force after stretch conditions was 2.4% higher, and the isometric steady-state force following shortening was not statistically different, relative to the corresponding isometric reference force at the same fiber length (**Table 2**). A similar increase in force (rFE) was observed in previous studies (using either Blebbistatin or BDM) on rabbit psoas muscle fibers (Cornachione and Rassier, 2012), mice soleus muscle fibers (Labeit et al., 2003) and frog tibialis anterior muscle (Bagni et al., 2002). A similar reduction, or even absence, of depressed forces (rFD) after shortening (during XB-inhibition) was observed in skinned psoas fibers from rabbits in the presence of BDM (Joumaa et al., 2012).

Assuming that potential titin-actin interactions do not require active force production and strong XB-binding to actin, the same contribution of titin-actin interactions to rFE would be expected in the Blebbistatin condition compared with the control condition. On the contrary, if titin-actin interactions depend on XB-force, no rFE is expected if Blebbistatin suppresses XB-force to a negligible level of maximum active force. The results of this study, obtained by administering Blebbistatin, revealed approximately 42% reduced rFE (relatively) due to 95% suppression of XB-interaction compared with the control condition (cf. results of **Tables 1**, **2**). Thus, active XB-binding is necessary — at least partially — for the full development of rFE. These findings are in line with previous investigations (Leonard and Herzog, 2010; Powers et al., 2014) showing that XB-inhibition (using BDM) decreases the magnitude of (r)FE — compared with strong XB-binding. Furthermore, experiments on rabbit psoas myofibrils at very long lengths (>4 μm) (Leonard and Herzog, 2010) support this hypothesis, as no rFE was observed in the absence of actin-myosin overlap for myofibrils actively stretched from about 4.5 μm to 6 μm. Leonard and Herzog (2010) and Powers et al. (2014) suggested that either 'active (actin-myosin based) force' or XB-attachment to actin is required to produce rFE.

Influence of XB-Inhibition on Mechanical Work During Shortening

When the skinned soleus fibers were activated, then stretched, and immediately shortened (SSC condition), the work done during the shortening phase was about 3.7 times greater compared with the work during shortening (Blebbistatin condition) (**Figure 4B**). From our knowledge, this is the first study investigating mechanical work in muscle preparations with inhibition of XB-interaction.

The quasi-linear increase in force upon active muscle stretching (**Figure 6** inset, first half), while actin–myosin interaction is suppressed, indicates that 'slippage' of attached XBs is dramatically reduced or even eliminated during fast active stretching in the presence of Blebbistatin. Therefore, the progressively increasing forces during active stretching at constant velocity indicate a continuous loading of non-XB elastic structures until the stretching has stopped. Consequently, stored elastic energy recoils in the shortening phase of SSCs. However, compared with the shortening phase of the SSC in the control condition (**Figure 5A**, the area below the blue line), work during the shortening phase of the SSC was reduced by 76% in the Blebbistatin condition (**Figure 5B**, the area below the blue line). This reduction in work is broadly in agreement with an observed decrease in rFE of 42% in the Blebbistatin compared with the control condition. Hence, reduced XB-binding by Blebbistatin (by 95%) might — at least partially — prevent titin-binding to actin and thus preloading of a shortened free titin spring during stretching.

There is an absolute work enhancement (work during the shortening phase of a SSC > work during active shortening) in both, the control and the Blebbistatin condition. However, this absolute work enhancement (**Figure 5A**, the area between the blue and the yellow line) was reduced by 64% in the Blebbistatin condition (**Figure 5B**, the area between the blue and the yellow line) compared to the control condition. Minor work enhancement under Blebbistatin might be, for example, due to the elastic energy that is stored and released in remaining XBs (approximately 5%) or a limited number of

titin-actin interaction. Furthermore, calcium-induced stiffening of titin (Labeit et al., 2003; Joumaa et al., 2008b) might also contribute to minor work enhancement in SSCs compared with shortening, due to stretching of stiffer titin in SSC but not in active shortening.

Since Blebbistatin seems to affect the XB force, our approach does not clearly separate XB and non-XB contributions. Accordingly, alternative inhibitors as *N*-benzyl-p-toluene sulfonamide (BTS) should be considered for further studies attempting to separate XB and non-XB contributions (Iwamoto, 2018; Ma et al., 2018).

CONCLUSION

The findings of this study reveal the following: (*I*) The SSC-effect is present at the single skinned muscle fiber level. Thus, there is direct evidence that the underlying mechanisms of the SSC-effect are within the sarcomere itself. (*II*) In the control condition, work and rFE are larger than in the Blebbistatin condition. From this, we conclude that XB-cycling contributes — at least partially — to the SSC-effect, which is likely to result from allowing titin-actin interaction. (*III*) The SSC-effect is still present in the Blebbistatin condition with a negligible number of active XBs. Consequently, non-XB structures contribute to the SSC-effect and rFE, probably through titin-actin interaction and calcium-induced stiffening of titin. To develop the full amount of increased titin-based force, active force production and strong XB-binding to actin is required. As this potentially titin-based increase in work is generated almost passively with no or negligible metabolic cost, based on our findings we conclude that titin contributes to the efficiency of SSCs. These assumptions are further supported by recent studies demonstrating that titin-based passive stress can activate the thick filament in skeletal muscle independent of calcium. This further supports a possible role of titin in the regulation of muscle contractility, likely mediated by the mechano-sensing signaling pathway in the myosin filament (Fusi et al., 2016; Brunello and Fusi, 2020).

The experimental findings of this study contribute to a detailed understanding of the SSC on the cellular level. With SSCs as the most basic everyday type of muscular contraction, this information not only promotes the basic understanding of muscle function underlying human locomotion but can also be used, i.e., for development of efficient humanoid drives with application in the field of movement science, medical engineering, robotics and prosthetics. Thus, there is a considerable significance of the implementation of SSC experiments in movement simulations — requiring a fundamental understanding of the underlying mechanisms.

DATA AVAILABILITY STATEMENT

All datasets presented in this study are included in the article/**Supplementary Material**.

ETHICS STATEMENT

The studies involving animals were reviewed and approved according to the regulations of the German animal protection law (Tierschutzgesetz, §4 (3); Permit Number: 35-9185.81/0491) by the Regierungspräsidium Stuttgart, Department of Landwirtschaft, Ländlicher Raum, Veterinär- und Lebensmittelwesen.

AUTHOR CONTRIBUTIONS

TS, DH, WS, and AT contributed to the conceptualization of the study. SW and AT performed the experiments. AT analyzed the data and prepared the figures. AT, TS, DH, WS, and SW analyzed and discussed the results. AT and TS drafted the first version of the manuscript. AT, DH, TS, and WS edited and revised the manuscript. All authors contributed to the article and approved the submitted version.

FUNDING

This work was supported by the Deutsche Forschungsgemeinschaft (DFG) under grants SI841/15-1, SI841/17-1, HA 5977/5-1, and SE 2109/2-1 as well as partially funded by the DFG as part of the German Excellence Strategy – EXC 2075 – 390740016.

SUPPLEMENTARY MATERIAL

The Supplementary Material for this article can be found online at: https://www.frontiersin.org/articles/10.3389/fphys.2020.00921/full#supplementary-material

REFERENCES

Abbott, B. C., and Aubert, X. M. (1952). The force exerted by active striated muscle during and after change of length. *J. Physiol.* 117, 77–86. doi: 10.1113/jphysiol.1952.sp004733

Bagni, M. A., Cecchi, G., and Colombini, B. (2005). Crossbridge properties investigated by fast ramp stretching of activated frog muscle fibres. *J. Physiol.* 565, 261–268. doi: 10.1113/jphysiol.2005.085209

Bagni, M. A., Cecchi, G., Colombini, B., and Colomo, F. (2002). A non-cross-bridge stiffness in activated frog muscle fibers. *Biophys. J.* 82, 3118–3127. doi: 10.1016/s0006-3495(02)75653-1

Bianco, P., Nagy, A., Kengyel, A., Szatmári, D., Mártonfalvi, Z., Huber, T., et al. (2007). Interaction forces between F-actin and titin PEVK domain measured with optical tweezers. *Biophys. J.* 93, 2102–2109. doi: 10.1529/biophysj.107.106153

Bobbert, M., Huijing, P., and van Ingen Schenau, G. (1986). A model of the human triceps surae muscle-tendon complex applied to jumping. *J. Biomech.* 19, 887–898. doi: 10.1016/0021-9290(86)90184-3

Bosco, C., Montanari, G., Ribacchi, R., Giovenali, P., Latteri, F., Iachelli, G., et al. (1987). Relationship between the efficiency of muscular work during jumping and the energetics of running. *Eur. J. Appl. Physiol. Occup. Physiol.* 56, 138–143. doi: 10.1007/BF00640636

Bottinelli, R., Canepari, M., Pellegrino, M. A., and Reggiani, C. (1996). Force-velocity properties of human skeletal muscle fibres: myosin heavy chain isoform and temperature dependence. *J. Physiol.* 495(Pt 2), 573–586. doi: 10.1113/jphysiol.1996.sp021617

Brenner, B. (1983). Technique for stabilizing the striation pattern in maximally calcium-activated skinned rabbit psoas fibers. *Biophys. J.* 41, 99–102. doi: 10.1016/s0006-3495(83)84411-7

Brunello, E., and Fusi, L. (2020). A new spring for titin. *J. Physiol.* 598, 213–214. doi: 10.1113/JP279314

Brunello, E., Fusi, L., Ghisleni, A., Park-Holohan, S. J., Ovejero, J. G., Narayanan, T., et al. (2020). Myosin filament-based regulation of the dynamics of contraction in heart muscle. *Proc. Natl. Acad. Sci. U.S.A.* 117, 8177–8186. doi: 10.1073/pnas.1920632117

Bullimore, S. R., Leonard, T. R., Rassier, D. E., and Herzog, W. (2007). History-dependence of isometric muscle force: effect of prior stretch or shortening amplitude. *J. Biomech.* 40, 1518–1524. doi: 10.1016/j.jbiomech.2006.06.014

Bullimore, S. R., MacIntosh, B. R., and Herzog, W. (2008). Is a parallel elastic element responsible for the enhancement of steady-state muscle force following active stretch? *J. Exp. Biol.* 211, 3001–3008. doi: 10.1242/jeb.021204

Burgoyne, T., Morris, E. P., and Luther, P. K. (2015). Three-dimensional structure of vertebrate muscle Z-band: the small-square lattice Z-band in rat cardiac muscle. *J. Mol. Biol.* 427, 3527–3537. doi: 10.1016/j.jmb.2015.08.018

Burkholder, T. J., and Lieber, R. L. (2001). Review sarcomere length operating range of vertebrate muscles during movement. *J. Exp. Biol.* 204, 1529–1536.

Campbell, K. S., and Lakie, M. (1998). A cross-bridge mechanism can explain the thixotropic short-range elastic component of relaxed frog skeletal muscle. *J. Physiol.* 510, 941–962. doi: 10.1111/j.1469-7793.1998.941bj.x

Campbell, K. S., and Moss, R. L. (2002). History-dependent mechanical properties of permeabilized rat soleus muscle fibers. *Biophys. J.* 82, 929–943. doi: 10.1016/s0006-3495(02)75454-4

Cavagna, G. A., Dusman, B., and Margaria, R. (1968). Positive work done by a previously stretched muscle. *J. Appl. Physiol.* 24, 21–32. doi: 10.1152/jappl.1968.24.1.21

Chen, J., Hahn, D., and Power, G. A. (2019). Shortening-induced residual force depression in humans. *J. Appl. Physiol.* 126, 1066–1073. doi: 10.1152/japplphysiol.00931.2018

Choi, S. J., and Widrick, J. J. (2010). Calcium-activated force of human muscle fibers following a standardized eccentric contraction. *Am. J. Physiol. Cell Physiol.* 299, 1409–1417. doi: 10.1152/ajpcell.00226.2010

Cohen, J. (1988). *Statistical Power Analysis for the Behavioral Sciences*, 2nd Edn. Hoboken, NJ: Taylor and Francis.

Cormie, P., Mcguigan, M., and Newton, R. (2011). Developing maximal neuromuscular Part 1 – biological basis of maximal power production. *Sports Med.* 41, 17–39.

Cornachione, A. S., and Rassier, D. E. (2012). A non-cross-bridge, static tension is present in permeabilized skeletal muscle fibers after active force inhibition or actin extraction. *Am. J. Physiol. Cell Physiol.* 302, C566–C574. doi: 10.1152/ajpcell.00355.2011

Dutta, S., Tsiros, C., Sundar, S. L., Athar, H., Moore, J., Nelson, B., et al. (2018). Calcium increases titin N2A binding to F-actin and regulated thin filaments. *Sci. Rep.* 8, 1–11.

Edman, K. A. P. (2012). Residual force enhancement after stretch in striated muscle. A consequence of increased myofilament overlap? *J. Physiol.* 590, 1339–1345. doi: 10.1113/jphysiol.2011.222729

Edman, K. A. P., Elzinga, G., and Noble, M. (1978). Enhancement of mechanical performance by stretch during tetanic contractions of vertebrate skeletal muscle fibres. *J. Physiol.* 281, 139–155. doi: 10.1113/jphysiol.1978.sp012413

Flitney, F., and Hirst, D. (1978). Cross-bridge detachment and sarcomere 'give' during stretch of active frog's muscle. *J. Physiol.* 449–465. doi: 10.1113/jphysiol.1978.sp012246

Fortuna, R., Kirchhuebel, H., Seiberl, W., Power, G. A., and Herzog, W. (2018). Force depression following a stretch-shortening cycle is independent of stretch peak force and work performed during shortening. *Sci. Rep.* 8:1534.

Freundt, J. K., and Linke, W. A. (2019). Titin as a force-generating muscle protein under regulatory control. *J. Appl. Physiol.* 126, 1474–1482. doi: 10.1152/japplphysiol.00865.2018

Fryer, M. W., Owen, V. J., Lamb, G. D., and Stephenson, D. G. (1995). Effects of creatine phosphate and P(i) on Ca2+ movements and tension development in rat skinned skeletal muscle fibres. *J. Physiol.* 482, 123–140. doi: 10.1113/jphysiol.1995.sp020504

Fukashiro, S., Hay, D., and Nagano, A. (2006). Biomechanical behavior of muscle-tendon complex during dynamic human movements measuring the muscle-tendon complex by ultrasonography. *J. Appl. Biomech.* 22, 131–147. doi: 10.1123/jab.22.2.131

Fukutani, A., and Herzog, W. (2019). Influence of stretch magnitude on the stretch-shortening cycle in skinned fibres. *J. Exp. Biol.* 222:jeb.206557. doi: 10.1242/jeb.206557

Fukutani, A., Joumaa, V., and Herzog, W. (2017). Influence of residual force enhancement and elongation of attached cross-bridges on stretch-shortening cycle in skinned muscle fibers. *Physiol. Rep.* 5:e13477. doi: 10.14814/phy2.13477

Fukutani, A., Leonard, T., and Herzog, W. (2019). Does stretching velocity affect residual force enhancement? *J. Biomech.* 89, 143–147. doi: 10.1016/j.jbiomech.2019.04.033

Fusi, L., Brunello, E., Yan, Z., and Irving, M. (2016). Thick filament mechano-sensing is a calcium-independent regulatory mechanism in skeletal muscle. *Nat. Commun.* 7:13281. doi: 10.1038/ncomms13281

Gregor, R. J., Roy, R. R., Whiting, W. C., Lovely, R. G., Hodgson, J. A., and Edgerton, V. R. (1988). Mechanical output of the cat soleus during treadmill locomotion: *in vivo* vs in situ characteristics. *J. Biomech.* 21, 721–732. doi: 10.1016/0021-9290(88)90281-3

Griffiths, P. J., Güth, K., Kuhn, H. J., and Rtiegg, J. C. (1980). Cross bridge slippage in skinned frog muscle fibres. *Biophys. Struct. Mech.* 7, 107–124. doi: 10.1007/bf00538402

Hahn, D., and Riedel, T. N. (2018). Residual force enhancement contributes to increased performance during stretch-shortening cycles of human plantar flexor muscles *in vivo*. *J. Biomech.* 77, 190–193. doi: 10.1016/j.jbiomech.2018.06.003

Haselgrove, J. C. (1975). X-ray evidence for conformational changes in the myosin filaments of vertebrate striated muscle. *J. Mol. Biol.* 92, 113–143. doi: 10.1016/0022-2836(75)90094-7

Herzog, W. (2018). The multiple roles of titin in muscle contraction and force production. *Biophys. Rev.* 10, 1187–1199. doi: 10.1007/s12551-017-0395-y

Herzog, W., and Leonard, T. R. (2000). The history dependence of force production in mammalian skeletal muscle following stretch-shortening and shortening-stretch cycles. *J. Biomech.* 33, 531–542. doi: 10.1016/s0021-9290(99)00221-3

Herzog, W., Schappacher, G., DuVall, M., Leonard, T. R., and Herzog, J. A. (2016). Residual force enhancement following eccentric contractions: a new mechanism involving Titin. *Physiology* 31, 300–312. doi: 10.1152/physiol.00049.2014

Huxley, A. F. (1957). Muscle structue and theories of contraction. *Prog. Biophys. Biophys. Chem.* 7, 255–318. doi: 10.1016/s0096-4174(18)30128-8

Huxley, H. (1969). The MECHANISM OF MUSCULAR CONTRAction. *Science* 164, 1356–1366.

Huxley, H. E., Stewart, A., Sosa, H., and Irving, T. (1994). X-ray diffraction measurements of the extensibility of actin and myosin filaments in contracting muscle. *Biophys. J.* 67, 2411–2421. doi: 10.1016/s0006-3495(94)80728-3

Iwamoto, H. (2018). Effects of myosin inhibitors on the X-ray diffraction patterns of relaxed and calcium-activated rabbit skeletal muscle fibers. *Biophys. Physicobiol.* 15, 111–120. doi: 10.2142/biophysico.15.0_111

Joumaa, V., Fitzowich, A., and Herzog, W. (2017). Energy cost of isometric force production after active shortening in skinned muscle fibres. *J. Exp. Biol.* 220, 1509–1515. doi: 10.1242/jeb.117622

Joumaa, V., and Herzog, W. (2013). Energy cost of force production is reduced after active stretch in skinned muscle fibres. *J. Biomech.* 46, 1135–1139. doi: 10.1016/j.jbiomech.2013.01.008

Joumaa, V., Leonard, T. R., and Herzog, W. (2008a). Residual force enhancement in myofibrils and sarcomeres. *Proc. Biol. Sci.* 275, 1411–1419. doi: 10.1098/rspb.2008.0142

Joumaa, V., Macintosh, B. R., and Herzog, W. (2012). New insights into force depression in skeletal muscle. *J. Exp. Biol.* 215, 2135–2140. doi: 10.1242/jeb.060863

Joumaa, V., Rassier, D. E., Leonard, T. R., and Herzog, W. (2008b). The origin of passive force enhancement in skeletal muscle. *Am. J. Physiol. Cell Physiol.* 294, C74–C78. doi: 10.1152/ajpcell.00218.2007

Katz, B. (1939). The relation between force and speed in muscular contraction. *J. Physiol.* 96, 45–64. doi: 10.1113/jphysiol.1939.sp003756

Kolega, J. (2004). Phototoxicity and photoinactivation of blebbistatin in UV and visible light. *Biochem. Biophys. Res. Commun.* 320, 1020–1025. doi: 10.1016/j.bbrc.2004.06.045

Komi, P. (2002). *Strength and Power in Sport (Encyclopaedia of Sports Medicine)*, ed. P. V. Komi (Hoboken, NJ: Blackwell Publishers).

Komi, P. V. (2000). Stretch-shorting cycle: a powerful model to study normal and fatigued muscle. *J. Biomech.* 33, 1197–1206. doi: 10.1016/s0021-9290(00)00064-6

Kurokawa, S., Fukunaga, T., Nagano, A., and Fukashiro, S. (2003). Interaction between fascicles and tendinous structures during counter movement jumping investigated *in vivo*. *J. Appl. Physiol.* 95, 2306–2314. doi: 10.1152/japplphysiol.00219.2003

Labeit, D., Watanabe, K., Witt, C., Fujita, H., Wu, Y., Lahmers, S., et al. (2003). Calcium-dependent molecular spring elements in the giant protein titin. *Proc. Natl. Acad. Sci. U.S.A.* 100, 13716–13721. doi: 10.1073/pnas.2235652100

Lee, H. D., Herzog, W., and Leonard, T. (2001). Effects of cyclic changes in muscle length on force production in in-situ cat soleus. *J. Biomech.* 34, 979–987. doi: 10.1016/S0021-9290(01)00077-X

Leonard, T. R., and Herzog, W. (2010). Regulation of muscle force in the absence of actin-myosin-based cross-bridge interaction. *Am. J. Physiol. Cell Physiol.* 299, C14–C20. doi: 10.1152/ajpcell.00049.2010

Li, Y., Unger, A., von Frieling-Salewsky, M., Rivas Pardo, J. A., Fernandez, J. M., and Linke, W. A. (2018). Quantifying the Titin contribution to muscle force generation using a novel method to specifically cleave the Titin springs *in situ*. *Biophys. J.* 114:645a. doi: 10.1016/j.bpj.2017.11.3480

Linari, M., Brunello, E., Reconditi, M., Fusi, L., Caremani, M., Narayanan, T., et al. (2015). Force generation by skeletal muscle is controlled by mechanosensing in myosin filaments. *Nature* 528, 276–279. doi: 10.1038/nature15727

Linari, M., Caremani, M., Piperio, C., Brandt, P., and Lombardi, V. (2007). Stiffness and fraction of Myosin motors responsible for active force in permeabilized muscle fibers from rabbit psoas. *Biophys. J.* 92, 2476–2490. doi: 10.1529/biophysj.106.099549

Lombardi, V., and Piazzesi, G. (1990). The contractile response during steady lengthening of stimulated frog muscle fibres. *J. Physiol.* 431, 141–171. doi: 10.1113/jphysiol.1990.sp018324

Luther, P. K. (2009). The vertebrate muscle Z-disc: sarcomere anchor for structure and signalling. *J. Muscle Res. Cell Motil.* 30, 171–185. doi: 10.1007/s10974-009-9189-6

Ma, W., Gong, H., and Irving, T. (2018). Myosin head configurations in resting and contracting murine skeletal muscle. *Int. J. Mol. Sci.* 19:2643. doi: 10.3390/ijms19092643

Maruyama, K., Natori, R., and Nonomura, Y. (1976). New elastic protein from muscle. *Nature* 262, 58–60. doi: 10.1038/262058a0

Morgan, D. L. (1977). Separation of active and passive components of short-range stiffness of muscle. *Am. J. Physiol.* 232, C45–C49. doi: 10.1038/sj.sc.3101154

Nagy, A. (2004). Differential actin binding along the PEVK domain of skeletal muscle titin. *J. Cell Sci.* 117, 5781–5789. doi: 10.1242/jcs.01501

Nishikawa, K. C., Monroy, J. A., Uyeno, T. E., Yeo, S. H., Pai, D. K., and Lindstedt, S. L. (2012). Is titin a "winding filament"? A new twist on muscle contraction. *Proc. R. Soc. B Biol. Sci.* 279, 981–990. doi: 10.1098/rspb.2011.1304

Noble, M. I. (1992). Enhancement of mechanical performance of striated muscle by stretch during contraction. *Exp. Physiol.* 77, 539–552. doi: 10.1113/expphysiol.1992.sp003618

Powers, K., Schappacher-Tilp, G., Jinha, A., Leonard, T., Nishikawa, K., and Herzog, W. (2014). Titin force is enhanced in actively stretched skeletal muscle. *J. Exp. Biol.* 217, 3629–3636. doi: 10.1242/jeb.105361

Rack, P., and Westbury, D. (1974). The short range stiffness of active mammalian muscle and its effect on mechanical properties. *J. Physiol.* 240, 331–350. doi: 10.1113/jphysiol.1974.sp010613

Ranatunga, K. W. (1982). Temperature-dependence of shortening velocity skeletal muscle. *J. Physiol.* 329, 465–483. doi: 10.1113/jphysiol.1982.sp014314

Ranatunga, K. W. (1984). The force-velocity relation of rat fast- and slow-twitch muscles examined at different temperatures. *J. Physiol.* 351, 517–529. doi: 10.2170/jjphysiol.34.1

Rassier, D. E. (2017). Sarcomere mechanics in striated muscles: from molecules to sarcomeres to cells. *Am. J. Physiol. Cell Physiol.* 313, C134–C145. doi: 10.1152/ajpcell.00050.2017

Rode, C., Siebert, T., and Blickhan, R. (2009). Titin-induced force enhancement and force depression: a "sticky-spring" mechanism in muscle contractions? *J. Theor. Biol.* 259, 350–360. doi: 10.1016/j.jtbi.2009.03.015

Schappacher-Tilp, G., Leonard, T., Desch, G., and Herzog, W. (2015). A novel three-filament model of force generation in eccentric contraction of skeletal muscles. *PLoS One* 10:e0117634. doi: 10.1371/journal.pone.0117634

Seiberl, W., Power, G. A., and Hahn, D. (2015a). Residual force enhancement in humans: current evidence and unresolved issues. *J. Electromyogr. Kinesiol.* 25, 571–580. doi: 10.1016/j.jelekin.2015.04.011

Seiberl, W., Power, G. A., Herzog, W., and Hahn, D. (2015b). The stretch-shortening cycle (SSC) revisited: residual force enhancement contributes to increased performance during fast SSCs of human m. *adductor pollicis*. *Physiol. Rep.* 3:e12401. doi: 10.14814/phy2.12401

Shalabi, N., Cornachione, A., Leite, F., Vengallatore, S., and Rassier, D. E. (2017). Residual force enhancement is regulated by titin in skeletal and cardiac myofibrils. *J. Physiol.* 595, 2085–2098. doi: 10.1113/JP272983

Siebert, T., Leichsenring, K., Rode, C., Wick, C., Stutzig, N., Schubert, H., et al. (2015). Three-dimensional muscle architecture and comprehensive dynamic properties of rabbit Gastrocnemius, Plantaris and Soleus: input for simulation studies. *PLoS One* 10:e0130985. doi: 10.1371/journal.pone.0130985

Soukup, T., Zachaøová, G., and Smerdu, V. (2002). Fibre type composition of soleus and extensor digitorum longus muscles in normal female inbred Lewis rats. *Acta Histochem.* 104, 399–405. doi: 10.1078/0065-1281-00660

Sugi, H. (1972). Tension changes during and after stretch in frog muscle fibres. *J. Physiol.* 225, 237–253. doi: 10.1113/jphysiol.1972.sp009935

Sugi, H., and Tsuchiya, T. (1988). Stiffness changes during enhancement and deficit of isometric force by slow length changes in frog skeletal muscle fibres. *J. Physiol.* 407, 215–229. doi: 10.1113/jphysiol.1988.sp017411

Tahir, U., Monroy, J. A., Rice, N. A., and Nishikawa, K. C. (2020). Effects of a titin mutation on force enhancement and force depression in mouse soleus muscles. *J. Exp. Biol.* 223:jeb197038. doi: 10.1242/jeb.197038

Tomalka, A., Rode, C., Schumacher, J., and Siebert, T. (2017). The active force – length relationship is invisible during extensive eccentric contractions in skinned skeletal muscle fibres. *Proc. R. Soc. B Biol. Sci.* 284:20162497. doi: 10.1098/rspb.2016.2497

Tomalka, A., Roehrle, O., Han, J.-C., Pham, T., Taberner, A. J., and Siebert, T. (2019). Extensive eccentric contractions in intact cardiac trabeculae: revealing compelling differences in contractile behaviour compared to skeletal muscles. *Proc. R. Soc. B Biol. Sci.* 286:20190719. doi: 10.1098/rspb.2019.0719

van Ingen Schenau, G. J., Bobbert, M. F., and de Haan, A. (1997). Does elastic energy enhance work and efficiency in the stretch-shortening cycle? *J. Appl. Biomech.* 13, 389–415. doi: 10.1123/jab.13.4.389

Van Ingen Schenau, G. J., Bobbert, M. F., and de Haan, A. (1997). Mechanics and energetics of the stretch-shortening cycle: a stimulating discussion. *J. Appl. Biomech.* 13, 484–496. doi: 10.1123/jab.13.4.484

Wakabayashi, K., Sugimoto, Y., Tanaka, H., Ueno, Y., Takezawa, Y., and Amemiya, Y. (1994).). X-ray diffraction evidence for the extensibility of actin and myosin filaments during muscle contraction. *Biophys. J.* 67, 2422–2435. doi: 10.1016/s0006-3495(94)80729-5

Widrick, J. J., Romatowski, J. G., Karhanek, M., and Fitts, R. H. (1997). Contractile properties of rat, rhesus monkey, and human type I muscle fibers. *Am. J. Physiol.* 272, R34–R42.

Conflict of Interest: The authors declare that the research was conducted in the absence of any commercial or financial relationships that could be construed as a potential conflict of interest.

frontiers in Physiology

ORIGINAL RESEARCH
published: 04 August 2020
doi: 10.3389/fphys.2020.00946

The Time-Course of Changes in Muscle Mass, Architecture and Power During 6 Weeks of Plyometric Training

Elena Monti[1,2†], Martino V. Franchi[1,2†], Francesca Badiali[2], Jonathan I. Quinlan[2,3,4], Stefano Longo[2,5] and Marco V. Narici[1,2,6*]*

[1] Institute of Physiology, Department of Biomedical Sciences, University of Padua, Padua, Italy, [2] MRC-ARUK Centre for Musculoskeletal Ageing, University of Nottingham, Derby, United Kingdom, [3] School of Sport, Exercise and Rehabilitation Sciences, University of Birmingham, Birmingham, United Kingdom, [4] NIHR Birmingham Biomedical Research Centre, University Hospitals Birmingham, NHS Foundation Trust and University of Birmingham, Birmingham, United Kingdom, [5] Department of Biomedical Sciences for Health, University of Milan, Milan, Italy, [6] CIR-Myo Myology Centre, Department of Biomedical Sciences, University of Padua, Padua, Italy

OPEN ACCESS

Edited by:
Geoffrey A. Power,
University of Guelph, Canada

Reviewed by:
Matt S. Stock,
University of Central Florida, United States
Jared R. Fletcher,
Mount Royal University, Canada

***Correspondence:**
Martino V. Franchi
martino.franchi@unipd.it
Marco V. Narici
marco.narici@unipd.it

[†] These authors have contributed equally to this work and share first authorship

Specialty section:
This article was submitted to Exercise Physiology, a section of the journal Frontiers in Physiology

Received: 29 May 2020
Accepted: 14 July 2020
Published: 04 August 2020

Citation:
Monti E, Franchi MV, Badiali F, Quinlan JI, Longo S and Narici MV (2020) The Time-Course of Changes in Muscle Mass, Architecture and Power During 6 Weeks of Plyometric Training. Front. Physiol. 11:946. doi: 10.3389/fphys.2020.00946

Purpose: To investigate the time-course of changes in knee-extensors muscle mass, architecture and function in response to plyometric training (PLT) performed on a novel training device, the Tramp-Trainer. This machine consists in a trampoline connected to an inclined sledge which allows the performance of repeated jumps while the subject is sitting on a chair.

Methods: Eight healthy males (173.6 ± 4.7 cm, 69.7 ± 13.5 kg, 25.3 ± 4.6 years) underwent 6 weeks of bilateral PLT on the tramp-trainer machine. Training was performed three times per week (between 120 and 150 bounces per session). Knee-extensor maximum voluntary torque (MVT) and power, quadriceps femoris (QF) volume (VOL), cross-sectional area from the 20% to the 60% of femur length and CSA_{mean}, together with vastus lateralis (VL) architecture (fascicle length, Lf, and pennation angle, PA) were assessed after 2, 4, and 6 weeks of PLT.

Results: All results are presented as changes versus baseline values. MVT increased by 17.8% (week 2, $p < 0.001$) and 22.2% (week 4, $p < 0.01$), respectively, and declined to 13.3% ($p < 0.05$) at week 6 of PLT. Power increased by 18.2% (week 4, $p < 0.05$) and 19.7% (week 6, $p < 0.05$). QF VOL increased by 4.7% (week 4, $p < 0.05$) and 5.8% (week 6, $p < 0.01$); VL VOL increased by 5.2%, ($p < 0.05$), 8.2%, ($p < 0.01$), and 9.6% ($p < 0.05$) at weeks 2, 4, and 6, respectively. An increase in Lf was detected already at wk 2 (2.2%, $p < 0.05$), with further increase at 4 and 6 weeks of PLT (4 and 4.4%, respectively, $p < 0.01$). PA increased by 5.8% ($p < 0.05$) at week 6. Significant positive correlations were found between CSA_{mean} and Power ($R^2 = 0.46$, $p < 0.001$) and between QF VOL and Power ($R^2 = 0.44$, $p < 0.024$).

Conclusions: PLT induced rapid increases in muscle volume, fascicle length, pennation angle, torque and power in healthy younger adults. Notably, changes in VL VOL and Lf were detectable already after 2 weeks, followed by increases in knee extensors

VOL and power from week 4 of PLT. Since the increase in CSA_{mean} and QF VOL cannot fully explain the increment in muscle power, it is likely that other factors (such as adaptations in neural drive or tendon mechanical properties) may have contributed to such fucntional changes.

Keywords: skeletal muscle, muscle volume, quadriceps cross-sectional area, muscle power, fascicle length, muscle hypertrophy

INTRODUCTION

Muscle power is a major contributor of performance both in sports and in daily life activities, and several studies have been carried out in order to understand how power could be improved in young, older, and clinical populations (Harries et al., 2012; Cook et al., 2013; Reid et al., 2015). In this regard, plyometric exercise has been shown to be particularly effective for improving muscular performance both in young athletes (Ramìrez-Campillo et al., 2014) and recreationally active people (Makaruk et al., 2011). During plyometric exercise, a physiological phenomenon called "stretch-shortening cycle" (SSC) is naturally occurring (Ishikawa and Komi, 2004; Taube et al., 2012). SSC is characterized by a deceleration of the body (where the agonist muscle-tendon unit -MTU- is stretched) followed immediately by an acceleration in the opposite direction (where the same MTU is rapidly shortened) (Komi, 1984). The SSC enhances the ability of the neuromuscular system to produce force in a brief amount of time, thus coupling the two major contributors to muscle power (i.e., muscle strength and contraction velocity) (Cardinale et al., 2011).

Increments in maximum isometric and explosive strength have been reported after plyometric training (PLT) protocols (de Villarreal et al., 2008; Behrens et al., 2016). Over a training period, the contributing factors to such increases can be found in (i) muscle morphological adaptations (i.e., architectural, whole muscle and muscle fibers size changes) (Pottiger Jeffrey et al., 1999; Blazevich et al., 2003; Malisoux et al., 2006b; McKinlay et al., 2012), (ii) tendon and joint stiffness properties (Hirayama et al., 2017), and (iii) modifications of neural activation (Behrens et al., 2014, 2016; Hirayama et al., 2017).

Although previous studies investigated the changes of skeletal muscle size, strength and power following plyometric training programs, to the present date and to the best of our knowledge, none of these studies focused on the time-course of the muscular adaptations to PLT. Defining when and how these changes occur may be beneficial in order to plan time-efficient protocols in healthy or clinical populations. In fact, when programming a training protocol aiming to elicit specific muscular adaptations (such as increases in explosive strength and power for athletes, or recovery of these qualities after injury) it is of extreme importance to know the timing and amplitude of such adaptations in order to plan personalized and efficient intervetions, with a well-defined progression of the load based on truly achievable goals.

However, one important aspect of the plyometric training methods reported in literature is that the majority of the studies exploited free-body plyometric exercise programs using different intensities, workloads, durations, number of sessions per week, and unilateral or bilateral modalities (Behrens et al., 2014; Piirainen et al., 2014; Hirayama et al., 2017). It follows that the guidelines for optimal PLT workloads are still unclear regarding the adaptations in muscle hypertrophy and function (Davies et al., 2015). Indeed, although specific laboratory tools (such as force platforms) may be useful to standardize PLT parameters, these tools are expensive and not always available where athletes train, nor at gyms and/or facilities where healthy and clinical population would carry out specific rehabilitation programs. Therefore, the use of easy accessible and user-friendly devices may be ideal for standardizing the work performed and the training intensties. In the present study we employed the tramp-trainer machine (FREI AG, Hinterzarten, Germany, EU) consisting of a trampoline attached to an inclined sledge, enabling the performance of repeated plyometric jumps while the subject is sitting on a chair with the back fully supported. With this device, exercise is performed seated and with a defined trajectory, which helps to standardize the exercise movement between different subjects. The trampoline offers to exercise on a compliant surface, and while being different from the stiffer ground exploited in the majority of the classical plyometric trainings, this is highly suitable for a wide range of users, from athletes during rehab, to healthy people, and even elderly frail populations (Franchi et al., 2019).

Hence, the aim of the present study was to investigate the time-course of knee-extensors changes in muscle size, architecture and function in response to a 6-week plyometric training performed on the tramp-trainer device. Based on previous reports that show that early adaptations in muscle architecture were observed with resistance exercise (Seynnes et al., 2007), our hypothesis was that changes in muscle architecture would characterize the early responses to plyometric training and that modifications in muscle size (i.e., cross-sectional area -CSA- and volume) and architecture would accompain increases in muscle torque and power.

MATERIALS AND METHODS

Participants

Fourteen young males were recruited to undergo a 6-weeks PLT program (height = 176.1 ± 6.3 cm, mass = 72.2 ± 13.8 kg, age = 25.4 ± 3.5 years). The pre-to-post adaptations to PLT (week 0 and week 6) are described in a previous study from our laboratory (Franchi et al., 2019). Among the fourteen participants, eight were randomly selected (height = 173.6 ± 4.7 cm, mass = 69.7 ± 13.5 kg, age = 25.3 ± 4.6 years; values are presented as mean ± SD)

to undergo the investigation of the time-course of morpho-functional assessments, which results are shown in this manuscript. All volunteers were healthy, fully independent and recreationally active; they had not performed any plyometric or heavy strength training within the past 6 months, and they were asked to not practice any other kind of physical activity during the study. During the 6-weeks of PLT, subjects were required to not change their lifestyle and recreational activity habits in comparison to the pre-training situation. All the subjects were medically screened by means of a medical questionnaire, to exclude sufferers of joint disease and metabolic, respiratory or cardiovascular impairments. All subjects provided written, informed consent. This study was approved by The University of Nottingham Ethics Committee and was compliant with the Declaration of Helsinki.

Trampoline-Trainer Exercise

Training was performed on the "Trampoline-Trainer" (tramp-trainer) exercise machine (**Figure 1**) (FREI AG, Hinterzarten, Germany, EU). As previously described (Franchi et al., 2019), the tramp-trainer is a device made up by an inclined trampoline connected to a 1.5 m inclined sledge. The user is seated on a movable chair attached to the sledge and is required to flex and extend the lower limbs on the trampoline against his own body weight. The legs are supported by two ankle braces connected to a spring, as shown in **Figure 1**. Briefly, the exercise can be compared, to a certain extent, to a leg press movement, where the workload is represented by the body mass and the inclination of the carriage. In order to elicit the greatest possible response to exercise, carriage inclination was set at the maximum angle allowed by the machine (22°) and kept constant for all the training sessions.

Volunteers exercising on the tramp-trainer start from a semi-squat position with their knees flexed to a range between 90 and 80 deg (counting 0 deg as anatomical zero/full leg extension). After a maximal push of the lower limb muscles (hip extensors, knee extensors, and plantar flexors), the body and chair are displaced along the rail, followed by a landing on the elastic trampoline and an immediate recoil as the subject bounces back off the trampoline, and the entire cycle is then repeated for successive jumps (Franchi et al., 2019). Thus, the movement can be also compared to a drop jump, with the evident differences of (i) the inclined falling trajectory and (ii) the compliant surface where the landing and bouncing actions are performed.

FIGURE 1 | Tramp Trainer exercise device.

Training Protocol and 30 Repetition Maximum (RM) Assessment

Prior to the first training session, on a separate day, participants were familiarized with the tramp-trainer, being asked to perform a maximum of only 5 submaximal bounces. During such familiarization session, each participant practiced starting and landing from a knee angle of ca. 90° measured with manual goniometer (full knee extension was taken as anatomical 0).

Training was performed 3 times per week (on the same days and at the same time for each session) for a period of 6 consecutive weeks. At least one resting day between training sessions was programmed. Training volume was based upon the guidelines of Chu (1998), who recommended that beginner and intermediate status athletes should not exceed 120 foot contacts per session when implementing a new PLT program. Training volume was set at 4 × 30 repetitions for the first 4 weeks, followed by 5 × 30 repetitions for the final 2 weeks. The 30 jumps were preformed consequently, while rest between sets was 120 s. The total duration of the training session was about 20–25 min (for the first 4 and the last 2 weeks, respectively). Before the beginning of the training session, a short warm up consisting in 10 squats was performed.

Training load was matched across subjects by determining 30RM values before the start of the program. 30RM is the training level at which subjects could perform no more than 30 repetitions without a decrease in bounce performance. To quantify bounce performance, a meter ruler was attached to the carriage of the training device to monitor, via an operator visual inspection, average bounce height during the assessment. Subjects were instructed to bounce at their 30RM, and if they fell significantly below their 30RM height for up to 3 consecutive bounces, they were prompted to increase bounce height in order to maintain a constant training load. A significant decrease was determined as 5 cm or more below the 30RM height.

As training progressed, loading increased progressively because the velocity of impact increased due to higher bounce distances. As bounce distance increased due to training adaptations, new 30RM values were identified and implemented to progressively increase the training load. 30RM values were re-checked every 7 days (before the start of the first session each new training week). When volunteers reached the highest value of the meter ruler attached to the carriage (i.e., the top of the carriage) for most (∼90%) of the repetitions in a single training session, a 15 kg weighted vest was provided from the successive session in order to further increase the training load. In addition, training load increase was provided by increasing the number of series from week 4 of the training period.

During each training session a red mark was placed on the side of the inclined plane rail-track as a visual target corresponding to a knee flexion of ca. 90°.

Functional and Morphological Parameters

To assess the time-course of training adaptations, test-sessions were performed before the beginning of the training (baseline), and after 2, 4, and 6 weeks of training. Testing sessions were scheduled right before the first training of the week, every 2 weeks, to allow a time lag of at least 48 h between the last training bout of the previous week and the testing day, in order to minimize exercise-induced edema. During all the test-sessions the following parameters were assessed: knee extensors isometric maximum voluntary contraction torque (MVT) and peak power production; vastus lateralis (VL) and quadriceps femoris muscle (QF) cross-sectional area (CSA) from the 20% to the 60% of the femur length, from which VL and QF volume were then estimated (see specific section below); VL muscle architecture at the 50% of the femur length. During the testing sessions, all participants were firstly scanned for US (VL architecture and QF CSAs) and afterward were randomly assigned to the following sequences (i) MVT testing first and power testing after (n = 4) or (ii) power testing first and MVT testing after (n = 4).

One week before baseline data collection -in the same day and time of the baseline session-, in 6 out of 8 subjects VL muscle architecture and QF and VL CSA were assessed, in order to evaluate the repeatability of the ultrasound operator through the Intraclass Correlation Coefficient (ICC) calculation.

Isometric MVT Testing

Isometric maximum voluntary torque was measured using an isokinetic dynamometer (Cybex Norm, Cybex International Inc., NY, United States) at a fixed joint angle of 70°, with full knee extension corresponding to 0°. The dynamometer had been previously calibrated following the manufacturer instructions, and gravity correction had been performed. After a brief warm-up, consisting of 10 short sub-maximal contractions at the 50% of MVT (1 s each), participants performed two maximum voluntary contractions, which lasted for 4 s, with a rest period of 30 s between contractions. Volunteers were provided with both real time visual feedback of torque production and a strong verbal encouragement during isometric contractions. The maximum isometric torque value (MVT peak) was chosen for data analysis.

Leg Extensor Power Testing

Knee extensors power was assessed using the Nottingham Power Rig (Nottingham University, Nottingham, United Kingdom). The power rig provides a measure of peak power during a hip and knee extension push againts a pedal (Bassey et al., 1992). Briefly, the device consist of a seat, and a lever (on which the feet are placed in order to exert force) which is connected to a flywheel by a chain. The leg extension movement is completed in 0.25–0.40 s. The resistance is minimal and remains nearly constant throughout the whole movement. On the testing day, participants were asked to push with both limbs as hard and as fast as possible (i.e., at their maximum velocity) on the raised foot plates through the full range of movement, and they were provided with strong verbal encouragement. Volunteers were required to perform a minimum of 5 repetitions of the leg-extension movement. If, within the 5 repetitions, a plateau was reached (i.e., the participant did not improve his performance from the 4th to the 5th repetition), the best value among the 5 trials was choosen for analysis. Conversely, if a progressive improvement in power was observed from the 4th repetition, unlimited efforts were allowed until a maximal power value was reached, and such value was considered for analysis. Participants were familiarized with the Nottingham Power Rig device, as at the first visit to the laboratory (prior to the first tesing session) they were asked to perform the exact protocol used for testing.

Muscle Cross-Sectional Area and Volume/Mass Calculation

Muscle CSA of the QF was measured *in vivo* using extended-field-of-view (EFOV) ultrasonography imaging (Mylab70, Esaote, Genoa, Italy). A 47 mm, 7.5 MHz linear array probe was used to obtain images at different muscle length percentages. Different region of interest were identified at the 20, 30, 40, 50, and 60% of the femur length (measured from greater trochanter to the mid patellar point) and marked on the skin (**Figure 2**). As shown in **Figure 2**, we considered the mid patellar point as the beginning of the QF and VL muscles (0%), and the great trochanter as their end (100%). The operator then positioned the probe transversally on the medial portion of the leg, thus starting the acquisition when the medial borders of the vastus medialis had been identified. The acquisition consisted in moving the transducer along the transverse plane and it was stopped after visualizing the lateral borders of the VL. An adjustable guide was used in each acquisition in order to keep the same transverse path. Care was taken in order to keep as constant as possible both pressure during all the image acquisition and acquisition velocity throughout the different testing sessions. Two CSA images per femur length percentage were acquired and used for analysis.

Quadriceps femoris and VL only CSAs were measured tracing the muscle borders using ImageJ image analysis software. Two measures per parameter were taken on each image, and the average of them was considered.

For simplicity, QF and VL muscle volume were estimated by using the truncated cone formula (shown in **Figure 2**), as previously reported (Tracy et al., 2003). Partial muscle volume values were calculated from the 20% to the 60% of the subjects' femur length using the CSAs data obtained from EFOV ultrasound scans. As no EFOV scans were performed below the 20% and above the 60% of the femur length marks, the remaining CSAs values for the 10, 70, 80, and 90% axials were estimated by fitting a spline curve (third order polynomial) through the CSA values that were truly measured (Seynnes et al., 2008).

The values corresponding to the 0 and 100% of the femur length were set as 0 (**Figure 2**). The calculated muscle volume, was assumed to closely approximate to muscle mass since muscle density is 1.0597 g/cm (Mendez and Keys, 1960).

Quadriceps femoris and VL volume were calculated as the sum of the calculated VOL between each femur length measured (20–60%) or estimated (10%, 70–90%) CSAs. In addition, QF CSA_{mean}

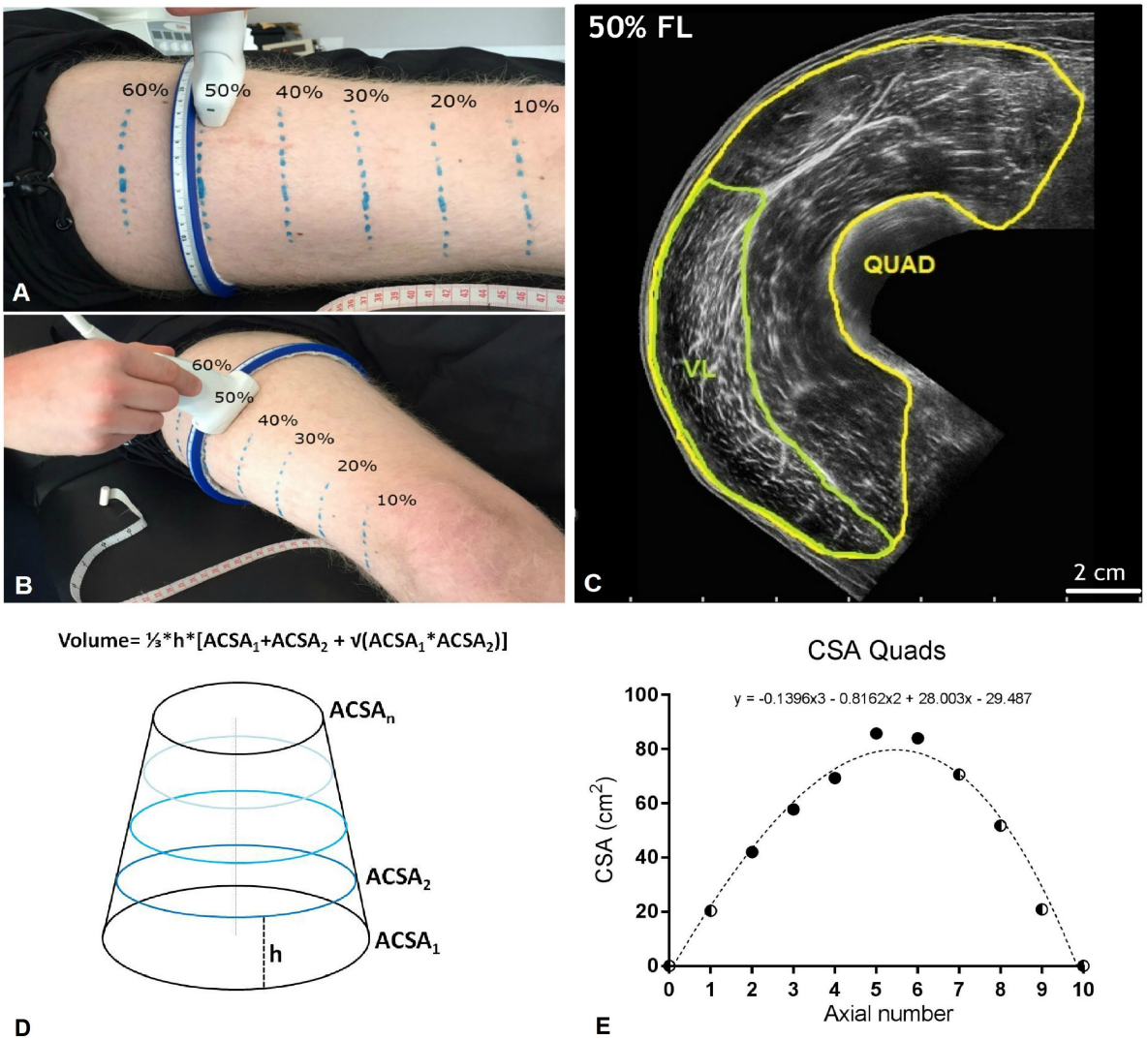

FIGURE 2 | (A,B) Ulatrsonographic assessment of quadriceps femoris (QF) cross-sectional area (CSA) at different percentages of the femur length (measured from the great throcanter to the mid-patellar point). Region of interests considered were 20, 30, 40, 50, and 60% of the femur length. **(C)** Quad and vastus lateralis (VL) CSA obtained at the 50% of the femur length from a representative subject. **(D)** Truncated cone formula. The muscle volume between each couple of contiguos axials was calculated as 1/3*h*[$ACSA_1$ + $ACSA_2$ + $\sqrt{(ACSA_1 * ACSA_2)}$], where ACSA stands for anatomical cross-sectional area. **(E)** Mathematical estimation of the lacking Quad CSA (10, 70, 80, and 90% of the femur length). A third order polynomial curve (reported for a representative subject) was fitted through the CSA values that were truly measured. For simplicity, the CSA values corresponding to the 0% and the 100% of the femur length were set as 0. Half and half symbols represent the estimated CSAs.

was calculated as the average value of the 10–90% femur length CSAs per each subject and time-point.

Muscle Architecture

Muscle architecture of the VL muscle was measured *in vivo* using B-mode ultrasonography (Mylab70, Esaote, Genoa, Italy). Ultrasound images were obtained on the right leg, while the participant was laying in supine position; the 50% of the femur length (measured from the great throcanther to the mid patellar point) was found and marked with a skin marker, and afterward the probe was orientated transversally and the medial and lateral borders of the VL were identified. The 50% of the distance between the VL borders was chosen for image acquisition. VL fascicle length (Lf) and pennation angle (PA) were measured using a 100 mm, 10–15 MHz, linear-array probe as described by Franchi et al. (2015): the probe was positioned over the belly of the VL, carefully adjusted to the fascicle plane while minimal pressure was applied. Three ultrasound scans were then analyzed using ImageJ image analysis software[1]. Briefly, fascicles were digitized using the segmented line tool (thus not neglecting any fascicle curvature within their visible portion). Then, fascicle length was determined through

[1]http://imagej.nih.gov/ij/

manual extrapolation (i.e., straight line tool used) of fibers and aponeuroses if a portion of the fascicle extended outside of the captured ultrasound image. Usually 2–3 fascicles were eveluated for each scan and their average value was taken as final Lf value. PA was measured at the intersection between the fascicles and the deep aponeurosis. An average of at least 3 PA measures per image was performed (Franchi et al., 2018).

Total External Mechanical Work

The total external mechanical work (W_{ext}, kJ) performed throughout the study was calculated as previously described (Franchi et al., 2019). Individual W_{ext} was calculated from body mass (plus 15 kg if participants were wearing the weighted vest), TT inclination, and average height reached during each bounce performed in each session relative to the maximum height of the track/carriage (i.e., every bounce height was recorded via visual inspection of an operator for all repetitions of set in each training session).

For a single set of 30 bounces, W_{ext} was calculated as follows:

$$W_{ext}\ (\text{kj}) = [(BM + VM) \times g \times (sin22)] \times (1.265\text{-}h_{ex}) \times 30$$

where BM (kg) represents the subject body mass, VM (kg) the mass of the weighted vest, g is the gravitational acceleration (9.81 $m{\cdot}s^{-2}$) multiplied by the sine of the pre-set inclination of the track, 22°(which was kept constant throughout the whole study), h_{ex} (m) represents the average height reached by every bounce in the set (relative to the total length of the track, 1.265 m), and 30 is the number of bounces performed per set.

Statistical Analysis

All data are presented as average values (and standard deviation).

A priori power analysis was performed using G*Power 3.1.9.4., using muscle power data obtained from a pilot study conducted in our laboratory. Power analysis revealed an actual power of 0.825 when considering a sample size of 8, with effect size being 1.02 and $\alpha = 0.05$.

All data met the normal distribution criteria, established on quantitative inspection by Shapiro–Wilk test. Repeatability of the measurements was tested for muscle mass (CSA) and architectural (Lf, PA) values via calculation of the Intraclass Correlation Coefficient (ICC) of the ultrasound operator performing all the data acquisition and analysis. ICC values were rated good to very good, and resulted as follows: QF CSA = 0.996 (CV = 0.01%); VL CSA = 0.993 (CV = 0.04%); VL PA = 0.962 (CV = 0.05%); VL Lf = 0.966 (CV = 0.09%).

In addition, basing on the same data used for the repeatability analysis (ICC), the minimum detectable change was calculated, following the approach suggested by Weir (2005). The percentage minimum detectable change values (i.e., the minimum percentage increase that would represent a real change, which would not be dictated by repeated measures errors) were as follows: QF CSA = 1.38% (±0.85 cm^2); VL CSA = 1.84% (±0.39 cm^2); VL PA = 1.93% (±0.35°); VL Lf = 1.38% (±0.11 cm).

Differences in the functional, morphological, and architectural muscle components of the study during the time-course (baseline vs. post 2, 4, and 6 weeks of training) were investigated using a one-way repeated measures analysis of variance (ANOVA). Tukey's multiple comparisons test was used to identify significance between the different time points. Significance level was set at $p < 0.05$.

Linear relationships between the percentage changes of the morphological and functional parameters during the time-course of PLT were tested using the Pearson's product-moment correlation coefficient (r). Linear regressions were also calculated and the coefficient of determination (R^2) was obtained. The level of significance was set at $p < 0.05$.

GraphPad Prism software (version 8.0; GraphPad software Inc., San Diego, CA, United States) was used to perform all statistical and *post hoc* analysis.

RESULTS

The average values for functional and morphological adaptations at each time point are presented in **Tables 1**, **2** (means ± S.D), while the percentage changes of the same parameters during the time-course -compared to baseline- are shown in **Figures 3**, **4**.

Time Course of Changes in Muscle Function

Mean MVT values increased by 17.8 ± 7.4% ($p < 0.001$) after only 2 weeks of PLT. After 4 weeks, MVT further increased (n.s. vs. week 2) reaching a peak percentage increment by 22.2 ± 12.2% compared to baseline ($p < 0.01$) (**Figure 3**). In contrast, post-training tests revealed a decrease in MVT values from week 4 to week 6 (n.s.); nonetheless pre-to-post MVT remained significantly different, presenting a total increase by 13.5 ± 10.8% ($p < 0.05$).

Power increased by 18.2 ± 15.4% ($p < 0.05$) after 4 weeks of PLT, reaching a final pre-to-post increment of 19.7 ± 13.5% ($p < 0.05$ vs. baseline) (**Figure 3**).

Time Course of Changes of QF and VL CSA and Volume

The time course of changes in muscle size is reported in **Table 2** and **Figures 3**, **4**.

Quadriceps femoris CSA showed significant adaptations after 2 weeks of PLT at 40 and 60% of the femur length, increasing, respectively, by 1.5 ± 1.0% and 3.5 ± 2.8% ($p < 0.05$). Similarly, VL CSA taken at the 40% and the 60% of the femur length increased, respectively, by 7.8 ± 4.9% and 4.9 ± 2.9% ($p < 0.05$) after 2 weeks of PLT.

From 4 weeks onwards, all the QF CSAs (except the one taken at the 20% of the femur length) showed a significant increment compared to baseline (at 20%: 5.6 ± 3.9%, $p < 0.05$; at 30%: 2.7 ± 2.6%, $p < 0.05$; at 50%: 2.4 ± 1.9%, $p < 0.05$; and at 60%: 4.2 ± 3.1%, $p < 0.05$). At 6 weeks, all QF CSAs were statistically larger compared to baseline (at 20%: 8.8 ± 4.9%, $p < 0.05$; at 30%: 7.7 ± 3.3%, $p < 0.001$; at 40%: 4.7 ± 2.2%, $p < 0.01$; at 50%: 3.1 ± 2.4%, $p < 0.05$; and at 60%: 5.1 ± 3.8%, $p < 0.05$).

Conversely, VL CSA increased only at the 40, 50, and 60% of the femur length after 4 ($p < 0.05$) and 6 weeks ($p < 0.05$)

TABLE 1 | Time-course of the muscle morphological and functional adaptations to a 6-week plyometric training.

	Baseline	Week 2	Week 4	Week 6	ANOVA
MVT (Nm)	230.37 ± 41.01	270.61 ± 46.98***	280.26 ± 52.46**	260.94 ± 51.06*	$F = 13.69$; $p = 0.0004$; $R^2 = 0.66$
Power (W)	519.64 ± 104.12	564.83 ± 125.20	609.54 ± 113.36*	617.50 ± 110.02*	$F = 11.42$; $p = 0.0042$; $R^2 = 0.66$
W_{Ext}/session (kJ)	27.67 ± 4.63	30.79 ± 6.25	31.22 ± 5.96*	39.41 ± 5.85***	$F = 52.03$ $p < 0.0001$ $R^2 = 0.88$
VL PA (deg)	16.50 ± 1.42	16.66 ± 1.56	17.27 ± 1.92	17.46 ± 1.73**	$F = 14.03$; $p = 0.0030$; $R^2 = 0.67$
VL Lf (cm)	7.79 ± 1.13	7.95 ± 1.05*	8.02 ± 1.11**	8.13 ± 1.17**	$F = 15.32$; $p = 0.0002$; $R^2 = 0.69$
QF CSA_{mean} (cm^2)	49.95 ± 8.37	51.74 ± 8.77	52.28 ± 8.78*	52.80 ± 8.66**	$F = 19.7$; $p = 0.0026$; $R^2 = 0.77$
QF volume (cm^3)	1867.70 ± 363.03	1934.19 ± 383.46	1954.40 ± 385.11*	1974.14 ± 382.01**	$F = 18.97$; $p = 0.0027$; $R^2 = 0.76$
VL volume (cm^3)	593.22 ± 123.46	623.71 ± 133.32*	640.99 ± 133.40**	648.70 ± 131.85*	$F = 14.91$; $p = 0.0016$; $R^2 = 0.71$

*All the parameters were assessed at baseline and at 2-, 4-, and 6-week time points. MVT, maximum voluntary torque; LEP, leg extensors muscles power; W_{ext}, external work; VL, vastus lateralis muscle; PA, pennation angle; Lf, fascicle length; QF, quadriceps femoris; CSA_{mean}, average of the cross-sectional areas taken at the 20, 30, 40, 50, and 60% of the femur length with the CSAs estimated at the 10, 80, and 90%. Results shown as Means ± SD. VS Baseline *p < 0.05, **p < 0.01, ***p < 0.001.*

TABLE 2 | Time-course of the vastus lateralis (VL) and quadriceps femoris (QF) cross-sectional areas (CSA) adaptations to a 6-week plyometric training.

VL CSA (cm^2)	Baseline	Week 2	Week 4	Week 6	ANOVA
20% FL	5.21 ± 2.01	5.69 ± 2.01	6.20 ± 1.93*	6.26 ± 2.32	$F = 4.916$; $p = 0.0307$; $R^2 = 0.50$
30% FL	11.28 ± 2.64	11.78 ± 2.48	12.39 ± 2.50	12.24 ± 2.63	$F = 8.602$; $p = 0.0096$; $R^2 = 0.63$
40% FL	17.24 ± 3.40	18.51 ± 3.51*	19.05 ± 3.55**	18.99 ± 3.49*	$F = 15.48$; $p = 0.0006$; $R^2 = 0.72$
50% FL	22.61 ± 4.76	23.65 ± 5.19	24.12 ± 5.23*	24.2 ± 4.91**	$F = 14.55$; $p = 0.0016$; $R^2 = 0.71$
60% FL	24.0 ± 4.04	25.19 ± 4.52*	25.86 ± 4.34***	26.65 ± 4.61*	$F = 7.702$; $p = 0.0231$; $R^2 = 0.56$
QF CSA (cm^2)	**Baseline**	**Week 2**	**Week 4**	**Week 6**	**ANOVA**
20% FL	37.79 ± 6.47	39.37 ± 8.44	40.33 ± 8.20	41.21 ± 7.96*	$F = 6.56$; $p = 0.0211$; $R^2 = 0.57$
30% FL	48.98 ± 10.52	50.41 ± 9.91	51.51 ± 10.15*	52.53 ± 10.30***	$F = 18.51$; $p \leq 0.0001$; $R^2 = 0.76$
40% FL	59.33 ± 11.20	60.14 ± 10.88**	60.74 ± 10.48	61.91 ± 10.42**	$F = 13.26$; $p = 0.0006$; $R^2 = 0.69$
50% FL	70.34 ± 10.21	71.01 ± 12.96	71.90 ± 12.94*	72.35 ± 12.74*	$F = 11.56$; $p = 0.0030$; $R^2 = 0.66$
60% FL	70.61 ± 12.16	72.92 ± 11.70*	73.42 ± 11.77*	73.96 ± 11.50*	$F = 14.41$; $p = 0.0060$; $R^2 = 0.71$

*CSAs are taken at the 20, 30, 40, 50, and 60% of the femur length (FL). Results shown as Means ± SD. VS Baseline *p < 0.05, **p < 0.01, ***p < 0.001.*

of PLT compared to baseline. Specifically, at 4 and 6 weeks, the percentage increment vs. baseline were, respectively: 10.9 ± 4.7% ($p < 0.01$) and 10.7 ± 7.1% ($p < 0.05$) for the 40%; 6.8 ± 4.0% ($p < 0.05$) and 7.4 ± 4.2% ($p < 0.01$) for the 50%; and 7.8 ± 2.6% ($p < 0.001$) and 11.2 ± 9.3% ($p < 0.05$) for the 60% of the femur length. Although, at week 6, VL CSA at the 20 and 30% of femur length showed a marked increase, this was not statistically significant (22.2 ± 19.6%, $p = 0.11$; and 9.2 ± 8.2%, $p = 0.07$; respectively).

Quadriceps femoris CSA_{mean} showed a progressive increment by 4.7 ± 2.8% at 4 weeks ($p < 0.05$ vs. baseline) and by 5.8 ± 2.7% at 6 weeks ($p < 0.01$ vs. baseline).

Quadriceps femoris volume increased by 4.7 ± 2.8% ($p < 0.05$) and 5.8 ± 2.6% ($p < 0.01$) after 4 and 6 weeks of PLT, respectively, compared to baseline. Compared to baseline, VL volume increased significantly by 5.2 ± 2.9% ($p < 0.05$) after only 2 weeks of PLT, by 8.2 ± 2.9% ($p < 0.01$) after 4 weeks, reaching an increment by 9.6 ± 5.7% ($p < 0.05$) at 6 weeks.

Time Course of VL Muscle Architecture Changes

Vastus lateralis Lf showed a significant increment by 2.2 ± 2.0% already after 2 weeks of training ($p < 0.05$), thereafter increasing linearly up to 4.0 ± 2.1% at week 4 compared to baseline ($p < 0.01$ vs. baseline and $p < 0.05$ vs. week 2) and by a further 0.4 ± 2.3% at week 6 (n.s. vs. week 4), reaching a final pre-to-post training increase by 4.4 ± 2.3% ($p < 0.01$) (**Figure 3**).

Vastus lateralis PA, instead, presented a significant increase only after 6 weeks of PLT ($p < 0.01$) by 5.8 ± 3.3% compared to baseline (**Figure 3**).

Correlations Between Changes in Muscle Function and Muscle Morphology

Significant correlations were found between training induced-changes in CSA_{mean} and Power ($R^2 = 0.46$, $p < 0.001$) as well as QF VOL and Power ($R^2 = 0.44$, $p < 0.024$).

None of the training induced-changes in muscle architecutre parameters (PA, Lf) were significantly correlated with the increase in Power.

Total External Mechanical Work

The total external mechanical work performed after the first training session (27 ± 4.6 kJ) was significantly different from the first session of the 4th week (31.2 ± 6 kJ, $P < 0.05$) and of the 6th (39.4 ± 5.9 kJ, $p < 0.001$) (**Table 1**). The average total work performed throughout the whole training period was 606.1 ± 124.6 kJ.

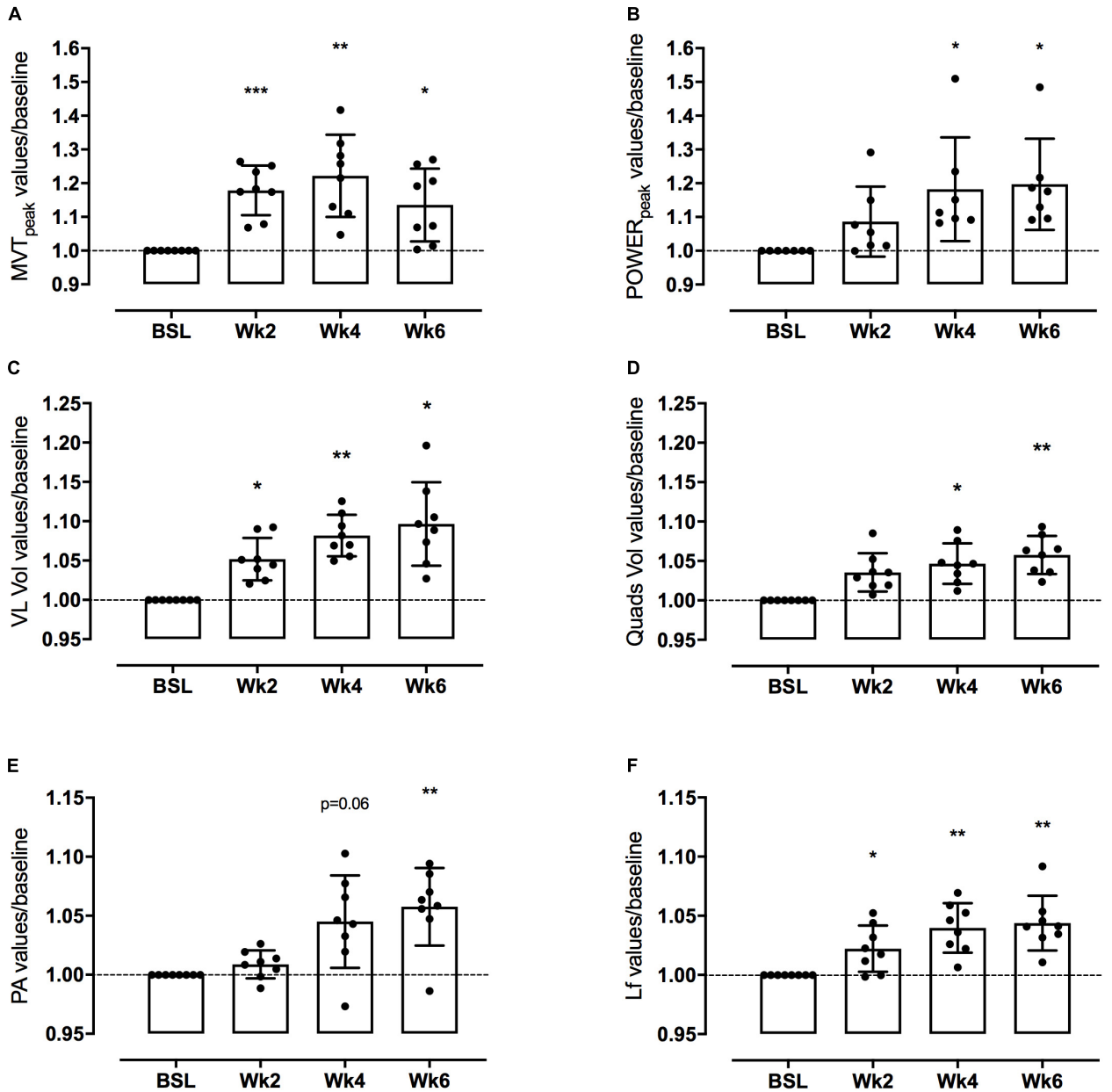

FIGURE 3 | Knee extensor maximum voluntary torque (MVT) and leg extensor power (LEP) (**A,B**, respectively), Vsatus Lateralis (VL) and quadriceps (QF) volume (**C,D**, respectively), Vastus Lateralis (VL) Pennation Angle (PA) and Length of fascicles (Lf) (**E,F**, respectively) adaptations to a 6-week PLT measured after 2, 4, and 6 weeks. Changes are expressed in percentage vs. baseline (Δ%). Results are normalized for baseline values and shown as Means with scattered plots ± SD. $^{*}p < 0.05$, $^{**}p < 0.01$, $^{***}p < 0.001$.

DISCUSSION

In the present study we investigated the time-course of changes in muscle mass, architecture and function in response to 6-week PLT performed on the tramp-trainer machine.

At the end of the training period, knee-extensors power was found to be increased by 19.7%, and this was accompanied by increments in both QF and VL volume and CSA_{mean}. In addition, VL Lf and PA increased by 4.4 and 5.8%, respectively.

Notably, early significant changes in muscle function (MVT), architecture (Lf) and morphology (VL and QF CSA, VL volume) were detectable after only 2 weeks of PLT. Among these changes, VL CSAs were found to be increased especially in muscle regions closer to the mid-belly, and a similar trend was observed for QF CSA. Furthermore, an increase in knee-extensors power (18.2%) was found just after 4 weeks of PLT, together with significant changes in QF volume (4.7%). Changes in QF

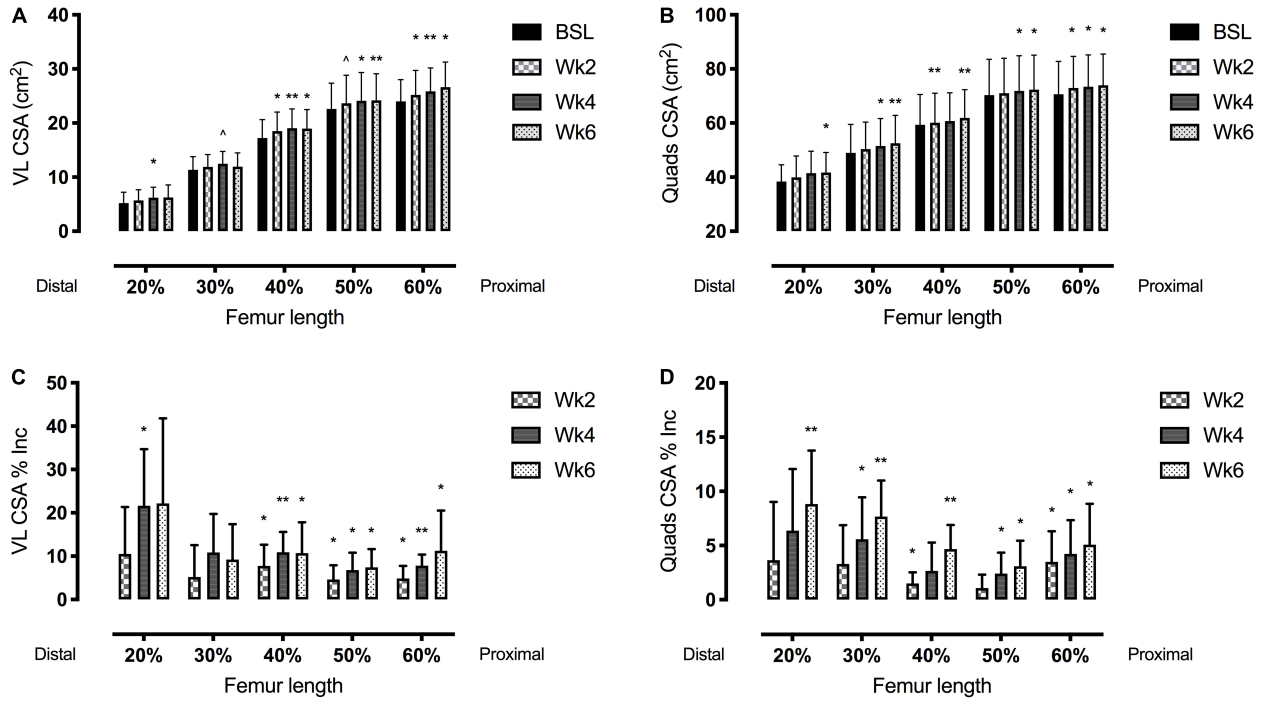

FIGURE 4 | Vastus lateralis (VL) (left side, **A,C**) and quadriceps femoris (right side, **B,D**) muscle cross-sectional area (CSA) adaptations to a 6-week plyometric training measured after 2, 4, and 6 weeks. Top panels represent muscle CSA changes in absolute values (cm^2). Bottom panels represent muscle CSA percentage changes (Δ%). Results are shown as Means ± SD. $^p = 0.05$, $^*p < 0.05$, $^{**}p < 0.01$.

volume significantly correlated with the increase in muscle power ($R^2 = 0.44$).

Adaptations in Muscle Function: Muscle Strength

The 6-week PLT intervention was highly effective for increasing knee-extensors MVT.

Consistent with previous studies investigating strength adaptations to training, the increase in MVT was very rapid, reaching 17.8% after just 2 weeks of training. A small portion of this increase can be explained by muscle hypertrophy (3.5% increase in QF CSA_{mean}), while it can be speculated that the main increment may be ascribable to an increased neural drive known to account for the early gain in muscle strength/power with resistance training (Narici et al., 1989; Häkkinen et al., 2001; Aagaard et al., 2002; Seynnes et al., 2007). As the training period progressed, MVT further increased to 22.2% at week 4 but no further increase was seen thereafter; in fact, at 6 weeks, the increase in MVT (13.3%) was 61% that of week 4. The slight decrement of MVT in the last 2 weeks of training is most likely due to a loading limitation (i.e., the training-load adjustments during the 6 weeks of PLT) of the plyometric training device used in this study. Indeed, as the participants bouncing performance improved, a 15 kg weighted vest was worn by the subjects to increase muscle loading, but as performance further improved at week 4, extra series were added to increase training volume. It seems thus that the combination of the 15 kg weighted vest plus the extra bounces series was not sufficient to provide enough muscle loading to achieve further gains in muscle strength after 4 weeks of training.

In addition, as gains in muscle strength appear to be training-specific (Tillin and Folland, 2014), another possible explanation could be related to the specificity of the movement used during plyometric training. In fact, this may have not been specific in relation to the one required to develop the maximal torque on the dynamometer device (i.e., isometric knee extension). Furthermore, only one joint angle (70°) was used to measure MVT throughout the whole study. Thus, we cannot exclude that a shift in the angle-torque relationship may have occurred in some volunteers as a resultant of more pronounced changes in muscle architectural features (Reeves et al., 2004). This would have in turn affected the force developed at a single joint angle (i.e., hence the 4-to-6 weeks drop in MVT).

The findings related to the increments in power and strength appear consistent with previous work, showing that exploiting combinations of countermovement jumps, drop-jumps, squat jumps and jumps using sledge apparatus would elicit enhancements in knee-extensors power and explosive force production (Pottiger Jeffrey et al., 1999; Fatouros et al., 2000; Kyröläinen et al., 2005; Piirainen et al., 2014). Some studies have shown that PLT could induce increases in knee-extensors maximum strength (Hakkinen et al., 1990; Fatouros et al., 2000; Malisoux et al., 2006b; Behrens et al., 2014), although others have reported no changes (Kyröläinen et al., 2005; Paleckis et al., 2015). The majority of these studies

included PLT performed on stiff grounds, which are different from the compliant surface of the tramp-trainer. However, the similarities of such results with the one of the present study, together with reports that PLT protocols conducted in different conditions [such as in water (Martel et al., 2005; Robinson et al., 2004)] lead to similar increases in torque and power outputs, seem to suggest that the adaptations observed for muscle function are in line with those found after "classic" PLTs.

A second critical point when comparing the results found in the literature to the ones of the present study could be the difference in training volume. Indeed, our participants performed a high number of jumps per session (i.e., ∼120–150). In this regard, de Villarreal et al. (2008) investigated the differences in knee-extensor strength and countermovement jump performance between low, medium and high frequency and volume PLT, showing that functional gains were not influenced by such variables.

Adaptations in Muscle Function: Muscle Power

It is noteworthy that, despite the lack of further gain in muscle torque, muscle power kept increasing till week 6.

Since power is the product of force and velocity, the increment of power may be expected to have been due to an increase in contraction speed. In this regard, a significant and progressive increase in fascicle length was found at all time points (2.2% at 2 weeks, 4.0% at 4 weeks and 4.4% at 6 weeks). A similar observation applies to CSA_{mean}, which showed a progressive increment (3.5% at 2 weeks, 4.7% at 4 weeks and 5.8% at 6 weeks). Hence, consistent with the notion that volume is the product CSA_{mean} and muscle length (Jones and Round, 2000) both an increase in fascicle length (reflecting a potential increase in the number of sarcomeres in series) and in CSA_{mean} likely contributed to the increase power observed in this study. This seems confirmed by the significant correlation between the % changes of CSA_{mean} ($R^2 = 0.46$, $p < 0.001$) and QF volume and power ($R^2 = 0.44$, $p < 0.024$).

In addition to these morphological factors, we cannot exclude that neural or tendon adaptations may have contributed to the increased force and power outputs. Previous studies have shown an increase in neural drive of knee-extensors (Behrens et al., 2013) and plantar flexors (Kubo et al., 2007) during MVT (Behrens et al., 2016) following PLT. In contrast, Kyröläinen et al. (2005) found a significant increase in plantar flexors activation following PLT but no differences were observed for the knee extensors. Interestingly, a higher knee extensors pre-activation when performing vertical jumps after PLT has been previously reported (Kyrölänen et al., 1991). Similarly, Hirayama et al. (2017) reported neuromuscular activity alterations of both agonist and antagonist of plantar flexors during a SSC performance, indicating that increased power output could be related to changes in leg muscle activation strategies (or inter-muscular coordination). Thus, although no complete agreement regarding the specific neural adaptations to PLT has been reached in the literature, it could be speculated that training-specific adaptations could have occurred and contributed to the changes in muscle function reported in this study.

In addition, tendon properties (CSA, stiffness, and young's modulus) are also known to be affected by the training-induced load (Bohm et al., 2015; Wiesinger et al., 2015; Kubo et al., 2017). Notwithstanding, the literature presents some controversial results when it comes to plyometric loading. Fouré et al. (2010) reported an increase in Achilles tendon stiffness after 14 weeks of PLT, and a similar result was found by Hirayama et al. (2017) after 12 weeks. On the other hand, Kubo et al. (2007) found an increase in ankle joint stiffness following 12 weeks of unilateral PLT, although no differences were found in Achilles tendon stiffness. This result was confirmed by a later study from the same authors (Kubo et al., 2017) that highlighted an increased active muscle stiffness with no changes in tendon CSA, stiffness and hysteresis following a 12-week PLT. The lack of changes in Achilles tendon CSA was also reported by Fouré et al. (2012) after 14 weeks training. The majority of the studies focusing on tendon adaptations to PLT have investigated the changes detectable in the Achilles tendon; to the best of our knowledge, only one study investigated the effects of drop-jumps training on patellar tendon so far (Paleckis et al., 2015), showing increases in CSA but not thickness of this tendon toward the end of the 9-days intervention protocols.

Taken together we cannot exclude that tendon adaptations may have occurred during the training period, but we cannot speculate toward which direction. Further research should aim to clarify this.

Adaptations in Muscle Size

We have also investigated the distribution of morphological changes of the QF and VL muscles, in terms of muscle volume and CSA values collected at different sites of femur length (**Figure 4**).

Both VL and QF muscle volume increased linearly throughout the training period; however, VL volume increment was significant after only 2 weeks, contributing to QF volume changes which were detectable after 4 weeks of PLT, in accordance with the increases in knee-extensors power.

Interestingly, the majority of the works focusing on PLT interventions did not evaluate the possible muscle hypertrophic responses to such training modality. Two studies from Kubo et al. (2007, 2017) reported increased plantar flexors muscle volume or thickness (respectively) following 12 weeks of PLT; on the other hand, Fouré et al. (2012) reported unchanged gastrocnemius medialis CSA measured by ultrasound after 14 weeks of intervention. As for the quadriceps muscle, few authors (Pottiger Jeffrey et al., 1999; Malisoux et al., 2006a,b) reported hypertrophy of both slow and fast fibers of the VL following 8 weeks of intervention. McKinlay et al. (2012) reported an 8.1% increased VL muscle thickness after 8 weeks of PLT, and Váczi et al. (2014) found a 2.5% increase in quadriceps CSA measured via magnetic resonance after 10 weeks of intervention in elderly people. Very interestingly, Earp et al. (2015) trained for 8 weeks 18 subjects with squat jumps (9 with parallel thigh depth jumps and 9 with volitional depth jumps), and found

increases in QF and VL CSA in the distal (33%) and mid (50%) sites of the muscles.

Our results also show that, consistently with the findings of Earp et al. (2015), the muscle volume adaptations were driven by specific regional hypertrophic responses, which appeared significant at different time points. The earliest changes in both VL and QF CSAs were detected in the mid-belly region (40–60% of femur length, after only 2 weeks of PLT) compared to the distal one (20–30% of the femur length, at week 4) (**Figure 4**). However, after 6 weeks, the highest percentage VL and QF CSA regional increments were reported distally.

The observed distal hypertrophy highlights the possible influence of the eccentric component of PLT. In fact, not only there is previous evidence of regional hypertrophy following different training modalities (Narici et al., 1989; Franchi et al., 2014), but also of a preferential distal growth of VL after eccentric exercise in comparison to a more marked mid-portion hypertrophy after concentric exercise (Franchi et al., 2014). Moreover, we previously reported regional differences in activation of mechanotransduction signaling (i.e., FAK, Meta-Vinculin), with the activation of such intergin-complex proteins being greater after pure eccentric training (Franchi et al., 2018). This could have induced greater potential for regional hypertrophic responses, as FAK has been shown to modulate muscle protein synthesis (Klossner et al., 2009). However, similar responses in muscle protein synthesis of mid muscle vs. distal sites were reported after 4 and 8 weeks of eccentric vs. concentric training (Franchi et al., 2015, 2018). Thus, such processes should be object of future investigations.

Regarding the significant changes in both VL and QF CSA after just 2 weeks of training (which in turn influence the changes in muscle volume), some authors have suggested that such early responses may be influenced by the edema provoked by the eccentric component of exercise in the first training sessions (Damas et al., 2018). The exact time point when an increase in CSA can be considered as true hypertrophy has been investigated by several studies and it is still currently under debate. DeFreitas et al. (2011) highlighted that 3-to-4 weeks of resistance training are sufficient to elicit muscle hypertrophy even when considering the potential bias introduced by muscle edema. Stock et al. (2017) investigated the hypertrophic adaptations to a concentric-only resistance training program, showing that after only 7 sessions (i.e., just over 2 weeks of training) significant hypertrophy could be detected. Furthermore, Wilkinson et al. (2014) demonstrated that cumulative myofibrillar protein synthesis is increased after only one bout of resistance training, peaking in day 2–4 post-exercise and then decreasing.

Lastly, in order to ensure our results not to be biased by the repeated measures error, we calculated the minimum detectable change, i.e., the minimum change required to assume that a real adaptation had occurred. For VL CSA, the minimal difference was found to be of 1.84%; within our subjects, only one of them showed increments lower than this at week 2 and week 4, and the average increases were at least 4.6% (week 2). For QF CSA, the minimal difference resulted of 1.38%; at week 2, 4 subjects presented increments higher than this value and 4 presented lower increments. However, the mean increment was higher than 1.38% (=minimum detectable change) in the CSAs taken at almost all the femur lengths, excluding the 50% (+1.06%) which resulted not significant. At weeks 4 and 6, all the subjects but 2 (week 4) and 1 (week 6) showed increments higher than 1.38%, and so did the average value calculated for all volunteers.

Thus, it is plausible that the observed adaptations in muscle size could be regarded as true hypertrophic responses.

Adaptations in Muscle Architecture

We observed a significant increase in fascicle length after 2 (2.2%), 4 (4%), and 6 (4.4%) weeks of training, while PA showed an increment (5.8%) only at the 6-week time point. Similarly to the approach used to detect whether these small (albeit significant) changes could be regarded as true adaptations (i.e., not biased by the repeated measures error) we calculated the minimum detectable change for both Lf and PA. For VL Lf, the minimum detectable change was 1.38%; at week 2, 3 out of 8 subjects showed increments lower than this value, while the average was higher. At weeks 4 and 6 only 1 subject displayed increments lower than 1.38%. VL PA minimum detectable change was 1.93%, and this value was not reached in 6 out of 8 subjects at week 2 (and also by the average in this time point), and by 1 subject at weeks 4 and 6. Accordingly, PA was significantly improved after 6 weeks and showed a trend after 4 weeks.

To the best of our knowledge, only very few studies have considered muscle architecture with respect of PLT. Blazevich et al. (2003) reported an increase in Lf after 5 weeks of sprinting and jumping training, accompanied by a decrease in PA compared to baseline. However, participants had been performing resistance training for the 4 weeks preceding training intervention, and thus the decrease in PA could be also related to the lack of weights in the 5 weeks of sprint and jump intervention. Aeles et al. (2017) investigated, in a cross-section study, the differences in gastrocnemius medialis muscle architecture between jumping athletes and untrained controls, finding no differences in Lf but higher PA in athletes.

Similarly to Blazevich et al. (2003), our results show increases in VL Lf following PLT; this phenomenon is expected to reflect an increase in the number of sarcomeres in series, and thus in maximum shortening velocity (Bodine et al., 1982). Animal studies have shown that sarcomere addition can occur already after 5, 10, and 28 days in response to training modalities involving muscle lengthening (Lynn et al., 1998; Butterfield et al., 2005; Chen et al., 2020). However, recent studies in intact whole mice muscle have described some variability in sarcomere length along different muscle regions (Moo et al., 2016), which become even more non-uniform upon activation (Moo et al., 2017). Thus, we can speculate that changes in Lf may represent a result of both sarcomere addition and change in sarcomere operating length.

The mechanisms responsible for the increase in fascicle length are likely related to the fascicle stretch caused by the repeated SSC involved in plyometric training. These SSCs are thought to involve consecutive muscle shortening (concentric) and lengthening (eccentric) contractions, but, at a muscle level, the real eccentric nature of the deceleration phase during the SSC has been often debated. Theoretically, the muscle is firstly lengthened before it rapidly contracts concentrically (Bosco et al., 1981):

however, some previous reports have suggested that the structures that stretch during the lengthening phase are the tendon complex and the series elastic components, while muscle fascicles behave "quasi isometrically" (Ishikawa and Komi, 2004). Nevertheless, these studies have been often conducted on the plantar-flexors MTU. Interestingly, two previous reports have observed, in addition to MTU and tendon lengthening, that VL fascicle lengthened during drop-jumps (Ishikawa, 2003) and countermovement jumps (Nikolaidou et al., 2017).

It follows that the mechanical stretch applied to the fascicles during training protocols involving a SSC may not be completely comparable to the one observed after pure eccentric contractions (Franchi et al., 2014). Notwithstanding, in the present study, during the landing-push off transition, volunteers were asked to maintain similar range of motion, corresponding to a maximum knee flexion of ca. 90°. In fact, previous work showed that isometric contractions at longer muscle lengths (at a knee joint angle similar to the one reached during bouncing in the present study) can lead to an increase in Lf (Noorkõiv et al., 2014). Lastly, we cannot exclude that the aponeuroses may have contributed to such adaptations in Lf: in fact, it has been shown that aponeurosis stiffness changes with muscle-tendon complex length (as would occur in the SCC), affecting fascicle strain (Raiteri et al., 2018). Fascicle stretch would in turn trigger mechanotransduction signaling pathways, which we have recently reported to be associated with changes in muscle architecture (Franchi et al., 2018).

Limitations

We acknowledge that the present study has some limitations.

First of all, we did not recruit a control group. However, we recommended our participants to not change their habitual levels of recreational physical activity and to not introduce any new exercise modality in the training period. Second, we acknowledge that the small sample size allow us to draw preliminary conclusions. Furthermore, our participants were not trained individuals and were novice to this training modality: it follows that the responses observed could be influenced by this aspect. Indeed, the relatively small (albeit significant) changes in muscle mass and architecture, and the observed increments in MVT and power could be less pronounced if the present PLT protocol would have been applied to an already trained population.

In addition, there are limitations linked to the plyometric training device we used. This device enables to increase the work output both by increasing the slope of the inclined sledge as well as by increasing the distance covered during the push as muscle power increases. To maximize the load, we used the maximum chair slope that could be set in this device. As the subject power increases with the training progression, he eventually reaches the end of the rail track along which the seat travels. To increase load intensity and prevent the subject reaching the end of the rail track we overloaded the subject with a 15-kg weighted vest. However, after 4 weeks of training, most participants were nearing the end run again, so to add extra work-volume we increased the number of series of sets of 30 bounces. This procedure was undoubtedly effective for increasing the total work performed but the overloading was probably insufficient to induce a further gain in muscle force.

On the other hand, also the use of the 15-kg weighted jacket could represent a potential limitation. Indeed, this was certainly sufficient for ensuring a gain in muscle strength up to 4 weeks of training but not enough to produce further gains after 4 weeks. However, despite these limitations, power output progressively increased up to the end of training period.

Lastly, we did not investigate either neural or tendon adaptations to the training protocol used (for a detailed discussion, see section "Adaptations in Muscle Function" paragraph).

CONCLUSION

The findings of the present study show that plyometric exercise training performed on the tramp-trainer is highly effective for inducing rapid gains in muscle volume, architecture, torque, and power in healthy younger adults.

Notably, changes in VL volume and fascicle length were detectable already after 2 weeks of training, followed by increases in knee-extensors volume and power from week 4 of PLT.

DATA AVAILABILITY STATEMENT

The raw data supporting the conclusions of this article will be made available by the authors, without undue reservation, to any qualified researcher.

ETHICS STATEMENT

The studies involving human participants were reviewed and approved by The University of Nottingham Ethics Committee and was compliant with the Declaration of Helsinki. The patients/participants provided their written informed consent to participate in this study.

AUTHOR CONTRIBUTIONS

MF, MN, and SL designed the study. EM, FB, JQ, and MF performed the experiments. EM and MF analyzed the data. EM, MF, SL, FB, JQ, and MN discussed the data. EM, MF, SL, and MN wrote the manuscript. All authors contributed to the article and approved the submitted version.

ACKNOWLEDGMENTS

The authors would like to acknowledge all the participants who took part to this study, Mrs. Amanda Gates and Dr. Philip Herrod for their contribution in the initial screening, and Miss Tereza Jandova for her help during the training sessions.

REFERENCES

Aagaard, P., Simonsen, E. B., Andersen, J. L., Magnusson, P., and Dyhre-Poulsen, P. (2002). Increased rate of force development and neural drive of human skeletal muscle following resistance training. *J. Appl. Physiol.* 93, 1318–1326. doi: 10.1152/japplphysiol.00283.2002

Aeles, J., Lenchant, S., Vanlommel, L., and Vanwanseele, B. (2017). Bilateral differences in muscle fascicle architecture are not related to the preferred leg in jumping athletes. *Eur. J. Appl. Physiol.* 117, 1453–1461. doi: 10.1007/s00421-017-3638-5

Bassey, E. J., Fiatarone, M. A., O'Neill, E. F., Kelly, M., Evans, W. J., and Lipsitz, L. A. (1992). Leg extensor power and functional performance in very old men and women. *Clin. Sci.* 82, 321–327. doi: 10.1042/CS0820321

Behrens, M., Mau-Moeller, A., and Bruhn, S. (2013). Effect of plyometric training on neural and mechanical properties of the knee extensor muscles. *Int. J. Sports Med.* 35, 101–119. doi: 10.1055/s-0033-1343401

Behrens, M., Mau-Moeller, A., and Bruhn, S. (2014). Effect of plyometric training on neural and mechanical properties of the knee extensor muscles. *Int. J. Sports Med.* 35, 101–109.

Behrens, M., Mau-Moeller, A., Mueller, K., Heise, S., Gube, M., Beuster, N., et al. (2016). Plyometric training improves voluntary activation and strength during isometric, concentric and eccentric contractions. *J. Sci. Med. Sport* 19, 170–176. doi: 10.1016/j.jsams.2015.01.011

Blazevich, A. J., Gill, N. D., Bronks, R., and Newton, R. U. (2003). Training-specific muscle architecture adaptation after 5-wk training in athletes. *Med. Sci. Sports Exerc.* 35, 2013–2022. doi: 10.1249/01.MSS.0000099092.83611.20

Bodine, S. C., Roy, R. R., Meadows, D. A., Zernicke, R. F., Sacks, R. D., Fournier, M., et al. (1982). Architectural, histochemical, and contractile characteristics of a unique biarticular muscle: the cat semitendinosus. *J. Neurophysiol.* 48, 192–201. doi: 10.1152/jn.1982.48.1.192

Bohm, S., Mersmann, F., and Arampatzis, A. (2015). Human tendon adaptation in response to mechanical loading: a systematic review and meta-analysis of exercise intervention studies on healthy adults. *Sport. Med. Open* 1:7. doi: 10.1186/s40798-015-0009-9

Bosco, C., Komi, P. V., and Ito, A. (1981). Prestretch potentiation of human skeletal muscle during ballistic movement. *Acta Physiol. Scand.* 111, 135–140. doi: 10.1111/j.1748-1716.1981.tb06716.x

Butterfield, T. A., Leonard, T. R., and Herzog, W. (2005). Differential serial sarcomere number adaptations in knee extensor muscles of rats is contraction type dependent. *J. Appl. Physiol.* 99, 1352–1358. doi: 10.1152/japplphysiol.00481.2005

Cardinale, M., Newton, R. U., and Nosaka, K. (2011). *Strength And Conditioning: Biological Principles And Practical Applications*. Hoboken, NJ: John Wiley & Sons.

Chen, J., Mashouri, P., Fontyn, S., Valvano, M., Elliott-Mohamed, S., Noonan, A. M., et al. (2020). The influence of training-induced sarcomerogenesis on the history dependence of force. *bioRxiv* [Preprint], doi: 10.1242/jeb.218776

Chu, D. (1998). *Jumping Into Plyometrics*. Champaign, IL: Human Kinetics.

Cook, C. J., Beaven, C. M., and Kilduff, L. P. (2013). Three weeks of eccentric training combined with overspeed exercises enhances power and running speed performance gains in trained athletes. *J. strength Cond. Res.* 27, 1280–1286. doi: 10.1519/JSC.0b013e3182679278

Damas, F., Libardi, C. A., and Ugrinowitsch, C. (2018). The development of skeletal muscle hypertrophy through resistance training: the role of muscle damage and muscle protein synthesis. *Eur. J. Appl. Physiol.* 118, 485–500. doi: 10.1007/s00421-017-3792-9

Davies, G., Riemann, B. L., and Manske, R. (2015). Current Concepts Of Plyometric Exercise. *Int. J. Sports Phys. Ther.* 10:760.

de Villarreal, E. S. S., González-Badillo, J. J., and Izquierdo, M. (2008). Low and moderate plyometric training frequency produces greater jumping and sprinting gains compared with high frequency. *J. strength Cond. Res.* 22, 715–725. doi: 10.1519/JSC.0b013e318163eade

DeFreitas, J. M., Beck, T. W., Stock, M. S., Dillon, M. A., and Kasishke, P. R. (2011). An examination of the time course of training-induced skeletal muscle hypertrophy. *Eur. J. Appl. Physiol.* 111, 2785–2790. doi: 10.1007/s00421-011-1905-4

Earp, J. E., Newton, R. U., Cormie, P., and Blazevich, A. J. (2015). Inhomogeneous quadriceps femoris hypertrophy in response to strength and power training. *Med. Sci. Sports Exerc.* 47, 2389–2397. doi: 10.1249/MSS.0000000000000669

Fatouros, I. G., Jamurtas, A. Z., Leontsini, D., Taxildaris, K., Aggelousis, N., Kostopoulos, N., et al. (2000). Evaluation of plyometric exercise training, weight training, and their combination on vertical jumping performance and leg strength. *J. Strength Cond. Res.* 14:470. doi: 10.1519/00124278-200011000-00016

Fouré, A., Nordez, A., and Cornu, C. (2010). Plyometric training effects on Achilles tendon stiffness and dissipative properties. *J. Appl. Physiol.* 109, 849–854. doi: 10.1152/japplphysiol.01150.2009

Fouré, A., Nordez, A., and Cornu, C. (2012). Effects of plyometric training on passive stiffness of gastrocnemii muscles and achilles tendon. *Eur. J. Appl. Physiol.* 112, 2849–2857. doi: 10.1007/s00421-011-2256-x

Franchi, M. V., Atherton, P. J., Reeves, N. D., Flück, M., Williams, J., Mitchell, W. K., et al. (2014). Architectural, functional and molecular responses to concentric and eccentric loading in human skeletal muscle. *Acta Physiol.* 210, 642–654. doi: 10.1111/apha.12225

Franchi, M. V., Monti, E., Carter, A., Quinlan, J. I., Herrod, P. J. J., Reeves, N. D., et al. (2019). Bouncing back! counteracting muscle aging with plyometric muscle loading. *Front. Physiol.* 10:178. doi: 10.3389/fphys.2019.00178

Franchi, M. V., Ruoss, S., Valdivieso, P., Mitchell, K. W., Smith, K., Atherton, P. J., et al. (2018). Regional regulation of focal adhesion kinase after concentric and eccentric loading is related to remodelling of human skeletal muscle. *Acta Physiol.* 223:e13056. doi: 10.1111/apha.13056

Franchi, M. V., Wilkinson, D. J., Quinlan, J. I., Mitchell, W. K., Lund, J. N., Williams, J. P., et al. (2015). Early structural remodeling and deuterium oxide-derived protein metabolic responses to eccentric and concentric loading in human skeletal muscle. *Physiol. Rep.* 3:e12593. doi: 10.14814/phy2.12593

Häkkinen, K., Kraemer, W. J., Newton, R. U., and Alen, M. (2001). Changes in electromyographic activity, muscle fibre and force production characteristics during heavy resistance/power strength training in middle-aged and older men and women. *Acta Physiol. Scand.* 171, 51–62. doi: 10.1046/j.1365-201X.2001.00781.x

Hakkinen, K., Pakarinen, A., Kyrolainen, H., Cheng, S., Kim, D. H., and Komi, P. V. (1990). Neuromuscular adaptations and serum hormones in females during prolonged power training. *Int. J. Sports Med.* 11, 91–98. doi: 10.1055/s-2007-1024769

Harries, S. K., Lubans, D. R., and Callister, R. (2012). Resistance training to improve power and sports performance in adolescent athletes: a systematic review and meta-analysis. *J. Sci. Med. Sport* 15, 532–540. doi: 10.1016/J.JSAMS.2012.02.005

Hirayama, K., Iwanuma, S., Ikeda, N., Yoshikawa, A., Ema, R., and Kawakami, Y. (2017). Plyometric training favors optimizing muscle-tendon behavior during depth jumping. *Front. Physiol.* 8:16. doi: 10.3389/fphys.2017.00016

Ishikawa, M. (2003). Effects of different dropping intensities on fascicle and tendinous tissue behavior during stretch-shortening cycle exercise. *J. Appl. Physiol.* 96, 848–852.

Ishikawa, M., and Komi, P. V. (2004). Effects of different dropping intensities on fascicle and tendinous tissue behavior during stretch-shortening cycle exercise. *J. Appl. Physiol.* 96, 848–852. doi: 10.1152/japplphysiol.00948.2003

Jones, D. A., and Round, J. M. (2000). "Strength and muscle growth," in *Paediatric Exercise Science and Medicine*, eds A. Armstrong and W. Van Mechelen (Oxford: Oxford University Press).

Klossner, S., Durieux, A. C., Freyssenet, D., and Flueck, M. (2009). Mechano-transduction to muscle protein synthesis is modulated by FAK. *Eur. J. Appl. Physiol.* 106, 389–398. doi: 10.1007/s00421-009-1032-1037

Komi, P. V. (1984). Physiological and biomechanical correlates of muscle function: effects of muscle structure and stretch-shortening cycle on force and speed. *Exerc. Sport Sci. Rev.* 12, 81–121.

Kubo, K., Ishigaki, T., and Ikebukuro, T. (2017). Effects of plyometric and isometric training on muscle and tendon stiffness in vivo. *Physiol. Rep.* 5:13374. doi: 10.14814/phy2.13374

Kubo, K., Morimoto, M., Komuro, T., Yata, H., Tsunoda, N., Kanehisa, H., et al. (2007). Effects of plyometric and weight training on muscle-tendon complex and jump performance. *Med. Sci. Sports Exerc.* 39, 1801–1810. doi: 10.1249/mss.0b013e31813e630a

Kyröläinen, H., Avela, J., McBride, J. M., Koskinen, S., Andersen, J. L., Sipilä, S., et al. (2005). Effects of power training on muscle structure and neuromuscular performance. *Scand. J. Med. Sci. Sport.* 15, 58–64. doi: 10.1111/j.1600-0838.2004.00390.x

Kyröläinen, H., Komi, P. V., and Kim, D. H. (1991). Effects of power training on neuromuscular performance and mechanical efficiency. *Scand. J. Med. Sci. Sports* 1, 78–87. doi: 10.1111/j.1600-0838.1991.tb00275.x

Lynn, R., Talbot, J. A., and Morgan, D. L. (1998). Differences in rat skeletal muscles after incline and decline running. *J. Appl. Physiol.* 85, 98–104. doi: 10.1152/jappl.1998.85.1.98

Makaruk, H., Winchester, J. B., Sadowski, J., Czaplicki, A., and Sacewicz, T. (2011). Effects of unilateral and bilateral plyometric training on power and jumping ability in women. *J. Strength Cond. Res.* 25, 3311–3318. doi: 10.1519/JSC.0b013e318215fa33

Malisoux, L., Francaux, M., Nielens, H., Renard, P., Lebacq, J., and Theisen, D. (2006a). Calcium sensitivity of human single muscle fibers following plyometric training. *Med. Sci. Sports Exerc.* 38, 1901–1908. doi: 10.1249/01.mss.0000232022.21361.47

Malisoux, L., Francaux, M., Nielens, H., and Theisen, D. (2006b). Stretch-shortening cycle exercises: an effective training paradigm to enhance power output of human single muscle fibers. *J. Appl. Physiol.* 100, 771–779. doi: 10.1152/japplphysiol.01027.2005

Martel, G. F., Harmer, M. L., Logan, J. M., and Parker, C. B. (2005). Aquatic plyometric training increases vertical jump in female volleyball players. *Med. Sci. Sports Exerc.* 37, 1814–1819. doi: 10.1249/01.mss.0000184289.87574.60

McKinlay, B., Wallace, P., Dotan, R., Long, D., Tokuno, C., Gabriel, D. A., et al. (2012). Effects of plyometric and resistance training on muscle strength, explosiveness, and neuromuscular function in young adolescent soccer players. *Strength Cond.* 26, 3039–3050. doi: 10.1519/jsc.0000000000002428

Mendez, J., and Keys, A. (1960). Density and composition of mammalian muscle. *Metabolism* 9, 184–188.

Moo, E. K., Fortuna, R., Sibole, S. C., Abusara, Z., and Herzog, W. (2016). In vivo sarcomere lengths and sarcomere elongations are not uniform across an intact muscle. *Front. Physiol.* 7:187. doi: 10.3389/fphys.2016.00187

Moo, E. K., Leonard, T. R., and Herzog, W. (2017). In vivo sarcomere lengths become more non-uniform upon activation in intact whole muscle. *Front. Physiol.* 8:1015. doi: 10.3389/fphys.2017.01015

Narici, M. V., Roi, G. S., Landoni, L., Minetti, A. E., and Cerretelli, P. (1989). Changes in force, cross-sectional area and neural activation during strength training and detraining of the human quadriceps. *Eur. J. Appl. Physiol. Occup. Physiol.* 59, 310–319. doi: 10.1007/bf02388334

Nikolaidou, M. E., Marzilger, R., Bohm, S., Mersmann, F., and Arampatzis, A. (2017). Operating length and velocity of human *M. vastus lateralis* fascicles during vertical jumping. *R. Soc. open Sci.* 4:170185. doi: 10.1098/rsos.170185

Noorkõiv, M., Nosaka, K., and Blazevich, A. J. (2014). Neuromuscular adaptations associated with knee joint angle-specific force change. *Med. Sci. Sports Exerc.* 46, 1525–1537. doi: 10.1249/MSS.0000000000000269

Paleckis, V., Mickevičius, M., Snieckus, A., Streckis, V., Pääsuke, M., Rutkauskas, S., et al. (2015). Changes in indirect markers of muscle damage and tendons after daily drop jumping exercise with rapid load increase. *J. Sports Sci. Med.* 14, 825–833.

Piirainen, J. M., Cronin, N. J., Avela, J., and Linnamo, V. (2014). Effects of plyometric and pneumatic explosive strength training on neuromuscular function and dynamic balance control in 60-70 year old males. *J. Electromyogr. Kinesiol.* 24, 246–252. doi: 10.1016/j.jelekin.2014.01.010

Pottiger Jeffrey, A., Lockwood, R. H., Haub, M. D., Dolezal, B. A., Almuzaini, K. S., Schroeder, J. M., et al. (1999). Muscle power and fiber characteristics following 8 weeks of plyometric training. *J. Strength Cond. Res.* 13, 275–279. doi: 10.1519/00124278-199908000-00016

Raiteri, B. J., Cresswell, A. G., and Lichtwark, G. A. (2018). Muscle-tendon length and force affect human tibialis anterior central aponeurosis stiffness in vivo. *Proc. Natl. Acad. Sci. U.S.A.* 115, E3097–E3105. doi: 10.1073/PNAS.1712697115

Ramìrez-Campillo, R., Alvarez, C., Henrìquez-Olgu, C., Baez, E. B., Martìnez, C., Andrade, D. C., et al. (2014). Effects of plyometric training on endurance and explosive strength performance in competitive middle- and long-distance runners. *J. Strength Cond. Res.* 28, 97–104. doi: 10.1519/JSC.0b013e3182a1f44c

Reeves, N. D., Narici, M. V., and Maganaris, C. N. (2004). In vivo human muscle structure and function: adaptations to resistance training in old age. *Exp. Physiol.* 89, 675–689. doi: 10.1113/expphysiol.2004.027797

Reid, K. F., Martin, K. I., Doros, G., Clark, D. J., Hau, C., Patten, C., et al. (2015). Comparative effects of light or heavy resistance power training for improving lower extremity power and physical performance in mobility-limited older adults. *J. Gerontol. A. Biol. Sci. Med. Sci.* 70, 374–380. doi: 10.1093/gerona/glu156

Robinson, L. E., Steven, T. D., Merrik, M. A., and Buckworth, J. (2004). The effects of land vs. aquatic plyometrics on power, torque, velocity, and muscle soreness in women. *J. Strength Cond. Res.* 18, 84–91. doi: 10.1519/00124278-200402000-00012

Seynnes, O. R., de Boer, M., and Narici, M. V. (2007). Early skeletal muscle hypertrophy and architectural changes in response to high-intensity resistance training. *J. Appl. Physiol.* 102, 368–373. doi: 10.1152/japplphysiol.00789.2006

Seynnes, O. R., Maganaris, C. N., De Boer, M. D., Di Prampero, P. E., and Narici, M. V. (2008). Early structural adaptations to unloading in the human calf muscles. *Acta Physiol.* 193, 265–274. doi: 10.1111/j.1748-1716.2008.01842.x

Stock, M. S., Mota, J. A., DeFranco, R. N., Grue, K. A., Jacobo, A. U., Chung, E., et al. (2017). The time course of short-term hypertrophy in the absence of eccentric muscle damage. *Eur. J. Appl. Physiol.* 117, 989–1004. doi: 10.1007/s00421-017-3587-z

Taube, W., Leukel, C., and Gollhofer, A. (2012). How neurons make us jump: the neural control of stretch-shortening cycle movements. *Exerc. Sport Sci. Rev.* 40, 106–115. doi: 10.1097/JES.0b013e31824138da

Tillin, N. A., and Folland, J. P. (2014). Maximal and explosive strength training elicit distinct neuromuscular adaptations, specific to the training stimulus. *Eur. J. Appl. Physiol.* 114, 365–374. doi: 10.1007/s00421-013-2781-x

Tracy, B. L., Ivey, F. M., Jeffrey Metter, E., Fleg, J. L., Siegel, E. L., and Hurley, B. F. (2003). A more efficient magnetic resonance imaging-based strategy for measuring quadriceps muscle volume. *Med. Sci. Sport. Exerc.* 35, 425–433. doi: 10.1249/01.MSS.0000053722.53302.D6

Váczi, M., Nagy, S. A., Koszegi, T., Ambrus, M., Bogner, P., Perlaki, G., et al. (2014). Mechanical, hormonal, and hypertrophic adaptations to 10weeks of eccentric and stretch-shortening cycle exercise training in old males. *Exp. Gerontol.* 58, 69–77. doi: 10.1016/j.exger.2014.07.013

Weir, J. P. (2005). Quantifying test-retest reliability using the intraclass correlation coefficient and the SEM. *J. Strength Cond. Res.* 19, 231–240. doi: 10.1519/15184.1

Wiesinger, H.-P., Kösters, A., Müller, E., and Seynnes, O. R. (2015). Effects of increased loading on in vivo tendon properties: a systematic review. *Med. Sci. Sports Exerc.* 47, 1885–1895. doi: 10.1249/MSS.0000000000000603

Wilkinson, D. J., Franchi, M. V., Brook, M. S., Narici, M. V., Williams, J. P., Mitchell, W. K., et al. (2014). A validation of the application of D2O stable isotope tracer techniques for monitoring day-to-day changes in muscle protein subfraction synthesis in humans. *Am. J. Physiol. Endocrinol. Metab.* 306:E571. doi: 10.1152/AJPENDO.00650.2013

Conflict of Interest: The authors declare that the research was conducted in the absence of any commercial or financial relationships that could be construed as a potential conflict of interest.

frontiers in Physiology

ORIGINAL RESEARCH
published: 18 August 2020
doi: 10.3389/fphys.2020.01028

Effects of Upper and Lower Limb Plyometric Training Program on Components of Physical Performance in Young Female Handball Players

Mehrez Hammami[1,2], Nawel Gaamouri[1,2], Katsuhiko Suzuki[3], Roy J. Shephard[4] and Mohamed Souhaiel Chelly[1,2]*

[1] Research Unit (UR17JS01), Sport Performance, Health & Society, Higher Institute of Sport and Physical Education of Ksar Saïd, Manouba University, Tunis, Tunisia, [2] Higher Institute of Sport and Physical Education of Ksar Saïd, Manouba University, Tunis, Tunisia, [3] Faculty of Sport Sciences, Waseda University, Tokorozawa, Japan, [4] Faculty of Kinesiology and Physical Education, University of Toronto, Toronto, ON, Canada

Purpose: This study examined the effects of a 10-week combined upper and lower limb plyometric training (ULLPT) programs on components of physical performance in young female handball players.

Methods: Participants aged 15.8 ± 0.2 years were randomly assigned between the experimental (EG; n = 17) and control (CG; n = 17) groups. Two-way analyses of performance (group × time) assessed changes in handgrip force, back extensor strength; medicine ball throwing, 30-m sprint times, change of direction (CoD) [Modified Illinois test (Illinois-MT)], four jumping tests [squat jump (SJ), countermovement jump (CMJ), CMJ with arms (CMJA) and 5 jump test (5JT), static and dynamic balance, and repeated sprint T-test scores (RSTT)].

Results: After 10 weeks of plyometric training (two sessions per week), group × time interactions showed significant changes in EG relative to CG in right and left handgrip force, back extensor strength and medicine ball throwing [$p < 0.001$, $d = 1.51$ (large); $p < 0.0001$, $d = 0.85$ (large); $p < 0.001$, $d = 0.90$ (large); $p < 0.0001$, $d = 0.52$ (medium), respectively]. Group × time interactions also showed improvements of EG relative to CG in sprint times [5 m ($p = 0.02$, $d = 0.80$ (large)); 10 m ($p < 0.0001$, $d = 1.00$ (large)); 20 m ($p = 0.02$, $d = 1.41$ (large)); and 30 m ($p = 0.02$, $d = 2.60$ (large))], CoD [Illinois-MT ($p < 0.001$, $d = 1.58$ (large))] and jumping [(SJ, CMJ, CMJA, and 5JT, $p = 0.001$, $d = 0.87$ (large); $p < 0.001$, $d = 1.17$ (large); $p < 0.001$, $d = 1.15$ (large); and $p = 0.006$, $d = 0.71$ (medium)) respectively]. Further, all RSTT scores (best time, mean time, total time, and fatigue index) improved significantly in the experimental group, with group × time interactions varying between $p < 0.001$ and $p = 0.049$ (d value large to medium). However, balance did not differ significantly between EG and CG.

Conclusion: We conclude that 10 weeks of ULLPT improved many measures of physical performance in young female handball players.

Keywords: change-of-direction, stork test, best time, mean time, push up jump, hurdle jump

OPEN ACCESS

Edited by:
Tobias Siebert,
University of Stuttgart, Germany

Reviewed by:
Olaf Prieske,
University of Applied Sciences for Sports and Management Potsdam, Germany
Jan Ruffieux,
University of Fribourg, Switzerland

****Correspondence:***
Mehrez Hammami
mahrez-10@hotmail.fr

Specialty section:
This article was submitted to Exercise Physiology, a section of the journal Frontiers in Physiology

Received: *28 May 2020*
Accepted: *28 July 2020*
Published: *18 August 2020*

Citation:
Hammami M, Gaamouri N, Suzuki K, Shephard RJ and Chelly MS (2020) Effects of Upper and Lower Limb Plyometric Training Program on Components of Physical Performance in Young Female Handball Players. Front. Physiol. 11:1028. doi: 10.3389/fphys.2020.01028

INTRODUCTION

The muscular power and strength of both the upper and the lower limbs are key contributors to performance in handball (Michalsik and Aagaard, 2015; Wagner et al., 2018), and plyometric training with quick and powerful multi-joint movements like jumping, hopping, and skipping is frequently used in handball to improve these aspects of a player's physical fitness (Chaabene et al., 2019; Hammami et al., 2019; Prieske et al., 2019). The response to such training depends on subject characteristics including age, sex, and initial training level, as well as program characteristics (type of training, exercise surface, and the rest interval between sets and training sessions) (Markovic and Mikulic, 2010; Ramirez-Campillo et al., 2018; Hammami et al., 2019). However, there is little information concerning its impact in young female handball players, especially in terms of upper limb training, although one might anticipate a particularly large response in those with minimal previous experience of plyometric training (Rubley et al., 2011). Hammami et al. (2019) found increases in both upper limb (handgrip force, back extensor strength, and medicine ball throwing) and lower limb [sprinting, change of direction (CoD), and jumping] performance after 9 weeks of combined upper and lower limb plyometric training (ULLPT) in U14 female handball players, and Chaabene et al. (2019) also reported increases in fitness measures after 8 weeks of plyometric training in young female handball players. On the other hand, Meszler and Vaczi (2019) found no significant changes in T agility test scores, balance, hamstring strength or H:Q ratio after 7 weeks of plyometric training in female basketball players aged less than 17 years. Haj-Sassi et al. (2011) concluded that players of a number of field and court sports performed many intermittent forward, backward, and lateral high speed movements during competitions. The ability to change direction is thus an important skill in many field and court sports. In team handball, it is essential to react quickly and perform powerful changes in direction, while moving quickly over short distances (Michalsik et al., 2014). In a typical handball game, there are 279 changes-of-direction, in response to visual or auditory cues (Cuesta, 1991). Players must change direction with a minimal loss of speed, balance, and motor control, and make short, maximal efforts with only brief recovery periods. Moreover, the ability to perform repeated sprints and changes of direction is regarded by many coaches and researchers as an important predictor of superior performance in intermittent and team sports (Wong Del et al., 2012).

No previous study has examined the impact of combined ULLPT on the ability of young females to change direction repeatedly. Thus, this study investigated the effects of a progressive in-season ULLPT training program on selected components of physical performance (strength, sprinting, jumping, CoD, balance, and repeated CoD) in young female handball players. We hypothesized that the inclusion of ULLPT into the regular training routine of young female handball players would generate larger improvements in physical performance than those obtained by standard handball training alone.

MATERIALS AND METHODS

Ethical Approval

All procedures were approved by the local ethical committee for the use of human participants. The study was conducted in accordance with the latest version of the Declaration of Helsinki. Written informed parental consent (for those <17 years) and participants' consent were obtained prior to commencing the study. All participants and their parents/legal representatives were fully informed about the experimental protocol and its potential risks and benefits.

Participants

The G power 3.0.10 program was used to calculate the minimal sample size needed in our study, with $Z_{1-\beta} = 1.03$ (power = 85%) and $Z_{\alpha/2} = 1.96$ (alpha = 5%). The study of Chaabene et al. (2019) showed the mean ± SD of 5-m sprint performance as 1.24 ± 0.12 (s) in the experimental group vs 1.17 ± 0.06 (s) in the control group (CG), and considering a ratio of one control for every case, there was a need for 15 experimental and 15 control subjects (Faul et al., 2007). Thirty-four young female handball players from two different clubs were randomly assigned between a plyometric training group (EG; $n = 17$; age = 15.8 ± 0.2 years; body mass = 64.2 ± 3.3 kg; height = 1.66 ± 0.03 m; body fat = 25.2 ± 3.8%; maturity-offset = 3.0 ± 0.5 years) and a CG who maintained their standard in-season regimen ($n = 17$; age = 15.8 ± 0.2 years; body mass = 63.0 ± 3.8 kg; height = 1.67 ± 0.04 m; body fat = 26.0 ± 3.3%; maturity-offset = 3.0 ± 0.4 years). All players were competing at the national level and were therefore classified as elite athletes. Their mean experience of handball competition was 5 years. They had 3 years' experience of plyometric training. All had already achieved a good overall physical preparation at the beginning of the season (a preliminary 6-week period of six training sessions per week). This preliminary phase was divided into two parts. During the first 3 weeks, a resistance training program aimed to improve muscular power and muscle volume by light loads (40–60%, one repetition maximum). The second 3-week period was devoted to improving muscular strength with higher loads (70–85%, one repetition maximum), supplemented by participation in friendly matches each weekend. Subjects continued to engage in five sessions per week of training during September, when the championship season began. The experimental intervention of biweekly ULLPT was undertaken during the second phase of the national championships (January to March). All participants had previously engaged in five to six training sessions per week (90-to-120 min each session). However, for 10 weeks, the EG replaced some of their handball-specific drills with a plyometric training program, although the overall training volume remained comparable for the two groups. It was decided that if any athlete missed more than 10% of the total training sessions and/or more than two consecutive sessions would be excluded from the study.

Experimental Design

The study was designed to test the effects of a 10-week ULLPT program on selected fitness measures in young female handball

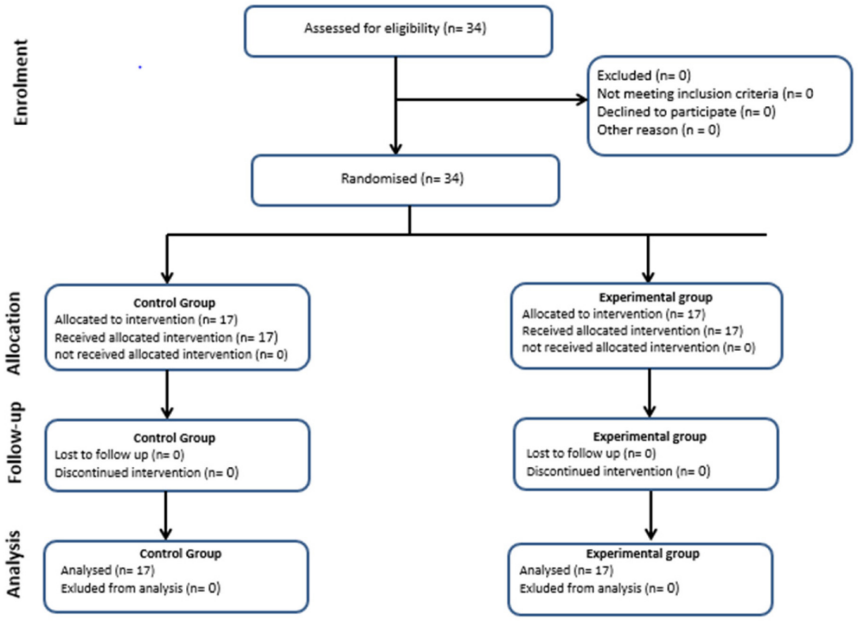

FIGURE 1 | The diagram (The CONSORT: Consolidated Standards of Reporting Trials) includes detailed information on the interventions received.

players. **Figure 1** presents a revised CONSORT diagram of the levels of reporting and explaining participant flow. The training intervention was conducted in-season during 2018–2019. In the week prior to the intervention, two 80- to 90-min sessions familiarized players with all test procedures. Measurements were made in a fixed order over 4 days, immediately before and 4 days after the last plyometric training session. Subjects did not participate in any exhausting exercise for 24 h before testing, and no food or caffeine-containing drinks were taken for 2 h before testing. A standardized warm-up (10–20 min of low- to moderate-intensity aerobic exercise and dynamic stretching) preceded all tests. On the first test day, participants made a 30-m sprint, followed by the modified Illinois change-of-direction test; three trials were allowed for each test (separated by 6–8 min of recovery) and the best performances as determined by paired photocells (Microgate, Bolzano, Italy) were noted. The second day was devoted to jumping [squat jump (SJ), countermovement jump (CMJ), CMJ with arms (CMJA), and horizontal 5-jump tests (5JT)] followed by dominant and non-dominant handgrip force assessments. On the third day, anthropometric measurements were followed by determinations of back extensor strength (three trials separated by at least 2 min of recovery) and medicine ball throw tests (two trials separated by 5 min of recovery), with the best attempts noted for further analyses. On the fourth day, the stork test, *Y* balance test and repeated sprint *T*-test (RSTT) were completed.

Testing Procedures

30-m Sprint Performance

Players started from a standing position, with the front foot 0.2 m from the first photocell beam and ran 30 m, with times recorded over distances of 5, 10, 20, and 30 m.

Modified Illinois Change-of-Direction Test (Illinois-MT)

Four cones formed the change-of-direction area for the modified Illinois test. On command, players sprinted 5 m, turned and ran back to the starting line, then, swerving in and out of the four markers, and completed two 5-m sprints (Hachana et al., 2014). No advice was given as to the most effective technique, but players were instructed to complete the test as quickly as possible without cutting over markers. Five minutes of rest was allowed between each of the three trials, and the fastest performance was used in subsequent analyses.

Vertical Jump

Jump height was assessed using an infrared photoelectric measurement device connected to a digital computer (Optojump System; Bolzano, Italy) that measured contact and flight times and the height of jump with a precision of 1/1,000 s. Participants begun the SJ at a knee angle of ∼90° (self-controlled, using a mirror), avoiding any downward movement, and pushed upward, keeping their legs straight throughout. The CMJ began from an upright position; a rapid downward movement to a knee angle of ∼90° (again self-controlled, using a mirror) accompanied the beginning of the push-off. During the CMJA, the hands were used freely while jumping. One minute of rest was allowed between three trials of each test, and the highest jump of each type was used in subsequent analyses.

Five Jump Test (5JT)

The test was performed as previously described (Hammami et al., 2019). From an upright standing position with both feet flat on the ground, participants tried to cover as much distance as possible with five forward jumps, alternating left- and right-leg ground contacts. Participants were allowed three maximal trials,

with 3 min of rest between efforts, and the best performance was used for analyses.

Handgrip Force

A hand dynamometer (Takei, Tokyo, Japan) was held with the arm at right angles and the elbows at the side of the body. The instrument was adjusted so that its base rested on the first metacarpal and the handle rested on the middle of the participant's four fingers. A maximal isometric effort was maintained for 5 s, without ancillary body movements. Two trials were made with each hand, with 1 min of rest between trials, and the highest readings were used in subsequent analyses.

Anthropometry

Anthropometric measurements included standing and sitting body height (stadiometer accuracy of 0.1 cm; Holtain, Crosswell, Crymych, Pembs, United Kingdom) and body mass (0.1 kg; Tanita BF683W scales, Munich, Germany). The overall percentage of body fat was estimated from the biceps, triceps, subscapular, and suprailiac skinfolds, using the equations of Durnin and Womersley (1974) for children and adolescent females:

$$\% \text{ Body fat} = (495/D) - 450$$

where $D = 1.1369 - 0.0598$ (Log sum of 4 skinfolds).

Maturity offset status was calculated from peak height velocity (Mirwald et al., 2002):

Maturity offset = −9.38 + (0.000188 × leg length × sitting height) + (0.0022 × age × leg length) + (0.00584 × age × sitting height) + (0.0769 × weight/height ratio).

Back Extensor Strength

Maximal isometric back extensor strength was measured using a back extensor dynamometer (Takei, Tokyo, Japan) (Hannibal et al., 2006). Participants stood on the dynamometer, with their feet a shoulder width apart and gripped the handle bar positioned across the patellae. The chain length was adjusted so that initially the legs were held straight and the back was flexed to 30°, as guided by wall markings. Participants then stood upright without bending their knees, pulling upward as strongly as possible.

Medicine Ball Throw

The test was performed using a 3-kg rubber medicine ball with 21.5-cm diameter (Tigar, Pirot, Serbia) powdered with magnesium carbonate. A familiarization session included a brief description of the optimal technique (Gillespie and Keenum, 1987). The seated player grasped the medicine ball with both hands, and on signal forcefully pushed the ball from the chest. The score was measured from the front of the sitting line to the powder-marked spot where the ball landed.

Stork Balance Test

Subjects stood on their dominant leg with their opposite foot resting against the inside of the supporting knee and both hands on their hips (Negra et al., 2017). On signal, they raised their heel; the test was terminated when the heel touched the ground or the foot moved away from the patella.

Dynamic Balance Test

Dynamic balance was assessed for both right and left legs, using the *Y*-balance test (Negra et al., 2017). Supine leg lengths were first determined from the anterior superior iliac spine to the most distal aspect of the medial malleolus. Subjects then stood barefoot and single-legged, with the tip of their great toe at the center of the grid, and reached in anterior, postero-medial and postero-lateral directions, marked on the floor by tape. The posterior lines extended at an angle of 135° from the anterior line. Trials were repeated if the participant (1) did not touch the required line with the reaching foot while maintaining weight-bearing on the stance leg, (2) lifted the stance foot from the center of the grid, (3) lost balance, (4) did not maintain start and return positions for one full second, or (5) touched the reaching foot to gain support. The maximal reach was measured in each direction, and a composite score calculated as [(maximum anterior + maximum postero-medial + maximum postero-lateral reach distance)/(leg length × 3) × 100] (Negra et al., 2017). Three trials were conducted in each direction, with two-minute rest intervals.

Repeated Sprint *T*-Test (RSTT)

This test offers a reliable and valid measurement (Pauole et al., 2000) of the ability to change directions rapidly, simulating a game with short, intense efforts, recovery periods and multi-directional displacements. Seven executions of the RSTT were made, with subjects walking back slowly to the next start point during 25-s recovery intervals. Measures included best time (RSTT-BT), mean time (RSTT-MT), total time (RSTT-TT) and a fatigue index (RSTT-FI) calculated as (Fitzsimons et al., 1993):

$$\text{FI} = [(\text{Total time}/(\text{Best time} \times 7)) \times 100] - 100$$

Plyometric Training Program

The intervention consisted of a progressive 10-week ULLPT program, based on the players' previous training records and research results (Hammami et al., 2019). It was completed during the mid-portion of the competitive season (from January to March) (**Table 1**). Biweekly plyometric sessions (Tuesdays and Thursdays) were performed immediately after the warm-up program, replacing some low-intensity technical-tactical handball drills. The intervention included push-up exercises for the upper limbs, and hurdling, lateral hurdling, and hurdle jumping (jumping with 180° rotation) exercises for the lower limbs. Exercises for the upper limbs were immediately followed by lower-limb exercises (i.e., 6 to 10 repetitions of dynamic push-ups + 6 to 8 repetitions of lower limb jumps), with no intervening rest periods (**Table 1**). The sequence of plyometric exercises for the upper and lower limbs lasted ∼10 s (Stojanovic et al., 2017). Recovery between sets was for 30 s. All plyometrics in general (i.e., upper and lower limb exercises) were performed with maximal effort, minimizing contact time in each repetition, and no resting was allowed between jumps. With the exception of competitive and friendly matches, the ULLPT replacement activity accounted for <10% of the total training load. During the intervention, the CG followed their regular handball training (i.e., mainly technical-tactical drills, small sided and simulated games, and injury prevention drills). The overall training load

TABLE 1 | Plyometric training program.

	Weeks 1–2	Weeks 3–4	Weeks 5–6	Weeks 7–8	Weeks 9–10
	S × R	S × R	S × R	S × R	S × R
Upper limb					
Push-up	10 × 6	10 × 6	10 × 6	10 × 6	10 × 6
Contacts number	60	60	60	60	60
	H × S × R	H × S × R	H × S × R	H × S × R	H × S × R
Lower limb					
Hurdle jump	0.3 m × 2 × 6	0.3 m × 3 × 6	0.35 m × 2 × 6	0.35 m × 3 × 6	0.4 m × 2 × 6
Lateral hurdle jump	0.3 m × 2 × 6	0.3 m × 3 × 6	0.35 m × 2 × 6	0.35 m × 3 × 6	0.4 m × 2 × 6
Stretched leg jump	0.25 m × 2 × 6	0.25 m × 3 × 6	0.30 m × 2 × 6	0.30 m × 3 × 6	0.35 m × 2 × 6
Hurdle jump (jump with 180° rotation)	0.25 m × 2 × 6	0.25 m × 3 × 6	0.30 m × 2 × 6	0.30 m × 3 × 6	0.35 m × 2 × 6
Horizontal jump	1.1 m × 2 × 6	1.1 m × 3 × 6	1.2 m × 2 × 6	1.2 m × 2 × 6	1.3 m × 2 × 6
Contact number	60	90	60	90	60

H, height; S, sets; R, reps.

was measured and comparable between groups using a rating of perceived exertion (Helms et al., 2016).

Statistics

Statistical analyses were carried out using the SPSS 20 program for Windows (SPSS, Inc., Armonk, NY: IBM Corp). Normality of all variables was tested using the Kolmogorov–Smirnov test procedure. A few results (Handgrip, *Y* Balance test and Stork balance test) showed some skewing of data, and both means and medians were reported for these measurements. Data are presented as mean (SD), and as median values for skewed variables. Between-group differences at baseline were examined using independent *t*-tests, and the effect of the intervention was determined by two-way analyses of variance (Experimental vs Control and Test vs Retest). To evaluate within-group pre-to-post performance changes, paired sample *t*-tests were applied. Effect sizes were calculated by converting partial eta squared values to Cohen's *d* [classified as small ($0.00 \leq d \leq 0.49$), medium ($0.50 \leq d \leq 0.79$), and large ($d \geq 0.80$)] (Cohen, 1988). Training-related effects were assessed by two-way analyses of variance (group × time). The criterion for statistical significance was set at $p < 0.05$, whether a positive or a negative difference was seen (i.e., a two-tailed test was adopted). The reliabilities of all dependent variables were assessed by calculating intra-class correlation coefficients (two-way mixed) and coefficients of variation.

RESULTS

No athletes missed more than 10% of the total training sessions and/or more than two consecutive sessions, so it was not necessary to exclude any participants from the study.

Reliability of the Tests

Test-retest reliabilities were generally above the accepted threshold, with intra-class correlation coefficients ranging from 0.63 to 0.98, and coefficients of variation of 1.4 to 58.4%. However, the stork left test had a poor reliability (ICC = 0.637/CV = 58.4) (**Table 2**).

TABLE 2 | Reliability and variability of performance tests.

	ICC	95% CI	CV
5 m	0.975	0.950–0.987	4.7
10 m	0.957	0.915–0.979	2.6
20 m	0.953	0.906–0.976	1.4
30 m	0.982	0.963–0.991	9.0
Illinois-MT	0.909	0.812–0.954	2.1
SJ	0.910	0.819–0.955	8.2
CMJ	0.978	0.956–0.989	7.5
CMJA	0.929	0.857–0.964	7.3
5JT	0.971	0.942–0.986	8.0
Handgrip right	0.896	0.791–0.948	7.3
Handgrip left	0.869	0.738–0.935	8.2
Back extensor	0.867	0.735–0.934	10.1
Medicine ball throw	0.978	0.955–0.989	18.1
Stork right	0.853	0.705–0.926	46.5
Stork left	0.637	0.274–0.819	58.4
Y balance test (RL/L)	0.977	0.54–0.988	11.0
Y balance test (RL/B)	0.894	0.788–0.947	9.8
Y balance test (RL/R)	0.942	0.883–0.971	19
Y balance test (LL/R)	0.982	0.963–0.991	9.0
Y balance test (LL/B)	0.942	0.883–0.971	8.5
Y balance test (LL/L)	0.973	0.946–0.987	21.8

CI, confidence intervals; CV, coefficient of variation; CMJ, counter-movement jump; CMJA, counter-movement jump; ICC, intraclass correlation coefficient; Illinois-MT, Illinois modified test; SJ, squat jump; B, background; L, left; R, right; LL, left leg; RL, right leg.

Between-Group Differences at Baseline

There were no significant initial intergroup differences for any of the dependent variables.

Training-Related Effects

All data for both groups increased significantly over the 10-week intervention, with the exception of the Stork balance test (left leg), which remained unchanged for the CG (**Tables 3**, **4**). The experimental group enhanced their upper limb performance

TABLE 3 | Upper-limb performance in experimental and control groups before and after the 10-week intervention.

	Experimental group (n = 17)					Control group (n = 17)					Anova group × time interaction	
	Pre	Post	% Δ change	Paired t test		Pre	Post	% Δ change	Paired t test		p	d (cohen)
				p	d (cohen)				p	d (cohen)		
Handgrip right (N)	233 ± 14	295 ± 17	26.3 ± 6.1	<0.001	4.10	231 ± 20	240 ± 19	4.1 ± 1.7	<0.001	0.48	<0.001	1.51
Handgrip left (N)	227 ± 22	279 ± 38 (267)[a]	23.0 ± 6.2	<0.001	1.73	226 ± 14	239 ± 13	5.8 ± 2.7	<0.001	0.99	0.001	0.85
Back extensor (N)	765 ± 97	980 ± 101	28.4 ± 4.5	<0.001	2.24	792 ± 56	861 ± 70	8.8 ± 6.0	<0.001	1.12	0.001	0.90
Medicine ball throw (m)	3.1 ± 0.5	4.0 ± 0.5	27.6 ± 9.6	<0.001	1.86	3.2 ± 0.6	3.4 ± 0.6	8.2 ± 7.8	<0.001	0.34	0.041	0.52

[a]*Median reported for rightward skewing data.*

scores: handgrip right (Δ = 26%, $p < 0.0001$, $d = -4.10$), handgrip left (Δ = 23%, $p < 0.0001$, $d = -1.13$), back extensor strength (Δ = 28%, $p < 0.0001$, $d = -2.24$), and medicine ball throw (Δ = 27.6%, $p < 0.0001$, $d = -1.86$), with significant group × time interactions [$p < 0.001$, $d = 1.51$ (large); $p < 0.0001$, $d = 0.85$ (large); $p < 0.001$, $d = 0.90$ (large); $p < 0.0001$, $d = 0.52$ (medium), respectively] (**Table 4**). The EG also enhanced their sprint performance over 5 m (Δ = 10%, $p < 0.0001$, $d = 2.43$), 10 m (Δ = 6.7%, $p < 0.0001$, $d = 2.89$), 20 m (Δ = 5.7%, $p < 0.0001$, $d = 4.33$), and 30 m (Δ = 7.8%, $p < 0.0001$, $d = 6.10$), with a group × time interaction [$p = 0.02$, $d = 0.80$ (large); $p < 0.0001$, $d = 1.00$ (large); $p = 0.02$, $d = 1.41$ (large); and $p = 0.02$, $d = 2.60$ (large), respectively]. Further, the EG improved their performance in the Illinois-MT (Δ = 7.4%, $p < 0.0001$, $d = 12.40$), with a group × time interaction [$p < 0.001$, $d = 1.58$ (large)] (**Table 4**). Jumping also improved significantly in the EG, with gains in the SJ (Δ = 18.2%, $p < 0.0001$, $d = -2.47$), CMJ (Δ = 21.1%, $p < 0.0001$, $d = -3.09$), CMJA (Δ = 20%, $p < 0.0001$, $d = -2.82$), and horizontal 5JT (Δ = 15.3%, $p < 0.0001$, $d = -3.50$), with group × time interactions at $p = 0.001$, $d = 0.87$ (large); $p = 0.02$, $d = 1.17$ (large); $p < 0.001$, $d = 1.15$ (large); and $p = 0.006$, $d = 0.71$ (medium), respectively. Again, all measures of RSTT performance increased significantly in the EG relative to the CG, with group × time interactions at $p < 0.001$, $d = 1.57$ (large); $p < 0.001$, $d = 1.81$ (large); $p < 0.001$, $d = 1.81$ (large); and $p = 0.049$, $d = 0.50$ (medium), in RSTT-BT, RSTT-MT, RSTT-TT, and RSTT-FI, respectively (**Table 4**). However, group × time interactions showed no significant inter-group differences in either static or dynamic balance (**Table 4**).

DISCUSSION

This study demonstrates that a 10-week in-season ULLPT program was effective in improving measures of upper body strength (handgrip force, back extensor, and medicine ball throwing), while permitting also substantial gains in sprinting, CoD, jumping, and RSTT performance in young female handball players, relative to participants who continued to follow the standard skills-based regimen. The findings confirm the observations of Hammami et al. (2019) who found improvements of handgrip force, back extensor strength, and medicine ball throwing in female handball players aged less than 14 years. Ignjatovic et al. (2012) also found increases in medicine ball throwing ($p < 0.01$), and in bench and shoulder press power ($p < 0.05$) relative to the controls after 12 weeks of medicine ball training in female handball players aged an average of 16.9 years (Ignjatovic et al., 2012), and Saeterbakken et al. (2011) reported a 4.9% increase in the maximal throwing velocity of female handball players aged 16.6 years after 6 weeks of medicine ball training ($p < 0.01$). Plyometric training improves strength through a combination of increased neural drive to the agonist muscles, improved intermuscular coordination, and changes in muscle size or architecture (Markovic and Mikulic, 2010). Increases in muscle strength and power after plyometric training could be due to neural and muscular adaptations such as changes in muscle architecture (i.e., a decrease in fascicle angle and an

TABLE 4 | Lower-limb performance in experimental and control groups before and after the 10-week intervention.

	Experimental group (n = 17)					Control group (n = 17)					Anova group × time interaction	
	Pre	Post	%Δ change	Paired t test		Pre	Post	%Δ change	Paired t test		p	d (cohen)
				p	d (cohen)				p	d (cohen)		
Sprint												
5 m (s)	1.25 ± 0.06	1.12 ± 0.05	10.0 ± 1.9	<0.001	2.43	1.28 ± 0.05	1.24 ± 0.05	3.3 ± 1.8	<0.001	0.82	0.002	0.80
10 m (s)	2.19 ± 0.05	2.05 ± 0.05	6.7 ± 1.5	<0.001	2.89	2.24 ± 0.05	2.20 ± 0.07	1.7 ± 2	0.002	2.37	<0.001	1.00
20 m (s)	3.77 ± 0.05	3.56 ± 0.05	5.7 ± 0.9	<0.001	4.33	3.75 ± 0.05	3.68 ± 0.07	1.8 ± 1	<0.001	1.19	<0.001	1.41
30 m (s)	4.64 ± 0.05	4.28 ± 0.07	7.8 ± 1.1	<0.001	6.10	5.54 ± 0.05	5.49 ± 0.07	1.0 ± 0.6	<0.001	0.85	<0.001	2.60
Change of direction												
Illinois-MT	13.07 ± 0.07	12.10 ± 0.09	7.4 ± 0.4	<0.001	12.40	13.11 ± 0.39	13 ± 0.39	0.8 ± 0.2	<0.001	0.29	<0.001	1.58
Jump												
SJ (cm)	22.4 ± 1.7	26.4 ± 1.9	18.2 ± 2.3	<0.001	2.47	22.8 ± 2.1	23.8 ± 1.6	4.5 ± 4.2	<0.001	0.55	0.001	0.87
CMJ (cm)	24.2 ± 1.6	29.3 ± 1.8	21.1 ± 3.3	<0.001	3.09	24.0 ± 2.0	24.9 ± 1.8	4.0 ± 3.3	<0.001	0.49	<0.001	1.17
CMJA (cm)	25.3 ± 1.6	30.4 ± 2.1	20.0 ± 2.8	<0.001	2.82	25.3 ± 2.1	25.8 ± 2.1	2.3 ± 1.1	<0.001	0.25	<0.001	1.15
5JT (m)	8.1 ± 0.3	9.3 ± 0.4	15.3 ± 1.4	<0.001	3.50	8.2 ± 1.5	8.5 ± 1.4	4.4 ± 3.3	<0.001	0.21	0.006	0.71
RSTT												
RSTT-BT (s)	12.61 ± 0.16	11.91 ± 0.18	5.5 ± 1.0	<0.001	4.24	12.61 ± 0.18	12.48 ± 0.23	1 ± 0.6	<0.001	0.65	<0.001	1.57
RSTT-MT (s)	12.93 ± 0.17	12.15 ± 0.16	6.1 ± 0.7	<0.001	4.87	12.90 ± 0.18	12.77 ± 0.23	1.0 ± 0.6	<0.001	0.65	<0.001	1.81
RSTT-TT (s)	90.5 ± 1.17	85.0 ± 1.15	6.1 ± 0.7	<0.001	4.89	90.30 ± 1.28	89.40 ± 1.58	1.0 ± 0.6	<0.001	0.65	<0.001	1.81
RSTT-FI (%)	2.52 ± 0.79 (2.15)[a]	1.97 ± 0.87	19.3 ± 35.5	<0.001	0.68	2.30 ± 0.03	2.32 ± 0.04	1.0 ± 0.6	<0.001	0.58	0.049	0.50
***Y* Balance test**												
Right support leg												
RL/A (cm)	75 ± 7	79 ± 8	4.9 ± 2.3	<0.001	0.55	73 ± 9	79 ± 9	9.1 ± 6.7	<0.001	0.69	0.501	0.16
RL/BL (cm)	89 ± 8	92 ± 9	4.2 ± 1.3	<0.001	0.36	87 ± 9	92 ± 10	5.4 ± 3.8	<0.001	0.54	0.831	0.006
RL/BR (cm)	46 ± 9 (44)[a]	52 ± 9 (51)[a]	12.4 ± 5.1	<0.001	0.69	48 ± 7	54 ± 7	15.3 ± 19	0.001	0.88	0.841	0.006
Left support leg												
LL/A (cm)	78 ± 5	82 ± 6	4.2 ± 1.3	<0.001	0.75	78 ± 9	84 ± 7	8.8 ± 9.8	0.001	0.77	0.356	0.22
LL/BR (cm)	92 ± 8	99 ± 7	7.5 ± 2.3	<0.001	0.96	96 ± 8	99 ± 7	3.9 ± 2.9	<0.001	0.41	0.372	0.22
LL/BL (cm)	48 ± 12 (43)[a]	51 ± 12	7.1 ± 3	<0.001	0.26	46 ± 8	50 ± 7	9.5 ± 7.6	<0.001	0.55	0.858	0.06
Stork balance test												
RL (s)	2.33 ± 1.16	3.37 ± 1.05	56.4 ± 39.8	<0.001	0.97	2.61 ± 1.16	3.92 ± 1.93 (3.41)[a]	55.9 ± 51.2	0.003	0.85	0.685	0.10
LL (s)	2.56 ± 1.46 (2.29)[a]	3.03 ± 1.46 (2.76)[a]	22.2 ± 8.6	<0.001	0.33	2.58 ± 1.58 (1.98)[a]	3.06 ± 1.43	40.1 ± 69.0	0.310	0.33	0.988	0.06

[a]*Median reported for rightward skewing data. Illinois-MT, Illinois modified test; SJ, squat jump; CMJ, countermovement jump; CMJA, countermovement jump with arms; 5JT, 5 jump test; RSTT, repeated sprint T-test; BT, best time; MT, mean time; TT, total time; FI, fatigue index; RL, right leg; A, anterior; BL, background left; BR, background right; LL, left leg.*

increase in fascicle length of knee extensors) (Blazevich et al., 2003); changes in the stiffness of various elastic components of the muscle-tendon complex of plantar flexors (Cornu et al., 1997; Kubo et al., 2007; Fouré et al., 2009; Grosset et al., 2009); and changes in single fiber mechanics of knee extensors (i.e., enhanced force, velocity and, consequently, power of slow, and fast muscle fibers) (Malisoux et al., 2007).

Plyometric training increases strength and power, with minimal effects on muscle volume (Markovic and Mikulic, 2010), so that gains in the upper limbs are unlikely to have negative consequences for sprinting ability. Hammami et al. (2019) previously found significant improvements in 20-m (p = 0.02, d = 0.557) and 30-m ($p < 0.001$, d = 1.07) performance after 9 weeks of ULLPT in U14 female handball players. Current results are consistent with these findings, with significant increases of speed over distances of 5–30 m. A meaningful portion of the ULLPT drills used during the current intervention implicated slow stretch-shortening cycle (SSC) muscle actions that mimicked those encountered during the acceleration phase of a sprint (Mero, 1988; Mero et al., 1992), contributing to the observed gains in sprint performance. Aside from the potential role of velocity-specific training, the direction of application of the muscle force may also contribute to the magnitude of the observed gains (Ramirez-Campillo et al., 2018). In this sense, the inclusion of horizontal jump drills may have contributed to the sprint improvements, given the importance of horizontal force production in sprinting (Morin et al., 2012; Kawamori et al., 2013). Improvement in sprint performance could be attributed to differences in the use of the SSC characteristics, as a SJ mainly consists of a concentric (push-off) phase, whereas a CMJ and other forms of plyometrics involve a coupling of eccentric and concentric phases (Markovic and Mikulic, 2010). The greatest benefits of plyometric training for sprint performance are dependent on the velocity of muscle action employed in training (Rimmer and Sleivert, 2000). Therefore, it has been suggested that greatest effects of PT on sprinting performance occur in the acceleration phase. It is known that slow SSC (long-response) plyometrics (>0.25 s), such as countermovement or SJs, transfer most directly to start and acceleration performance, whereas fast SSC (short-response) plyometrics (<0.25 s), such as drop jumps, have more transfer to maximum running velocity (Rimmer and Sleivert, 2000; Plisk et al., 2008).

The present results also showed a large effect group × time interaction in the Illinois-MT performance, matching the responses observed in the meta-analysis of Asadi et al. (2016) and Chaabene et al. (2019) but not Meszler and Vaczi (2019) (studies where training was limited to the lower limbs). Meszler and Vaczi (2019) explained their lack of response by fatigue, due to an incomplete recovery between sessions, but the regimen used also did not include any form of exercise where athletes had to change direction. Neural adaptations and enhancement of motor-unit recruitment may be mechanisms that can lead to an improvement on the CoD test (Aagaard et al., 2002).

A recent meta-analysis and other studies (Rubley et al., 2011; Chaabene et al., 2019; Meszler and Vaczi, 2019) have demonstrated increases in the jump performance of female athletes after plyometric training (Stojanovic et al., 2017), and the present results show that this benefit can be obtained if the regimen includes lower limb training. The improvement in jump performance is due to enhancing the elastic properties of the musculotendon unit and optimizing the neural sequencing and firing rates of the motor units involved (Ignjatovic et al., 2012). The increases observed in jump performance after ULLPT could be due to neuromuscular adaptations, such as an increased neural drive to the agonist muscles, changes in muscle-tendon mechanical-stiffness characteristics, alterations in muscle size and/or architecture, and changes in single-fiber mechanics (Maffiuletti et al., 2002; De Villarreal et al., 2009; Thomas et al., 2009). Other possible aspects of neural adaptation to plyometric training include (i) changes in leg muscle activation strategies (or inter-muscular coordination) during vertical jumping, particularly during the preparatory (i.e., pre-landing) jump phase; and (ii) changes in the stretch reflex excitability (Bishop and Spencer, 2004; De Villarreal et al., 2009).

This present study is the first to investigate the effect of plyometric training on repeated change of direction (RSTT) performance in young female handball players. It showed increases in all RSTT scores [best time ($p < 0.001$; d = 1.57); mean time ($p < 0.001$; d = 1.81); total time ($p < 0.001$; d = 1.81), and fatigue index (p = 0.49; d = 50)]. However, Rosas et al. (2017) previously noted increases in running anaerobic sprint test (RAST) after plyometric training in female soccer players, and (Hammami et al., 2016) found increases in 2 of 3 parameters (best time and total time) after 8 weeks of plyometric training in adolescent soccer players. Plyometric training affects nervous factors. It allows faster recruitment of motor units, a higher maximum discharge frequency, a greater quantity of innervation doublets, and better synchronization of motor units. All of the combined create a higher level of strength and a faster muscle contraction speed.

No significant gains in static or dynamic balance were seen after plyometric training. Others, also, have found no effects on balance from lower limb plyometrics alone. Thus, Hammami et al. (2019) found no effects on static and dynamic balance after 9 weeks of plyometric training in U14 female handball players, and Meszler and Vaczi (2019) saw no effects after 7 weeks of plyometric training in female basketball players aged less than 17 years, although Cherni et al. (2019) did report a significant improvement in the static balance test of adult female basketball players after plyometric training, and Benis et al. (2016) noted improved postural control and lower-limb stability as assessed by the *Y* balance test when adult female basketball players undertook body-weight neuromuscular training.

Certain limitations of this study must be acknowledged. The training load was not monitored over the training intervention using, for instance, external and/or internal load measures. If the group of players played an official match, then a friendly match or physical work was scheduled for the other group so that the load was the same for the two groups. Nevertheless, there is a difference in feeling between an official match, a friendly match and physical workload. This could potentially be checked by a mental trainer or by a psychology questionnaire, but unfortunately this is not the case in the current study. Notwithstanding, the general training description was quite

detailed, with both groups following similar technical/tactical training over six training sessions per week, and we are confident that the total training load was similar between groups.

CONCLUSION

This study demonstrated that the in-season combined ULLPT (two sessions per week) can substantially improve upper limb performance in young female handball players, while conserving the gains anticipated from lower limb plyometrics. The ULLPT intervention lasted a total of only 35 min per session, making it a time-efficient training method that can be routinely carried out in a sporting environment, with few resources required.

Upper and lower limb plyometric training is a time-efficient and a highly beneficial method for improving the physical performance of both upper and lower limbs in young female handball players. Further research is needed to examine the effects of ULLPT on muscle morphology and neural adaptations, and to explore the impact of maturation status as a potential moderator variable.

DATA AVAILABILITY STATEMENT

The raw data supporting the conclusions of this article will be made available by the authors, without undue reservation.

ETHICS STATEMENT

The studies involving human participants were reviewed and approved by Manouba University Ethics Committee. Written informed consent to participate in this study was provided by the participants' legal guardian/next of kin.

AUTHOR CONTRIBUTIONS

MH designed the study, conducted analyses, and wrote the manuscript. NG, RS, and KS assisted in acquisition, analysis and interpretation of data, and reviewed and edited the article. MH and MC administered the project. MC and KS made substantial contribution including conception and a critical revision of the article. All authors read and approved the final manuscript.

FUNDING

"Ministry of Higher Education and Scientific Research, Tunis, Tunisia" for the financial support of the experiment. The publication of this article was funded by the Waseda University Grant for Special Research Projects.

ACKNOWLEDGMENTS

We thank the "Ministry of Higher Education and Scientific Research, Tunis, Tunisia" for the financial support. We also thank Associate Professor Ridha Aouedi, Ph.D. [Research Unit (UR17JS01) "Sport Performance, Health and Society," Higher Institute of Sport and Physical Education of Ksar Saïd, Manouba University, Tunis, Tunisia] for the valuable statistical help. The publication of this article was funded by the Waseda University Grant for Special Research Projects.

REFERENCES

Aagaard, P., Simonsen, E. B., Andersen, J. L., Magnusson, P., and Dyhre-Poulsen, P. (2002). Increased rate of force development and neural drive of human skeletal muscle following resistance training. *J. Appl. Physiol.* 93, 1318–1326. doi: 10.1152/japplphysiol.00283.2002

Asadi, A., Arazi, H., Young, W. B., and Saez De Villarreal, E. (2016). The Effects of Plyometric Training on Change-of-Direction Ability: A Meta-Analysis. *Int. J. Sports Physiol. Perform.* 11, 563–573. doi: 10.1123/ijspp.2015-0694

Benis, R., Bonato, M., and La Torre, A. (2016). Elite female basketball players' body-weight neuromuscular training and performance on the Y-balance test. *J. Athl. Train* 51, 688–695. doi: 10.4085/1062-6050-51.12.03

Bishop, D., and Spencer, M. (2004). Determinants of repeated-sprint ability in well-trained team-sport athletes and endurance-trained athletes. *J. Sports Med. Phys. Fitness* 44, 1–7.

Blazevich, A. J., Gill, N. D., Bronks, R., and Newton, R. U. (2003). Training-specific muscle architecture adaptation after 5-wk training in athletes. *Med. Sci. Sports Exerc.* 35, 2013–2022. doi: 10.1249/01.mss.0000099092.83611.20

Chaabene, H., Negra, Y., Moran, J., Prieske, O., Sammoud, S., Ramirez-Campillo, R., et al. (2019). Plyometric training improves not only measures of linear speed, power, and change-of-direction speed but also repeated sprint ability in female young handball players. *J. Strength Cond. Res.* doi: 10.1519/JSC.0000000000003128 [Epub ahead of print].

Cherni, Y., Jlid, M. C., Mehrez, H., Shephard, R. J., Paillard, T., Chelly, M. S., et al. (2019). Eight weeks of plyometric training improves ability to change direction and dynamic postural control in female basketball players. *Front. Physiol.* 10:726.

Cohen, J. (1988). *Statistical Power Analysis for the Behavioral Sciences*. Hillsdale, NJ: Lawrence Erlbaum.

Cornu, C., Almeida Silveira, M., and Goubel, F. (1997). Influence of plyometric training on the mechanical impedance of the human ankle joint. *Eur. J. Appl. Physiol. Occup. Physiol.* 76, 282–288. doi: 10.1007/s004210050249

Cuesta, G. (1991). *Balonmano (Handball)*. Madrid: Spanish Handball Association.

De Villarreal, E. S., Kellis, E., Kraemer, W. J., and Izquierdo, M. (2009). Determining variables of plyometric training for improving vertical jump height performance: a meta-analysis. *J. Strength Cond. Res.* 23, 495–506. doi: 10.1519/jsc.0b013e318196b7c6

Durnin, J. V., and Womersley, J. (1974). Body fat assessed from total body density and its estimation from skinfold thickness: measurements on 481 men and women aged from 16 to 72 years. *Br. J. Nutr.* 32, 77–97. doi: 10.1079/bjn19740060

Faul, F., Erdfelder, E., Lang, A. G., and Buchner, A. (2007). G*Power 3: a flexible statistical power analysis program for the social, behavioral, and biomedical sciences. *Behav. Res. Methods* 39, 175–191. doi: 10.3758/bf03193146

Fitzsimons, M., Dawson, B., Ward, D., and And Wilkinson, A. (1993). Cycling and running tests of repeated sprint ability. *Aust. J. Sci. Med. Sport* 8, 82–87.

Fouré, A., Nordez, A., Guette, M., and Cornu, C. (2009). Effects of plyometric training on passive stiffness of gastrocnemii and the musculo-articular complex of the ankle joint. *Scand. J. Med. Sci. Sports* 19, 811–818. doi: 10.1111/j.1600-0838.2008.00853.x

Gillespie, J., and Keenum, S. (1987). A validity and reliability analysis of the seated shot put as a test of power. *J. Hum. Mov. Stud.* 13, 97–105.

Grosset, J. F., Piscione, J., Lambertz, D., and Chantal, P. (2009). Paired changes in electromechanical delay and musculo-tendinous stiffness. *Eur. J. Appl. Physiol.* 105, 1673–1683.

Hachana, Y., Chaabene, H., Ben Rajeb, G., Khlifa, R., Aouadi, R., Chamari, K., et al. (2014). Validity and reliability of new agility test among elite and subelite under 14-soccer players. *PLoS One* 9:e95773. doi: 10.1371/journal.pone.0095773

Haj-Sassi, R., Dardouri, W., Gharbi, Z., Chaouachi, A., Mansour, H., Rabhi, A., et al. (2011). Reliability and validity of a new repeated agility test as a measure of anaerobic and explosive power. *J. Strength Cond. Res.* 25, 472–480. doi: 10.1519/jsc.0b013e3182018186

Hammami, M., Negra, Y., Aouadi, R., Shephard, R. J., and Chelly, M. S. (2016). Effects of an in-season plyometric training program on repeated change of direction and sprint performance in the junior soccer player. *J. Strength Cond. Res.* 30, 3312–3320. doi: 10.1519/jsc.0000000000001470

Hammami, M., Ramirez-Campillo, R., Gaamouri, N., Aloui, G., Shephard, R. J., and Chelly, M. S. (2019). Effects of a combined upper- and lower-limb plyometric training program on high-intensity actions in female U14 handball players. *Pediatr. Exerc. Sci.* 31, 465–472. doi: 10.1123/pes.2018-0278

Hannibal, N. S., Plowman, S. A., Looney, M. A., and Brandenburg, J. (2006). Reliability and validity of low back strength/muscular endurance field tests in adolescents. *J. Phys. Act Health* 3, S78–S89.

Helms, E. R., Cronin, J., Storey, A., and Zourdos, M. C. (2016). Application of the repetitions in reserve-based rating of perceived exertion scale for resistance training. *Strength Cond. J.* 38, 42–49. doi: 10.1519/ssc.0000000000000218

Ignjatovic, A. M., Markovic, Z. M., and Radovanovic, D. S. (2012). Effects of 12-week medicine ball training on muscle strength and power in young female handball players. *J. Strength Cond. Res.* 26, 2166–2173. doi: 10.1519/jsc.0b013e31823c477e

Kawamori, N., Nosaka, K., and Newton, R. U. (2013). Relationships between ground reaction impulse and sprint acceleration performance in team sport athletes. *J. Strength Cond. Res.* 27, 568–573. doi: 10.1519/jsc.0b013e318257805a

Kubo, K., Morimoto, M., Komuro, T., Tsunoda, N., Kanehisa, H., and Fukunaga, T. (2007). Influences of tendon stiffness, joint stiffness, and electromyographic activity on jump performances using single joint. *Eur. J. Appl. Physiol.* 99, 235–243. doi: 10.1007/s00421-006-0338-y

Maffiuletti, N. A., Dugnani, S., Folz, M., Di Pierno, E., and Mauro, F. (2002). Effect of combined electrostimulation and plyometric training on vertical jump height. *Med. Sci. Sports Exerc.* 34, 1638–1644. doi: 10.1097/00005768-200210000-00016

Malisoux, L., Francaux, M., and Theisen, D. (2007). What do single-fiber studies tell us about exercise training? *Med. Sci. Sports Exerc.* 39, 1051–1060. doi: 10.1249/mss.0b13e318057aeb

Markovic, G., and Mikulic, P. (2010). Neuro-musculoskeletal and performance adaptations to lower-extremity plyometric training. *Sports Med.* 40, 859–895. doi: 10.2165/11318370-000000000-00000

Mero, A. (1988). Force-time characteristics and running velocity of male sprinters during the acceleration phase of sprinting. *Res. Q. Exerc. Sport* 59, 94–98. doi: 10.1080/02701367.1988.10605484

Mero, A., Komi, P. V., and Gregor, R. J. (1992). Biomechanics of sprint running. A review. *Sports Med.* 13, 376–392. doi: 10.2165/00007256-199213060-00002

Meszler, B., and Vaczi, M. (2019). Effects of short-term in-season plyometric training in adolescent female basketball players. *Physiol. Int.* 106, 168–179. doi: 10.1556/2060.106.2019.14

Michalsik, L. B., and Aagaard, P. (2015). Physical demands in elite team handball: comparisons between male and female players. *J. Sports Med. Phys. Fitness* 55, 878–891.

Michalsik, L. B., Madsen, K., and Aagaard, P. (2014). Match performance and physiological capacity of female elite team handball players. *Int. J. Sports Med.* 35, 595–607. doi: 10.1055/s-0033-1358713

Mirwald, R. L., Baxter-Jones, A. D., Bailey, D. A., and Beunen, G. P. (2002). An assessment of maturity from anthropometric measurements. *Med. Sci. Sports Exerc.* 34, 689–694. doi: 10.1097/00005768-200204000-00020

Morin, J. B., Bourdin, M., Edouard, P., Peyrot, N., Samozino, P., and Lacour, J. R. (2012). Mechanical determinants of 100-m sprint running performance. *Eur. J. Appl. Physiol.* 112, 3921–3930. doi: 10.1007/s00421-012-2379-8

Negra, Y., Chaabene, H., Sammoud, S., Bouguezzi, R., Abbes, M. A., Hachana, Y., et al. (2017). Effects of plyometric training on physical fitness in prepuberal soccer athletes. *Int. J. Sports Med.* 38, 370–377. doi: 10.1055/s-0042-122337

Pauole, K., Madole, K., Garhammer, J., Lacourse, M., Rozenek, R. (2000). Reliability and validity of the t-test as a measure of agility leg power, and leg speed in college-aged men and women. *J. Strength Cond. Res.* 14, 443–450. doi: 10.1519/00124278-200011000-00012

Plisk, S., Beachle, T. R., and Earle, R. W. (2008). "Speed, agility, and speed-endurance development," in *Essentials of Strength Training and Conditioning*, eds T. R. Baechle, and R. W. Earle (Champaigh, IL: Human Kinetics), 458–485.

Prieske, O., Chaabene, H., Puta, C., Behm, D. G., Busch, D., and Granacher, U. (2019). Effects of drop height on jump performance in male and female elite adolescent handball players. *Int. J. Sports Physiol. Perform.* 14, 674–680. doi: 10.1123/ijspp.2018-0482

Ramirez-Campillo, R., Garcia-Pinillos, F., Garcia-Ramos, A., Yanci, J., Gentil, P., Chaabene, H., et al. (2018). Effects of Different Plyometric Training Frequencies on Components of Physical Fitness in Amateur Female Soccer Players. *Front. Physiol.* 9:934.

Rimmer, E., and Sleivert, G. (2000). Effects of a plyometrics intervention program on sprint performance. *J. Strength Cond. Res.* 14, 295–301. doi: 10.1519/00124278-200008000-00009

Rosas, F., Ramirez-Campillo, R., Martinez, C., Caniuqueo, A., Canas-Jamet, R., Mccrudden, E., et al. (2017). Effects of plyometric training and beta-alanine supplementation on maximal-intensity exercise and endurance in female soccer players. *J. Hum. Kinet.* 58, 99–109. doi: 10.1515/hukin-2017-0072

Rubley, M. D., Haase, A. C., Holcomb, W. R., Girouard, T. J., and Tandy, R. D. (2011). The effect of plyometric training on power and kicking distance in female adolescent soccer players. *J. Strength Cond. Res.* 25, 129–134. doi: 10.1519/jsc.0b013e3181b94a3d

Saeterbakken, A. H., Van Den Tillaar, R., and Seiler, S. (2011). Effect of core stability training on throwing velocity in female handball players. *J. Strength Cond. Res.* 25, 712–718. doi: 10.1519/jsc.0b013e3181cc227e

Stojanovic, E., Ristic, V., Mcmaster, D. T., and Milanovic, Z. (2017). Effect of plyometric training on vertical jump performance in female athletes: a systematic review and meta-analysis. *Sports Med.* 47, 975–986. doi: 10.1007/s40279-016-0634-6

Thomas, K., French, D., and Hayes, P. R. (2009). The effect of two plyometric training techniques on muscular power and agility in youth soccer players. *J. Strength Cond. Res.* 23, 332–335. doi: 10.1519/jsc.0b013e318183a01a

Wagner, H., Fuchs, P., Fusco, A., Fuchs, P., Bell, W. J., and Duvillard, S. P. (2018). Physical performance in elite male and female team handball players. *Int. J. Sports Physiol. Perform*. doi: 10.1123/ijspp.2018-0014 [Epub ahead of print].

Wong Del, P., Chan, G. S., and Smith, A. W. (2012). Repeated-sprint and change-of-direction abilities in physically active individuals and soccer players: training and testing implications. *J. Strength Cond. Res.* 26, 2324–2330. doi: 10.1519/jsc.0b013e31823daeab

Conflict of Interest: The authors declare that the research was conducted in the absence of any commercial or financial relationships that could be construed as a potential conflict of interest.

frontiers in Physiology

ORIGINAL RESEARCH
published: 12 November 2020
doi: 10.3389/fphys.2020.592183

Contribution of Stretch-Induced Force Enhancement to Increased Performance in Maximal Voluntary and Submaximal Artificially Activated Stretch-Shortening Muscle Action

Martin Groeber[1], Savvas Stafilidis[1], Wolfgang Seiberl[2] and Arnold Baca[1]*

[1] Department of Biomechanics, Kinesiology and Computer Science in Sport, Centre for Sport Science and University Sports, University of Vienna, Vienna, Austria, [2] Department of Human Movement Science, Institute of Sport Science, Bundeswehr University Munich, Neubiberg, Germany

In everyday muscle action or exercises, a stretch-shortening cycle (SSC) is performed under different levels of intensity. Thereby, compared to a pure shortening contraction, the shortening phase in a SSC shows increased force, work, and power. One mechanism to explain this performance enhancement in the SSC shortening phase is, besides others, referred to the phenomenon of stretch-induced increase in muscle force (known as residual force enhancement; rFE). It is unclear to what extent the intensity of muscle action influences the contribution of rFE to the SSC performance enhancement. Therefore, we examined the knee torque, knee kinematics, m. vastus lateralis fascicle length, and pennation angle changes of 30 healthy adults during isometric, shortening (CON) and stretch-shortening (SSC) conditions of the quadriceps femoris. We conducted maximal voluntary contractions (MVC) and submaximal electrically stimulated contractions at 20%, 35%, and 50% of MVC. Isometric trials were performed at 20° knee flexion (straight leg: 0°), and dynamic trials followed dynamometer-driven ramp profiles of 80°–20° (CON) and 20°–80°–20° (SSC), at an angular velocity set to 60°/s. Joint mechanical work during shortening was significantly ($p < 0.05$) enhanced by up to 21% for all SSC conditions compared to pure CON contractions at the same intensity. Regarding the steady-state torque after the dynamic phase, we found significant torque depression for all submaximal SSCs compared to the isometric reference contractions. There was no difference in the steady-state torque after the shortening phases between CON and SSC conditions at all submaximal intensities, indicating no stretch-induced rFE that persisted throughout the shortening. In contrast, during MVC efforts, the steady-state torque after SSC was significantly less depressed compared to the steady-state torque after the CON condition ($p = 0.034$), without significant differences in the m. vastus lateralis fascicle length and pennation angle. From these results, we concluded that the contribution of the potential enhancing factors in SSCs of the m. quadriceps femoris is dependent on the contraction intensity and the type of activation.

Keywords: force enhancement, force depression, elastic energy, electrical stimulation, muscular activation, concentric, eccentric

OPEN ACCESS

Edited by:
Li Zuo,
The Ohio State University,
United States

Reviewed by:
Mark Willems,
University of Chichester,
United Kingdom
Huub Maas,
Vrije Universiteit Amsterdam,
Netherlands

****Correspondence:***
Martin Groeber
martin.groeber@univie.ac.at

Specialty section:
This article was submitted to Striated Muscle Physiology, a section of the journal Frontiers in Physiology

Received: *06 August 2020*
Accepted: *19 October 2020*
Published: *12 November 2020*

Citation:
Groeber M, Stafilidis S, Seiberl W and Baca A (2020) Contribution of Stretch-Induced Force Enhancement to Increased Performance in Maximal Voluntary and Submaximal Artificially Activated Stretch-Shortening Muscle Action. Front. Physiol. 11:592183. doi: 10.3389/fphys.2020.592183

INTRODUCTION

A stretch-shortening cycle (SSC) is a muscle action that often occurs in everyday movements or sporting exercises. During a SSC, a lengthening contraction is immediately followed by a shortening contraction. This results in increased performance during the shortening phase compared to pure shortening contractions ("SSC-effect") (Komi and Gollhofer, 1997; Komi, 2000). The mechanisms attributed to the enhanced force or work during the concentric phase of the SSC are the stretch-reflex (Dietz et al., 1979), the release of stored passive-elastic energy (Finni et al., 2001; Kawakami et al., 2002) and the pre-activation of muscles (Bobbert and Casius, 2005). The reflex motor response can enhance the ongoing contraction and thus stretch reflexes can make a net contribution to muscle stiffness in the SSC (Komi and Gollhofer, 1997). Tendinous tissue can store and recoil passive elastic energy, which can be utilized in a SSC (Finni et al., 2001). Pre-activation describes the time required for force development. In the SSC, the initial stretch allows muscles to build up force before shortening begins (van Schenau et al., 1997). An additional SSC mechanism that has been particularly under discussion in recent literature is related to stretch-induced force enhancing effects within the contractile element of muscles (Seiberl et al., 2015b; Hahn and Riedel, 2018; Tomolka et al., 2020).

It is well accepted that—compared to a length- and activation-matched reference contraction—an eccentric muscle action provides increased force or torque during, but also after, the lengthening phase, when the muscle is kept active in an isometric steady-state. The force or torque response to stretch is described to have two components. First, a velocity-dependent force enhancement (FE) throughout the stretch period (Edman, 2012). And second, the long-lasting component, which is known as the phenomenon of residual force enhancement (rFE) (Herzog, 2004). There is some experimental evidence that mechanisms related to stretch-induced rFE also contribute to enhanced performance in the SSC (Seiberl et al., 2015b; Fortuna et al., 2017; Fukutani et al., 2017a; Hahn and Riedel, 2018; Groeber et al., 2019). Different parameters influence the amount of rFE. For example, with increased stretch amplitude, the amount of rFE rises (Edman, 1978; Sugi and Tsuchiya, 1988), and it occurs at all muscle lengths (Rassier et al., 2003). On the other hand, no influence of stretch velocity could be detected for slow and moderate speeds (Edman et al., 1982; Lee and Herzog, 2002), whereas for fast stretch speeds, no significant rFE could be found (Fukutani et al., 2019a). These findings suggested rFE to be a muscle property which could be observed at different structural muscle levels (Abbott and Aubert, 1952; Edman, 1978; Herzog et al., 2003; Bullimore et al., 2007) and in different muscle groups (Oskouei and Herzog, 2006b; Pinniger and Cresswell, 2007; Seiberl et al., 2013). A very frequently used approach to explain rFE is the protein titin, which is thought to act as a kind of molecular spring. The binding of Ca^{2+} might enhance intramolecular attraction and compactness in the PEVK region of titin, which would be expected to increase titin stiffness (Rode et al., 2009; Herzog, 2014; Linke, 2018; Fukutani and Herzog, 2019). However, the exact role of titin is still unclear.

In contrast to an active stretch, the steady-state force or torque after a concentric contraction is reduced compared to an isometric reference contraction at the same muscle length (residual force depression, rFD) (Herzog, 2004). Thereby, an increase in shortening speed is associated with a decrease in rFD (Herzog and Leonard, 2000). In conformity with the force-velocity relationship (Hill, 1938), increased contraction velocities lead to reduced force capacities resulting in reduced work produced during shortening. Thus, the amount of rFD increases with the amount of work during shortening. Accordingly, rFD declines with decreasing shortening magnitude (Maréchal and Plaghki, 1979; Herzog and Leonard, 1997). Stress-induced inhibition of the actin-myosin overlap zone is the primary mechanism suggested for rFD (Herzog, 2004; Joumaa et al., 2017). In addition, the protein titin might bind to actin upon muscle activation. This could lead to an inhibition of cross bridges by less binding sites for myosin on the actin filament due to bound titin (Rode et al., 2009).

These often independently researched phenomena of rFD and rFE are directly confronted in stretch-shortening cycles. If analyzed together in the context of SSCs, conflicting results for the interaction of these force-enhancing and -depressing history-dependent properties are presented in literature. For example, Seiberl et al. (2015b) and Fortuna et al. (2017) reported a contribution of rFE to the SSC performance enhancement by counteracting the development of rFD which is established during the concentric phase. In contrast, Herzog and Leonard (2000) and Lee et al. (2001) reported the same amount of rFD after a SSC as for pure concentric muscle actions. Thus, possible interactions of rFE- and rFD-related mechanisms in SSC, thereby influencing muscle performance, are still not well understood.

The standardized protocols for evaluating the history-dependent properties of muscle action may not adequately represent everyday movements like walking or running, since the operating conditions vary during muscle action with these natural movements (Bohm et al., 2018). However, in some resistance training exercises the magnitude and velocity of the eccentric and concentric phase is kept constant, especially when using lower intensities (Sakamoto and Sinclair, 2006, 2012). Although these parameters are similar in the eccentric and concentric phase, the entire SSC is often performed under different levels of intensity in resistance training exercises in order to regulate training exposure (Wernbom et al., 2007).

Concerning above mentioned mechanisms related to the performance enhancement in SSCs, it can be assumed, that the intensity of muscle action differently affects their contributions to increased force, work or power. For example, it is reported that rFE increases with increasing contraction intensity (Oskouei and Herzog, 2006a). However, this result could not be confirmed in a feedback-controlled submaximal knee extension protocol study (Seiberl et al., 2012). Owing to that, if contraction intensity could influence rFE, it would also influence performance in a SSC. Also, if the proposed mechanism of titin—which spans from the Z line to the M band of the sarcomere (Leonard and Herzog, 2010)—contributes to the enhancing effects, elastic titin forces might increase upon higher muscle activation (Fukutani and Herzog, 2019), meaning elevated Ca^{2+} ion concentration in the

environment of the myofibrils (Gehlert et al., 2015). Additionally, tendon elongation should be greater with increasing muscle force (Wang, 2006; Fukutani et al., 2017b), resulting in more elastic energy stored in the tendon during the eccentric phase, which is beneficial in the shortening phase of the SSC, but should not account solely for enhanced performance in a SSC (Seiberl et al., 2015b). Hence, the focus of this work was to examine the influence of contraction intensity on the history-dependent properties of muscle action in a SSC.

We hypothesized that with increasing intensity the SSC-effects are larger; possibly due to increased rFE, which should be observable by enhanced torque compared to a pure concentric (CON) muscle action in the steady-state after the SSC.

MATERIALS AND METHODS

Participants

Thirty healthy adults initially participated in this study. Three subjects did not complete the tests, or data was missing; therefore, they were excluded from further analysis. Finally, data were obtained from 12 female and 15 male adults (age: 26.6 ± 6.2 years, height: 175.4 ± 8.7 cm, body mass: 71.8 ± 11.3 kg), they all participated voluntarily and provided written informed consent prior to the study. The suitability of participation was determined with an anamnesis questionnaire to determine the risk factors for physical activity. The participants had no neuromuscular disorders, cardiovascular problems or injury to the right leg. The Ethics Committee of the University of Vienna approved the experimental protocol (reference number: 00364).

Experimental Setup

Knee joint torque was measured using an isokinetic dynamometer (HUMAC Norm, Model 770; CSMi) at the right leg. We captured all analog signals of the isokinetic dynamometer with the Vicon Nexus A/D card (16 bit) with a sampling frequency of 2 kHz. The upper body was fixed to the dynamometer by straps (100° seat back angle). The sitting position was precisely adapted to each test person. The lateral femoral condyles of every participant were aligned with the rotation axis of the dynamometer.

Synchronously, kinematic data was recorded with a Vicon Nexus motion-capturing system (Oxford, United Kingdom, 100 Hz) using nine cameras (Vantage V8). Eight reflective markers were captured, fixed at the following positions: trochanter major, the most prominent points of the medial and lateral femoral condyles, medial and lateral malleolus of the right leg. Additionally, we placed one marker at the axis of the dynamometer and two markers on the dynamometer's arm (one of them at the point of force application defining the lever arm as the distance between the line of action of the applied extension force and the dynamometer's axis of rotation).

For all voluntary contractions, the EMG signals of the m. vastus medialis and m. rectus femoris were captured (Delsys, Trigno Wireless EMG System, United States, 2 kHz) and recorded synchronously with the torque and kinematic data. The electrodes were attached following the guidelines of the SENIAM group (Hermens et al., 2000). The sensors had an inter-electrode spacing of 10 mm (Delsys, Trigno Avanti Sensor).

Muscle contractions were evoked at specific intensities by electrical stimulation (Digitimer DS8R, United Kingdom). The areas of the skin were shaved and cleaned with alcohol for the later application of the electrodes. The muscle motor points of m. vastus lateralis and m. vastus medialis were identified by scanning the skin's surface with a motor point pen (COMPEX, United Kingdom). Two electrodes (5 × 5 cm) were placed precisely on the previously identified motor points (Gobbo et al., 2014). Repetitive 100 μs square-wave pulses at 100 Hz were used. The train duration was approximately 6 s long.

For the investigation of history dependent effects in muscle action it is crucial that experimental conditions concerning muscle activity and muscle length are well controlled. Especially muscle length not necessarily follows dynamometer angular settings in a linear manner for different conditions and intensities, what can bias the interpretation of force capacities according to the force-length relationship of the knee extensors. For this reason, we additionally used ultrasonography (Telemed ArtUS EXT-1H, IT, 70 Hz) to determine the underlying fascicle length changes and pennation angle of the m. vastus lateralis (see **Figure 1**). A linear probe (LV8-5N60-A2) with a field of view of 60 mm was used. The probe was fixed to the muscle belly of the m. vastus lateralis with a custom-made bracket. To synchronize the video data with the other data recorded with Vicon Nexus, an analog signal (0–3 V) was generated when the video was started and stopped. This analog signal was captured by the Vicon system.

Experimental Protocol

On test day, the participants first had a general warm-up (bicycle ergometer, 5 min, between 80 and 90 W), which was followed by a specific warm-up of the quadriceps femoris on the isokinetic dynamometer (several submaximal contractions, 5 min). After the warm-up, the subjects had to perform two maximal voluntary contractions (MVCs) at a 20° dynamometer angle (full knee extension was defined as 0°). There was no statistical difference (t-test paired, p = 0.089) between the two MVC contractions (3.8% on average) and the average of peak joint torque of both

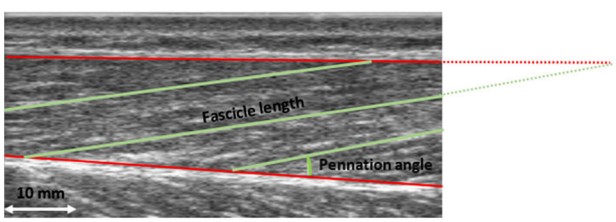

FIGURE 1 | Ultrasound image of the m. vastus lateralis. Fascicle length and pennation angle were determined for three fascicles. Pennation angle was calculated between the muscle fascicle and the deep aponeurosis. Fascicle length was defined as the distance between the intersection of the upper aponeurosis with the muscle fascicle and the intersection of the lower aponeurosis and muscle fascicle. The mean of the three measured values was used for further analysis.

trials was defined as 100% intensity. As a next step, current was applied and incrementally increased until the desired isometric knee torque was reached (20, 35, and 50% of MVC). Once the desired intensity was reached, the stimulus was maintained for several seconds to ensure a steady torque response. These current intensity settings were used for the entire experiment. The settings were checked again after a pause of one minute. The protocol comprised isometric contraction (ISO), pure shortening contractions (CON) and stretch-shortening cycles (SSC). It should be noted that the term 'isometric' is used for simplicity, although it actually refers to a fixed-end muscle-tendon unit contraction, where some muscle shortening at initial activation is likely, even when the joint angle is constant (Fukashiro et al., 1995). The angular velocity was fixed at 60°/s, and a fixed range of motion adjusted by the dynamometer (ISO: 20°, CON: 80°–20°, SSC: 20°–80°–20°) was used. This range of motion refers to the ascending limb of the knee extensor torque-angle relationship (Hahn et al., 2007) and reflects SSC ranges as found in many everyday movements such as walking, running or hopping (Jin and Hahn, 2019). In randomized order, MVC and different submaximal contraction intensities were tested (20, 35, and 50% of MVC) that were triggered through electrical stimulation. For simplified designation, tests under maximal voluntary contraction will be referred to as 100% (**Figure 2**). Rest between the contractions was two minutes in order to prevent fatigue (Tilp et al., 2011).

Dynamic contractions had an isometric pre-activation period before the dynamic phase (until a plateau was reached) followed by an isometric hold phase (steady-state) after the knee rotation. At the end of the experimental protocol, the subjects had to perform one fixed-end MVC at 20° dynamometer angle.

Data Processing

Torque and dynamometer angle data were low-pass filtered (zero-delay, fourth-order Butterworth) with a cut-off frequency of 10 Hz. Gravitational forces acting on the dynamometer arm system were corrected for all subjects. Each contraction was repeated twice and mean values were used for further analysis. CON and SSC were compared at T1 (80° dynamometer angle, end of stretch for SSC condition) and at 50° dynamometer angle (midpoint of 80°–20° range, T2) in the shortening phase. ISO, CON, and SSC were compared at the isometric steady-state, 1–1.5 s after the dynamic phase (T3, 20° dynamometer angle), while at that point the average values of 0.5 s were used (**Figure 3**).

Additionally, the mechanical work during angular rotation was calculated as the integral of torque during the shortening phase, using a numerical trapezoidal method.

$$W = \int M \, d\varphi = \int M \cdot \omega \, dt \tag{1}$$

with W as mechanical work [J], M as torque [Nm], and ω as rotational velocity [rad/s].

Due to difficulties in the standardization of the knee angle range of motion at high torque levels, mechanical work values were additionally adjusted to the respective range of motion in each individual trial (see results section). Different knee angles between CON and SSC at T1 affect the results of the absolute mechanical work during the shortening. Therefore, we decided to adjust mechanical work to the respective range of motion to avoid this problem.

Kinematic data was also low-pass filtered using a cutoff frequency of 10 Hz. Knee-joint angle was compared between conditions at time points T1, T2, and T3. It had been previously shown that due to the compliance of the dynamometer and the tissue deformation, a shift of both knee joint and dynamometer axis occurs, and therefore differences between the measured and the resultant knee joint moments exist. To address this shortcoming, we implemented the inverse dynamic approach proposed by (Arampatzis et al., 2004).

$$M_{res} = M_{Meas} \cdot \frac{d_K}{d_B} \tag{2}$$

with $\boldsymbol{M}_{res}$ as the corrected joint moment, $\boldsymbol{M}_{Meas}$ the initially measured moment, $\boldsymbol{d}_B$ as the lever arm of the applied force to the dynamometer axis and $\boldsymbol{d}_K$ as the lever arm of force to the knee joint [according to the free body diagram reported by Arampatzis et al. (2004)].

EMG data were band-pass filtered (10–400 Hz, fourth-order Butterworth), rectified, smoothed (250 ms moving average). Mean difference in m. rectus femoris and m. vastus medialis activity was used for analysis.

Pennation angle was calculated between the muscle fascicle and the deep aponeurosis. Fascicle length was defined as the

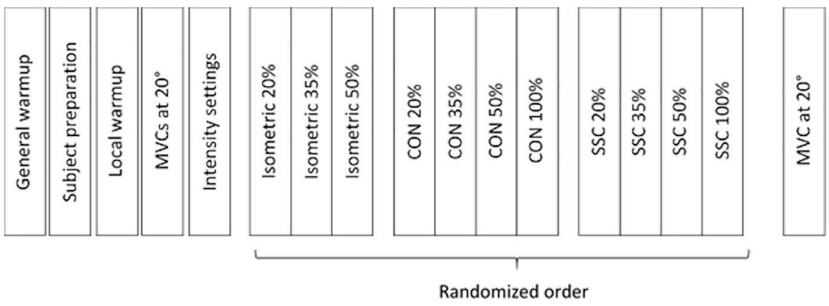

FIGURE 2 | Experimental protocol work flow. The test protocol comprised maximal voluntary contractions (100%) and submaximal electrical stimulated contractions at 20%, 35%, and 50% of MVC.

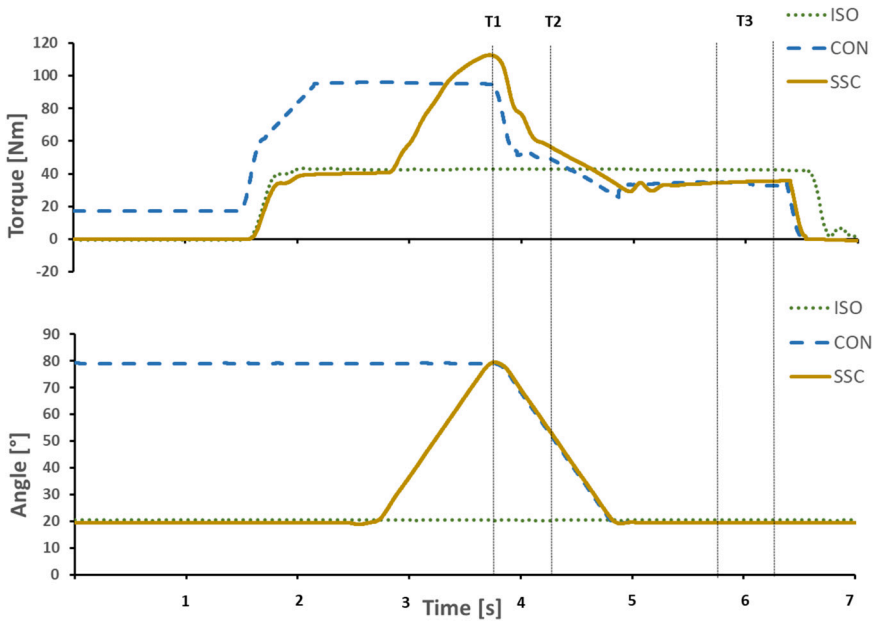

FIGURE 3 | Exemplary representation of torque-time and angle-time traces. Vertical lines indicate the time point at the end of stretch (T1), midpoint of shortening (T2), and the steady-state interval where the mean steady-state torque was calculated (T3). Continuous yellow line SSC, dotted green line ISO, and dashed blue line CON.

distance between the intersection of the superficial aponeurosis with the muscle fascicle and the intersection of the deep aponeurosis and muscle fascicle. This was always done for three fascicles and the mean value was calculated (see **Figure 1**). If the muscle fascicle was no longer visible on the image section, the point of intersection was calculated by assuming a linear continuation. Trigonometry was used to estimate the part of the fascicle that was not visible. This approach has been widely used before; nevertheless, it should be noted that this linear approach could result in an error. However, it was reported that this error is less than 2.4% (Narici et al., 2003; Reeves and Narici, 2003). Two evaluators digitized the ultrasound image separately for testing on interrater reliability, using open-source software (Tracker, Open Source Physics, Version 5.1.1).

The synchronization of all the data was achieved by use of the ultrasound device's start-stop analog signal.

Statistical Analysis

Data was tested for normality using a Kolmogorov–Smirnov test. Depending on the number of conditions to be compared, either a paired t-test with dependent variables or repeated measures ANOVA was employed. If sphericity was violated, Greenhouse-Geisser correction was used. Two-way ANOVA (within-within subject design) was adopted to examine the interaction (condition × intensity) and main effect (condition and intensity) for knee joint torque, mechanical work, knee angle, fascicle length and pennation angle. If the interaction (condition × intensity) was significant, subsequent *post hoc* comparisons with Bonferroni adjustments were conducted for comparing CON and SSC at each level of intensity. One-way ANOVA or paired t-test was utilized for EMG. The level of significance was set to $p < 0.05$. The effect size was assessed with partial eta squared (η^2). Interrater reliability for pennation angle and fascicle length measurements was analyzed by calculating the intraclass correlation coefficient (ICC, two-way mixed model; single measures).

By means of a paired *t*-test, the MVC at the end of the test session was compared with the MVC at the beginning to determine possible fatigue. For comparison of ISO, CON, and SSC conditions, the previously described time points (T1–T3) were used. Data are presented as mean ± SD.

RESULTS

Initial Conditions

The achieved isometric (ISO) joint torque at the specified percentages (20, 35, and 50% of MVC) reached a mean value of 23.2 ± 6.0%, 36.2 ± 8.0%, and 49.3 ± 9.4%, respectively, at the same dynamometer angle of 20°.

Further, a *t*-test revealed no statistical difference between MVCs at the beginning (92.5 ± 29.9 Nm) and at the end of the test protocol (91.3 ± 29.2 Nm), indicating no fatigue.

Joint Torque and Work Measurements

Two-way ANOVA revealed a significant interaction (condition × intensity) of torque after the stretch phase (T1) ($p = 0.023$, $\eta^2 = 0.159$). Main effect of intensity ($p < 0.001$, $\eta^2 = 0.843$) and for condition ($p < 0.001$, $\eta^2 = 0.501$) revealed increased torque with higher intensity and for the SSC condition. For the intensities of 35, 50, and 100%, the torque after the

stretch phase (T1) in SSCs was significantly higher compared to the isometric pre-activation in the CON conditions at the same activation level and the corresponding dynamometer angle (35%: $p = 0.013$; 50%: $p = 0.001$, and 100%: $p = 0.032$). This resulted in 13.7, 32.2, and 10.7% FE in the 35, 50, and 100% intensity conditions. No FE could be found for the lowest (20%) activation level ($p = 0.103$) (see **Figure 4** and **Table 1**).

Significant interaction (condition × intensity) was found for the range-adjusted mechanical work ($p = 0.049$, $\eta^2 = 0.123$). Main effect of intensity ($p < 0.001$, $\eta^2 = 0.839$) and condition ($p < 0.001$, $\eta^2 = 0.708$) revealed increased mechanical work with higher intensity and for the SSC condition. Range-adjusted mechanical work during shortening was significantly higher for all SSCs compared to CON contractions at the same activation level (20%: $p < 0.001$; 35%: $p < 0.001$; 50%: $p < 0.001$; 100%: $p = 0.001$) (see **Figure 5** and **Table 2**). The absolute mechanical work during shortening was also significantly higher for all SSC conditions compared to the CON conditions at the same intensity ($p < 0.05$). The percentage increase of normalized mechanical work in the SSC compared to CON contraction (referred to as SSC-effect) was 17.4, 17.7, 20.9, and 13.1% for the 20, 35, 50, and 100% intensities, respectively.

Regarding the steady-state torque after the dynamic phase (T3), two-way ANOVA with repeated measures revealed a significant interaction ($p = 0.004$, $\eta^2 = 0.207$). Main effect of intensity ($p < 0.001$, $\eta^2 = 0.856$) and condition ($p < 0.001$, $\eta^2 = 0.530$) was significant. *Post hoc* comparisons revealed significant rFD for all SSCs compared to the isometric reference conditions for all submaximal levels of contractions (20–50%). A significant torque depression of the CON contractions (CON_35%: 11.1%, CON_50%: 12.7%, CON_100%: 11.8%) could be found for all activation levels except 20% of MVC (CON_20%: 6.6%, no significance, $p = 0.288$). The only difference between CON and SSC was found under 100% ($p = 0.034$), where the SSC steady-state torque was significantly less depressed than in the CON condition (see **Figure 6** and **Table 1**).

TABLE 1 | Mean (±SD; $n = 27$) values of knee joint torque at T1 (onset of shortening) and T3 (steady-state after dynamic phase).

Contraction intensity	Knee joint torque [Nm ± SD]				
	T1		T3		
	CON	SSC	ISO	CON	SSC
20%	31.1 ± 10.7	29.8 ± 10.3	18.2 ± 4.8	17.1 ± 4.5	16.7 ± 3.6*
35%	**47.2 ± 19.6**	**53.7 ± 25.8**	29.9 ± 6.9	26.6 ± 7.0*	25.7 ± 6.1*
50%	**71.6 ± 37.8**	**94.7 ± 50.3**	40.4 ± 9.6	35.3 ± 10.7*	34.0 ± 10.1*
100%	**180.7 ± 62.1**	**200.0 ± 66.4**	76.4 ± 23.5	**67.4 ± 22.2***	**74.1 ± 25.1**

Bold values indicate significant ($p < 0.05$) differences between the shortening (CON) and stretch-shortening (SSC) condition at the respective intensity level and time-point. Asterisks indicate a significant difference of CON or SSC to the isometric reference contraction (ISO) at the respective intensity level and time-point.

Knee Angle

For knee angle, no significant interaction (condition × intensity) was found at all time points (T1: $p = 0.251$, $\eta^2 = 0.052$; T2: $p = 0.309$, $\eta^2 = 0.015$; T3: $p = 0.736$, $\eta^2 = 0.012$). Main effect of intensity was found at all three time points (T1: $p < 0.001$, $\eta^2 = 0.800$; T2: $p < 0.001$, $\eta^2 = 0.648$; T3: $p < 0.001$, $\eta^2 = 0.412$),

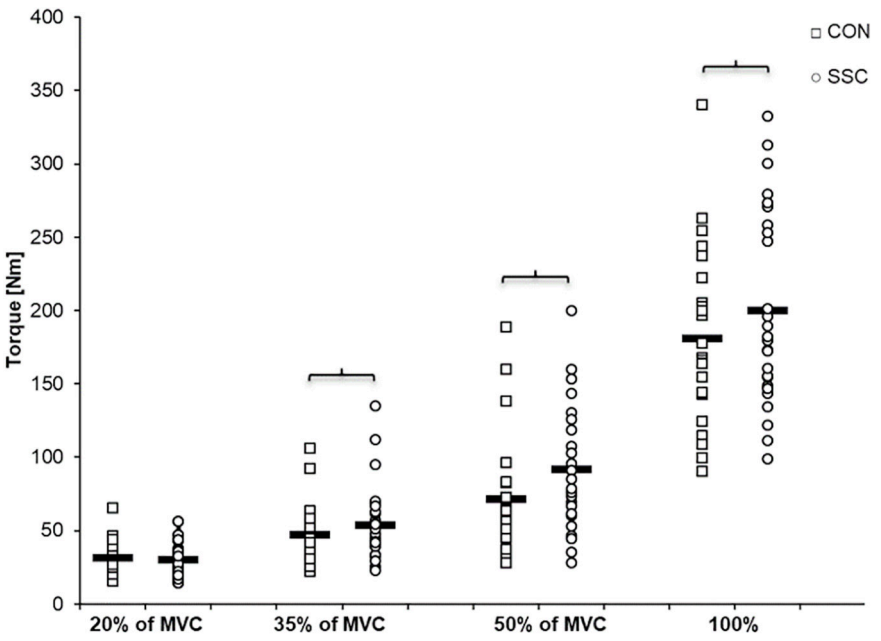

FIGURE 4 | Mean ($n = 27$, thick horizontal line) (and mean of each individual subject) values of joint torque at the onset of shortening (T1). Squares represent concentric condition (CON), whereas circles represent stretch-shortening conditions (SSC). Braces indicate significant ($p < 0.05$) differences between CON and SSC at the same intensity level.

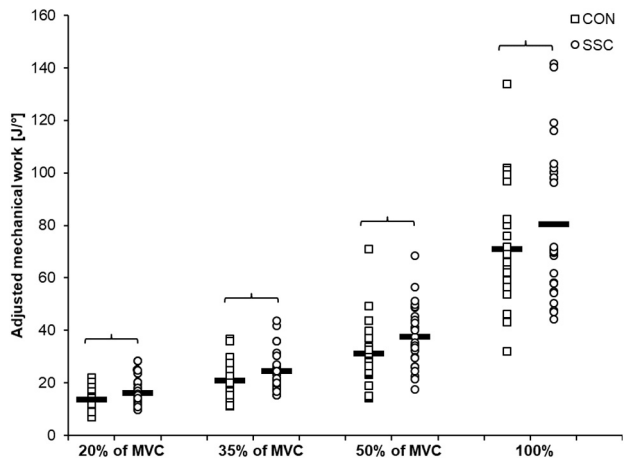

FIGURE 5 | Mean (n = 27, thick horizontal line) (and mean of each individual subjects) values of mechanical work adjusted to the actual knee rotation during the shortening phase. Squares represent concentric condition (CON), whereas circles represent stretch-shortening conditions (SSC). Braces indicate significant ($p < 0.05$) differences between CON and SSC at the same intensity level.

TABLE 2 | Mean (±SD; n = 27) values of the absolute mechanical work and the work adjusted to the actual knee rotation during shortening.

Contraction intensity	Absolute mechanical work [J ± SD]		Adjusted mechanical work [J/° ± SD]	
	CON	SSC	CON	SSC
20%	**763.8 ± 184.2**	**869.8 ± 182.2**	**13.8 ± 3.5**	**16.2 ± 4.4**
35%	**1150.0 ± 321.6**	**1295.9 ± 365.3**	**20.9 ± 6.9**	**24.6 ± 7.6**
50%	**1648.1 ± 525.5**	**1911.6 ± 558.0**	**31.1 ± 11.9**	**37.6 ± 11.7**
100%	**3458.9 ± 1044.9**	**3733.6 ± 1182.6**	**71.1 ± 24.0**	**80.4 ± 28.6**

Bold values indicate significant ($p < 0.05$) differences between the shortening (CON) and stretch-shortening (SSC) condition at the respective intensity.

knee joint flexion angle decreased significantly as the intensity raised. The main effect of condition was only significant at T1 ($p < 0.001$, $\eta^2 = 0.557$), knee joint flexion angle was significantly higher at the CON condition compared to the SSC condition (see **Figure 7**).

Muscle Architectural Changes

Analysis of the fascicle length and pennation angle was obtained by two independent investigators. Mean ICC across all measurements was 0.84 (ranging from 0.80 to 0.87 for subjects) for fascicle length and 0.81 (ranging 0.77–0.85 for subjects) for pennation angle, indicating good interrater reliability (Koo and Li, 2016).

The interaction (condition × intensity) was not significant for fascicle length at all time points (T1: $p = 0.667$, $\eta^2 = 0.015$; T2: $p = 0.638$, $\eta^2 = 0.021$; T3: $p = 0.717$, $\eta^2 = 0.021$). Main effect of intensity showed significant shorter fascicle length with increased intensity (T1: $p < 0.001$, $\eta^2 = 0.582$; T2: $p < 0.001$, $\eta^2 = 0.588$; T3: $p < 0.001$, $\eta^2 = 0.456$). Main effect of condition was not significant at all time points (T1: $p = 0.068$, $\eta^2 = 0.150$; T2: $p = 0.413$, $\eta^2 = 0.032$; T3: $p = 0.257$, $\eta^2 = 0.061$) (see **Figure 8**).

Two-way ANOVA revealed no significant interaction (condition × intensity) of pennation angle at all time points (T1: $p = 0.620$, $\eta^2 = 0.021$; T2: $p = 0.232$, $\eta^2 = 0.067$; T3: $p = 0.742$, $\eta^2 = 0.015$). Whereas the main effect of intensity showed, that pennation angle was increased with higher intensity (T1: $p < 0.001$, $\eta^2 = 0.550$; T2: $p < 0.001$, $\eta^2 = 0.630$; T3: $p < 0.001$, $\eta^2 = 0.452$). Pennation angle was significant higher in the CON condition compared to the SSC at T1. No statistical difference could be found at T2 and T3 (T1: $p = 0.023$, $\eta^2 = 0.224$; T2: $p = 0.392$, $\eta^2 = 0.035$; T3: $p = 0.984$, $\eta^2 < 0.001$) (see **Figure 9**).

Muscle Activity

For the comparison of SSC and CON muscle activity, we did not find any differences for all analyzed muscles and time points ($p > 0.05$). Between SSC and CON conditions the mean difference in m. rectus femoris activity was 3.1 ± 4.8%, 5.5 ± 5.6%, and 4.3 ± 4.0% at T1, T2, and T3, respectively. For m. vastus medialis, the mean difference between SSC and CON activity at T1, T2, and T3 was 8.6 ± 9.8%, 6.1 ± 5.0%, and 2.6 ± 3.4%.

At T3, in the steady-state phases after shortening, SSC and CON muscle activity was additionally compared to isometric references. Here, m. rectus femoris also did not show any statistical difference between conditions. For m. vastus medialis, compared to the ISO condition we found significantly lower muscle activity for both, the CON (22.5 ± 30.9%) and the SSC (20.6 ± 30.3%) condition ($p < 0.001$, $\eta^2 = 0.36$).

DISCUSSION

The study was designed to investigate the influence of the contraction intensity on stretch-induced performance enhancement in a SSC. We hypothesized that the SSC-effects (enhanced work during shortening phase) are larger with increasing intensity, partly explainable by increased contributions of stretch-induced mechanisms related to rFE. As expected, we found that the average work values were significantly greater for all SSCs compared to the corresponding concentric contractions. The SSC-effect was about 20% in the submaximal electrically stimulated trials, and about 13% in MVCs. Interestingly and against our expectations, despite the clear performance enhancement during SSCs, all shortening phases ended in significant rFD, except for SSCs performed at 100% intensity.

Similar to other studies, we found increased joint torque at the end of stretch compared to the isometric pre-activation in the CON condition (Power et al., 2013; Seiberl et al., 2015b; Hahn and Riedel, 2018), but not for all intensity levels. We did not see a FE at the end of stretches with the lowest activation (20% of MVC), but increasing FE from 13 to 32% with increasing electrical stimulation (**Figure 4**). Thus, our results indicate that the FE during the stretch phase is intensity dependent—at least during electrical stimulation. During voluntarily maximally activated SSCs, the torque was also significantly enhanced compared with

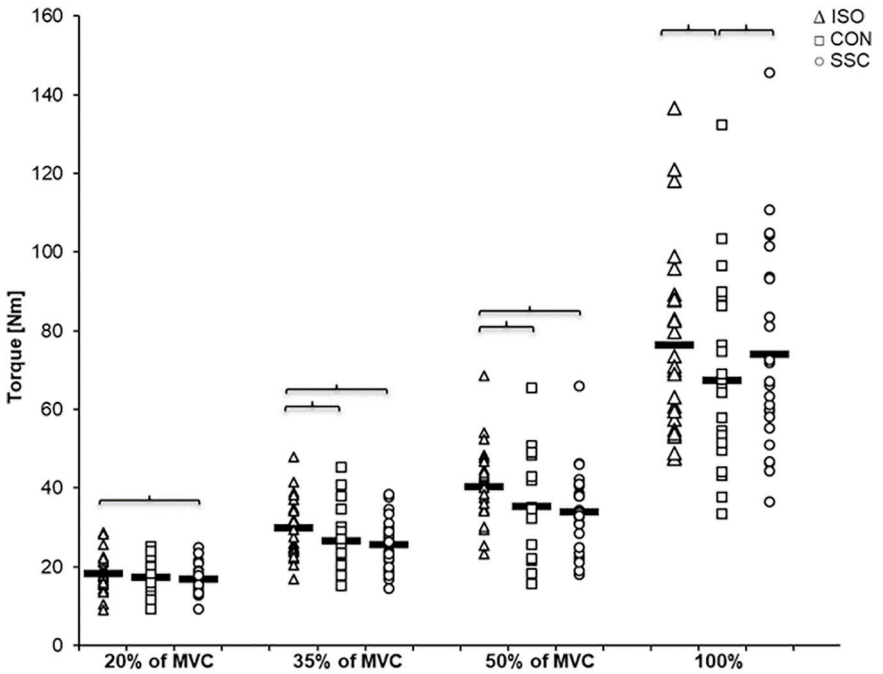

FIGURE 6 | Mean (n = 27, thick horizonal line) (and mean of each individual subject) values of joint torque in the steady-state after the dynamic phase (T3). Triangles represent purely isometric torque at 20° knee flexion (ISO), squares represent concentric condition (CON), whereas circles represent stretch-shortening conditions (SSC). Braces indicate significant ($p < 0.05$) differences between the conditions.

isometric pre-activation of the CON condition; but this FE of about 11% at 100% intensity was slightly lower than the FE at 35% intensity in the electrically stimulated trials. Similar to our study, Lee and Herzog (2002) compared peak forces during eccentric contractions in m. adductor pollicis and also found that slightly less FE was produced under MVC conditions compared to electrically stimulated contractions at an intensity the subjects could comfortably tolerate. A lack of increased force in voluntary eccentric contractions is typically associated with an inhibition of the neural drive (Westing et al., 1990; Webber and Kriellaars, 1997), which could explain the lower relative FE at MVCs compared with the submaximally electrically stimulated trials (≥35%). However, examination of the EMG data at the end of the stretch phase in SSCs showed no significant differences ($p > 0.05$) to the CON condition at the respective time point in the isometric pre-activation phase before shortening, which further means that also an inhibition of neural drive cannot explain these results. Our results indicate that relative FE increases with higher submaximal intensities. At the MVC level, the relative FE is smaller than during the electrically stimulated attempts (>35%).

The kinematic analysis revealed that there was a discrepancy between dynamometer-defined and measured knee angle. In the CON condition, the knee joint angle was significantly more flexed compared to the SSC condition. Although we did not find any statistical interaction (condition × intensity), the difference in knee joint angle between the conditions had the tendency to get bigger with increasing intensity. Accordingly, the highest discrepancy was found at the end of the stretch (T1) during MVC stretch-shortening trials, where the highest absolute torques were measured. Although the subjects were firmly strapped to the seat of the dynamometer, the high torques during the eccentric phases can lead to a slight elevation of the pelvis, what in turn gives way for the thigh and counteracts exact dynamometer-driven knee flexion. The significantly lower knee joint angles (more extended) at T1 led to architectural differences in pennation angle of m. vastus lateralis in these trials. Although we found no statistical difference in fascicle length (**Figure 8**), it can be assumed that the differences in knee joint and pennation angle influenced force and torque production according to the force-length and torque-angle relationship of knee extensors. As during this experiment the knee extensors likely worked on the ascending limb of the torque-angle relationship (Marginson and Eston, 2001; Hahn et al., 2007), the standardization difficulties possibly lead to an underestimation of the relative force enhancement at the end of stretch. We assume that a perfectly matched eccentric-concentric turning-point at a greater knee flexion angle would have generated even higher FE. This is also supported by data from the m. vastus lateralis confirming that the presented fascicle lengths in this work can be related to the ascending limb of the respective force-length relationship (Nikolaidou et al., 2017). Therefore, we believe it is safe to assume that there was clear FE in all SSC conditions, except for at the lowest intensities. However, since we did not assess the force-length relationship of each individual subject, the interpretation of an underestimated FE in these cases remains speculative. As already mentioned before, the range of motion was deliberately chosen, since it reflects SSC ranges as found in many everyday movements (Jin and Hahn, 2019). However, it should be noted that the

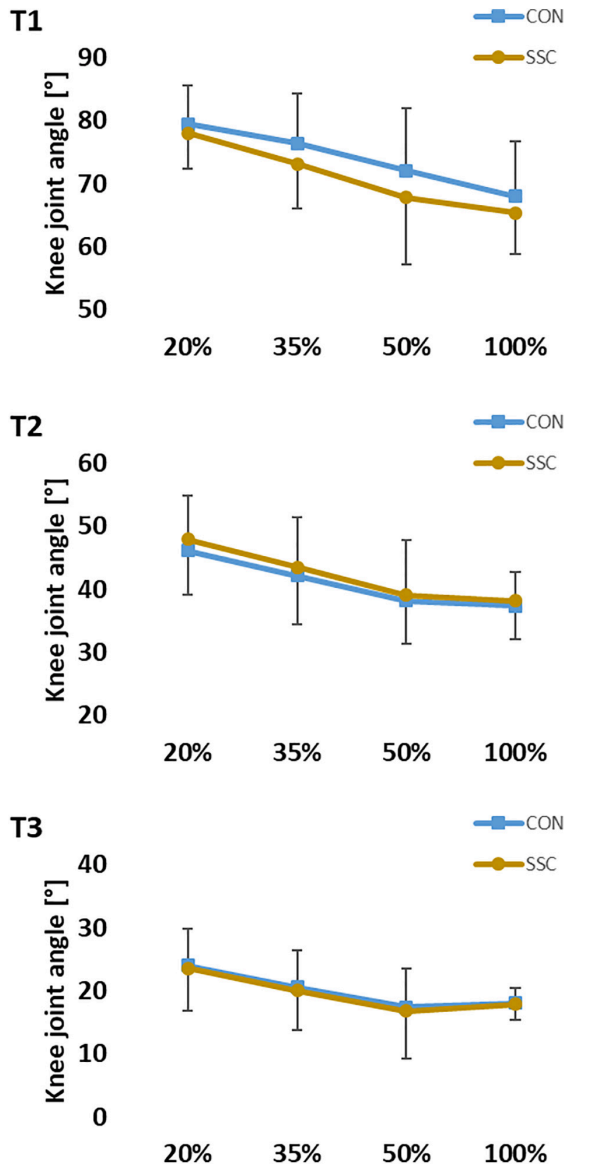

FIGURE 7 | Mean (±SD, n = 27) values of knee joint angle at different contraction intensities (% of MVC). T1 is the time-point at the onset of shortening, T2 in the middle of the shortening phase, T3 the time-point at steady-state after the dynamic phase. No significant interaction (condition × intensity) was found. Main effect of condition revealed, that knee joint flexion angle was significantly ($p < 0.05$) higher at the CON compared to the SSC condition at T1.

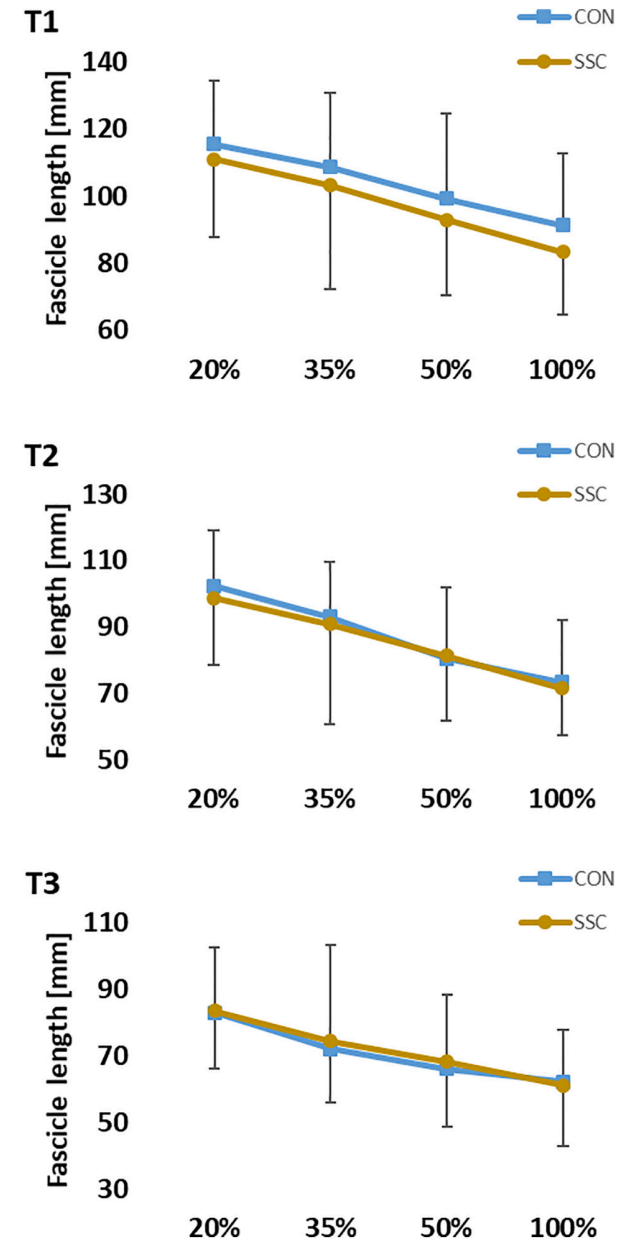

FIGURE 8 | Mean (±SD, n = 27) values of fascicle length at different contraction intensities (% of MVC). T1 is the time-point at the onset of shortening, T2 in the middle of the shortening phase, T3 the time-point at steady-state after the dynamic phase. No significant interaction (condition × intensity) was found. Main effect of condition was also not significant ($p > 0.05$).

results could be also different dependent on where the muscle operates on the force-length relationship. Under well controlled conditions *in vitro* or *in situ* studies, eccentric force enhancement during and after stretch is typically greater at longer sarcomeres or fascicle lengths (Granzier et al., 1989; Hisey et al., 2009). However, *in vivo* studies showing greater FE during stretch in multi-joint contractions (Hahn et al., 2014). In contrast to that, Linnamo et al. (2006) reported the same FE at short and long muscle lengths during single joint contractions.

Due to the fact that the knee joint angle at T1 was different between the SSC and CON conditions—which led to a greater angle change in the CON conditions—we adjusted calculations of mechanical work to the actual knee angle range during shortening for better comparability of conditions. The results confirmed that the work performed during shortening is significantly greater for all SSCs compared to the corresponding

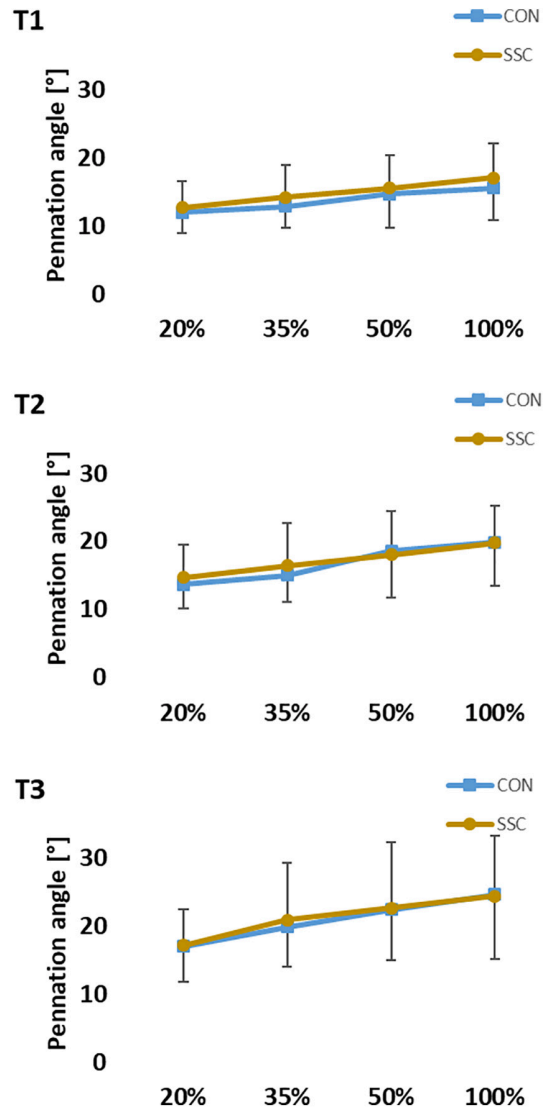

FIGURE 9 | Mean (±SD, n = 27) values of pennation angle at different contraction intensities (% of MVC). T1 is the time-point at the onset of shortening, T2 in the middle of the shortening phase, T3 the time-point at steady-state after the dynamic phase. No significant interaction (condition × intensity) was found. Main effect of condition revealed, that the pennation angle was significantly ($p < 0.05$) higher at the SSC compared to the CON condition at T1.

CON contractions. Even absolute mechanical work was greater for all SSC contractions, although the knee angle change during shortening, and thus the absolute range, was greater in the CON conditions. In literature, several mechanisms are presented to explain an enhancement of mechanical work during shortening in a SSC. Activation dynamics, i.e., the time required to fully establish muscle activation, can play a major role in movements with or without a counter-movement (Fukutani et al., 2019b). However, muscle activation has no influence on our results of performance enhancement in SSCs, since we always had an isometric pre-activation phase before the dynamic phases. This means that for every level of intensity, trials for both conditions started with an identical muscle activity. Additionally, the stretch-reflex activity is discussed in order to contribute to increased work in SSCs. However, we consider the relevance of stretch-reflex contributions in our settings to be negligible or even non-existent for two reasons. First, stretch reflexes are expected in fast movements with fast muscle lengthening—such as hopping (Komi and Gollhofer, 1997)—and should not be relevant in our experiment with a movement velocity of 60°/s. Second, electrical stimulation was used in all submaximal trials, where clear SSC-effects were evident. In addition, by the visual inspection of the EMG data we did not identify any suspicious activation peaks at the onset of stretch. For these reasons, we are confident that the stretch-reflex also has no or negligible influence on our results.

As already mentioned at the beginning of this paper, this leaves two remaining mechanisms that most likely explain the entire SSC performance enhancement found in our work. The lengthening of passive elastic structures leads to the storage of elastic energy that is released during shortening and thereby contributes to enhanced work during shortening in the SSC (Finni et al., 2001). Additionally, tendon elongation can affect changes in muscle length, resulting in enhanced force-generating capability due to the force-velocity relationship (Hill, 1938; Ishikawa et al., 2005). The amount of tendon elongation is dependent on the force applied to the tendon (Reeves et al., 2003), which in our experiment means that with higher intensity, more energy can be stored in the tendon. This is true for the absolute forces and work during SSCs; however, the relative SSC-effect was nearly constant for all submaximal intensities ranging between 17 and 21% increased work, and slightly lower SSC-effects were found during MVCs. Contrary to what we expected, no influence of intensity on the relative mechanical work during shortening in the SSC was found, whereas the type of activation (electrically stimulated vs. voluntary) seems to have an influence on the SSC-effects.

The main question for this experiment was whether, and to what extent, stretch-induced force-enhancing effects within the contractile element of muscles can contribute to enhanced work during the shortening. In contrast to the discussed mechanisms above, a contribution of rFE-related mechanisms to increased work during shortening in SSC should be visible also after the shortening phase (Seiberl et al., 2015b). It was speculated that if rFE-related mechanisms contribute to the SSC-effects, then the increased force/torque should be triggered during the stretch phase, contribute to the performance enhancement during the shortening phase, and should be visible as a history-dependent property in the steady-state phases after the SSC. Joint torque in the steady-state (T3) after the pure CON trials was significantly depressed compared to the ISO reference contraction (range 6.6–12.7%, not significant for 20% intensity), which is in line with previous studies that reported a rFD between 5 and 25% at knee extensions (Lee et al., 1999, 2000; Altenburg et al., 2008; Dargeviciute et al., 2013). No statistical difference of rFD was found for pure CON muscle action and SSC at the same activation level, except for the test under maximal voluntary activation (CON_100%: rFD of 11.8% and SSC_100%: rFD of 3.1%), without any difference in m. vastus lateralis fascicle length

and pennation angle. This indicates that mechanisms related to rFE are responsible for the less depressed steady-state torque in our experiment during the maximum voluntary SSC condition, which further means that the intensity of contraction and/or the type of activation in a SSC has an influence on this long-lasting component. Based on this finding, it might be concluded that there is an activation threshold where no significant rFD in the SSC of the m. quadriceps femoris remains. However, one needs to be careful comparing the submaximal and MVC conditions in this work, as there are important differences between voluntary and electrically elicited contractions. Electrically stimulated muscles do not mirror the asynchronous and varied firing frequencies voluntary activation shows (Lee et al., 1999) what likely influences muscle function as well. History-dependent effects show way more variability during voluntary contractions, than what we would expect from the 'facts' derived from animal models and electrically stimulated muscle action (Seiberl et al., 2015a). The reasons are still not well understood. We decided to use electrical stimulation for all submaximal contractions, since torque or EMG feedback-controlled trials are experimentally difficult to implement, and it can be only matched at the isometric state before and after the dynamic phase. This is not the case for MVCs, but extremely high stimulation intensities would be too painful and not tolerable for participants. For this reason, voluntary contractions were used for 100% intensity trials that additionally better represent everyday tasks or exercises like the squat, where we also have a stretch of the m. quadriceps femoris directly followed by a shortening contraction.

In literature, a current approach to explaining rFE is related to a titin-actin interaction (Rode et al., 2009; Herzog et al., 2016; Linke, 2018; Fukutani and Herzog, 2019). Titin stiffness increases with higher muscle activation, which could result in a reduced rFD in our SSC under maximal voluntary contraction. As previously reported, there are conflicting results in literature regarding the effects of rFE in the SSC (Groeber et al., 2019). Some authors reported that any stretch-induced rFE was abolished during the shortening in SSCs (Herzog and Leonard, 2000; Lee et al., 2001; Fukutani et al., 2019b), whereas others observed significantly higher force or torque values in the steady-state after the SSC compared to pure shortening muscle action (Seiberl et al., 2015b; Fortuna et al., 2017; Hahn and Riedel, 2018). Seiberl et al. (2015b) and Hahn and Riedel (2018) used electrical stimulation at 50–60% and 32.9% of MVC respectively, but they both had quite high shortening velocities in their test protocol, which is associated with reduced rFD (Herzog and Leonard, 2000). Additionally, Fortuna et al. (2017) reported that shortening affects rFD in SSC contractions in a time-dependent manner. The authors found that with a longer shortening time, a greater rFD was produced. However, the same authors still reported a reduced rFD after the SSC at an intensity level of 50–60% of MVC when the shortening phase was 1 s in length as was the case in our protocol. Their results come from the m. adductor pollicis, which—compared to the m. quadriceps femoris—is of a smaller size and has a short tendon. Since the mechanism for different rFD values with different muscle group sizes remain unknown (Chen et al., 2019), one can only speculate about the possible influence of muscle size on rFD in a SSC contraction.

CONCLUSION

To our knowledge, this is the first study considering the steady-state torque after a SSC of the m. quadriceps femoris under maximal voluntary contractions and under different submaximal contraction intensities. We hypothesized that with increasing intensity, the SSC-effects are larger, possibly due to increased rFE.

In conclusion, we observed increased mechanical work during the shortening phase of the SSC for all contraction intensities. Additionally, reduced rFD in the SSC condition compared to CON was only found for 100% intensity. Under reduced activation, the stretch-induced force-enhancing effects were only visible during the shortening phase. Our results indicate that the magnitude of contribution of the potential mechanisms in SSCs of the m. quadriceps femoris changes with the intensity and type of activation. Furthermore, the complete attenuation of rFE in the lower intensities despite greater mechanical work during the shortening phase should be examined in future studies.

DATA AVAILABILITY STATEMENT

The raw data supporting the conclusions of this article will be made available by the authors, without undue reservation.

ETHICS STATEMENT

The studies involving human participants were reviewed and approved by the Ethics Committee of the University of Vienna. The patients/participants provided their written informed consent to participate in this study.

AUTHOR CONTRIBUTIONS

MG, SS, and AB conceived and designed the experiment. MG performed the experiment. MG and SS analyzed the data. MG, SS, WS, and AB discussed the results, made a substantial contribution to the interpretation of data, and contributed to the elaboration of the manuscript. All authors contributed to the article and approved the submitted version.

FUNDING

Open access funding was provided by the University of Vienna, and partial funding was provided by the German Research Foundation (DFG) under the grant number SE 2109/2-1.

ACKNOWLEDGMENTS

We thank Philipp Kornfeind and Markus Kleinberger for their assistance in the laboratory. We also would like to thank all participants for their time and motivation.

REFERENCES

Abbott, B. C., and Aubert, X. M. (1952). The force exerted by active striated muscle during and after change of length. *J. Physiol.* 117, 77–86.

Altenburg, T. M., de Ruiter, C. J., Verdijk, P. W. L., van Mechelen, W., and de Haan, A. (2008). Vastus lateralis surface and single motor unit EMG following submaximal shortening and lengthening contractions. *Appl. Physiol. Nutr. Metab.* 33, 1086–1095. doi: 10.1139/h08-092

Arampatzis, A., Karamanidis, K., de Monte, G., Stafilidis, S., Morey-Klapsing, G., and Brüggemann, G.-P. (2004). Differences between measured and resultant joint moments during voluntary and artificially elicited isometric knee extension contractions. *Clin. Biomechan. (Bristol, Avon)* 19, 277–283. doi: 10.1016/j.clinbiomech.2003.11.011

Bobbert, M. F., and Casius, L. J. R. (2005). Is the effect of a countermovement on jump height due to active state development? *Med. Sci. Sports Exerc.* 37, 440–446. doi: 10.1249/01.MSS.0000155389.34538.97

Bohm, S., Marzilger, R., Mersmann, F., Santuz, A., and Arampatzis, A. (2018). Operating length and velocity of human vastus lateralis muscle during walking and running. *Sci. Rep* 8:5066. doi: 10.1038/s41598-018-23376-23375

Bullimore, S. R., Leonard, T. R., Rassier, D. E., and Herzog, W. (2007). History-dependence of isometric muscle force: effect of prior stretch or shortening amplitude. *J. Biomechan.* 40, 1518–1524. doi: 10.1016/j.jbiomech.2006.06.014

Chen, J., Hahn, D., and Power, G. A. (2019). Shortening-induced residual force depression in humans. *J. Appl. Physiol. (1985)* 126, 1066–1073. doi: 10.1152/japplphysiol.00931.2018

Dargeviciute, G., Masiulis, N., Kamandulis, S., Skurvydas, A., and Westerblad, H. (2013). Residual force depression following muscle shortening is exaggerated by prior eccentric drop jump exercise. *J. Appl. Physiol. (1985)* 115, 1191–1195. doi: 10.1152/japplphysiol.00686.2013

Dietz, V., Schmidtbleicher, D., and Noth, J. (1979). Neuronal mechanisms of human locomotion. *J. Neurophys.* 42, 1212–1222. doi: 10.1152/jn.1979.42.5.1212

Edman, K. A. (1978). Maximum velocity of shortening in relation to sarcomere length and degree of activation of frog muscle fibres proceedings. *J. Physiol.* 278, 9–10.

Edman, K. A., Elzinga, G., and Noble, M. I. (1982). Residual force enhancement after stretch of contracting frog single muscle fibers. *J. General Physiol.* 80, 769–784. doi: 10.1085/jgp.80.5.769

Edman, K. A. P. (2012). Residual force enhancement after stretch in striated muscle. a consequence of increased myofilament overlap? *J. Physiol.* 590, 1339–1345. doi: 10.1113/jphysiol.2011.222729

Finni, T., Ikegawa, S., and Komi, P. V. (2001). Concentric force enhancement during human movement. *Acta Physiol. Scand.* 173, 369–377. doi: 10.1046/j.1365-201X.2001.00915.x

Fortuna, R., Groeber, M., Seiberl, W., Power, G. A., and Herzog, W. (2017). Shortening-induced force depression is modulated in a time- and speed-dependent manner following a stretch-shortening cycle. *Physiol. Rep.* 5:e13279. doi: 10.14814/phy2.13279

Fukashiro, S., Itoh, M., Ichinose, Y., Kawakami, Y., and Fukunaga, T. (1995). Ultrasonography gives directly but noninvasively elastic characteristic of human tendon in vivo. *Eur. J. Appl. Physiol. Occupat. Physiol.* 71, 555–557. doi: 10.1007/BF00238560

Fukutani, A., and Herzog, W. (2019). Current understanding of residual force enhancement: cross-bridge component and non-cross-bridge component. *Int. J. Mol. Sci.* 20:5479. doi: 10.3390/ijms20215479

Fukutani, A., Joumaa, V., and Herzog, W. (2017a). Influence of residual force enhancement and elongation of attached cross-bridges on stretch-shortening cycle in skinned muscle fibers. *Physiol. Rep.* 5:13477. doi: 10.14814/phy2.13477

Fukutani, A., Misaki, J., and Isaka, T. (2017b). Relationship between joint torque and muscle fascicle shortening at various joint angles and intensities in the plantar flexors. *Sci. Rep.* 7:290. doi: 10.1038/s41598-017-00485-481

Fukutani, A., Leonard, T., and Herzog, W. (2019a). Does stretching velocity affect residual force enhancement? *J. Biomechan.* 89, 143–147. doi: 10.1016/j.jbiomech.2019.04.033

Fukutani, A., Shimoho, K., and Isaka, T. (2019b). Pre-activation affects the effect of stretch-shortening cycle by modulating fascicle behavior. *Biol. Open* 8:bio044651. doi: 10.1242/bio.044651

Gehlert, S., Bloch, W., and Suhr, F. (2015). Ca2+-dependent regulations and signaling in skeletal muscle: from electro-mechanical coupling to adaptation. *Int. J. Mol. Sci.* 16, 1066–1095. doi: 10.3390/ijms16011066

Gobbo, M., Maffiuletti, N. A., Orizio, C., and Minetto, M. A. (2014). Muscle motor point identification is essential for optimizing neuromuscular electrical stimulation use. *J. Neuroeng. Rehabilitation* 11:17. doi: 10.1186/1743-0003-11-17

Granzier, H. L., Burns, D. H., and Pollack, G. H. (1989). Sarcomere length dependence of the force-velocity relation in single frog muscle fibers. *Biophys. J.* 55, 499–507. doi: 10.1016/S0006-3495(89)82843-7

Groeber, M., Reinhart, L., Kornfeind, P., and Baca, A. (2019). The contraction modalities in a stretch-shortening cycle in animals and single joint movements in humans: a systematic review. *J. Sports Sci. Med.* 18, 604–614.

Hahn, D., Herzog, W., and Schwirtz, A. (2014). Interdependence of torque, joint angle, angular velocity and muscle action during human multi-joint leg extension. *Eur. J. Appl. Physiol.* 114, 1691–1702. doi: 10.1007/s00421-014-2899-5

Hahn, D., and Riedel, T. N. (2018). Residual force enhancement contributes to increased performance during stretch-shortening cycles of human plantar flexor muscles in vivo. *J. Biomechan.* 77, 190–193. doi: 10.1016/j.jbiomech.2018.06.003

Hahn, D., Seiberl, W., and Schwirtz, A. (2007). Force enhancement during and following muscle stretch of maximal voluntarily activated human quadriceps femoris. *Eur. J. Appl. Physiol.* 100, 701–709. doi: 10.1007/s00421-007-0462-463

Hermens, H. J., Freriks, B., Disselhorst-Klug, C., and Rau, G. (2000). Development of recommendations for SEMG sensors and sensor placement procedures. *J. Electromyography Kinesiol.* 10, 361–374. doi: 10.1016/S1050-6411(00)00027-24

Herzog, W. (2004). History dependence of skeletal muscle force production: implications for movement control. *Hum. Movem. Sci.* 23, 591–604. doi: 10.1016/j.humov.2004.10.003

Herzog, W. (2014). Mechanisms of enhanced force production in lengthening (eccentric) muscle contractions. *J. Appl. Physiol. (*1985) 116, 1407–1417. doi: 10.1152/japplphysiol.00069.2013

Herzog, W., and Leonard, T. R. (1997). Depression of cat soleus forces following isokinetic shortening. *J. Biomechan.* 30, 865–872. doi: 10.1016/S0021-9290(97)00046-48

Herzog, W., and Leonard, T. R. (2000). The history dependence of force production in mammalian skeletal muscle following stretch-shortening and shortening-stretch cycles. *J. Biomechan.* 33, 531–542. doi: 10.1016/s0021-9290(99)00221-223

Herzog, W., Schachar, R., and Leonard, T. R. (2003). Characterization of the passive component of force enhancement following active stretching of skeletal muscle. *J. Exp. Biol.* 206, 3635–3643. doi: 10.1242/jeb.00645

Herzog, W., Schappacher, G., DuVall, M., Leonard, T. R., and Herzog, J. A. (2016). Residual force enhancement following eccentric contractions: a new mechanism involving titin. *Physiology (Bethesda, Md.)* 31, 300–312. doi: 10.1152/physiol.00049.2014

Hill, A. V. (1938). The heat of shortening and the dynamic constants of muscle. *Proc. R. Soc. Lond. B* 126, 136–195. doi: 10.1098/rspb.1938.0050

Hisey, B., Leonard, T. R., and Herzog, W. (2009). Does residual force enhancement increase with increasing stretch magnitudes? *J. Biomechan.* 42, 1488–1492. doi: 10.1016/j.jbiomech.2009.03.046

Ishikawa, M., Komi, P. V., Grey, M. J., Lepola, V., and Bruggemann, G.-P. (2005). Muscle-tendon interaction and elastic energy usage in human walking. *J. Appl. Physiol. (1985)* 99, 603–608. doi: 10.1152/japplphysiol.00189.2005

Jin, L., and Hahn, M. E. (2019). Comparison of lower extremity joint mechanics between healthy active young and middle age people in walking and running gait. *Sci. Rep.* 9:5568. doi: 10.1038/s41598-019-41750-9

Joumaa, V., Fitzowich, A., and Herzog, W. (2017). Energy cost of isometric force production after active shortening in skinned muscle fibres. *J. Exp. Biol.* 220, 1509–1515. doi: 10.1242/jeb.117622

Kawakami, Y., Muraoka, T., Ito, S., Kanehisa, H., and Fukunaga, T. (2002). In vivo muscle fibre behaviour during counter-movement exercise in humans reveals a significant role for tendon elasticity. *J. Physiol.* 540, 635–646. doi: 10.1113/jphysiol.2001.013459

Komi, P. V. (2000). Stretch-shortening cycle: a powerful model to study normal and fatigued muscle. *J. Biomechan.* 33, 1197–1206. doi: 10.1016/S0021-9290(00)00064-66

Komi, P. V., and Gollhofer, A. (1997). Stretch reflexes can have an important role in force enhancement during SSC exercise. *J. Appl. Biomechan.* 13, 451–460. doi: 10.1123/jab.13.4.451

Koo, T. K., and Li, M. Y. (2016). A guideline of selecting and reporting intraclass correlation coefficients for reliability research. *J. Chiropractic Med.* 15, 155–163. doi: 10.1016/j.jcm.2016.02.012

Lee, H.-D., and Herzog, W. (2002). Force enhancement following muscle stretch of electrically stimulated and voluntarily activated human adductor pollicis. *J. Physiol.* 545, 321–330. doi: 10.1113/jphysiol.2002.018010

Lee, H.-D., Herzog, W., and Leonard, T. (2001). Effects of cyclic changes in muscle length on force production in in-situ cat soleus. *J. Biomechan.* 34, 979–987. doi: 10.1016/s0021-9290(01)00077-x

Lee, H. D., Suter, E., and Herzog, W. (1999). Force depression in human quadriceps femoris following voluntary shortening contractions. *J. Appl. Physiol. (1985)* 87, 1651–1655. doi: 10.1152/jappl.1999.87.5.1651

Lee, H.-D., Suter, E., and Herzog, W. (2000). Effects of speed and distance of muscle shortening on force depression during voluntary contractions. *J. Biomechan.* 33, 917–923. doi: 10.1016/s0021-9290(00)00070-71

Leonard, T. R., and Herzog, W. (2010). Regulation of muscle force in the absence of actin-myosin-based cross-bridge interaction. *Am. J. Physiol. Cell Physiol.* 299, C14–C20. doi: 10.1152/ajpcell.00049.2010

Linke, W. A. (2018). Titin gene and protein functions in passive and active muscle. *Annu. Rev. Physiol.* 80, 389–411. doi: 10.1146/annurev-physiol-021317-121234

Linnamo, V., Strojnik, V., and Komi, P. V. (2006). Maximal force during eccentric and isometric actions at different elbow angles. *Eur. J. Appl. Physiol.* 96, 672–678. doi: 10.1007/s00421-005-0129-x

Maréchal, G., and Plaghki, L. (1979). The deficit of the isometric tetanic tension redeveloped after a release of frog muscle at a constant velocity. *J. General Physiol.* 73, 453–467. doi: 10.1085/jgp.73.4.453

Marginson, V., and Eston, R. (2001). The relationship between torque and joint angle during knee extension in boys and men. *J. Sports Sci.* 19, 875–880. doi: 10.1080/026404101753113822

Narici, M. V., Maganaris, C. N., Reeves, N. D., and Capodaglio, P. (2003). Effect of aging on human muscle architecture. *J. Appl. Physiol. (1985)* 95, 2229–2234. doi: 10.1152/japplphysiol.00433.2003

Nikolaidou, M. E., Marzilger, R., Bohm, S., Mersmann, F., and Arampatzis, A. (2017). Operating length and velocity of human M. vastus lateralis fascicles during vertical jumping. *R Soc. Open Sci.* 4:170185. doi: 10.1098/rsos.170185

Oskouei, A. E., and Herzog, W. (2006a). Force enhancement at different levels of voluntary contraction in human adductor pollicis. *Eur. J. Appl. Physiol.* 97, 280–287. doi: 10.1007/s00421-006-0167-z

Oskouei, A. E., and Herzog, W. (2006b). The dependence of force enhancement on activation in human adductor pollicis. *Eur. J. Appl. Physiol.* 98, 22–29. doi: 10.1007/s00421-006-0170-174

Pinniger, G. J., and Cresswell, A. G. (2007). Residual force enhancement after lengthening is present during submaximal plantar flexion and dorsiflexion actions in humans. *J. Appl. Physiol. (1985)* 102, 18–25. doi: 10.1152/japplphysiol.00565.2006

Power, G. A., Makrakos, D. P., Rice, C. L., and Vandervoort, A. A. (2013). Enhanced force production in old age is not a far stretch: an investigation of residual force enhancement and muscle architecture. *Physiol. Rep.* 1:e00004. doi: 10.1002/phy2.4

Rassier, D. E., Herzog, W., and Pollack, G. H. (2003). Dynamics of individual sarcomeres during and after stretch in activated single myofibrils. *Proc. Biol. Sci.* 270, 1735–1740. doi: 10.1098/rspb.2003.2418

Reeves, N. D., Maganaris, C. N., and Narici, M. V. (2003). Effect of strength training on human patella tendon mechanical properties of older individuals. *J. Physiol.* 548, 971–981. doi: 10.1111/j.2003.t01-1-00971.x

Reeves, N. D., and Narici, M. V. (2003). Behavior of human muscle fascicles during shortening and lengthening contractions in vivo. *J. Appl. Physiol. (1985)* 95, 1090–1096. doi: 10.1152/japplphysiol.01046.2002

Rode, C., Siebert, T., and Blickhan, R. (2009). Titin-induced force enhancement and force depression: a 'sticky-spring' mechanism in muscle contractions? *J. Theoretical Biol.* 259, 350–360. doi: 10.1016/j.jtbi.2009.03.015

Sakamoto, A., and Sinclair, P. J. (2006). Effect of movement velocity on the relationship between training load and the number of repetitions of bench press. *J. Strength Condition. Res.* 20, 523–527. doi: 10.1519/16794.1

Sakamoto, A., and Sinclair, P. J. (2012). Muscle activations under varying lifting speeds and intensities during bench press. *Eur. J. Appl. Physiol.* 112, 1015–1025. doi: 10.1007/s00421-011-2059-2050

Seiberl, W., Hahn, D., Herzog, W., and Schwirtz, A. (2012). Feedback controlled force enhancement and activation reduction of voluntarily activated quadriceps femoris during sub-maximal muscle action. *J. Electromyography Kinesiol.* 22, 117–123. doi: 10.1016/j.jelekin.2011.10.010

Seiberl, W., Paternoster, F., Achatz, F., Schwirtz, A., and Hahn, D. (2013). On the relevance of residual force enhancement for everyday human movement. *J. Biomechan.* 46, 1996–2001. doi: 10.1016/j.jbiomech.2013.06.014

Seiberl, W., Power, G. A., and Hahn, D. (2015a). Residual force enhancement in humans: current evidence and unresolved issues: current evidence and unresolved issues. *J. Electromyography Kinesiol.* 25, 571–580. doi: 10.1016/j.jelekin.2015.04.011

Seiberl, W., Power, G. A., Herzog, W., and Hahn, D. (2015b). The stretch-shortening cycle (SSC) revisited: residual force enhancement contributes to increased performance during fast SSCs of human m. *adductor pollicis*. *Physiol. Rep.* 3:e12401. doi: 10.14814/phy2.12401

Sugi, H., and Tsuchiya, T. (1988). Stiffness changes during enhancement and deficit of isometric force by slow length changes in frog skeletal muscle fibres. *J. Physiol.* 407, 215–229. doi: 10.1113/jphysiol.1988.sp017411

Tilp, M., Steib, S., Schappacher-Tilp, G., and Herzog, W. (2011). Changes in fascicle lengths and pennation angles do not contribute to residual force enhancement/depression in voluntary contractions. *J. Appl. Biomechan.* 27, 64–73. doi: 10.1123/jab.27.1.64

Tomolka, A., Weidner, S., Hahn, D., Seiberl, W., and Siebert, T. (2020). Cross-bridges and sarcomeric non-cross-bridge structures contribute to increased work in stretch-shortening cycles. *Front. Physiol.* 11:921. doi: 10.3389/fphys.2020.00921

van Schenau, G. J. I., Bobbert, M. F., Haan, A., and de. (1997). Mechanics and energetics of the stretch-shortening cycle: a stimulating discussion. *J. Appl. Biomechan.* 13, 484–496. doi: 10.1123/jab.13.4.484

Wang, J. H.-C. (2006). Mechanobiology of tendon. *J. Biomechan.* 39, 1563–1582. doi: 10.1016/j.jbiomech.2005.05.011

Webber, S., and Kriellaars, D. (1997). Neuromuscular factors contributing to in vivo eccentric moment generation. *J. Appl. Physiol. (1985)* 83, 40–45. doi: 10.1152/jappl.1997.83.1.40

Wernbom, M., Augustsson, J., and Thomeé, R. (2007). The influence of frequency, intensity, volume and mode of strength training on whole muscle cross-sectional area in humans. *Sports Med. (Auckland, N.Z.)* 37, 225–264. doi: 10.2165/00007256-200737030-200737034

Westing, S. H., Seger, J. Y., and Thorstensson, A. (1990). Effects of electrical stimulation on eccentric and concentric torque-velocity relationships during knee extension in man. *Acta Physiol. Scand.* 140, 17–22. doi: 10.1111/j.1748-1716.1990.tb08971.x

Conflict of Interest: The authors declare that the research was conducted in the absence of any commercial or financial relationships that could be construed as a potential conflict of interest.

frontiers in Physiology

ORIGINAL RESEARCH
published: 03 December 2020
doi: 10.3389/fphys.2020.567641

Transmission-Mode Ultrasound for Monitoring the Instantaneous Elastic Modulus of the Achilles Tendon During Unilateral Submaximal Vertical Hopping

Scott C. Wearing[1,2], Larissa Kuhn[1], Torsten Pohl[2], Thomas Horstmann[2] and Torsten Brauner[3]*

[1] Institute of Health and Biomedical Innovation, Queensland University of Technology, Brisbane, QLD, Australia, [2] Faculty of Sports and Health Sciences, Technical University of Munich, Munich, Germany, [3] Department of Sport Science, German University of Health and Sport, Ismaning, Germany

OPEN ACCESS

Edited by:
Daniel Hahn, Ruhr University Bochum, Germany

Reviewed by:
Olivier Seynnes, Norwegian School of Sport Sciences, Norway
Jack Martin, University of Wisconsin-Madison, United States
Josh Baxter, University of Pennsylvania, United States

***Correspondence:**
Scott C. Wearing
s.wearing@qut.edu.au

Specialty section:
This article was submitted to Exercise Physiology, a section of the journal Frontiers in Physiology

Received: *30 May 2020*
Accepted: *11 November 2020*
Published: *03 December 2020*

Citation:
Wearing SC, Kuhn L, Pohl T, Horstmann T and Brauner T (2020) Transmission-Mode Ultrasound for Monitoring the Instantaneous Elastic Modulus of the Achilles Tendon During Unilateral Submaximal Vertical Hopping. Front. Physiol. 11:567641. doi: 10.3389/fphys.2020.567641

Submaximal vertical hopping capitalizes on the strain energy storage-recovery mechanism associated with the stretch-shortening cycle and is emerging as an important component of progressive rehabilitation protocols in Achilles tendon injury and a determinant of readiness to return to sport. This study explored the reliability of transmission mode ultrasound in quantifying the instantaneous modulus of elasticity of human Achilles tendon during repetitive submaximal hopping. A custom-built ultrasound transmission device, consisting of a 1 MHz broadband emitter and four regularly spaced receivers, was used to measure the axial velocity of ultrasound in the Achilles tendon of six healthy young adults (mean ± SD; age 26 ± 5 years; height 1.78 ± 0.11 m; weight 79.8 ± 13.6 kg) during steady-state unilateral hopping (2.5 Hz) on a piezoelectric force plate. Vertical ground reaction force and lower limb joint kinematics were simultaneously recorded. The potential sensitivity of the technique was further explored in subset of healthy participants (n = 3) that hopped at a slower rate (1.8 Hz) and a patient who had undergone Achilles tendon rupture-repair (2.5 Hz). Reliability was estimated using the mean-within subject coefficient of variation calculated at each point during the ground-contact phase of hopping, while cross-correlations were used to explore the coordination between lower limb kinematics ground reaction forces and ultrasound velocity in the Achilles tendon. Axial velocity of ultrasound in the Achilles tendon was highly reproducible during hopping, with the mean within-subject coefficient of variation ranging between 0.1 and 2.0% across participants. Ultrasound velocity decreased immediately following touch down (−19 ± 13 ms^{-1}), before increasing by 197 ± 81 ms^{-1}, on average, to peak at 2230 ± 87 ms^{-1} at 67 ± 3% of ground contact phase in healthy participants. Cross-correlation analysis revealed that ultrasound velocity in the Achilles tendon during hopping was strongly associated with knee (mean r = 0.98, range 0.95–1.00) rather than ankle (mean r = 0.67, range 0.35–0.79) joint motion. Ultrasound velocity was sensitive to changes

in hopping frequency in healthy adults and in the surgically repaired Achilles tendon was characterized by a similar peak velocity (2283 ± 13 ms^{-1}) but the change in ultrasound velocity (447 ± 21 ms^{-1}) was approximately two fold that of healthy participants (197 ± 81 ms^{-1}). Although further research is required, the technique can be used to reliably monitor ultrasound velocity in the Achilles tendon during hopping, can detect changes in the instantaneous elastic modulus of tendon with variation in hopping frequency and tendon pathology and ultimately may provide further insights into the stretch-shortening cycle and aid clinical decision concerning tendon rehabilitation protocols and readiness to return to sport.

Keywords: speed of sound, tendon, stretch-shortening cycle, muscle, biomechanics, elastic modulus, elasticity

INTRODUCTION

Hopping capitalizes on the strain energy storage-recovery mechanism associated with the stretch-shortening cycle (Cavagna, 1977) and is emerging as an important component of progressive rehabilitation protocols in Achilles tendon injury and a determinant of readiness to return to sport following anterior cruciate ligament reconstruction (Noyes et al., 1991; Sancho et al., 2019; Silbernagel et al., 2020). The stretch-shortening cycle is characterized by pre-activation of the muscle followed by lengthening of the musculotendinous unit while the muscle remains activated and subsequent shortening of the musculotendinous unit, which is thought to make use of the elastic properties of tendon and optimize locomotor efficiency (Bobbert and Casius, 2011; Taube et al., 2012). This mechanism is dependent, in part, on the material stiffness (i.e., elastic modulus) of the posterior ankle tendons, and allows optimal function of the posterior muscles of the leg (Lichtwark and Wilson, 2005).

To date, measures of the elastic modulus of the Achilles tendon during hopping have typically been derived secondarily from estimates of tendon displacement and loading using B-mode ultrasound and indirect techniques, including inverse dynamics, and electromyography-to-force processing (Lichtwark and Wilson, 2005; Bogey and Barnes, 2017). Such indirect approaches are based on estimates of joint centers and tendon moment arms and require assumptions regarding the contribution of agonist and antagonist muscles to the net ankle joint moment, which may result in overestimation of tendon loads by as much as 50% compared to direct measures (Gregor et al., 1991; Fukashiro et al., 1993) and tendon work loops (hysteresis) that are physiologically implausible (Zelik and Franz, 2017).

While alternative approaches have been used to quantify soft tissue properties or loading *in vivo*, such as mechanical vibration and elastography (Martin et al., 2018; Corrigan et al., 2019; Keuler et al., 2019), transmission-mode ultrasound is emerging as potentially useful quantitative technique for the measurement of the mechanical properties of soft tissues such as tendon and ligament during activities of daily living (Miles et al., 1996; Kuo et al., 2001; Pourcelot et al., 2005a). The axial transmission velocity of ultrasound in tendon (V) is dependent on its instantaneous elastic modulus (E, material stiffness) and mass density (ρ) and, in tendon, is governed by the classic Newtonian–Laplace equation with adjustment for Poisson's effects (ν) in elastic media (Miles et al., 1996; Pourcelot et al., 2005a; Crevier-Denoix et al., 2009; Vergari et al., 2012);

$$V = \sqrt{\frac{E}{\rho}\frac{(1-\nu)}{(1+\nu)(1-2\nu)}} \qquad \text{(Equation 1)}$$

Animal studies have confirmed that tensile stress applied to the tendon results in a nonlinear though monotonic increase in ultrasound velocity (Kuo et al., 2001; Pourcelot et al., 2005a; Crevier-Denoix et al., 2009). Hence, while the variation in the transmission speed of ultrasound with the application of mechanical load to tendon represents a limitation of most sonographic approaches (Ooi et al., 2014), ultrasound transmission techniques take advantage of this relationship, along with the nonlinear properties of tendon, to quantify the instantaneous elastic modulus of superficial human tendon *in vivo* under physiological loading conditions (Wearing et al., 2013, 2014; Wulf et al., 2015). Recently, the technique has been successfully applied to quantify tendon biomechanics during both static and dynamic activities of daily living such as walking and rising from a chair (Pourcelot et al., 2005b; Wearing et al., 2014, 2016) and has been shown to be sufficiently sensitive to detect changes in the instantaneous elastic modulus of Achilles tendon with footwear (Wearing et al., 2014), footstrike pattern (Wearing et al., 2019) and tendon pathology (Wulf et al., 2018). Although the technique has also been shown to be sufficiently sensitive to detect changes in the instantaneous elastic modulus of Achilles tendon with changes in walking speed (Brauner et al., 2017), there is debate as to whether the Achilles tendon normally operates within the elastic "toe" region under conditions of physiological loading or the "linear" elastic region, where Young's elastic modulus is traditionally measured *in vitro* and ultrasound transmission velocity would approach a constant value (Maganaris and Paul, 1999; Biewener and Roberts, 2000). This is further compounded by direct measures of physiological loading in the Achilles tendon during submaximal hopping in which peak loads were found, rather unexpectedly, to be approximately twice those observed walking (Komi et al., 1992) and jumping (Fukashiro et al., 1995). Consequently, it remains unknown if the technique is suitable for individualized measurement of human Achilles tendon during hopping.

FIGURE 1 | Illustration of the experimental setup. The custom-built ultrasound probe was positioned over the posterior Achilles tendon (insert).

The primary aim of the current study, therefore, was to investigate the feasibility and reliability of transmission mode ultrasound in quantifying the instantaneous modulus of elasticity of human Achilles tendon during repetitive submaximal hopping. As a secondary aim, the coordination patterns between lower limb kinematics and ultrasound velocity profiles in the Achilles tendon were also explored. Finally, to further study the potential clinical utility and sensitivity of the technique, changes in peak ultrasound transmission velocity in the Achilles tendon were examined in a subgroup of participants hopping at a slower frequency and in a patient with a rupture-repaired Achilles tendon. It was anticipated that, as a surrogate measure of the instantaneous elastic modulus of the Achilles tendon, ultrasound velocity in the tendon would be lower when hopping at a faster rate, corresponding with a lower ankle joint moment (Otsuka et al., 2018), and also lower in rupture-repaired Achilles tendon as a consequence of a lower material stiffness and impaired ankle plantarflexion strength (Oda et al., 2017).

MATERIALS AND METHODS

Participants

A convenience sample of six healthy young adults (three males, three females) participated in the study. The mean (±SD) age, height, and weight of healthy participants was 26 ± 5 years, 1.78 ± 0.11 m, and 79.8 ± 13.6 kg, respectively. In order to further explore the potential of transmission-mode ultrasound to evaluate the stretch shortening cycle, a female patient (age, 24 years; height, 1.76 m and weight, 54.0 kg) who had undergone unilateral surgical repair for rupture of the Achilles tendon was also evaluated. The participant was 24 months post-operation, pain free and had successfully returned to sport and normal activities of daily living and was individually matched to a healthy female participant to within five years of age and five kilograms. All participants were recreationally active, and regularly competed in structured sport (4 h per week). No participant reported a medical history of diabetes, familial hypercholesterolemia, inflammatory arthritis, or neuromuscular disease or a prior history of chronic Achilles tendon pain. All participants attended the laboratory on a single occasion for testing and provided written informed consent to the procedures of the study, which received approval from the University Human Research Ethics Committee.

Equipment

Axial transmission velocity of ultrasound was measured in the Achilles tendon using a custom-built ultrasonic device described previously (Wearing et al., 2014, 2016). The device incorporated a five-element ultrasound probe consisting of a 1 MHz broadband pulse emitter and four regularly spaced receivers. The skin

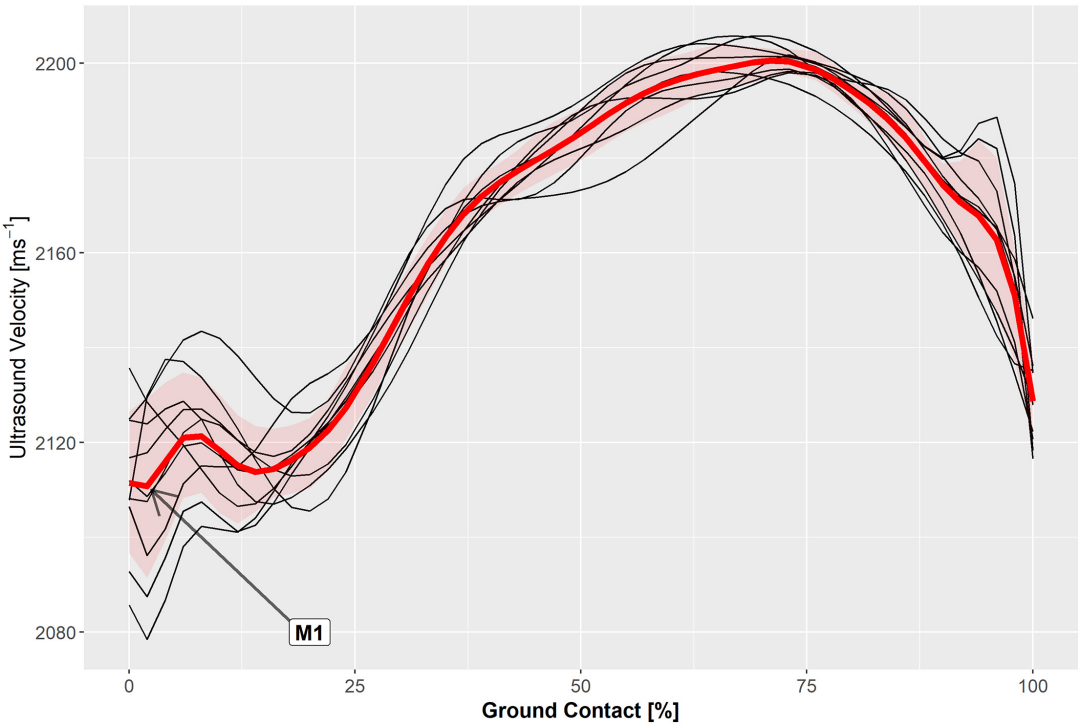

FIGURE 2 | Axial velocity of ultrasound measured in the Achilles tendon during the ground contact phase of ten hop cycles (black traces) and the ensemble average (red trace) in a representative participant.

overlying the posterior Achilles tendon was prepared and cleaned using standard alcohol abrading methods (Cram and Rommen, 1989). The probe was positioned over the midline of the posterior aspect of the Achilles tendon during quiet bipedal stance, with the emitter located 1-cm superior to the calcaneus (**Figure 1**). Adhesive coupling medium and elasticized bandage were used to ensure the probe was maintained in close contact with the skin. Received ultrasonic signals were digitized at 20 MHz and the time of flight of the first arriving transient between receivers was estimated using the first-zero crossing criterion (Camus et al., 2000; Bossy et al., 2002). Average transmission velocity was subsequently calculated given the known distance between receivers (7.5 mm) and the measured time of flight. Measurement precision for axial transmission velocity of ultrasound is better than 3 ms^{-1} (Crevier-Denoix et al., 2009).

A 3D motion analysis system (Vicon Nexus 2.6, Vicon Motion Systems Ltd., Oxford, United Kingdom) was used to simultaneously record ankle and knee kinematics during the hopping task. The system consisted of eight high-resolution infra-red cameras (T10-series) that captured the kinematics of 16 reflective markers (14 mm diameter), positioned on standard anatomical landmarks of the hip, thigh, shank, and foot in accordance with Vicon's Plug-in Gait Lower Body model (Kadaba et al., 1990; Davis et al., 1991). Sagittal plane motion of the knee and ankle joints during hopping were sampled at a rate of 200 Hz. Vertical ground reaction forces were also measured using a piezoelectric force platform (Kistler 9655, Kistler Instrument Corp., Amherst, NY, United States, natural frequency ∼600 Hz) sampling at 1000 Hz. Kinematic, kinetic and ultrasound data were collected synchronously using a common trigger.

Protocol

A modified version of the repetitive hopping protocol outlined by Brauner et al. (2014) was employed. Prior to testing all participants were afforded a 5-min warm up in which they familiarized themselves with the sub-maximal hopping exercise. The protocol required participants to perform 20 s of single-limb hopping. Initially, participants stood erect for approximately 3 s, allowing a static calibration of lower extremity joint centers and coordinate systems, and then commenced hopping in place on the left limb until instructed to stop. A digital metronome (MA-30, KORG Inc., Japan) was used to set a hopping frequency of 2.5 Hz for all participants. To avoid the potential influence of arm movement, participants performed the hopping task with their hands laterally positioned on their waist. The hopping frequency was specifically selected, as the human leg is known to behave as an elastic spring at hopping rates above 2.2 Hz (Farley et al., 1991). To further explore the effect of hoping rate on ultrasound velocity measurements, three participants consented to repeat the hopping task at a slower rate (1.8 Hz) task.

Data Reduction and Statistical Analysis

All data were low-pass filtered using a fourth-order, zero-lag Butterworth filter with a cut-off frequency of 30 Hz as determined by residual analysis. Data from the central ten steady-state hopping cycles over the 20 s period were selected for

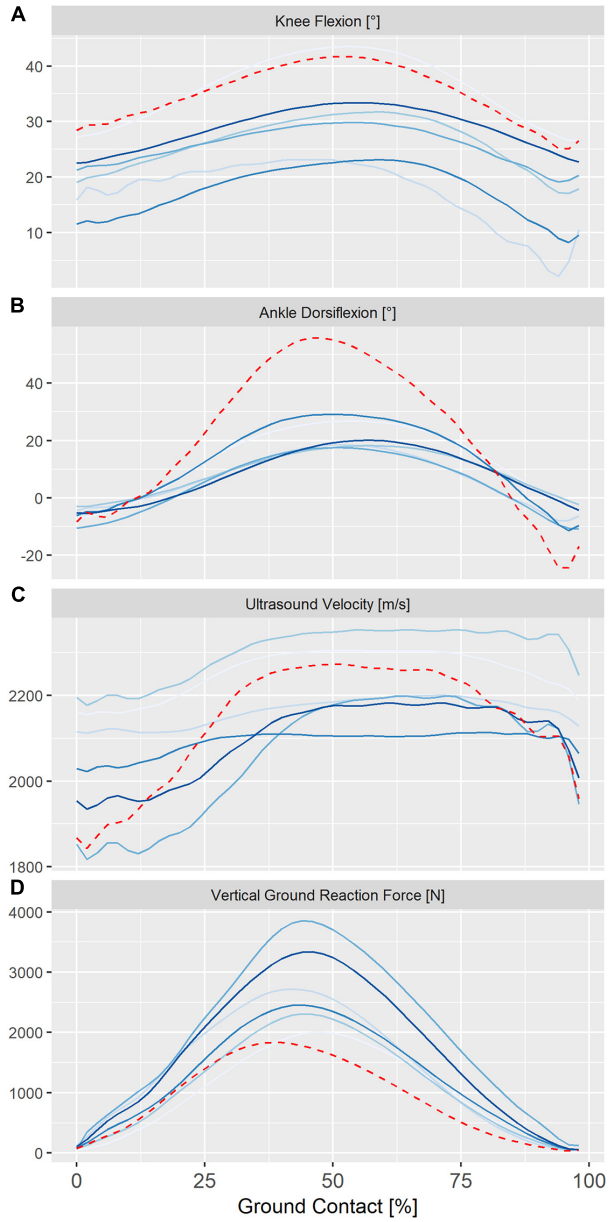

FIGURE 3 | Individual ensemble histories for knee kinematics **(A)** ankle kinematics **(B)**, ultrasound velocity in the Achilles tendon **(C)** and vertical ground reaction forces **(D)** during the ground contact phase of steady-state hopping in six healthy adults (solid lines) and in a single adult, 24 months post-surgical repair (dashed line). Positive values for sagittal knee and ankle kinematics represent flexion and dorsiflexion, respectively.

each participant for subsequent analysis. Each hopping cycle was identified based on vertical ground reaction force signals and resampled to 100 points per cycle. Peak vertical ground reaction force and peak loading rates for each hop cycle were subsequently determined (McSweeney et al., 2019). Sagittal ankle and knee angles and external moments during each hop cycle were calculated using standard "bottom-up" inverse dynamics via Plug-in-Gait. Maximum and minimum ultrasound velocity and sagittal ankle and knee angles were also identified. To allow direct comparison to previous studies, leg stiffness (K_{dyn}) was defined as the instantaneous ratio of ground reaction force (F_G) to the vertical displacement of the center of mass (ΔL) as given by;

$$K_{dyn}\,(t) = F_G(t)/\Delta L(t) \qquad \text{(Equation 2)}$$

where t equals time and the vertical displacement of the virtual hip joint center was used to describe the center of mass (Riese and Seyfarth, 2012). Importantly, the definition is equal to that cited by Farley and Morgenroth (1999) for the instant of maximum displacement of the center of mass.

All data were evaluated for normality using the Shapiro–Wilk test (IBM-SPSS statistical software package, Version 21 for Windows, IBM Corp. Armonk, NY, United States). As variables were determined to be normally distributed, means and standard deviations have been used as summary statistics. The within-subject coefficient of variation (SD/mean) for each participant was calculated at each point of the ground contact phase of all 10 hoping cycles and the mean was used as an estimate of intra-test (within-subject) variability. To visually compare data between participants, ensemble averages and standard deviations were computed. The standard deviation of mean within-subject data (i.e., mean across ten hopping cycles) was later used to estimate between-subject variability. The coordination between ultrasound velocity profiles in the Achilles tendon and lower limb kinematics and ground reaction forces were explored using cross-correlations (Winter and Patla, 1997; Mullineaux et al., 2001; Nelson-Wong et al., 2009). Absolute differences in mean peak ultrasound values that exceeded the minimum detectable change were used to compare the individual data of participants hopping at a slower rate and in the participant with a history of Achilles tendon rupture. The minimum detectable change was computed from the SEM using the equation described by Weir (2005).

RESULTS

Measured hopping frequencies were 2.51 ± 0.02 Hz for all participants and 1.86 ± 0.02 Hz for the three participants that repeated the exercise at a slower rate and coinciding with a hopping height of 3.6 to 4.1 cm. The ultrasound velocity profile in the Achilles tendon was highly reproducible (**Figure 2**) and was typically characterized by a local minimum (M1) and maximum (P1) during the contact phase of unilateral steady-state hopping (**Figure 3**). Variability in ultrasound velocity in the Achilles tendon tended to be greatest during initial touchdown (1.1%) and lowest at around the time of peak vertical ground reaction force, where the mean within-subject coefficient of variation for ultrasound velocity in the tendon was, on average, less than 0.3%. The mean within-subject coefficient of variation for ultrasound velocity over the entire ground contact phase of the hopping cycle was 0.9% and ranged between 0.1 and 2.0% across all participants.

Ensemble averages for knee and ankle kinematics and axial velocity of ultrasound in the Achilles tendon for all participants are shown in **Figure 3**. On average, peak ultrasound velocity in the Achilles tendon of healthy participants decreased by 19 ± 13 ms^{-1} immediately following touch down at 4 ± 2% of

TABLE 1 | Mean (SD) kinematic, kinetic, and ultrasound parameters during the contact phase of hopping in healthy adults (n = 6).

	Contact	M1	P1	Toe off	Time to M1 (%)†	Time to Peak (%)†
Knee angle (°)	20 (5)	–	31 (8)	18 (7)	–	54 (6)
Ankle angle (°)	−6 (3)	–	22 (5)	−6 (3)	–	54 (3)
Ultrasound velocity (ms^{-1})	2051 (131)	2032 (141)	2230 (87)	2097 (113)	4 (2)	67 (3)
Vertical ground reaction force (BW)		–	3.6 (0.5)		–	45 (2)
Leg stiffness (kNm^{-1})		–	32 (12)		–	21 (13)

†*Expressed as a percentage of the duration of ground contact; BW, normalized to bodyweight. Positive knee and ankle angles reflect flexion and dorsiflexion, respectively.*

TABLE 2 | Cross correlation (range) and lag† of kinematic, kinetic and ultrasound parameters during hopping.

	Ultrasound velocity	Knee angle	Ankle angle	Vertical ground reaction force
Knee angle	0.98 (0.95 to 1.00)			
Lag (%)	0 (0 to 0)			
Ankle angle	0.67 (0.35 to 0.79)	0.73 (0.36 to 0.86)		
Lag (%)	3 (−14 to 28)	9 (−4 to 20)		
Vertical ground reaction force	0.85 (0.83 to 0.87)	0.91 (0.89 to 0.95)	0.90 (0.62 to 0.99)	
Lag (%)	4 (0 to 8)	3 (−2 to 6)	8 (6 to 10)	
Leg stiffness	0.91 (0.88 to 0.93)	0.95 (0.92 to 0.96)	0.83 (0.53 to 0.94)	0.96 (0.94 to 0.98)
Lag (%)	2 (0 to 4)	6 (0 to 12)	19 (16 to 22)	10 (6 to 16)

†*Expressed as a percentage of the duration of ground contact.*

ground contact, before increasing to peak at 2230 ± 87 ms^{-1} at 67 ± 3% of ground contact phase (**Table 1**). The between-subject variability, as defined by the mean ensemble standard deviation (100 ± 21 ms^{-1}), was approximately five-fold greater than the intra-test (within-subject) variability. Cross-correlation analysis revealed that ultrasound velocity in the Achilles tendon during hopping was strongly associated with knee (mean r = 0.98, range 0.95–1.00) rather than ankle (mean r = 0.67, range 0.35–0.79) joint motion in the six healthy participants (**Table 2**).

Ensemble ankle moments and ultrasound velocity in the Achilles tendon at slow (1.8 Hz) and fast (2.5 Hz) hopping rates in a healthy individual are shown in **Figure 4**. Hopping at a faster rate resulted in a qualitative reduction in knee and ankle movement and an increase in peak ground reaction force and ultrasound velocity in the Achilles tendon of two healthy participants but a lower peak ultrasound velocity and external ankle moment in the third participant (**Figure 4A**). **Figure 4** also demonstrates ultrasound velocity and ankle moments during hopping (2.5 Hz) in the participant that had undergone operative repair of the Achilles tendon relative to that of an age-, weight-, and sex-matched healthy control. Hopping in the surgically repaired Achilles tendon was characterized by markedly lower ankle moment (**Figure 4B**). Although peak ultrasound velocity (2283 ± 13 ms^{-1}) was comparable to healthy participants hopping at the same frequency, the change in ultrasound velocity from touch down to peak velocity (447 ± 21 ms^{-1}) was approximately two fold that of healthy participants on average (197 ± 81).

DISCUSSION

Measurement of ultrasound velocity was well tolerated by participants in the current study and without technical difficulty. The ultrasound velocity profile in the Achilles tendon was characterized by a local minimum and maximum during the contact phase of unilateral steady-state hopping. Axial velocity of ultrasound in the Achilles tendon was highly reproducible between hopping cycles, with a mean intra-test (within-subject) coefficient of variation of less than 1% over the entire ground contact phase. Between-subject variability in ultrasound velocity, however, was about five times higher than within-subject variability. The greater variability between subjects presumably reflects the various hopping movement patterns or strategies adopted by individuals during hopping (Chang et al., 2008). However, given that animal models have shown the coefficient of variation in mass density of different tendons to be in the order of 2.8% (Vergari et al., 2012), the variability in ultrasound velocity observed between healthy participants in the current study may also reflect differences in tendon cross-sectional area and density between participants. Nonetheless, the maximum and minimum ultrasound velocities measured in the Achilles tendon during the stretch-shortening cycle in hopping in this study (approximately 2000–2230 ms^{-1}) are somewhat higher than those reported previously in healthy adults (approximately 1850–2050 ms^{-1}) during walking at preferred speed (Pourcelot et al., 2005a,b; Wearing et al., 2014)). Assuming a mass density of approximately 1100 kg/m^3 (Vergari et al., 2012), and a Poisson's ratio of around 0.46 (Thorpe et al., 2014), the minimum and maximum ultrasound velocity observed in the Achilles tendon during the stretch-shortening cycle of hopping in the current study equate to an elastic modulus of 0.98 and 1.2 GPa, respectively, which is comparable to that estimated for human cadaveric tendon (819 ± 208 MPa) during quasistatic tensile testing (Wren et al., 2001).

Peak vertical ground reaction force, joint kinematics and estimates of leg stiffness in the current study were consistent with those reported for hopping in healthy adults at similar

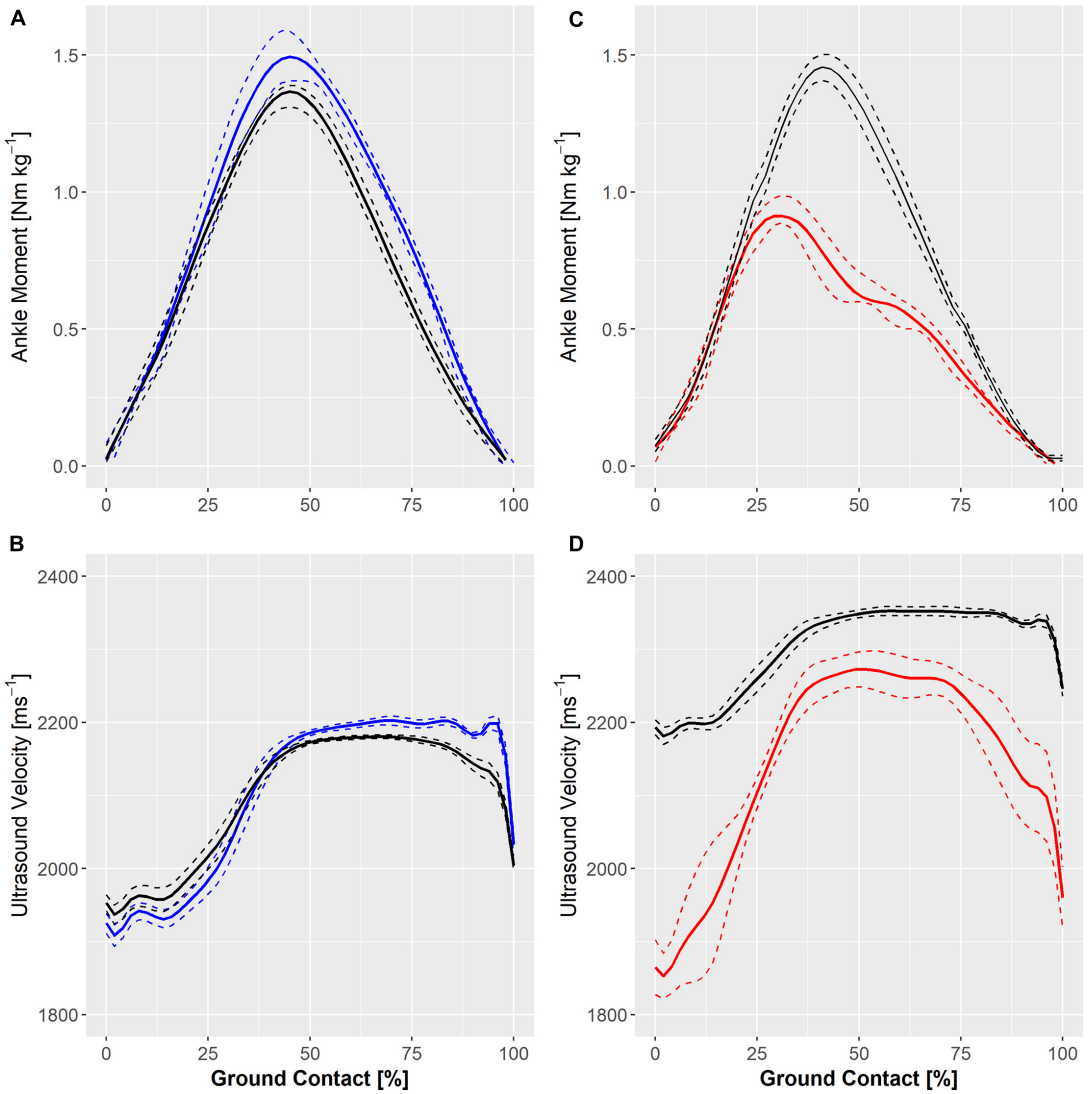

FIGURE 4 | Individual ensemble histories for external ankle moments (upper panels) and ultrasound velocity in the Achilles tendon (lower panels) of a healthy adult during hopping at 1.8 Hz (solid blue line) and 2.5 Hz **(A,B)** and in an adult with a surgically repaired Achilles tendon (solid red line) and a matched healthy control hopping at 2.5 Hz **(C,D)**. Standard deviations are represented by dashed lines.

frequencies (Farley et al., 1991). Leg stiffness during hopping at frequencies above 2.2 Hz have previously been suggested to predominantly reflect ankle joint stiffness (Farley and Morgenroth, 1999; Hobara et al., 2011). Although ankle joint stiffness may be regulated through a number of mechanisms, passive tissue properties, stretch reflexes, and muscle activation are all thought to contribute to physiological joint stiffness (Weiss et al., 1986a,b, 1988). In the absence of the ankle joint approaching the limits of its range of motion, simultaneous co-activation of agonist-antagonist muscles has been suggested to be a prime method for increasing the mechanical stiffness of the ankle joint, without necessarily affecting the angle or net torque (Wind and Rouse, 2020). Hence, co-activation of antognist muscle groups, as has been previously reported with jumping (Arai et al., 2013), may be one explanation for the elevated velocity of ultrasound in Achilles tendon during the propulsive phase of hopping; despite a concomittent reduction in vertical ground reaction force. Interestingly, ultrasound velocity in the Achilles tendon was more closely correlated with knee flexion than ankle movement in the current study. Although this observation highlights the challenge associated with deconvoluting the contribution of agonist and antagonist muscles to the net joint moment, especially of biarticular muscles such as the triceps surae, it also suggests that, at least in this study, the ultrasound velocity profile developed within the triceps surae muscle unit was related more to knee flexion than ankle movement during hopping in healthy adults. This observation is consistent with synergistic interaction of the ankle and knee joints proposed by João et al. (2014), in which the knee extensors were considered critical to the vertical acceleration of

the center of mass, while the ankle plantarflexors acted to stabilize the foot and ankle.

The ultrasound transmission technique also appears sufficiently sensitive to demonstrate individual responses to changes in hopping frequency and to characterize deficits in dynamic tendon function in a participant with a history of Achilles tendon rupture repair. It is noteworthy that, in the latter case, that the participant was asymptomatic, reported good function and had returned to sport. Ankle joint dorsiflexion but not knee flexion was markedly increased during hopping in the rupture-repaired tendon. Increased ankle dorsiflexion during hopping is a well-known complication following Achilles tendon rupture repair (Tengman and Riad, 2013). Despite having the lowest external ankle joint moment of any participant, peak ultrasound velocity in the repaired Achilles tendon was comparable to that of healthy participants (2120–2358 ms^{-1}). Interestingly, the change in ultrasound velocity during hopping in the surgically repaired tendon was twice that of healthy tendon, suggesting that the muscle-tendon unit of rupture-repaired Achilles tendon may be more compliant than that of healthy tendon. While this initial finding is consistent with previous research demonstrating that repaired Achilles tendon is longer (Rosso et al., 2013), has a lower material stiffness (Wulf et al., 2018) and is associated with lower ankle plantarflexion strength than healthy tendon (Horstmann et al., 2012), further prospective research in surgically repaired, contralateral and healthy Achilles tendon under both static and dynamic loading conditions is warranted to further elucidate the effect of tendon repair on tendon function.

Although the change in ultrasound transmission velocity in tendon over the hop cycle provides an indication of the stress developed in the muscle-tendon unit as a whole, it should be noted that tendon stress is influenced by tendon cross-sectional area. As the Achilles is a conjoined tendon of the soleus and medial and lateral gastrocnemius muscles, differential muscle activity and loading within the tendon may also occur (Arndt et al., 1998). Hence, whether the ultrasound velocity pattern observed in the current study is applicable to the entire tendon structure is unknown. Similarly, variations in ultrasound transmission velocity during hopping are influenced by both active (muscle) and passive components of loading. Hence, the role of active and passive loading mechanisms could not be readily delineated. While future studies may benefit from evaluating tendon properties in the absence of external loads and under passive loading conditions, it is recognized that *in vivo* measurement of tendon slack is not straightforward (Hug et al., 2013). Moreover, the transmission of ultrasound waves in tendon is also influenced by factors such as the density and temperature of the tissue (Miles et al., 1996). Although it may reasonably be assumed that, for a given individual, tendon density and temperature remained stable during the short-term, steady-state hopping conditions tested in the current study, repeated cyclic loading of tendon has been estimated to induce considerable thermal effects in equine tendon when applied over an extended period (Wilson and Goodship, 1994). Marked variation in such factors may then make comparisons between-individuals more difficult. In addition, the technique is only suitable for evaluating the biomechanics of relatively superficial tendons. It should also be noted that this study employed conventional motion analysis to model the foot as a rigid segment to estimate ankle joint movement, which undoubtedly overestimates peak osseous ankle movement. The range of ankle joint movement during hopping in the current study, however, is consistent with that reported for the tibiotalar joint when bone pins and dyanamic radiographic approaches were used to track osseous movement (Pitcairn et al., 2020).

Nonetheless, the limited data presented in this study have shown that transmission-mode ultrasound can be reliably used to quantify tendon biomechanics during hopping in healthy and injured Achilles tendons. As ultrasound velocity is directly related to the instantaneous elastic modulus of the Achilles tendon, and the change in velocity reflects the change in applied stress to the tendon, the technique also has the potential to provide new insights into muscle-tendon unit function during the stretch-shortening cycle, particularly if combined with synchronous measures of muscle activity and fascicle behavior. Hence, the technique has application for research concerning the neuromuscular control of movement, the role of elasticity in hopping and neuromuscular adaptation and pathology. Moreover, the ultrasound technique shows promise for near real-time clinical monitoring of Achilles tendon properties during hopping, which is emerging as an important component of progressive rehabilitation protocols and a key clinical determinant of the readiness to return to sport.

DATA AVAILABILITY STATEMENT

Summary data supporting the conclusions of this article will be made available by the authors, without undue reservation.

ETHICS STATEMENT

This study was reviewed and approved by the University of Applied Health Sciences Rhein-Neckar. The participants provided their written informed consent to participate in this study.

AUTHOR CONTRIBUTIONS

LK, SW, TB, and TP designed the experiment. LK and TP collected the data. SW, TB, and TP performed the statistical analysis. SW, TB, and TH interpreted the results. SW wrote the first draft of the manuscript. SW and TB prepared the figures. All authors contributed to the manuscript revision, read, and approved the submitted version.

ACKNOWLEDGMENTS

We thank Dr. James Smeathers and Dr. Wolfgang Seiberl for their assistance in preparing the manuscript.

REFERENCES

Arai, A., Ishikawa, M., and Ito, A. (2013). Agonist–antagonist muscle activation during drop jumps. *Eur. J. Sport Sci.* 13, 490–498. doi: 10.1080/17461391.2013.764930

Arndt, A. N., Komi, P. V., Brüggemann, G. P., and Lukkariniemi, J. (1998). Individual muscle contributions to the in vivo achilles tendon force. *Clin. Biomech.* 13, 532–541. doi: 10.1016/s0268-0033(98)00032-1

Biewener, A. A., and Roberts, T. J. (2000). Muscle and tendon contributions to force, work, and elastic energy savings: a comparative perspective. *Exerc. Sport Sci. Rev.* 28, 99–107.

Bobbert, M. F., and Casius, L. J. R. (2011). Spring-like leg behaviour, musculoskeletalmechanics and control in maximum and submaximum height human hopping. *Phil. Trans. R. Soc. Lond. B Biol. Sci.* 366, 1516–1529. doi: 10.1098/rstb.2010.0348

Bogey, R. A., and Barnes, L. A. (2017). An EMG-to-Force Processing approach for estimating in vivo hip muscle forces in normal human walking. *IEEE Trans. Neural Syst. Rehabil. Eng.* 25, 1172–1179. doi: 10.1109/tnsre.2016.2613021

Bossy, E., Talmant, M., and Laugier, P. (2002). Effect of bone cortical thickness on velocity measurements using ultrasonic axial transmission: a 2D simulation study. *J. Acoust. Soc. Am.* 112, 297–307. doi: 10.1121/1.1480836

Brauner, T., Hooper, S. L., Pourcelot, P., Crevier-Denoix, N., Horstmann, T., and Wearing, S. C. (2017). Load in the achilles tendon is progressively increased with reductions in walking speed. *Med. Sci. Sports Exerc.* 49, 2001–2008. doi: 10.1249/mss.0000000000001322

Brauner, T., Sterzing, T., Wulf, M., and Horstmann, T. (2014). Leg stiffness: comparison between unilateral and bilateral hopping tasks. *Hum. Mov. Sci.* 33, 263–272. doi: 10.1016/j.humov.2013.08.009

Camus, E., Talmant, M., Berger, G., and Laugier, P. (2000). Analysis of the axial transmission technique for the assessment of skeletal status. *J. Acoust. Soc. Am.* 108, 3058–3065. doi: 10.1121/1.1290245

Cavagna, G. A. (1977). Storage and utilization of elastic energy in skeletal muscle. *Exerc. Sports. Sci. Rev.* 5, 89–127.

Chang, Y.-H., Roiz, R. A., and Auyang, A. G. (2008). Intralimb compensation strategy depends on the nature of joint perturbation in human hopping. *J. Biomech.* 41, 1832–1839. doi: 10.1016/j.jbiomech.2008.04.006

Corrigan, P., Zellers, J. A., Balascio, P., Silbernagel, K. G., and Cortes, D. H. (2019). Quantification of mechanical properties in healthy achilles tendon using continuous shear wave elastography: areliability and validation study. *Ultrasound Med. Biol.* 45, 1574–1585. doi: 10.1016/j.ultrasmedbio.2019.03.015

Cram, J. R., and Rommen, D. (1989). Effects of skin preparation on data collected using an EMG muscle-scanning procedure. *Biofeedback Self Regul.* 14, 75–82. doi: 10.1007/bf00999342

Crevier-Denoix, N., Ravary-Plumioen, B., Evrard, D., and Pourcelot, P. (2009). Reproducibility of a non-invasive ultrasonic technique of tendon force measurement, determined in vitro in equine superficial digital flexor tendons. *J. Biomech.* 42, 2210–2213. doi: 10.1016/j.jbiomech.2009.06.005

Davis, R., Ounpuu, S., Tyburski, D., and Gage, J. R. (1991). A gait analysis collection and reduction technique. *Hum. Mov. Sci.* 10, 575–587. doi: 10.1016/0167-9457(91)90046-z

Farley, C. T., Blickhan, R., Saito, J., and Taylor, C. R. (1991). Hopping frequency in humans: a test of how springs set stride frequency in bouncing gaits. *J. Appl. Physiol.* 71, 2127–2132. doi: 10.1152/jappl.1991.71.6.2127

Farley, C. T., and Morgenroth, D. C. (1999). Leg stiffness primarily depends on ankle stiffness during human hopping. *J. Biomech.* 32, 267–273. doi: 10.1016/s0021-9290(98)00170-5

Fukashiro, S., Komi, P., Järvinen, M., and Miyashita, M. (1993). Comparison between the directly measured achilles tendon force and the tendon force calculated from the ankle joint moment during vertical jumps. *Clin. Biomech.* 8, 25–30. doi: 10.1016/s0268-0033(05)80006-3

Fukashiro, S., Komi, P. V., Järvinen, M., and Miyashita, M. (1995). In vivo achilles tendon loading' during jumping in humans. *Eur. J. Appl. Physiol. Occup. Physiol.* 71, 453–458. doi: 10.1007/bf00635880

Gregor, R. J., Komi, P. V., Browning, R. C., and Järvinen, M. (1991). A comparison of the triceps surae and residual muscle moments at the ankle during cycling. *J. Biomech.* 24, 287–297. doi: 10.1016/0021-9290(91)90347-p

Hobara, H., Inoue, K., Omuro, K., Muraoka, T., and Kanosue, K. (2011). Determinant of leg stiffness during hopping is frequency-dependent. *Eur. J. Appl. Physiol.* 111, 2195–2201. doi: 10.1007/s00421-011-1853-z

Horstmann, T., Lukas, C., Merk, J., Brauner, T., and Mündermann, A. (2012). Deficits 10-years after achilles tendon repair. *Int. J. Sports Med.* 33, 474–479. doi: 10.1055/s-0032-1301932

Hug, F., Lacourpaille, L., Maïsetti, O., and Nordez, A. (2013). Slack length of gastrocnemius medialis and achilles tendon occurs at different ankle angles. *J. Biomech.* 46, 2534–2538. doi: 10.1016/j.jbiomech.2013.07.015

João, F., Veloso, A., Cabral, S., Moniz-Pereira, V., and Kepple, T. (2014). Synergistic interaction between ankle and knee during hopping revealed through induced acceleration analysis. *Hum. Mov. Sci.* 33, 312–320. doi: 10.1016/j.humov.2013.10.004

Kadaba, M. P., Ramakrishnan, H. K., and Wootten, M. E. (1990). Measurement of lower extremity kinematics during level walking. *J. Orthop. Res.* 8, 383–392. doi: 10.1002/jor.1100080310

Keuler, E. M., Loegering, I. F., Martin, J. A., Roth, J. D., and Thelen, D. G. (2019). Shear wave predictions of achilles tendon loading during human walking. *Sci. Rep.* 9:13419.

Komi, P. V., Fukashiro, S., and Järvinen, M. (1992). Biomechanical loading of achilles tendon during normal locomotion. *Clin. Sports Med.* 11, 521–531. doi: 10.1016/s0278-5919(20)30506-8

Kuo, P. L., Li, P. C., and Li, M. L. (2001). Elastic properties of tendon measured by two different approaches. *Ultrasound Med. Biol.* 27, 1275–1284. doi: 10.1016/s0301-5629(01)00442-2

Lichtwark, G. A., and Wilson, A. M. (2005). In vivo mechanical properties of the human achilles tendon during one-legged hopping. *J. Exp. Biol.* 208, 4715–4725. doi: 10.1242/jeb.01950

Maganaris, C. N., and Paul, J. P. (1999). In vivo human tendon mechanical properties. *J. Physiol.* 521, 307–313.

Martin, J. A., Brandon, S. C. E., Keuler, E. M., Hermus, J. R., Ehlers, A. C., Segalman, D. J., et al. (2018). Gauging force by tapping tendons. *Nat. Commun.* 9:1592.

McSweeney, S., Reed, L. F., and Wearing, S. C. (2019). Vertical ground reaction forces during gait in children with and without calcaneal apophysitis. *Gait Posture* 71, 126–130. doi: 10.1016/j.gaitpost.2019.04.027

Miles, C. A., Fursey, G. A., Birch, H. L., and Young, R. D. (1996). Factors affecting the ultrasonic properties of equine digital flexor tendons. *Ultrasound Med. Biol.* 22, 907–915. doi: 10.1016/0301-5629(96)00085-3

Mullineaux, D. R., Bartlett, R. M., and Bennett, S. (2001). Research design and statistics in biomechanics and motor control. *J. Sport Sci.* 19, 739–760. doi: 10.1080/026404101317015410

Nelson-Wong, E., Howarth, S., Winter, D. A., and Callaghan, J. P. (2009). Application of autocorrelation and crosscorrelation analyses in human movement and rehabilitation research. *J. Orthop. Sports Phys. Ther.* 39, 287–295. doi: 10.2519/jospt.2009.2969

Noyes, F. R., Barber, S. D., and Mangine, R. E. (1991). Abnormal lower limb symmetry determined by function hop tests after anterior cruciate ligament rupture. *Am. J. Sports Med.* 19, 513–518. doi: 10.1177/036354659101900518

Oda, H., Sano, K., Kunimasa, Y., Komi, P. V., and Ishikawa, M. (2017). Neuromechanical modulation of the achilles tendon during bilateral hopping in patients with unilateral achilles tendon rupture, over 1 year after surgical repair. *Sports Med.* 47, 1221–1230. doi: 10.1007/s40279-016-0629-3

Ooi, C. C., Malliaras, P., Schneider, M. E., and Connell, D. A. (2014). "Soft, hard, or just right?" Applications and limitations of axial-strain sonoelastography and shear-wave elastography in the assessment of tendon injuries. *Skeletal Radiol.* 43, 1–12. doi: 10.1007/s00256-013-1695-3

Otsuka, M., Kurihara, T., and Isaka, T. (2018). Bilateral deficit of spring-like behaviour during hopping in sprinters. *Eur. J. Appl. Physiol.* 118, 475–481. doi: 10.1007/s00421-017-3791-x

Pitcairn, S., Kromk, J., Hogan, M., and Anderst, W. (2020). Validation and application of dynamic biplane radiography to study in vivo ankle joint kinematics during high-demand activities. *J. Biomech.* 103:109696. doi: 10.1016/j.jbiomech.2020.109696

Pourcelot, P., Defontaine, M., Ravary, B., Lemâtre, M., and Crevier-Denoix, N. (2005a). A non-invasive method of tendon force measurement. *J. Biomech.* 38, 2124–2129. doi: 10.1016/j.jbiomech.2004.09.012

Pourcelot, P., Van Den Bogert, A. J., Huang, X., and Crevier-Denoix, N. (2005b). Achilles tendon loads at walk measured using a novel ultrasonic

technique. *Comput. Methods Biomech. Biomed. Eng.* 8, 221–222. doi: 10.1080/10255840512331389055

Riese, S., and Seyfarth, A. (2012). Stance leg control: variation of leg parameters supports stable hopping. *Bioinspir. Biomim.* 7:016006. doi: 10.1088/1748-3182/7/1/016006

Rosso, C., Vavken, P., Polzer, C., Buckland, D. M., Studler, U., Weisskopf, L., et al. (2013). Long-term outcomes of muscle volume and achilles tendon length after achilles tendon ruptures. *Knee Surg. Sports Traumatol. Arthrosc.* 21, 1369–1377. doi: 10.1007/s00167-013-2407-1

Sancho, I., Morrissey, D., Willy, R. W., Barton, C., and Malliaras, P. (2019). Education and exercise supplemented by a pain-guided hopping intervention for male recreational runners with midportion achilles tendinopathy: a single cohort feasibility study. *Phys. Ther. Sport* 40, 107–116. doi: 10.1016/j.ptsp.2019.08.007

Silbernagel, K. G., Hanlon, S., and Sprague, A. (2020). Current clinical concepts: conservative management of achilles tendinopathy. *J. Athl. Train.* 55, 438–447. doi: 10.4085/1062-6050-356-19

Taube, W., Leukel, C., and Gollhofer, A. (2012). How neurons make us jump: the neural controlof stretch-shortening cycle movements. *Exerc. Sport Sci. Rev.* 40, 106–115. doi: 10.1097/jes.0b013e31824138da

Tengman, T., and Riad, J. (2013). Three-dimensional gait analysis following achilles tendon rupture with nonsurgical treatment reveals long-term deficiencies in muscle strength and function. *Orthop. J. Sports Med.* 1:2325967113504734.

Thorpe, C. T., Riley, G. P., Birch, H. L., Clegg, P. D., and Screen, H. R. C. (2014). Effect of fatigue loading on structure and functional behaviour of fascicles from energy-storing tendons. *Acta Biomater.* 10, 3217–3224. doi: 10.1016/j.actbio.2014.04.008

Vergari, C., Ravary-Plumioën, B., Evrard, D., Laugier, P., Mitton, D., Pourcelot, P., et al. (2012). Axial speed of sound is related to tendon's nonlinear elasticity. *J. Biomech.* 45, 263–268. doi: 10.1016/j.jbiomech.2011.10.032

Wearing, S. C., Davis, I. S., Brauner, T., Hooper, S. L., and Horstmann, T. (2019). Do habitual foot-strike patterns in running influence functional achilles tendon properties during gait? *J. Sport Sci.* 37, 2735–2743. doi: 10.1080/02640414.2019.1663656

Wearing, S. C., Hooper, S. L., Locke, S., and Smeathers, J. E. (2013). Non-invasive clinical measurement of the viscoelastic properties of tendon using acoustic wave transmission. *Dtsch Z. Sportme.* 64:148.

Wearing, S. C., Hooper, S. L., Smeathers, J. E., Pourcelot, P., Crevier-Denoix, N., and Brauner, T. (2016). Tendinopathy alters ultrasound transmission in the patellar tendon during squatting. *Scand. J. Med. Sci. Sports* 26, 1415–1422. doi: 10.1111/sms.12602

Wearing, S. C., Reed, L., Hooper, S. L., Bartold, S., Smeathers, J. E., and Brauner, T. (2014). Running shoes increase achilles tendon load in walking: an acoustic propagation study. *Med. Sci. Sports Exerc.* 46, 1604–1609. doi: 10.1249/mss.0000000000000256

Weir, J. P. (2005). Quantifying test-retest reliability using the intraclass correlation coefficient and the SEM. *J. Strength Cond. Res.* 19, 231–240. doi: 10.1519/15184.1

Weiss, P. L., Hunter, I. W., and Kearney, R. E. (1988). Human ankle joint stiffness over the full range of muscle activation levels. *J. Biomech.* 21, 539–544. doi: 10.1016/0021-9290(88)90217-5

Weiss, P. L., Kearney, R. E., and Hunter, I. W. (1986a). Position dependence of ankle joint dynamics – i. passive mechanics. *J. Biomech.* 19, 727–735. doi: 10.1016/0021-9290(86)90196-x

Weiss, P. L., Kearney, R. E., and Hunter, I. W. (1986b). Position dependence of ankle joint dynamics – ii. active mechanics. *J. Biomech.* 19, 737–751. doi: 10.1016/0021-9290(86)90197-1

Wilson, A. M., and Goodship, A. E. (1994). Exercise-induced hyperthermia as a possible mechanism for tendon degeneration. *J. Biomech.* 27, 899–905. doi: 10.1016/0021-9290(94)90262-3

Wind, A. M., and Rouse, E. J. (2020). Neuromotor regulation of ankle stiffness is comparable to regulation of joint position and torque at moderate levels. *Sci. Rep.* 10:10383.

Winter, D. A., and Patla, A. E. (1997). *Signal Processing and Linear Systems for the Movement Sciences*. Waterloo, ON: Waterloo Biomechanics.

Wren, T. A., Yerby, S. A., Beaupré, G. S., and Carter, D. R. (2001). Mechanical properties of the human achilles tendon. *Clin. Biomech.* 16, 245–251.

Wulf, M., Shanker, M., Schuetz, M., Lutz, M., Langton, C. M., Hooper, S. L., et al. (2018). Lower material stiffness in rupture-repaired achilles tendon during walking: transmission-mode ultrasound for post-surgical tendon evaluation. *Knee Surg. Sports Traumatol. Arthrosc.* 26, 2030–2037. doi: 10.1007/s00167-017-4624-5

Wulf, M., Wearing, S. C., Hooper, S. L., Smeathers, J. E., Horstmann, T., and Brauner, T. (2015). achilles tendon loading patterns during barefoot walking and slow running on a treadmill: an ultrasonic propagation study. *Scand. J. Med. Sci. Sports* 25, 868–875. doi: 10.1111/sms.12455

Zelik, K. E., and Franz, J. R. (2017). It's positive to be negative: achilles tendon work loops during human locomotion. *PLoS ONE* 12:e0179976. doi: 10.1371/journal.pone.0179976

Conflict of Interest: The authors declare that the research was conducted in the absence of any commercial or financial relationships that could be construed as a potential conflict of interest.

frontiers in Physiology

ORIGINAL RESEARCH
published: 18 January 2021
doi: 10.3389/fphys.2020.567538

Energy Cost of Force Production After a Stretch-Shortening Cycle in Skinned Muscle Fibers: Does Muscle Efficiency Increase?

Venus Joumaa[1], Atsuki Fukutani[2] and Walter Herzog[1,3]*

[1] Human Performance Laboratory, Faculty of Kinesiology, University of Calgary, Calgary, AB, Canada, [2] Faculty of Sport and Health Science, Ritsumeikan University, Kusatsu, Japan, [3] Biomechanics Laboratory, School of Sports, Federal University of Santa Catarina, Florianopolis, Brazil

Muscle force is enhanced during shortening when shortening is preceded by an active stretch. This phenomenon is known as the stretch-shortening cycle (SSC) effect. For some stretch-shortening conditions this increase in force during shortening is maintained following SSCs when compared to the force following a pure shortening contraction. It has been suggested that the residual force enhancement property of muscles, which comes into play during the stretch phase of SSCs may contribute to the force increase after SSCs. Knowing that residual force enhancement is associated with a substantial reduction in metabolic energy per unit of force, it seems reasonable to assume that the metabolic energy cost per unit of force is also reduced following a SSC. The purpose of this study was to determine the energy cost per unit of force at steady-state following SSCs and compare it to the corresponding energy cost following pure shortening contractions of identical speed and magnitude. We hypothesized that the energy cost per unit of muscle force is reduced following SSCs compared to the pure shortening contractions. For the SSC tests, rabbit psoas fibers ($n = 12$) were set at an average sarcomere length (SL) of 2.4 μm, activated, actively stretched to a SL of 3.2 μm, and shortened to a SL of 2.6 or 3.0 μm. For the pure shortening contractions, the same fibers were activated at a SL of 3.2 μm and actively shortened to a SL of 2.6 or 3.0 μm. The amount of ATP consumed was measured over a 40 s steady-state total isometric force following either the SSCs or the pure active shortening contractions. Fiber stiffness was determined in an additional set of 12 fibers, at steady-state for both experimental conditions. Total force, ATP consumption, and stiffness were greater following SSCs compared to the pure shortening contractions, but ATP consumption per unit of force was the same between conditions. These results suggest that the increase in total force observed following SSCs was achieved with an increase in the proportion of attached cross-bridges and titin stiffness. We conclude that muscle efficiency is not enhanced at steady-state following SSCs.

Keywords: mechanical work, ATPase activity, cross-bridge cycling, stiffness, force depression, residual force enhancement, titin

OPEN ACCESS

Edited by:
Jared R. Fletcher, Mount Royal University, Canada

Reviewed by:
Vincenzo Lombardi, University of Florence, Italy
Ramona Ritzmann, Clinic Rennbahn AG, Switzerland

****Correspondence:***
Venus Joumaa
vjoumaa@ucalgary.ca

Specialty section:
This article was submitted to Exercise Physiology, a section of the journal Frontiers in Physiology

Received: *29 May 2020*
Accepted: *23 December 2020*
Published: *18 January 2021*

Citation:
Joumaa V, Fukutani A and Herzog W (2021) Energy Cost of Force Production After a Stretch-Shortening Cycle in Skinned Muscle Fibers: Does Muscle Efficiency Increase? Front. Physiol. 11:567538. doi: 10.3389/fphys.2020.567538

INTRODUCTION

Muscle force is enhanced during shortening, when shortening is preceded by an active stretch. This phenomenon is known as the stretch-shortening cycle (SSC) effect. The detailed molecular mechanisms responsible for the increase in force and work during SSCs remain unknown. It has been suggested that the SSC effect may be caused by tendon elongation (Cavagna and Citterio, 1974; Finni et al., 2001; Kawakami et al., 2002), stretch-induced reflex responses (Nichols and Houk, 1973; Dietz et al., 1979), pre-activation (cross-bridge elongation) of muscles (Bobbert et al., 1996; Bobbert and Casius, 2005), and residual force enhancement (Seiberl et al., 2015; Fukutani et al., 2017).

Recently, in experiments performed in skinned muscle fibers, Fukutani et al. (2017) showed that the increase in force observed in the shortening phase of SSCs can be maintained at steady-state following stretch-shortening compared to pure shortening contractions of identical speed and magnitude. Fukutani et al. (2017) argued that since experiments were performed in skinned muscle fibers, in which the effects of tendon elongation and reflex activation were eliminated, and the effects of muscle pre-activation (associated with cross-bridge elongations) dissipate quickly, residual force enhancement is likely the primary factor causing the increase in steady-state force following SSCs. This hypothesis was further supported by studies on *in vivo* muscles (Seiberl et al., 2015; Fortuna et al., 2019).

Abbott and Aubert (1952) were the first to systematically show that the steady-state isometric force after active stretching of muscles was higher than the purely isometric force at the corresponding lengths. This property of skeletal muscle became known as residual force enhancement and has been systematically observed in whole muscle preparations (Morgan et al., 2000; Herzog and Leonard, 2002; Pinniger et al., 2006), human skeletal muscles (Oskouei and Herzog, 2006; Shim and Garner, 2012; Power et al., 2013), single fibers (Sugi and Tsuchiya, 1988; Edman and Tsuchiya, 1996; Pinnell et al., 2019), and single myofibrils and sarcomeres (Joumaa et al., 2008; Leonard et al., 2010). Residual force enhancement is known to increase with the magnitude of stretch (Abbott and Aubert, 1952; Edman et al., 1978), and is long lasting (more than 20 s in cat soleus), but can be abolished instantaneously by deactivating the muscle long enough for force to drop to zero (Morgan et al., 2000; Herzog and Leonard, 2002). Furthermore, it has been found that the energy cost per unit of force is reduced by more than 15% in the force enhanced compared to the purely isometric reference state, while stiffness was the same for the two conditions, suggesting that the proportion of attached cross-bridges was similar for the force enhanced and the isometric reference states (Joumaa and Herzog, 2013). This finding suggests that residual force enhancement is accompanied by an increase in muscle efficiency.

Knowing that residual force enhancement may contribute to the increase in force following SSCs, and that residual force enhancement is associated with an increase in muscle efficiency, it is plausible that efficiency is also increased following SSCs. SSCs are common during everyday movement and an increase in muscle efficiency caused by SSCs might be more important than the mechanical advantage of an increase in force.

The purpose of this study was to investigate the energy cost of force production at steady-state following SSCs and compare it to the energy cost following pure shortening contractions. We hypothesized that the energy cost is reduced following SSCs compared to pure shortening contractions. Skinned fibers from rabbit psoas were used for all experiments, and energy cost (ATP consumed) was quantified by measuring the amount of phosphate released during contraction using a malachite green assay (Fujita et al., 1999; Karpowich et al., 2015; Utter et al., 2015). Fibers were stretched to a long sarcomere length of 3.2 μm before being shortened (Fukutani et al., 2017) in order to maximize residual force enhancement and its potential effect on force production.

MATERIALS AND METHODS

Skinned Fiber Preparation

Rabbits were euthanized by an intravenous injection of 1 ml of a pentobarbital solution (240 mg/ml), a protocol approved by the University of Calgary's Animal Care and Ethics Committee. Strips of psoas muscle were dissected, tied to small wooden sticks and stored in a rigor solution for 12 h at 4°C, then in a rigor-glycerol (50:50) solution at −20°C for 2 weeks (Joumaa and Herzog, 2013). On the day of the experiments, a single fiber segment was dissected from the skinned muscle biopsy using a binocular microscope and transferred to an experimental glass chamber containing the relaxing solution. One end of the fiber was glued to the hook of a length controller and the other end to the hook of a force transducer (Aurora Scientific Inc, Ontario, Canada), allowing control of length and force measurements, respectively. Sarcomere lengths were measured using optical diffraction of a He-Ne laser beam. All experiments were performed at ∼24°C.

Mechanical Tests

SSC and Active Shortening to a Sarcomere Length of 2.6 μm

For the SSC test (SSC-2.6), skinned fibers ($n = 12$) were set at an average sarcomere length (SL) of 2.4 μm (L_0) in a relaxing solution, activated, stretched to a SL of 3.2 μm in 4 s, and immediately shortened to a SL of 2.6 μm in 2 s. Fibers were held at this length for 15 s, and then transferred to another bath of activating solution for 40 s, then to a relaxing solution (**Figure 1**). For the active shortening contractions without a prior stretch (CTL-2.6), the same fibers were passively stretched to an average SL of 3.2 μm in 4 s, held for 40 s, and then activated and shortened to a SL of 2.6 μm in 2 s. Fibers were held at this length for 15 s, and then transferred to another bath of activating solution for 40 s, then to a relaxing solution (**Figure 1**).

Fibers were given a 5 min rest period between tests. After each test, the activating solutions in which the fiber was bathed for 40 s were collected for the assessment of ATP consumed.

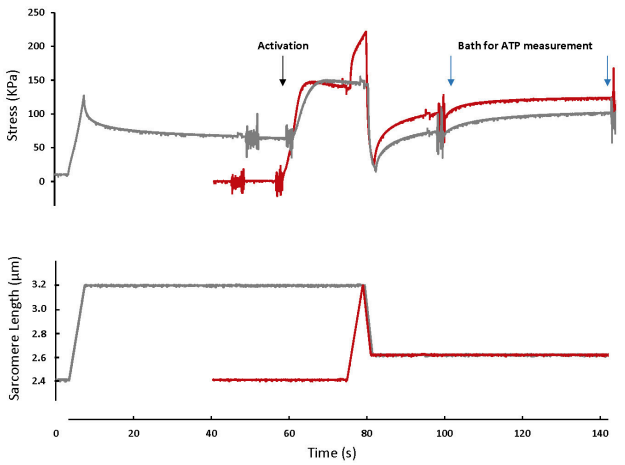

FIGURE 1 | A typical fiber response to an active shortening without a prior stretch (gray) and a stretch-shortening cycle (red). For the active shortening contraction, the fiber was passively stretched from a SL of 2.4 μm to a SL of 3.2 μm, activated and then actively shortened to a SL of 2.6 μm. After 15 s, the fiber was transferred to a fresh activating solution for 40 s and then deactivated. For the SSC contraction, the fiber was activated at a SL of 2.4 μm, actively stretched to a SL of 3.2 μm and immediately shortened to a SL of 2.6 μm. After 15 s the fiber was transferred to a bath of fresh activating solution for 40 s. The activating solutions in which the fibers were bathed for 40 s were used for ATP measurement. Note that the rate of force redevelopment and the steady-state force after shortening are smaller in the active shortening without prior stretch test compared to the SSC test. A fiber was activated by adding first a washing solution (free of EGTA and calcium) and then an activating solution (with high concentration of calcium). The noise on the graph indicates the time when the solution was changed. Active shortening lasted long enough to favor force depression.

SSC and Active Shortening to a Sarcomere Length of 3.0 μm

Experiments were identical to those outlined in the previous paragraph, except that the active shortening performed during the SSC (SSC-3.0) and shortening (CTL-3.0) contractions was from a SL of 3.2 μm to a SL of 3.0 μm in 1 s.

Metabolic Cost

Metabolic cost was quantified by measuring ATPase activity using the malachite green phosphate method (Kodama et al., 1986; Fujita et al., 1999; Karpowich et al., 2015; Utter et al., 2015). The activating solution in which the fiber was bathed during the last 40 s of activation following shortening in the SSC-2.6, SSC-3.0, CTL-2.6, and CTL-3.0 tests was diluted 10 times. Then, inorganic phosphate (Pi) was determined by measuring the absorbance at 620 nm of the green complex formed between malachite green, molybdate and Pi (Sigma-Aldrich MAK307).

The absorbance signal was calibrated by using a known amount of Pi and monitoring the green complex absorbance. Sensitivity of this method to small changes in ATP concentration was also tested (**Figure 2**). Pi produced by the fibers during activation was calculated and converted to amount of ATP used during contraction by assuming that ATP used during contraction is equal to Pi produced (Huxley, 1957).

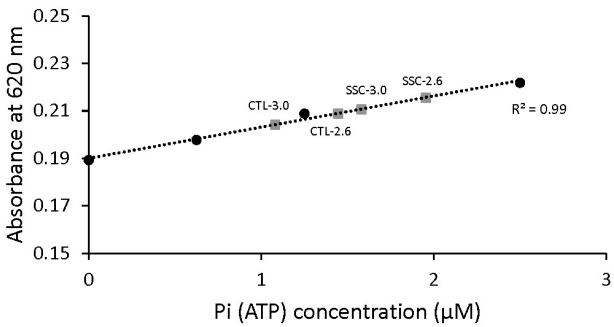

FIGURE 2 | Malachite green absorbance as a function of Pi (ATP) concentration. The standard curve was established by adding known amounts of Pi. When the concentration of Pi increased, the amount of malachite green increased and therefore the absorbance was increased too. Examples of the absorbance of malachite green in the diluted solutions of active shortening (CTL-2.6 and CTL-3.0) and SSCs (SSC-2.6 and SSC-3.0) contractions are also shown. The malachite green assay used in this study could detect differences in the concentration of Pi in the order of 0.1 μM.

Stiffness Measurements

An additional group of 12 fibers was used to measure stiffness after the stretch shortening cycles and purely active shortening stretches. Stiffness was measured using sinusoidal length changes of a peak-to-peak amplitude of 0.2% of L_0 at 0.5 kHz (Regnier et al., 1998) for 50 ms at sarcomere lengths of 2.6 and 3.0 μm, 15 s following shortening in the SSC and active shortening tests.

Metabolic Cost After Residual Force Enhancement

It has been shown that residual force enhancement is accompanied by a decrease in the energy cost per unit of force (Joumaa and Herzog, 2013). In order to check our ability to reproduce similar results in this study, we used another group of fibers ($n = 5$) to determine the energy cost of force production after active stretch compared to a purely isometric reference contraction performed at the same final fiber length. For the reference contraction condition, fibers were set at an average sarcomere length of 3.2 μm, activated, held for 15 s, transferred to another activating solution bath for 40 s and then deactivated. After a rest period of 5 min, the active stretch contraction was performed. Fibers were activated at a sarcomere length of 2.4 μm, then actively stretched to a sarcomere length of 3.2 μm. Fibers were held at this length for 15 s, transferred to another bath of activating solution for 40 s, and then relaxed. After a rest period of 5 min, reference and active stretch contraction tests were repeated. The activating solutions in which the fibers were bathed for 40 s were used for metabolic cost assessment.

Data Analysis

Steady-State Stress

Steady-state total stress at sarcomere lengths of 2.6 and 3.0 μm was determined as the average stress produced during the last 40 s of activation following shortening in the SSC-2.6, SSC-3.0, CTL-2.6, and CTL-3.0 tests.

Mechanical Work

Mechanical work during shortening in the SSC and active shortening tests was calculated by trapezoidal numerical integration of the total force-displacement, curve during the shortening phase.

Metabolic Cost

The amount of ATP used during the last 40 s of activation following shortening in the SSC-2.6, SSC-3.0, CTL-2.6, and CTL-3.0 tests was divided by the average steady-state total force produced during this time in order to obtain the ATPase activity per unit of force.

Stiffness

Stiffness, expressed as Young's modulus (N/mm^2), was measured from the sinusoidal length changes applied to the fiber, as the average peak-to-peak change in stress divided by the peak-to-peak change in length for 10 consecutive cycles.

Statistical Analysis

The outcome measures were compared between the SSC condition and the pure isometric shortening condition at a given sarcomere length (at a sarcomere length of 2.6 μm: SSC-2.6 vs. CTL-2.6, and at a sarcomere length of 3.0 μm: SSC-3.0 vs. CTL-3.0), and therefore the non-parametric Wilcoxon matched-pair signed-rank test ($\alpha = 0.05$) was used. Bonferroni correction was used for multiple comparisons.

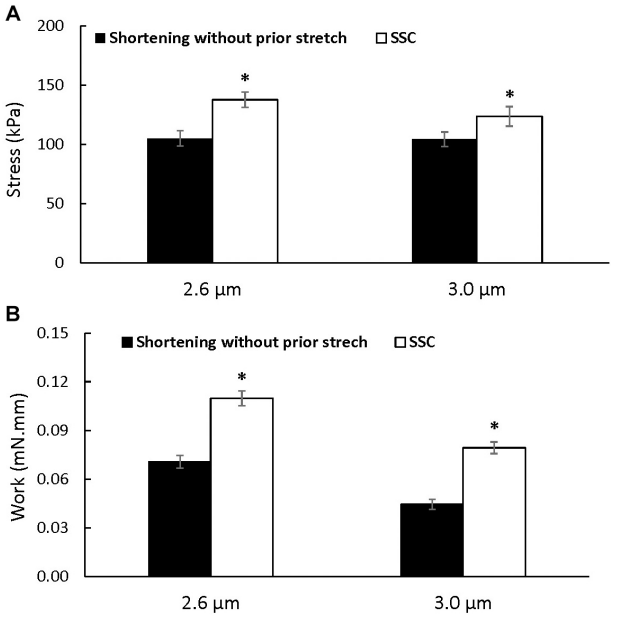

FIGURE 3 | Average total stress **(A)** and work performed during shortening **(B)** (±SEM) for the active shortening and SSC contractions at sarcomere lengths of 2.6 and 3.0 μm. Total stress and the work performed during shortening were greater after SSCs compared to the pure shortening contractions. *Indicates a significant difference from the corresponding pure active shortening contraction.

RESULTS

Figure 1 shows the force-time history of a typical SSC and active shortening experiment.

Steady-state force: Steady-state total force produced during the last 40 s of activation was greater after the SSCs compared to the pure shortening conditions at sarcomere lengths of 2.6 μm ($p = 0.009$) and 3.0 μm ($p = 0.003$) (**Figure 3A**). On average, the increase in total force following the SSCs was (mean ± SEM) 29.8 ± 3.2% and 17.9 ± 1.8% at sarcomere lengths of 2.6 and 3.0 μm, respectively.

Mechanical Work

Mechanical work during the shortening phase was enhanced in the SSC conditions compared to the pure shortening conditions ($p = 0.002$ and 0.002 for sarcomere lengths of 2.6 and 3.0 μm, respectively) (**Figure 3B**).

Metabolic Cost

There was a trend for an increase in the absolute amount of ATP consumed at a sarcomere length of 2.6 μm after the SSC condition compared to the pure shortening contraction ($p = 0.083$), but the absolute amount of ATP consumed was higher after the SSC contraction compared to the pure shortening condition at a sarcomere length of 3.0 μm ($p = 0.016$), and when the data for both sarcomere lengths was combined ($p = 0.022$) (**Figure 4A**). However, ATP consumption per unit of total force was not different between the SSC and the pure shortening conditions at sarcomere lengths of 2.6 μm ($p = 0.221$) and 3.0 μm ($p = 0.262$) (**Figure 4B**).

Stiffness

Stiffness (**Figure 5A**) increased after the SSC conditions compared to the pure shortening conditions at sarcomere lengths of 2.6 μm ($p = 0.002$) and 3.0 ($p = 0.002$) by (mean ± SEM) 16 ± 1 and 18 ± 2%, respectively (**Figure 5B**). Total stress observed at steady-state after SSCs and active shortening tests normalized to stiffness was not different between the SSC and the pure shortening conditions at sarcomere lengths of 2.6 μm ($p = 0.687$) and 3.0 μm ($p = 0.227$) (**Figure 5C**).

Metabolic Cost of Residual Force Enhancement

The energy cost per unit of total force was significantly reduced after active stretch compared to the purely isometric reference contraction ($p = 0.022$) (**Figure 4C**), confirming the previously reported reduction in the energy cost of total force production after an active stretch (Joumaa and Herzog, 2013).

DISCUSSION

The purpose of this study was to investigate the energy cost of force production at steady-state after a SSC and compare it to the energy cost of force after shortening contractions without a prior stretch. Our main finding was that force and ATP consumption

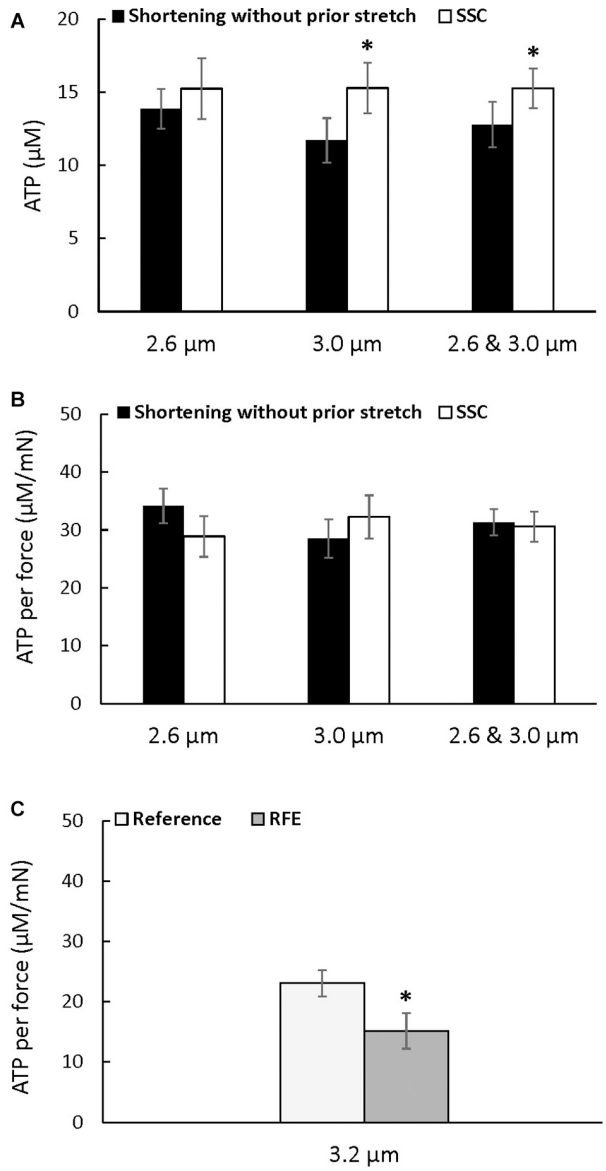

FIGURE 4 | Average ATP consumption **(A)**, average ATP consumption per unit of force **(B)** for the active shortening and the SSC contractions at sarcomere lengths of 2.6, 3.0, and 2.6 μm and 3.0 μm combined, and average ATP consumption per unit of force for the residual force enhancement **(C)** (±SEM). ATP consumption was greater after SSCs at a sarcomere length of 3.0 μm, and when 2.6 μm and 3.0 μm were combined, compared to the pure shortening contractions. ATP consumption per unit of force was not different after SSCs compared to the corresponding active shortening contractions but was reduced in the RFE compared to the isometric reference contractions. The residual force enhancement tests were performed twice, and results were combined for the first and second reference and active stretch contractions. *Indicates a significant difference from the corresponding pure shortening contraction ($p < 0.05$).

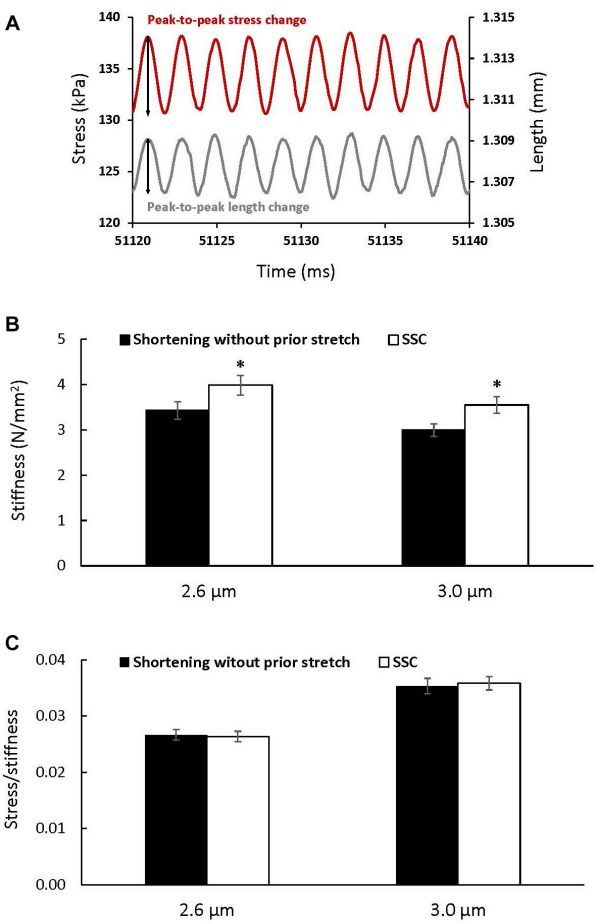

FIGURE 5 | The change in stress (red) in response to the sinusoidal length changes (gray) performed to measure stiffness **(A)**, and average stiffness **(B)** and stress relative to stiffness **(C)** (±SEM) for the active shortening and SSC contractions at sarcomere lengths of 2.6 and 3.0 μm. Stiffness was calculated as the average change in stress (peak-to-peak stress change) divided by the change in the initial fiber length (peak-to-peak length change expressed as strain) for 10 consecutive cycles. *Indicates a significant difference from the corresponding active shortening contraction ($p < 0.05$).

were enhanced at steady-state after SSCs, and that the energy cost per unit of force was the same for both experimental conditions.

Active stretch and residual force enhancement have been associated with a substantial increase in muscle efficiency, as measured by a reduction in the metabolic energy cost per unit of force (Joumaa and Herzog, 2013). Based on these earlier findings, we hypothesized that the metabolic energy cost per unit of force after SSCs may also be reduced compared to pure shortening contractions. We used long stretches (to a sarcomere length of 3.2 μm) in our experimental protocols in order to maximize the effect of active stretching on force in the SSCs. However, the steady-state force was enhanced following SSCs compared to the corresponding pure shortening contractions and so was the ATP consumption, resulting in similar metabolic costs per unit of force for the two experimental conditions, and thus, a similar efficiency.

The absence of the expected increase in muscle efficiency following SSCs may be due to the fact that the increase in force following the SSCs was likely accompanied by a corresponding increase in the proportion of attached cross-bridges compared to

the pure shortening contractions. This suggestion is supported by the proportional increase in stiffness with force and the absence of a change in the ratio of force to stiffness in the SSC compared to the corresponding pure shortening conditions (**Figures 5B,C**). Stiffness measurements must be viewed with caution when interpreting them as a measure of the proportion of attached cross-bridges alone, since other elements like titin contribute to active stiffness, and this titin-based stiffness increases after activation (Powers et al., 2020) and stretch (Herzog, 2014). Although titin contribution to passive stiffness is minimal compared to that of cross-bridges (about 0.04 pN/nm per titin molecule (Linke et al., 1998) vs. 1.21 pN/nm per cross-bridge (Linari et al., 2007), Powers et al. (2020) have shown that titin-associated stiffness during muscle contraction is about two order of magnitudes larger than what has been reported for passive conditions. This suggests that in our experiments titin contributes to stiffness in addition to the cross-bridges. Furthermore, knowing that the force produced by titin does not require ATP, the fact that there is a trend toward an increase in absolute ATP consumption after SSC-2.6 and not a statistically significant increase in ATP consumption, suggests that the observed increase in stiffness following SSC-2.6 was in part caused by an increase in titin force after active stretch and shortening, in addition to the increase in the proportion of attached cross-bridges. Since the increase in stiffness after SSC-3.0 was accompanied by an increase in absolute ATP consumption, the contribution of titin to the increase in stiffness after SSC-3.0 seems lower than at SSC-2.6. Although titin-based force is normally lower at a sarcomere length of 2.6 μm compared to a sarcomere length of 3.0 μm, titin contribution to force and stiffness at steady-state after SSC-2.6 seems greater than that after SSC-3.0. We speculate that this could result from a greater restoring force developed by a stretch-stiffened titin when actively shortened to a shorter sarcomere length of 2.6 μm compared to a sarcomere length of 3.0 μm.

Why do the proportion of attached cross-bridges and cross-bridge-based stiffness increase at steady-state after SSCs compared to the corresponding pure shortening contractions? It has been observed that the steady-state isometric force after active shortening of muscles is reduced compared to the purely isometric force at the corresponding length (Abbott and Aubert, 1952; Edman, 1975; Granzier and Pollack, 1989). Furthermore, experiments using whole muscles (Lee and Herzog, 2003) and single fibers (Sugi and Tsuchiya, 1988; Joumaa et al., 2012; Pinnell et al., 2019) have consistently shown that force depression is associated with a proportional decrease in stiffness that has been interpreted as a decrease in the proportion of attached cross-bridges, compared to isometric contractions at the corresponding length. Our finding that the proportion of attached cross-bridges after SSCs was greater than that after a shortening contraction suggests that, somehow, an active stretch preceding a shortening contraction effectively prevented the reduction in cross-bridges during a pure shortening contraction.

It is hard to reconcile the suggested increase in attached cross-bridges observed after SSCs compared to pure shortening contractions with the stress-induced inhibition of cross-bridge hypothesis suggested by Marechal and Plaghki (1979) to explain force depression. Marechal and Plaghki (1979) suggested that active shortening might be associated with a stress-induced inhibition of cross-bridge formation in the newly formed overlap zone created during the active shortening. This hypothesis has been supported by data showing that the decrease in force at steady-state after an active shortening increases with the amount of stress and mechanical work performed during shortening: the greater the work during shortening, the lower the stiffness and the lower the force at steady-state after shortening, likely because of a greater inhibition of cross-bridge formation (Meijer et al., 1997; Herzog et al., 2000; Joumaa et al., 2017). However, although the mechanical work performed during the shortening phase of the SSC was greater than the work performed during the pure shortening contractions (**Figure 3B**), stiffness and force were greater after SSCs compared to the corresponding shortening contractions. Similar findings, showing great force following SSCs despite a high amount of work produced during the shortening phase, were obtained in previous studies using fibers (Fukutani et al., 2017; Fukutani and Herzog, 2019; Fukutani and Isaka, 2019) and *in vivo* muscles (Fortuna et al., 2018, 2019; Hahn and Riedel, 2018). One possible explanation for these findings may be that the stress-induced inhibition of cross-bridges during the shortening phase of the SSC was compensated for by an increase in cross-bridge recruitment and formation during and after the initial lengthening phase of the SSC. However, if this interpretation was correct, residual force enhancement at steady-state following active stretching would be accompanied by an increase in the proportion of attached cross-bridges compared to the corresponding pure isometric contraction. However, this is not the case and the proportion of attached cross-bridges does not increase in the force enhanced state compared to the corresponding pure isometric contractions (Sugi and Tsuchiya, 1988; Joumaa and Herzog, 2013). Therefore, an increase in cross-bridge recruitment would not occur in the stretch phase of the SSCs but would have to occur in the shortening phase. A plausible explanation for a reduced inhibition of cross-bridge formation during the shortening phase of SSC was suggested by Fortuna et al. (2019) and further supported by Tomalka et al. (2020). These authors argued that in pure shortening contractions, work is produced primarily by cross-bridges, while in SSC contractions, a substantial amount of the shortening work is produced by the recoil of the passive structures that elongated during the stretch phase of the SSCs (Fortuna et al., 2019). In this case, the stress on actin filaments, and associated cross-bridge inhibition, might be reduced compared to pure shortening contractions, which in turn, could result in the observed increase in the proportion of attached cross-bridges following SSCs compared to pure shortening contractions.

Another possibility is based on the direct effect of the recruitment of the passive structures (titin) during the active stretch on the contractile filaments. It has been demonstrated using myofibrillar models (Hanft et al., 2013) and x-ray diffraction (Irving et al., 2011; Ait-Mou et al., 2016) that titin passive force induces stretch-based alterations in the structural arrangement and flexibility of the contractile filaments. Therefore, we speculate that the stretch phase of the SSCs and the associated substantial increase in titin-based force

could stabilize the contractile filaments and reduce actin conformational distortion and stress-induced inhibition of cross-bridges during the shortening phase. This will result in more cross-bridges at steady-state following SSCs compared to pure shortening contractions, in which titin-based force is relatively low and has limited capacity to stabilize the nanostructure of the contractile filaments. Nevertheless, further research is warranted to investigate the impact of active lengthening on titin, the contractile filaments and cross-bridge formation and inhibition during SSCs.

LIMITATIONS AND FUTURE DIRECTIONS

In this study, we investigated whether the increase in force after a SSC was accompanied by an increase in muscle efficiency, and found that muscle efficiency at steady-state after a SSC was not improved. This result might not apply readily to everyday activities as most daily movements involving SSCs are not followed by long isometric contractions. However, this result provides insights into the potential mechanisms of the increase in force at steady-state after SSCs. A major limitation of this study was that ATP consumption could not be measured in real time during the dynamic phases of SSCs. Future experiments should aim at addressing this limitation by assessing the energy cost of force in real time during the stretching and shortening phases of SSCs. Furthermore, although the frequency of the sinusoidal perturbations used in this study to measure stiffness has been used by others (e.g., Regnier et al., 1998), it could be argued that a greater frequency should have been used to prevent the effect of force recovery on stiffness.

CONCLUSION

We have shown that force was enhanced at steady-state following SSCs, but there was no difference in the metabolic energy cost of force following SSCs and pure shortening contractions. The increase in force is likely caused by an increase in the proportion of attached cross-bridges and titin stiffness following SSCs compared to pure shortening contractions.

DATA AVAILABILITY STATEMENT

The raw data supporting the conclusions of this article will be made available by the authors, without undue reservation.

ETHICS STATEMENT

The animal study was reviewed and approved by the University of Calgary's Animal Care and Ethics Committee.

AUTHOR CONTRIBUTIONS

VJ, AF, and WH conceived and designed research, interpreted results of experiments, edited and revised manuscript, and approved final version of manuscript. VJ performed the experiments, analyzed the data, and drafted the manuscript. All authors contributed to the article and approved the submitted version.

FUNDING

The financial support of CIHR (10013332), the Killam Foundation (10001203), and the Canada Research Chair Program (RT730101), is greatly acknowledged.

REFERENCES

Abbott, B. C., and Aubert, X. M. (1952). The force exerted by active striated muscle during and after change of length. *J. Physiol.* 117, 77–86.

Ait-Mou, Y., Hsu, K., Farman, G. P., Kumar, M., Greaser, M. L., Irving, T. C., et al. (2016). Titin strain contributes to the Frank-Starling law of the heart by structural rearrangements of both thin- and thick-filament proteins. *Proc. Natl. Acad. Sci. U S A.* 113, 2306–2311. doi: 10.1073/pnas.1516732113

Bobbert, M. F., and Casius, L. J. R. (2005). Is the effect of a countermovement on jump height due to active state development? *Med. Sci. Sports Exerc.* 37, 440–446. doi: 10.1249/01.mss.0000155389.34538.97

Bobbert, M. F., Gerritsen, K. G., Litjens, M. C., and Van Soest, A. J. (1996). Why is countermovement jump height greater than squat jump height? *Med. Sci. Sports Exerc.* 28, 1402–1412. doi: 10.1097/00005768-199611000-00009

Cavagna, G. A., and Citterio, G. (1974). Effect of stretching on the elastic characteristics and the contractile component of frog striated muscle. *J. Physiol.* 239, 1–14. doi: 10.1113/jphysiol.1974.sp010552

Dietz, V., Schmidtbleicher, D., and Noth, J. (1979). Neuronal mechanisms of human locomotion. *J. Neurophysiol.* 42, 1212–1222. doi: 10.1152/jn.1979.42.5.1212

Edman, K. A. (1975). Mechanical deactivation induced by active shortening in isolated muscle fibres of the frog. *J. Physiol.* 246, 255–275. doi: 10.1113/jphysiol.1975.sp010889

Edman, K. A., and Tsuchiya, T. (1996). Strain of passive elements during force enhancement by stretch in frog muscle fibres. *J. Physiol.* 490(Pt 1), 191–205. doi: 10.1113/jphysiol.1996.sp021135

Edman, K. A., Elzinga, G., and Noble, M. I. (1978). Enhancement of mechanical performance by stretch during tetanic contractions of vertebrate skeletal muscle fibres. *J. Physiol.* 281, 139–155. doi: 10.1113/jphysiol.1978.sp012413

Finni, T., Ikegawa, S., and Komi, P. V. (2001). Concentric force enhancement during human movement. *Acta Physiol. Scand.* 173, 369–377. doi: 10.1046/j.1365-201X.2001.00915.x

Fortuna, R., Goecking, T., Seiberl, W., and Herzog, W. (2019). Force depression following a stretch-shortening cycle depends on the amount of residual force enhancement established in the initial stretch phase. *Physiol. Rep.* 7:14188.

Fortuna, R., Kirchhuebel, H., Seiberl, W., Power, G. A., and Herzog, W. (2018). Force depression following a stretch-shortening cycle is independent of stretch peak force and work performed during shortening. *Sci. Rep.* 8:8.

Fujita, K., Ye, L. H., Sato, M., Okagaki, T., Nagamachi, Y., and Kohama, K. (1999). Myosin light chain kinase from skeletal muscle regulates an ATP-dependent interaction between actin and myosin by binding to actin. *Mol. Cell. Biochem.* 190, 85–90. doi: 10.1007/978-1-4615-5543-8_11

Fukutani, A., and Herzog, W. (2019). Influence of stretch magnitude on the stretch–shortening cycle in skinned muscle fibres. *J. Exp. Biol.* 222:206557

Fukutani, A., and Isaka, T. (2019). Influence of muscle length on the stretch-shortening cycle in skinned rabbit soleus. *Sci. Rep.* 9, 1–5. doi: 10.1038/s41598-019-54959-5

Fukutani, A., Joumaa, V., and Herzog, W. (2017). Influence of residual force enhancement and elongation of attached cross-bridges on stretch-shortening cycle in skinned muscle fibers. *Physiol. Rep.* 5:13477.

Granzier, H. L., and Pollack, G. H. (1989). Effect of active pre-shortening on isometric and isotonic performance of single frog muscle fibres. *J. Physiol.* 415, 299–327. doi: 10.1113/jphysiol.1989.sp017723

Hahn, D., and Riedel, T. N. (2018). Residual force enhancement contributes to increased performance during stretch-shortening cycles of human plantar flexor muscles in vivo. *J. Biomech.* 77, 190–193. doi: 10.1016/j.jbiomech.2018.06.003

Hanft, L. M., Greaser, M. L., and McDonald, K. S. (2013). Titin-mediated control of cardiac myofibrillar function. *Arch. Biochem. Biophys.* 552-553, 83–91. doi: 10.1016/j.abb.2013.11.005

Herzog, W. (2014). Mechanisms of enhanced force production in lengthening (eccentric) muscle contractions. *J. Appl. Physiol.* 116, 1407–1417. doi: 10.1152/japplphysiol.00069.2013

Herzog, W., and Leonard, T. R. (2002). Force enhancement following stretching of skeletal muscle: a new mechanism. *J. Exp. Biol.* 205, 1275–1283.

Herzog, W., Leonard, T. R., and Wu, J. Z. (2000). The relationship between force depression following shortening and mechanical work in skeletal muscle. *J. Biomech.* 33, 659–668. doi: 10.1016/s0021-9290(00)00008-7

Huxley, A. F. (1957). Muscle structure and theories of contraction. *Prog. Biophys. Biophys. Chem.* 7, 255–318. doi: 10.1016/s0096-4174(18)30128-8

Irving, T., Wu, Y., Bekyarova, T., Farman, G. P., Fukuda, N., and Granzier, H. (2011). Thick-filament strain and interfilament spacing in passive muscle: effect of titin-based passive tension. *Biophys. J.* 100, 1499–1508. doi: 10.1016/j.bpj.2011.01.059

Joumaa, V., and Herzog, W. (2013). Energy cost of force production is reduced after active stretch in skinned muscle fibres. *J. Biomechan.* 46, 1135–1139. doi: 10.1016/j.jbiomech.2013.01.008

Joumaa, V., Fitzowich, A., and Herzog, W. (2017). Energy cost of isometric force production after active shortening in skinned muscle fibres. *J. Exp. Biol.* 220, 1509–1515. doi: 10.1242/jeb.117622

Joumaa, V., Leonard, T. R., and Herzog, W. (2008). Residual force enhancement in myofibrils and sarcomeres. *Proc. Biol. Sci.* 275, 1411–1419. doi: 10.1098/rspb.2008.0142

Joumaa, V., Macintosh, B. R., and Herzog, W. (2012). New insights into force depression in skeletal muscle. *J. Exp. Biol.* 215, 2135–2140. doi: 10.1242/jeb.060863

Karpowich, N. K., Song, J. M., Cocco, N., and Wang, D.-N. (2015). ATP binding drives substrate capture in an ECF transporter by a release-and-catch mechanism. *Nat. Struct. Mol. Biol.* 22, 565–571. doi: 10.1038/nsmb.3040

Kawakami, Y., Muraoka, T., Ito, S., Kanehisa, H., and Fukunaga, T. (2002). In vivo muscle fibre behaviour during counter-movement exercise in humans reveals a significant role for tendon elasticity. *J. Physiol.* 540, 635–646. doi: 10.1113/jphysiol.2001.013459

Kodama, T., Fukui, K., and Kometani, K. (1986). The Initial Phosphate Burst in ATP Hydrolysis by Myosin and Subfragment-1 as Studied by a Modified Malachite Green Method for Determination of Inorganic Phosphate. *J. Biochem.* 99, 1465–1472. doi: 10.1093/oxfordjournals.jbchem.a135616

Lee, H. D., and Herzog, W. (2003). Force depression following muscle shortening of voluntarily activated and electrically stimulated human adductor pollicis. *J. Physiol.* 551, 993–1003. doi: 10.1113/jphysiol.2002.037333

Leonard, T. R., DuVall, M., and Herzog, W. (2010). Force enhancement following stretch in a single sarcomere. *Am. J. Physiol. Cell Physiol.* 299, C1398–C1401.

Linari, M., Caremani, M., Piperio, C., Brandt, P., and Lombardi, V. (2007). Stiffness and Fraction of Myosin Motors Responsible for Active Force in Permeabilized Muscle Fibers from Rabbit Psoas. *Biophys. J.* 92, 2476–2490. doi: 10.1529/biophysj.106.099549

Linke, W. A., Ivemeyer, M., Mundel, P., Stockmeier, M. R., and Kolmerer, B. (1998). Nature of PEVK-titin elasticity in skeletal muscle. *Proc. Natl. Acad. Sci. U S A.* 95, 8052–8057. doi: 10.1073/pnas.95.14.8052

Marechal, G., and Plaghki, L. (1979). The deficit of the isometric tetanic tension redeveloped after a release of frog muscle at a constant velocity. *J. Gen. Physiol.* 73, 453–467. doi: 10.1085/jgp.73.4.453

Meijer, K., Grootenboer, H. J., Koopman, B. F. J. M., and Huijing, P. A. (1997). Fully Isometric Length-Force Curves of Rat Muscle Differ from Those during and after Concentric Contractions. *J. Appl. Biomech.* 13, 164–181. doi: 10.1123/jab.13.2.164

Morgan, D. L., Whitehead, N. P., Wise, A. K., Gregory, J. E., and Proske, U. (2000). Tension changes in the cat soleus muscle following slow stretch or shortening of the contracting muscle. *J. Physiol.* 522(Pt 3), 503–513. doi: 10.1111/j.1469-7793.2000.t01-2-00503.x

Nichols, T. R., and Houk, J. C. (1973). Reflex Compensation for Variations in the Mechanical Properties of a Muscle. *Science* 181, 182–184. doi: 10.1126/science.181.4095.182

Oskouei, A. E., and Herzog, W. (2006). The dependence of force enhancement on activation in human adductor pollicis. *Eur. J. Appl. Physiol.* 98, 22–29. doi: 10.1007/s00421-006-0170-4

Pinnell, R. A. M., Mashouri, P., Mazara, N., Weersink, E., Brown, S. H. M., and Power, G. A. (2019). Residual force enhancement and force depression in human single muscle fibres. *J. Biomech.* 91, 164–169. doi: 10.1016/j.jbiomech.2019.05.025

Pinniger, G. J., Ranatunga, K. W., and Offer, G. W. (2006). Crossbridge and non-crossbridge contributions to tension in lengthening rat muscle: force-induced reversal of the power stroke. *J. Physiol.* 573, 627–643. doi: 10.1113/jphysiol.2005.095448

Power, G. A., Makrakos, D. P., Rice, C. L., and Vandervoort, A. A. (2013). Enhanced force production in old age is not a far stretch: an investigation of residual force enhancement and muscle architecture. *Physiol. Rep.* 1:e00004. doi: 10.1002/phy2.4

Powers, J. D., Bianco, P., Pertici, I., Reconditi, M., Lombardi, V., and Piazzesi, G. (2020). Contracting striated muscle has a dynamic I-band spring with an undamped stiffness 100 times larger than the passive stiffness. *J. Physiol.* 598, 331–345. doi: 10.1113/JP278713

Regnier, M., Lee, D. M., and Homsher, E. (1998). ATP Analogs and Muscle Contraction: Mechanics and Kinetics of Nucleoside Triphosphate Binding and Hydrolysis. *Biophys. J.* 74, 3044–3058. doi: 10.1016/S0006-3495(98)78012-9

Seiberl, W., Power, G. A., Herzog, W., and Hahn, D. (2015). The stretch-shortening cycle (SSC) revisited: residual force enhancement contributes to increased performance during fast SSCs of human m. adductor pollicis. *Physiol. Rep.* 3:12401.

Shim, J., and Garner, B. (2012). Residual force enhancement during voluntary contractions of knee extensors and flexors at short and long muscle lengths. *J. Biomech.* 45, 913–918. doi: 10.1016/j.jbiomech.2012.01.026

Sugi, H., and Tsuchiya, T. (1988). Stiffness changes during enhancement and deficit of isometric force by slow length changes in frog skeletal muscle fibres. *J. Physiol.* 4, 215–229. doi: 10.1113/jphysiol.1988.sp017411

Tomalka, A., Weidner, S., Hahn, D., Seiberl, W., and Siebert, T. (2020). Cross-Bridges and Sarcomeric Non-cross-bridge Structures Contribute to Increased Work in Stretch-Shortening Cycles. *Front. Physiol.* 11:921. doi: 10.3389/fphys.2020.00921

Utter, M. S., Ryba, D. M., Li, B. H., Wolska, B. M., and Solaro, R. J. (2015). Omecamtiv Mecarbil, a Cardiac Myosin Activator, Increases Ca2+ Sensitivity in Myofilaments With a Dilated Cardiomyopathy Mutant Tropomyosin E54K. *J. Cardiovasc. Pharmacol.* 66, 347–353. doi: 10.1097/FJC.0000000000000286

Conflict of Interest: The authors declare that the research was conducted in the absence of any commercial or financial relationships that could be construed as a potential conflict of interest.

frontiers in Physiology

ORIGINAL RESEARCH
published: 29 March 2021
doi: 10.3389/fphys.2021.648019

Non-cross Bridge Viscoelastic Elements Contribute to Muscle Force and Work During Stretch-Shortening Cycles: Evidence From Whole Muscles and Permeabilized Fibers

Anthony L. Hessel[1†], Jenna A. Monroy[2†] and Kiisa C. Nishikawa[3]*

[1]Institute of Physiology II, University of Muenster, Muenster, Germany, [2]W.M. Keck Science Department, Claremont Colleges, Claremont, CA, United States, [3]Department of Biological Sciences, Northern Arizona University, Flagstaff, AZ, United States

OPEN ACCESS

Edited by:
Geoffrey A. Power, University of Guelph, Canada

Reviewed by:
Arthur J. Cheng, York University, Canada
Atsuki Fukutani, University of Calgary, Canada

***Correspondence:**
Jenna A. Monroy
JMonroy@keckscl.claremont.edu

[†]These authors have contributed equally to this work and share first authorship

Specialty section:
This article was submitted to Striated Muscle Physiology, a section of the journal Frontiers in Physiology

Received: *31 December 2020*
Accepted: *08 March 2021*
Published: *29 March 2021*

Citation:
Hessel AL, Monroy JA and Nishikawa KC (2021) Non-cross Bridge Viscoelastic Elements Contribute to Muscle Force and Work During Stretch-Shortening Cycles: Evidence From Whole Muscles and Permeabilized Fibers. Front. Physiol. 12:648019. doi: 10.3389/fphys.2021.648019

The sliding filament–swinging cross bridge theory of skeletal muscle contraction provides a reasonable description of muscle properties during isometric contractions at or near maximum isometric force. However, it fails to predict muscle force during dynamic length changes, implying that the model is not complete. Mounting evidence suggests that, along with cross bridges, a Ca^{2+}-sensitive viscoelastic element, likely the titin protein, contributes to muscle force and work. The purpose of this study was to develop a multi-level approach deploying stretch-shortening cycles (SSCs) to test the hypothesis that, along with cross bridges, Ca^{2+}-sensitive viscoelastic elements in sarcomeres contribute to force and work. Using whole soleus muscles from wild type and *mdm* mice, which carry a small deletion in the N2A region of titin, we measured the activation- and phase-dependence of enhanced force and work during SSCs with and without doublet stimuli. In wild type muscles, a doublet stimulus led to an increase in peak force and work per cycle, with the largest effects occurring for stimulation during the lengthening phase of SSCs. In contrast, *mdm* muscles showed neither doublet potentiation features, nor phase-dependence of activation. To further distinguish the contributions of cross bridge and non-cross bridge elements, we performed SSCs on permeabilized psoas fiber bundles activated to different levels using either $[Ca^{2+}]$ or $[Ca^{2+}]$ plus the myosin inhibitor 2,3-butanedione monoxime (BDM). Across activation levels ranging from 15 to 100% of maximum isometric force, peak force, and work per cycle were enhanced for fibers in $[Ca^{2+}]$ plus BDM compared to $[Ca^{2+}]$ alone at a corresponding activation level, suggesting a contribution from Ca^{2+}-sensitive, non-cross bridge, viscoelastic elements. Taken together, our results suggest that a tunable viscoelastic element such as titin contributes to: (1) persistence of force at low $[Ca^{2+}]$ in doublet potentiation; (2) phase- and length-dependence of doublet potentiation observed in wild type muscles and the absence of these effects in *mdm* muscles; and (3) increased peak force and work per cycle in SSCs. We conclude that non-cross bridge viscoelastic elements, likely titin, contribute substantially to muscle force and work, as well as the phase-dependence of these quantities, during dynamic length changes.

Keywords: 2,3-butanedione monoxime, calcium-dependence, doublet potentiation, skeletal muscle, titin, work loop, history-dependence

INTRODUCTION

As scientific theories evolve, paradigms often shift as seemingly obscure facts that resisted explanation by an accepted theory take on new importance (Kuhn, 1962). In the sliding-filament, swinging cross bridge theory of muscle contraction (Huxley and Hanson, 1954; Huxley and Niedergerke, 1954; Huxley, 1957), the isometric force-length relationship (Gordon et al., 1966), and the isotonic force-velocity relationship (Huxley, 1957) played important roles in establishing the theory as fact. However, several key observations including enhancement of force with stretch and depression of force with shortening resisted explanation by the accepted theory (Abbott and Aubert, 1952; Edman, 1975; Edman et al., 1982; Tsuchiya and Sugi, 1988). The perceived importance of these history-dependent muscle properties has increased over recent decades with the recognition that they play essential roles in human and animal movement by enhancing work and power output, dissipating force, and providing instantaneous stabilization during unexpected perturbations (Daley and Biewener, 2011; Nishikawa et al., 2013; Seiberl et al., 2013). Additionally, there is increasing recognition that muscle models based on the isometric force-length and isotonic force-velocity relationships fail to predict muscle force during dynamic *in vivo* movement (Siebert et al., 2008; Lee et al., 2013; Dick et al., 2017), perhaps because a critical element is missing (Rode et al., 2009; Heidlauf et al., 2017; Nishikawa et al., 2018; Nishikawa, 2020).

Accumulating evidence suggests that Ca^{2+}-sensitive, non-cross bridge, viscoelastic elements in sarcomeres of skeletal muscles (Monroy et al., 2012; Colombini et al., 2016; Nishikawa et al., 2019), are responsible for history-dependent muscle properties during changes in length (Nocella et al., 2014; Nishikawa, 2016; Herzog, 2018). It has also become increasingly accepted that the giant titin protein is a Ca^{2+}-sensitive, viscoelastic element in muscle sarcomeres (Nishikawa, 2020). Titin is the largest known protein, extending from the Z-line to the M-band (Bang et al., 2001; Linke, 2018). In the Z-line and A-band, titin is bound to the thin and thick filaments, respectively. In contrast, I-band titin is a freely extensible, viscoelastic spring, that is predominantly comprised of a relatively compliant proximal Ig domain region, a stiff PEVK region, (named for its predominant residues), and an N2A region that spans between the two springs (Linke et al., 1998a,b). Because of its location within the sarcomere, titin is responsible for nearly all longitudinal force in relaxed myofibrils (Granzier and Irving, 1995) and was suggested to function as a Ca^{2+}-dependent spring in active muscle (Leonard and Herzog, 2010; Nishikawa et al., 2012; Linke, 2018). Recent work has demonstrated that the N2A region of titin binds to actin in a Ca^{2+}-dependent manner (Dutta et al., 2018; Nishikawa et al., 2019), which would shorten titin's free length and allow for stretch of only the stiffer PEVK region in active muscle. The *mdm* mutation in mice produces a small deletion in N2A titin (Garvey et al., 2002), which profoundly reduces active muscle stiffness (Powers et al., 2016; Hessel and Nishikawa, 2017; Monroy et al., 2017), leading to a reduction in both force enhancement with stretch and force depression with shortening (Tahir et al., 2020), apparently by preventing N2A titin–actin binding (Dutta et al., 2018; Nishikawa et al., 2019).

Many previous experiments have evaluated force during isovelocity stretch-hold (i.e., force enhancement) or shorten-hold (i.e., force depression) contractions (recently reviewed by Herzog, 2018; Chen et al., 2019). While these experiments provide important details about the history-dependence of force during and after isovelocity stretch and shortening, they fail to capture the history-dependent properties of muscles during SSCs (Seiberl et al., 2015b; Hahn and Riedel, 2018; Fukutani and Herzog, 2020b), in which energy stored during stretch can be recovered during shortening to increase net work per cycle (Hahn and Riedel, 2018; Fukutani and Herzog, 2020b). Most previous *ex vivo* studies using SSCs typically varied the velocity or amplitude of length changes (Askew and Marsh, 1997, 1998), but only rarely have such studies examined the effects of cross-bridge inhibition on muscle force and work (Fukutani and Herzog, 2020b). While it is now widely believed that cross bridges contribute relatively little to energy storage during active stretch (Linari et al., 2003; Pinniger et al., 2006), the mechanisms and extent of contributions from non-cross bridge elements such as titin to energy storage and recovery in SSCs remains to be elucidated. Based on the above arguments, it seems reasonable that a Ca^{2+}-activated, non-cross bridge, viscoelastic element, specifically titin, contributes to muscle force and work during SSCs.

In this study, we used a multi-level, *ex vivo* approach to test broadly for contributions of Ca^{2+}-activated, non-cross bridge, viscoelastic elements to SSCs in two different experimental preparations and muscles: whole soleus muscles and permeabilized psoas fibers. In whole muscle experiments, we used doublet stimuli at different phases of SSCs in wild type and *mdm* muscles to test for a role of titin in activation-and phase-dependence of peak force and work. In permeabilized psoas fibers, we used the myosin inhibitor, BDM to investigate contributions of Ca^{2+}-sensitive non-cross bridge elements at different activation levels. By taking similar approaches that vary activation in the two preparations, we aim to further our understanding of the role of titin in regulating muscle force and work during SSCs.

For whole muscles, our strategy was to use doublet stimuli at varying phases of SSCs in wild type and *mdm* soleus muscles to test whether titin contributes not only to muscle force and work, but also to doublet potentiation as well as to the phase-dependence of activation, which feature prominently in the biomechanics of *in vivo* movements (Dickinson et al., 2000; Seiberl et al., 2015a; Paternoster et al., 2016). Doublet stimuli, when added to a train of low-frequency stimuli, potentiate muscle force (Burke et al., 1970, 1976) for up to hundreds of milliseconds after the single extra stimulus (Sandercock and Heckman, 1997). Although few previous studies have investigated doublet potentiation in SSCs, a single stimulus has been observed to increase work per cycle by up to 50% (Stevens, 1996). While this property of muscle has been known for more than 50 years, the underlying mechanisms are not well explained by the sliding filament-swinging cross bridge theory of muscle contraction (Burke et al., 1970; Sandercock and Heckman, 1997;

Binder-Macleod and Kesar, 2005; Nishikawa et al., 2018). Several studies have shown that the Ca^{2+} transient associated with the doublet stimulus returns to control levels within ~25 ms (Abbate et al., 2002; Cheng et al., 2013; Bakker et al., 2017), but the increase in muscle force that persists for hundreds of milliseconds cannot be explained by current theories (Burke et al., 1970; Binder-Macleod and Kesar, 2005; Nishikawa, 2018). Previous studies have suggested that, similar to invertebrate "catch" (Butler and Siegman, 2010), engagement of a Ca^{2+}-activated elastic element could potentially explain the sustained force at low [Ca^{2+}] following doublet stimulation (Parmiggiani and Stein, 1981; Sandercock and Heckman, 1997; Binder-Macleod and Kesar, 2005; Nishikawa, 2018). By varying the phase of doublet stimulation in SSCs, we also investigated a potential role for titin in the phase-dependence of activation (Dickinson et al., 2000; Ahn, 2012).

For permeabilized muscle fibers, we developed a different strategy to investigate the relative contributions of Ca^{2+}-sensitive cross bridges and non-cross bridge elements to muscle force and work in SSCs. Many previous studies have reported that, as activation increases in SSCs, peak force during lengthening also increases, which correlates with increased positive work during the subsequent shortening phase (Seiberl et al., 2015b; Fortuna et al., 2017; Fukutani and Herzog, 2020a). Of note, treatment of single muscle fibers with 10 mM BDM (~50% maximum activation level) enhanced shortening work during SSCs relative to a shortening-only contraction (Fukutani and Herzog, 2020b), suggesting that a Ca^{2+}-sensitive, non-cross bridge viscoelastic element remains engaged during myosin inhibition. Here, we extend these observations to a wide range of concentration of calcium ions (pCa)- and BDM-regulated activation levels (15–100%). If a Ca^{2+}-sensitive, non-cross bridge viscoelastic element remains engaged during myosin inhibition, then we expect that peak force and work during SSCs will be greater in BDM-treated than in Ca^{2+}-activated fiber bundles matched to the same level of activation. We measured force and work of permeabilized fiber bundles during SSCs across differing levels of activation, achieved by varying the pCa and the myosin inhibitor, 2,3-butanedione monoxime (BDM) in a series of activating solutions. BDM reduces the proportion of actin-bound myosin heads (Griffiths et al., 2006), and therefore the isometric force of Ca^{2+}-activated fibers. We matched activation levels of mouse psoas fiber bundles activated using solutions with different pCa to similar bundles activated using varying doses of BDM at pCa = 4.2. By comparing BDM-controlled and pCa-controlled fibers at a given activation level, we sought to determine whether force and work during SSCs were produced by cross bridges alone, or whether there was evidence for a contribution of additional Ca^{2+}-dependent, viscoelastic elements.

In summary, our multi-level approach focuses on varying activation levels in SSCs: using pCa and BDM in psoas fiber bundles, and changing stimulation patterns (i.e., doublets and stimulation phase) in whole soleus muscles. At the whole muscle level, we hypothesize that titin contributes to doublet potentiation of muscle force and work during SSCs, and that the *mdm* mutation reduces not only the doublet effect but also the phase-dependence of activation on muscle force and work. At the level of permeabilized fibers, we predicted that, if only cross bridges contribute to force and work, and then there should be no difference in SSCs between BDM-controlled vs. pCa-controlled fibers across activation levels. However, if Ca^{2+}-dependent viscoelastic elements also contribute, then BDM-controlled fibers should show greater force and work than pCa-controlled fibers.

MATERIALS AND METHODS

Animal use was approved by the Institutional Animal Care and Use Committees of the University Clinic Muenster (LANUV NRW, 81-02.04.2019.A472), Northern Arizona University (NAU IACUC Protocol #18-002), and the Claremont Colleges (CC IACUC Protocol #017-003). Adult mice were euthanized by an isoflurane gas overdose, cervical dislocation, and cardiac puncture. For whole muscle studies, wild type and homozygous recessive (*mdm*) B6C3Fe a/a-Ttn ^{mdm}/J mice from a C57BL/6 J background were obtained from a breeding colony at Northern Arizona University. Homozygous *mdm* mice can be identified by their small size, stiff gait, and hunchback posture at 10–12 days of age (Garvey et al., 2002; Lopez et al., 2008). Fiber studies were conducted on wild type mice with the same genetic background (C57BL/6 J) from a colony at University of Muenster.

Whole Muscle Experiments

Whole muscle experiments were conducted on 11 wild type and 18 *mdm* soleus muscles from age-matched mice of both sexes (average wild type age = 44.4 ± 2.0 days; average *mdm* age = 49.6 ± 2.9 days, $p = 0.12$). Because wild type mice were larger in body size than *mdm* mice, muscle mass, optimal length (L_0), and maximum isometric force were significantly greater in wild type compared to *mdm* soleus (**Table 1**), as reported previously (Taylor-Burt et al., 2015; Hessel and Nishikawa, 2017; Monroy et al., 2017; Hessel et al., 2019; Tahir et al., 2020). Maximum isometric stress was also lower in *mdm* muscles, likely because titin transmits cross bridges forces from the A-band to the Z-disk (Horowits et al., 1986; Nishikawa, 2020). Neither Ca^{2+} sensitivity nor the force-velocity relationship differs between genotypes (Hessel and Nishikawa, 2017; Tahir et al., 2020). To account for differences in length and stress, muscle length was normalized to optimal length (L_0) and relative differences in stress were compared between genotypes.

To obtain force and length measurements during SSCs, the distal end of each muscle was attached to an inflexible hook,

TABLE 1 | Physiological characteristics of wild type and *mdm* soleus muscles.

	mdm	Wild type
Body mass (g)	7.5 ± 0.30*	23.4 ± 0.49
Muscle mass (mg)	1.96 ± 0.53*	9.3 ± 0.67
L_0 (mm)	7.13 ± 0.26*	11.27 ± 0.33
Max isometric force (N) ForForcewFocforce (N)	0.008 ± 0.006*	0.14 ± 0.01
P_0 (Ncm^{-2})	4.1 ± 1.2*	15.6 ± 1.53

*Data expressed as mean ± SEM, mdm: n = 18, wild type: n = 11. *indicates p < 0.05.*

and the proximal end was attached to a dual servomotor muscle lever (Aurora Scientific, Inc., Series 300B, Aurora, ON, Canada). A custom LabVIEW (National Instruments Corp., Austin, TX, United States) program was used to control the muscle lever and record force, length and time at a sampling rate of 4 kHz. Muscles were kept in a Krebs–Henseleit bath (in mM: 137 NaCl, 5 KCl, 1 NaH_2PO_4, 24 $NaHCO_3$, 2 $CaCl_2$, 1 $MgSO_4$, and 11 dextrose, pH 7.4), buffered with 95% O_2 and 5% CO_2. Because SSC experiments can fatigue muscles quickly, whole muscles were maintained at a constant temperature (21–23°C), at which the maximum isometric tetanic force remains stable for several hours and within 10% of the maximum isometric stress at normal body temperature of 37°C (James et al., 2015).

Maximum isometric tetanic force was measured from soleus muscles stimulated at 70–80 Hz for 800–1,500 ms at supramaximal voltage (Monroy et al., 2017). Periodically, the maximum isometric tetanic force was measured, and a muscle was removed from the analysis if force dropped by more than 10% from the initial value. At the start of each SSC experiment, muscles were set to optimal length (L_0), defined as the length at which maximum isometric twitch force was produced. The maximum isometric stress (P_0, Ncm^{-2}) was determined by dividing maximum isometric force by the physiological cross-sectional area, calculated using standard methods (Hakim et al., 2013; Monroy et al., 2017).

We measured the effects of doublet potentiation at different phases during SSCs in wild type and *mdm* soleus muscles to determine not only whether titin contributes to muscle force and work, but also to the activation- and phase-dependence of these quantities. Small amounts of doublet potentiation in fast-twitch muscles stimulated at nearly the maximum frequency can be explained by an increased number of cross bridges (Bakker et al., 2017), but not the larger and longer lasting effects that are observed at lower stimulation frequencies (see e.g., Abbate et al., 2002). Long-lasting doublet potentiation in soleus muscles that persists for >200 ms also is not readily explained by cross-bridge models (Sandercock and Heckman, 1997). By measuring muscle work during SSCs in wild type and *mdm* soleus muscles with and without doublet stimulation, we can determine whether titin likely contributes to doublet potentiation of muscle force and work. Muscles were subjected to ±5% L_0 SSCs at a frequency of 5 Hz for a total of four cycles with and without doublet stimulation (**Figures 1A,C**). The cycle phase is defined here as the percent of an individual stretch-shortening cycle (SSC), where a phase of 0% denotes a muscle at its shortest length (−5% L_0) at the onset of lengthening, a phase of 50% denotes a muscle at its longest length (+5% L_0) at the onset of shortening, and the cycle ends at a phase of 100% (**Figures 1B,D**). Muscles were stimulated submaximally at 30 Hz for 100 ms.

To investigate the phase dependence of doublet stimulation, activation was initiated at six different phases within the SSC (8.3, 25, 33.3, 50, and 83.3%), which determined muscle length at the onset of stimulation as well as the direction of the work loop (clockwise for positive work and counter-clockwise for negative work). Each activation onset was repeated with and without a single doublet stimulus. Doublet stimuli were added 10 ms following the initial stimulus, for a total of three or four stimuli per cycle (see **Figure 1**; doublet stimulus indicated by black arrow). Passive and maximally stimulated (i.e., 75–80 Hz stimulus frequency) work loops were also obtained at each phase of stimulation. Muscles were rested 5–7 min between trials to minimize fatigue. For each trial, peak stress (Ncm^{-2}) and mass-specific net, negative, and positive work were measured from the third cycle of each trial (James et al., 1995) using MATLAB (2019) [version 9.7.0. (R2019b) Natick, Massachusetts: The MathWorks Inc.].

Permeabilized Fiber Bundle Experiments

Permeabilized ("skinned") fibers were prepared from wild type mouse psoas muscles (n = 8 mice, five male/three female, age range 3–6 months) using standard glycerol techniques (Hessel et al., 2019). Extracted muscles were permeabilized and stored in a relaxing solution [in mmol l^{-1}: potassium propionate (170), magnesium acetate (2.5), MOPS (20), K_2EGTA (5), and ATP (2.5), pH 7.0] for 12 h at 4°C, then moved to a relaxing: glycerol (50:50) or rigor: glycerol solution [KCl (100), $MgCl_2$ (2), EGTA (5), Tris (10), DTT (1), 50% glycerol, and pH 7.0] at −20°C for a minimum of 3 weeks. To limit protein degradation, all solutions contained one tablet of protease inhibitor (Complete, Roche Diagnostics, Mannheim, Germany) per 100 ml of solution. On the day of experiments, permeabilized muscles were removed from the storage solution and vigorously washed in relaxing solution on ice. Small bundles of 3–10 fibers were separated from the muscle. The ends of the fibers were wrapped with fine sutures and placed in custom-made clips to secure the fibers in place. Fibers bundles were attached lengthwise to a piezomotor on one end and a force transducer on the other end *via* aluminum clamps (Scientific Instruments, Heidelberg, Germany). All mechanical experiments were performed at 21°C. Force data were recorded at 1,000 Hz. Each fiber bundle was suspended in a bath of relaxing solution and then transferred to other baths as needed. Sarcomere length (SL) was measured by laser diffraction and initially set to an average length of 2.6 μm SL. Length changes were accomplished by computer-control of the length motor. Force was set to slack length = 0 mN for each sample. Total force is a combination of passive and active force components.

To separate the effects of $[Ca^{2+}]$ on cross bridge and non-cross bridge elements, we conducted mechanical experiments on fiber bundles activated to different levels by either: (1) changing the level of $[Ca^{2+}]$ (expressed as pCa = $-\log[Ca^{2+}]$); or (2) reducing cross bridge force production using the myosin inhibitor BDM at supramaximal pCa = 4.2. Different activating solutions were prepared from the same stock activating solution [in mmol l^{-1}: potassium propionate (170), magnesium acetate (2.5), MOPS (10), ATP (2.5), and pH 7.0] by adding CaEGTA and K_2EGTA in different proportions to obtain different pCa levels. For pCa-controlled experiments, we prepared activating solutions with a final pCa range between 4.2 and 6.2 to achieve a range of isometric forces (confirmed during pilot tests). For the BDM-controlled solutions, we added BDM to supramaximal activation solutions (pCa 4.2) to final concentrations between

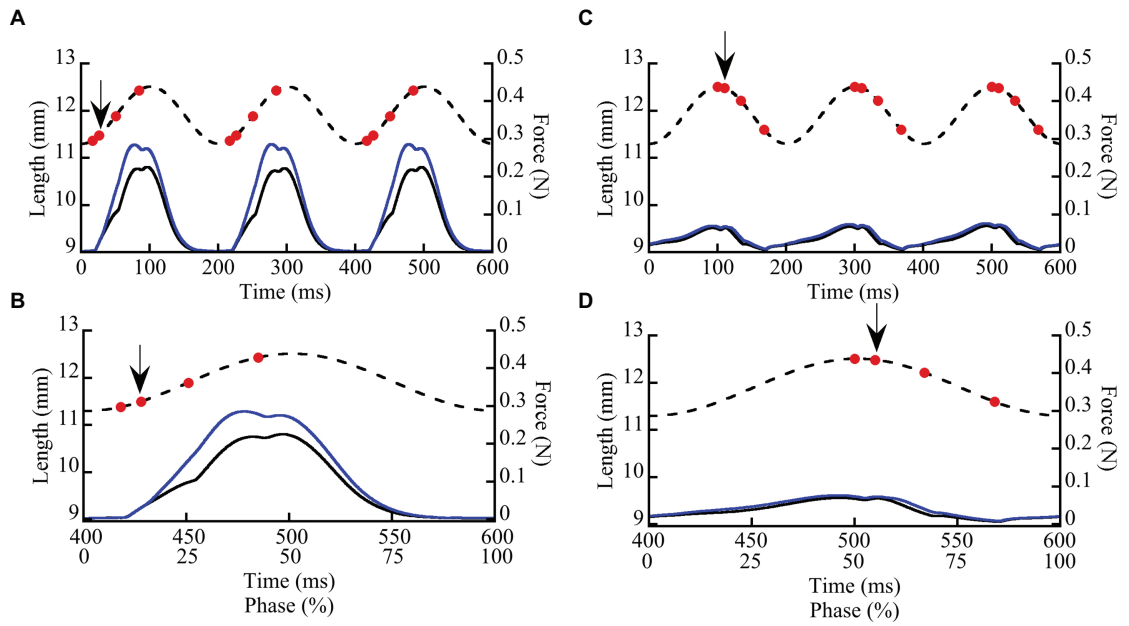

FIGURE 1 | Representative stretch-shortening cycles (SSCs) from whole wild type soleus muscles stimulated at two phases of activation (8.3 and 50%). Muscles were subjected to 3–4 SSCs at strain amplitude of ±5% L_0 and a frequency of 5 Hz (200 ms/cycle). In this example, a muscle was stimulated at a phase of 8.3% **(A,B)** when the muscle was lengthening and at a phase of 50% **(C,D)** at the onset of muscle shortening. **(A,C)** illustrate three successive cycles. **(B,D)** show the third cycle from each trial, as well as the relationship between time (ms) and phase (0–100%). Dashed lines show length vs. time and solid lines show force vs. time. Muscle force (solid lines) is shown for SSCs with (blue lines) and without (black lines) a doublet stimulus added 10 ms after the first stimulus in each cycle. Red dots indicate individual stimuli, the arrow indicates the doublet.

0 and 30 mM BDM, to achieve a range of isometric forces from 100 to ~15% of maximum isometric force. The goal was to perform SSCs on individual fiber bundles over as a wide range of activation levels as possible to reduce variability associated with comparing data across different samples. Fibers were subjected to either the BDM- or the pCa- controlled protocols, but not both; we found that some level of force-reduction remained after BDM treatment, even with thorough washing.

The SSC protocol was as follows (**Figure 2**): muscle fibers were either kept relaxed or isometrically activated at 2.6 μm SL until isometric force was reached (1.5–4 min), and then cycled through eight successive triangular SSCs, from 2.6 to 3.0 μm SL at 2 Hz (1.6 μm SL s^{-1}). After completion of SSCs, fibers were held at constant length (2.6 μm SL) for 30 s, and finally deactivated in relaxing solution. All fibers were tested in the following order: (1) Passive fibers were moved through the SSC protocol in a relaxed state 3–5 times to pre-stress the sample, which makes the force data more consistent (Li et al., 2020; Rivas-Pardo et al., 2020). The final passive SSC protocol was saved and used as the relaxed state. (2) Fibers were maximally activated (pCa 4.2) and moved through the SSC protocol. (3) The SSC protocol was repeated from lowest to highest activating solutions (increasing activation level for both BDM and pCa trials), up to seven different activating solutions per fiber, with at least 3 min rest in fresh relaxing solution between trials. This order was followed to maximize the number of tests that could be performed on a single fiber bundle before the force it produced dropped below 85% of its original maximum force, after which the fiber bundle was no longer used in experiments. We chose to use seven trials per sample after an extensive pilot study in which we subjected fiber bundles to various levels of pCa and measured changes in force over time. At certain submaximal activation levels, we found that fiber bundles could be activated up to 20 times before forces dropped below 85% of starting values. The conservative seven-trial cutoff was chosen to ensure that most fibers would be able to complete the experiment with minimal decrease in force. For each fiber bundle, the activation level (%) was calculated as the isometric force prior to the SSC divided by the maximum isometric force of the same fiber bundle at pCa = 4.2.

Generally, activation led to a typical leveling-off of isometric force over time, but the time to reach maximum force increased as activation level decreased (see **Figures 2A,B**). Some experiments at the lowest activation levels (>25 mM BDM; > pCa 6.1) required up to 4 min to develop maximum isometric force. Therefore, we used relatively long isometric activations before SSCs in all trials. After each trial, the fibers were visually assessed for damage using a 10x dissection microscope. We excluded the data and terminated the experiment if fibers tore, or if the passive force of relaxed fibers changed after the SSC protocol by >5%. In the present study, 12/43 fiber bundles were discarded. To compare across different fiber bundles, force data (mN total force) were normalized to stress ($mN*mm^2$) using standard methods (Hessel et al., 2019). Length data were

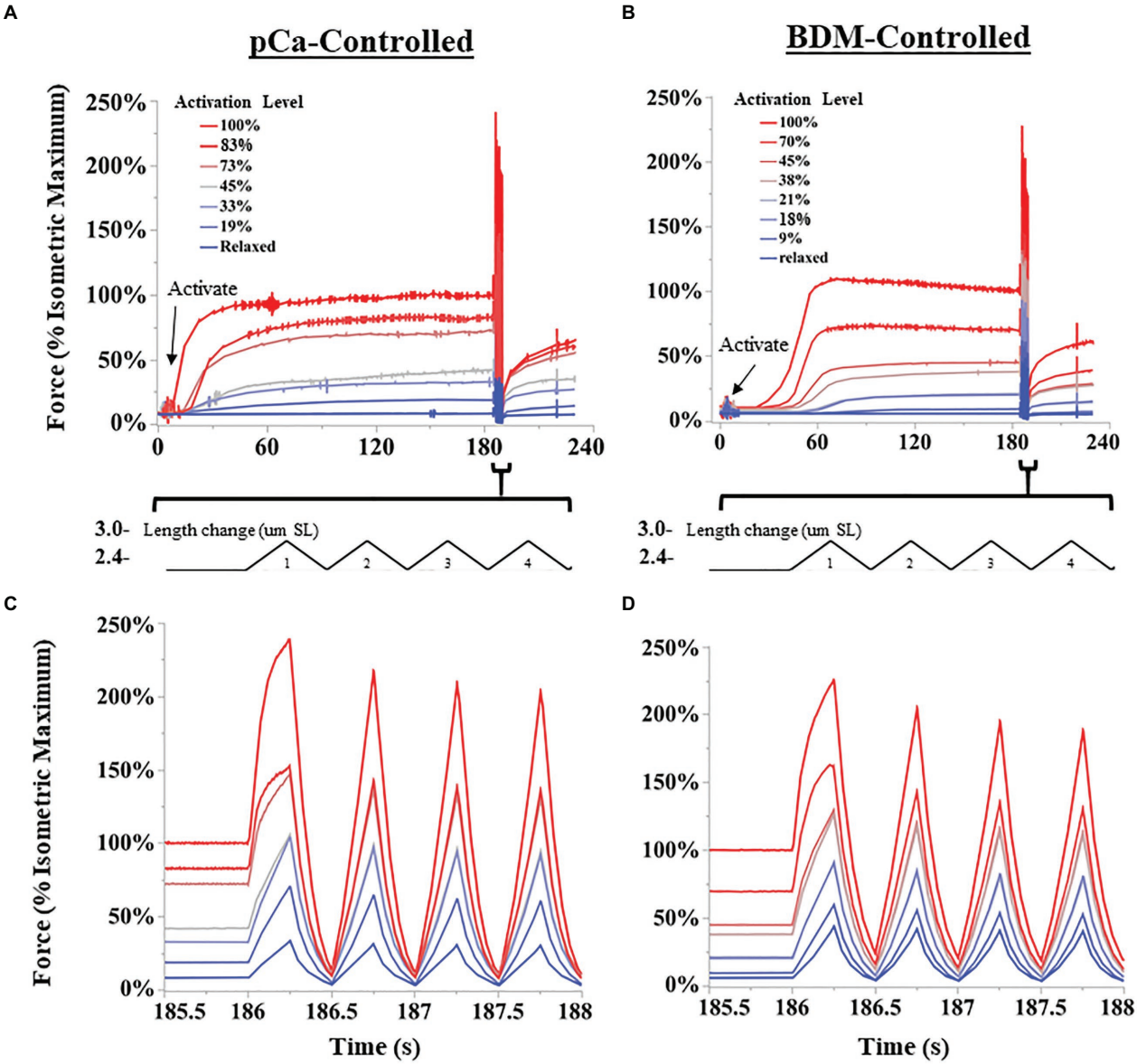

FIGURE 2 | Representative SSC experiments from permeabilized fiber bundles. Activation levels were controlled either by decreasing the concentration of calcium ions (pCa; **A,C**), or by 2,3-butanedione monoxime (BDM)-induced myosin inhibition **(B,D)**. Length changes were performed using a "triangular" length trajectory between 2.4 and 3.0 μm SL at 2 Hz. **(A,B)** show all force trials collected for a representative fiber bundle for pCa-controlled and BDN-controlled fibers, respectively. Bundles were activated until force leveled off, and then subjected to multiple SSCs. **(C,D)** show the first four cycles at a higher time resolution for pCa and BDM trials, respectively.

normalized to strain using the initial length of 2.6 μm SL. Peak force and specific work were normalized to the fiber's isometric force at pCa 4.2 (reference trial). In total, we collected contraction trials from 16 and 15 fiber bundles in BDM and pCa-controlled protocols, respectively.

Statistical Analysis

Statistical analyses were conducted using the lme4, lmtest, tidyverse, car (Fox and Weisberg, 2010), and MASS packages in R Studio statistical software (R Studio Team, 2020), Microsoft Excel (v11, Microsoft Inc., Seattle, WA, United States), and JMP (JMP Pro 14, SAS Institute). Alpha values were set at 0.05. Data were best Box-Cox transformed to meet assumptions of normality and homoscedasticity when necessary. Data are presented as mean ± SE (sem).

Whole Muscle Experiments

To assess effects of genotype and phase of stimulation on SSC variables, we used a linear mixed model with genotype and

phase as main effects, the genotype × phase interaction, and individual nested within genotype as a random effect. The dependent variables were the differences between the control and doublet conditions for peak stress, net work, positive work, and negative work per cycle. Because peak stress, net, and negative work changed curvilinearly with phase of stimulation, a quadratic term for phase and the interaction between the quadratic term and genotype was added to the model. A log likelihood ratio test was used to determine the significance of each independent variable. The quadratic term was not significant and therefore not included in the model describing the difference in positive work across genotypes and phase of activation. Because maximum isometric stress was significantly smaller in *mdm* muscles, the dependent variables were recalculated as the % difference relative to the control and the analysis was repeated. All variables changed curvilinearly with phase of stimulation, therefore a quadratic term for phase and the interaction between the quadratic term and genotype was also included in the model.

Fiber Bundle Experiments

We compared four SSC variables across activation levels and between pCa-controlled and BDM-controlled conditions. From the stress-time traces, we calculated the forces at the longest length (peak force) during each SSC. Negative (lengthening phase), positive (shortening phase), and net (total) specific work per cycle were also calculated for each SSC. For clarity, and because trends are similar between SSCs, we only present analysis of SSC 1 in the main text, while data for all SSCs are available in supplemental information (see **Supplementary Figure S1**). We plotted relative values of force and specific work against activation level.

To assess the effects of condition and force on all four variables, we ran an analysis of covariance (ANCOVA) in JMP. The model included condition (pCa vs. BDM) as the main effect, activation level as the covariate, the condition by activation level interaction, and individual nested within condition as a random effect. To compare fibers activated with Ca^{2+} or Ca^{2+} plus BDM, the ANCOVA analyses were conducted for peak force and work in SSCs from 52 pCa and 76 BDM-controlled fibers across activation levels (% isometric force before the SSCs).

RESULTS

Whole Muscle Experiments

In general, when wild type muscles were activated with doublet stimulation during lengthening (phase < 50%) force and work increased, and the increase persisted throughout shortening for 100 ms after stimulation ceased (**Figure 3A**). When activated during shortening (phase = 50%), doublet stimulation resulted in smaller changes in positive and negative work (**Figure 3B**). Activation at the end of shortening and through the beginning of lengthening (phase > 70%) caused a large increase in negative work but small change in positive work (**Figure 3C**). Across all phases of activation, *mdm* muscles exhibited little doublet potentiation of force or work (**Figures 3D–F**).

There was a significantly greater increase in peak stress with doublet stimulation in wild type than in *mdm* muscles (**Figure 4**; $F = 52.3$, $p < 0.0001$). There was also a significant interaction between the quadratic term and genotype, indicating a difference in curvature of the stress-phase relationship between genotypes (**Figure 4**; $F = 13.3$, $p = 0.0004$). In wild type soleus, the greatest increase in peak stress occurred at phase = 25%. However, only two muscles were stimulated at this phase, so the mean value may be an over-estimate. For all other phases, at least seven muscles were included in the analysis. In general, the greatest increase in peak stress with doublet stimulation occurred when muscles were activated during lengthening and the smallest increase occurred during shortening. A separate analysis of only *mdm* data showed no effect of phase ($F = 0.2$, $p = 0.65$) or the quadratic term ($F = 0.04$, $p = 0.85$) on peak stress in *mdm* muscles (**Figure 4**). Similarly, the relative increase in peak stress with doublet stimulation was greater in wildtype compared to *mdm* muscles (**Supplementary Figure S1**; **Supplementary Table S1**; $F = 23.7$, $p < 0.0001$). However, there was no significant interaction between genotype and the quadratic term, indicating that the relationship between the relative increase in peak stress and phase did not differ between genotypes ($F = 0.49$, $p = 0.48$).

Wild type muscles exhibited a significantly greater increase in net ($F = 43.84$, $p < 0.0001$), negative ($F = 14.51$, $p = 0.0007$), and positive work ($F = 50.43$, $p < 0.0001$) with doublet stimulation compared to *mdm* muscles (**Figure 5**). Similar to peak stress, the greatest increase in work occurred when muscles were activated during lengthening and the smallest increase occurred when muscles were activated during shortening. Wild type muscles exhibited a 3-fold greater increase in negative work with doublet stimulation than *mdm* muscles, and there was a significant interaction between the quadratic term and genotype on both net ($F = 49.81$, $p < 0.0001$) and negative work ($F = 40.87$, $p < 0.0001$), indicating that the curvature of the relationship between these variables and phase differed between genotypes (**Figures 5A,B**). Positive work decreased linearly with phase and the slope of this relationship was five times greater in wild type than *mdm* muscles (**Figure 5C**; $F = 20.88$, $p < 0.0001$). Relative changes in net, negative, and positive work were similar to absolute differences (**Supplementary Figure S2**; **Supplementary Table S1**). During lengthening, the relative increases in both negative and positive work were more than 20% greater in wild type compared to *mdm* muscles. Interestingly, at phase = 33%, when wild type muscles were stimulated at the end of lengthening and through the beginning of shortening, there was a more than 2-fold increase in positive work with doublet stimulation, causing net work to shift from negative to positive and to increase by more than 150% (**Supplementary Figure S2**).

Permeabilized Fiber Bundle Experiments

Initial total isometric stress of fiber bundles in pCa 4.2 solution with no BDM was similar (ANOVA; $F = 0.07$; $p = 0.79$) between pCa-controlled ($N = 15$; force = 2.05 ± 0.24 mN; PCSA = 0.017 ± 0.008 mm^2; stress = 116.60 ± 4.2 mN^*mm^2) and BDM-controlled fibers ($N = 16$; force = 2.24 ± 0.38;

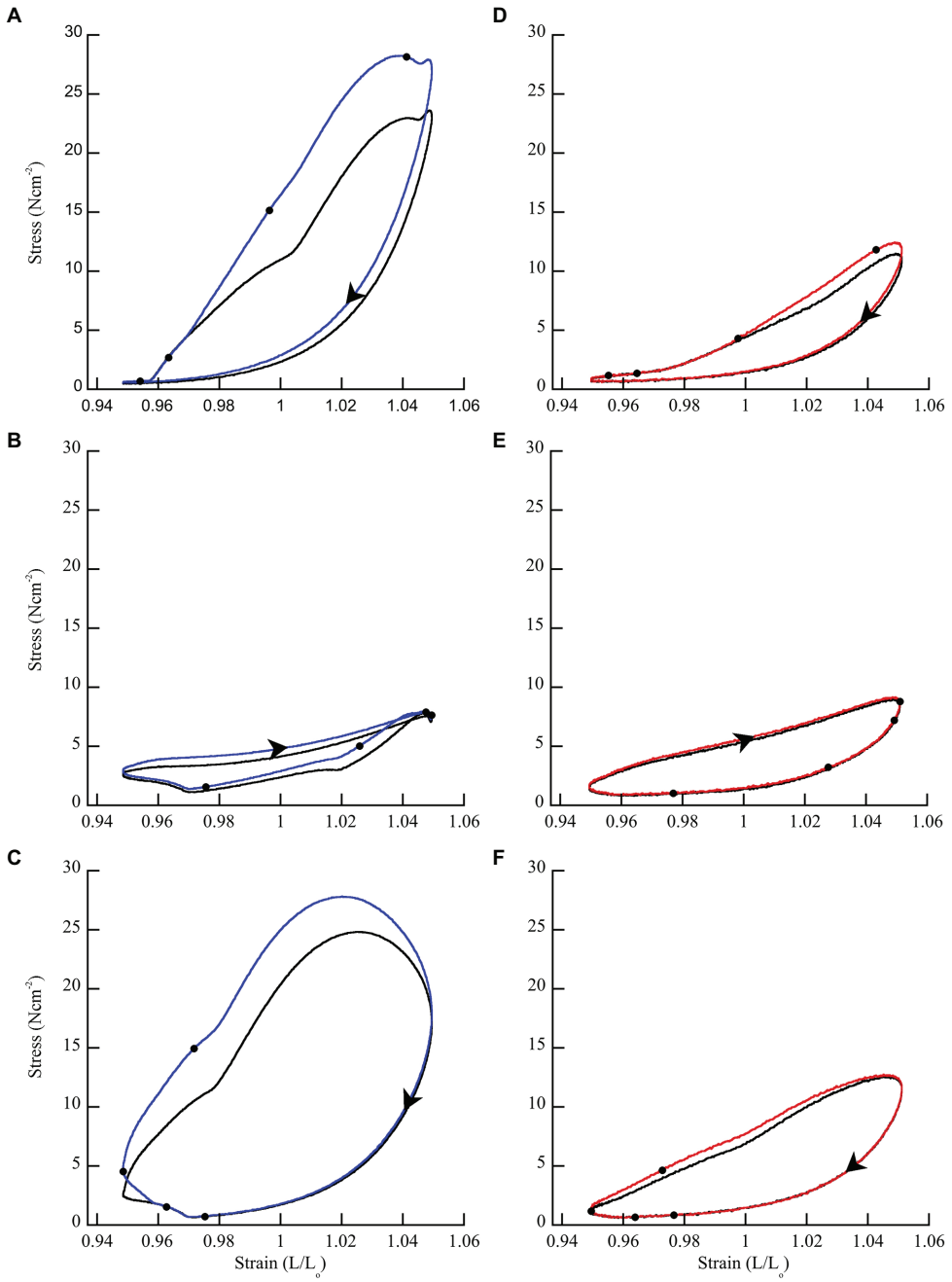

FIGURE 3 | Representative work loops from wild type and *mdm* soleus muscles stimulated with (blue = wild type; red = *mdm*) and without (black) a doublet. **(A,D)** Phase = 8.3% when the muscle is lengthening. **(B,E)** Phase = 50% when the muscle is shortening. **(C,F)** Phase = 83.3% when the muscle is shortening followed by lengthening. The effect of doublet stimulation on work per cycle (area within the work loop) changes with the phase of activation and is greatest when stimulation occurs during lengthening (phase < 50%). Black dots indicate individual stimuli. Arrows indicate the direction of a work loop.

PCSA 0.019 ± 0.012 mm^2; stress = 119.02 ± 7.9 mN^*mm^2), as expected. Furthermore, the initial isometric stress of relaxed fibers (passive, relaxing solution with no BDM at 2.6 μm SL) was also similar (ANOVA; F = 0.52; p = 0.48) between pCa-controlled (12.989 ± 9.4 mN^*mm^2) and BDM-controlled fibers (10.42 ± 5.9 mN^*mm^2).

During the eight SSCs, the first SSC always produced the largest peak force (up to 250% maximal isometric force), with subsequent SSCs decreasing in force until SSC 5–8 when the force became approximately constant (**Supplementary Figure S3**). The relationship between peak force during the first SSC vs. activation level differed between pCa- and BDM-controlled

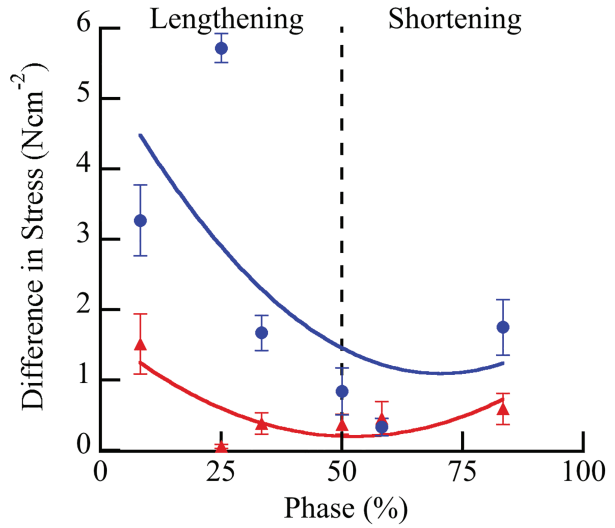

FIGURE 4 | Differences in peak stress with vs. without doublet stimulation across phase of stimulation in wild type (blue) and *mdm* (red) soleus. Doublet potentiation of peak stress is reduced in *mdm* muscles compared to wild type at all phases of activation ($F = 52.3$, $p < 0.0001$). Phase = 0% indicates a muscle at its shortest length at the onset of lengthening and phase = 50% indicates a muscle at its longest length just prior to shortening. Data represent means ± SE, $N = 28$ individuals, 112 trials.

fibers (**Figure 6A**). ANCOVA showed that peak force increased with increasing activation level for both conditions (activation level covariate $F = 680.71$, $p < 0.001$). Furthermore, compared to pCa-controlled fibers, the peak force of the BDM-controlled fibers was higher at a given activation level (condition $F = 12.59$, $p = 0.0014$) and trended toward a steeper slope than in pCa-controlled fibers (interaction $F = 3.78$, $p = 0.055$; **Figure 6A**).

The relationships between specific positive, negative, and net work per cycle vs. activation level also differed between pCa- and BDM-controlled fibers (**Figures 6B–D**). For all three work variables, there was a significant positive relationship between work and activation level (positive work $F = 612.07$, $p < 0.001$; negative work $F = 1318.01$, $p < 0.001$; net work $F = 1399.58$, $p < 0.001$). The relationship between positive work vs. activation level for BDM-controlled fibers produced a slightly steeper slope than for pCa-controlled fibers (interaction $F = 7.53$, $p = 0.0072$), and there was no significant difference between intercepts (condition $F = 0.41$, $p = 0.53$; **Figure 6B**). In contrast, the relationship between negative work vs. activation level produced steeper slopes (interaction $F = 4.75$, $p = 0.031$) and increased intercepts (condition $F = 14.89$, $p < 0.001$) in BDM-controlled fibers compared to pCa-controlled fibers (**Figure 6C**). Finally, the relationship between net work vs. activation level increased in BDM-controlled fibers compared to pCa-controlled fibers (condition $F = 26.78$, $p < 0.001$), but with similar slopes (interaction $F = 1.90$, $p = 0.1709$; **Figure 6D**). Taken together, our data indicate that specific negative and net work per cycle is greater in BDM- vs. pCa-controlled fibers.

DISCUSSION

The focus of our study was to conduct SSC experiments at two different levels of muscle organization to test the hypothesis that Ca^{2+}-activated, non-cross bridge, viscoelastic elements contribute to muscle force and work during dynamic changes in length. We used whole muscle and single fiber preparations to ask whether the traditional sliding filament – swinging cross bridge theory alone can account for muscle force and work during SSCs. Together, both approaches provided support for the hypothesis that a Ca^{2+}-dependent, non-cross bridge element, likely titin, contributes to force and work during SSCs.

Whole Muscle Experiments

Three observations from whole muscle studies support the existence of non-cross bridge forces in SSCs. (1) In wild type muscles, potentiation of force and work persists for ~100 ms after doublet stimulation, long after ~25 ms [Ca^{2+}] transients associated with a doublet stimulus have subsided (Bakker et al., 2017). (2) Adding a doublet stimulus to a submaximal pulse train during SSCs increased force and work in a phase-dependent manner, with stimulation during the eccentric phase producing the greatest increase. (3) The response to doublet stimulation was significantly reduced in *mdm* muscles with a small deletion in N2A titin (Garvey et al., 2002), showing almost no long-lasting effects throughout an SSC.

Results from the present study showed that doublet potentiation of force and work persisted throughout an SSC for 100 ms after stimulation ceased in wild type muscles. This observation corroborates previous findings which showed a rapid increase in force with doublet stimulation that can be sustained for long periods up to 250 ms under isometric conditions (Burke et al., 1970; Zajac and Young, 1980; Stein and Parmiggiani, 1981; Hennig and Lømo, 1987; Sandercock and Heckman, 1997; Abbate et al., 2002). Recent work by Bakker et al. (2017) showed that doublet stimulation increases intracellular [Ca^{2+}] for the first 20–30 ms following stimulation. They suggested that the [Ca^{2+}] transient might saturate the second Ca^{2+}-binding site on TnC and lead to faster initiation of cross-bridge cycling, although this hypothesis remains to be tested experimentally. Nevertheless, the proposed increase in rate of cross-bridge cycling *via* saturation of TnC cannot account neither for increased force with doublet stimulation nor for persistence of the potentiated force for up to hundreds of milliseconds (Burke et al., 1976; Sandercock and Heckman, 1997) after the [Ca^{2+}] level has returned to baseline levels (Abbate et al., 2002; Cheng et al., 2013; Bakker et al., 2017). Thus, while the rate of cross-bridge cycling may increase with a transient increase in [Ca^{2+}] and therefore contribute to the rapid increase in force, neither the time constants of Ca^{2+} release and re-uptake nor the saturation of TnC are consistent with the sustained increase in force and work that occurs in response to doublet stimulation.

The increased effect of doublet stimulation during the eccentric phase of an SSC that we observed here matches previous work demonstrating that stretch of a muscle during doublet stimulation

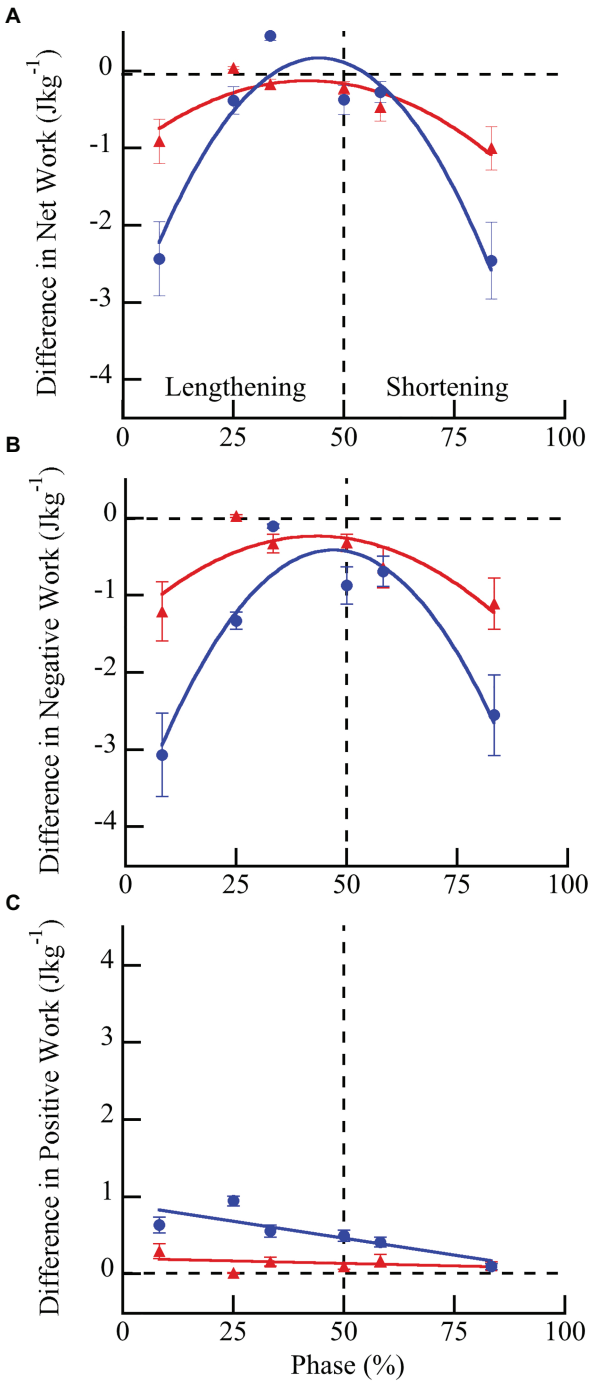

FIGURE 5 | Differences in net **(A)**, negative **(B)**, and positive **(C)** work per cycle with vs. without doublet stimulation across phase of activation in wild type (blue) and *mdm* (red) muscles. The greatest increase in work with doublet stimulation occurred when muscles were activated during lengthening and the smallest increase occurred when muscles were activated during shortening. Wild type muscles exhibited a significantly greater increase in net ($F = 43.84$, $p < 0.0001$), negative ($F = 14.51$, $p = 0.007$), and positive ($F = 50.43$, $p < 0.0001$) work than *mdm* muscles across all phases of activation. Phase = 0% indicates a muscle at its shortest length at the onset of lengthening and phase = 50% indicates a muscle at its longest length just prior to shortening. Data represent means ± SE, $N = 28$ individuals, 112 trials.

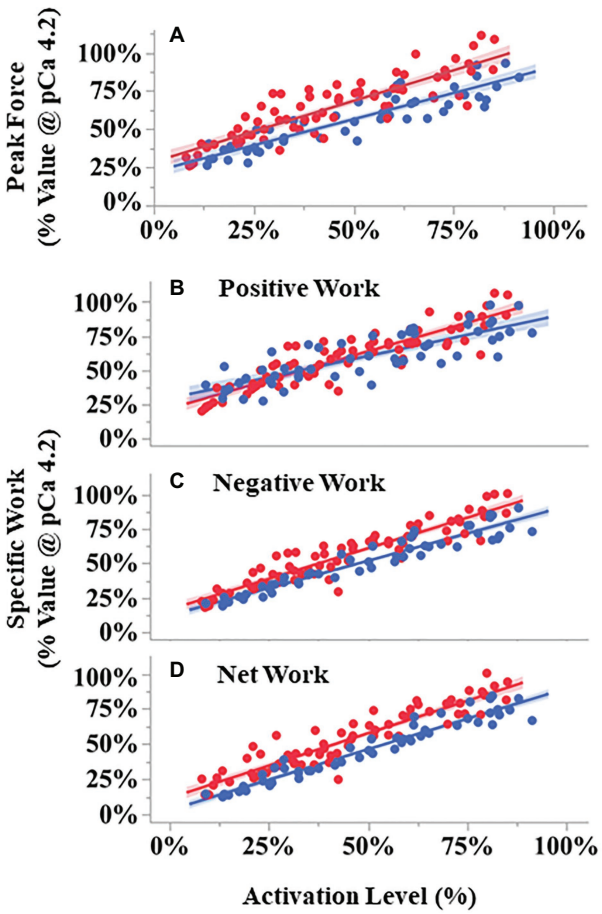

FIGURE 6 | Peak force and work during SSCs vs. activation level for pCa- (blue) and BDM- (red) controlled fibers. All variables scaled linearly with activation level analysis of covariance (ANCOVA covariate effect < 0.001). Peak forces **(A)** were larger in BDM- vs. pCa- controlled trials across activation levels ($p = 0.0014$). Both negative ($p < 0.001$) and total work ($p = 0.014$) components were also larger in BDM vs. pCa controlled fibers. Compared to pCa-controlled trials, BDM-controlled trials had a modest but statistically significant steeper increase with activation level for positive work (**B**, ANCOVA interaction effect, $p = 0.0072$) and negative work (**C**, $p = 0.031$), but not for net work (**D**, $p = 0.16$). The 95% CIs are shown by the shaded regions around the lines. $N = 15$ pCa and 16 BDM experiments, $n = 52$ pCa and 76 BDM trials.

enhances force, whereas shortening abolishes the doublet effect (Sandercock and Heckman, 1997). Isometric studies have also shown that doublet potentiation is greatest at short muscle lengths on the ascending limb of the length-tension relationship and decreases as muscle length increases (Burke et al., 1976; Sandercock and Heckman, 1997). In addition, Stevens (1996) showed that adding a single doublet stimulus to an SSC can increase net work per cycle by more than 50%. The length-dependence of doublet potentiation is not easily explained by cross bridge models, but instead suggests the engagement of a Ca^{2+}-dependent viscoelastic element (Binder-Macleod and Kesar, 2005) that stores elastic energy during stretch and releases energy during shortening, thereby increasing muscle force and work during eccentric SSCs (Nishikawa et al., 2018).

Interestingly, results from the present study also showed that doublet potentiation is markedly reduced in *mdm* muscles, which are characterized by a small deletion in the N2A region of titin (Garvey et al., 2002). The difference between wild type and *mdm* muscles was greatest when the muscles were activated during lengthening, where doublets increased negative, positive, and net work per cycle in wild type but not *mdm* soleus. These observations are consistent with other studies on *mdm* muscles, which demonstrated reduced force enhancement during active stretch and reduced force depression with active shortening (Tahir et al., 2020), as well as reduced net work during eccentric SSCs (Hessel and Nishikawa, 2017).

To our knowledge, this study is the first to test the hypothesis that titin contributes to doublet potentiation. Previous studies have suggested a role for elastic elements other than cross bridges (Stein and Parmiggiani, 1981; Sandercock and Heckman, 1997; Binder-Macleod and Kesar, 2005), but the mechanism for doublet potentiation remains unclear. Doublet potentiation is similar to "catch" in molluscan muscles, in that force is maintained for hours at low [Ca^{2+}] (Butler and Siegman, 2010). The mechanism for molluscan catch has been shown to involve binding of twitchin, a giant sarcomeric protein related to titin, to thin filaments (Butler and Siegman, 2010), similar to N2A titin-actin binding which is thought to be responsible for titin activation (Dutta et al., 2018; Nishikawa, 2020). The addition of a doublet at the onset of a submaximal stimulus train causes a transient increase in [Ca^{2+}], which likely increases in titin-actin binding in addition to cross bridge formation. However, once [Ca^{2+}] returns to baseline levels between stimuli (~25 ms), cross bridges release but force remains elevated due to the much slower off rates (~200 ms) of titin-actin interactions (Dutta et al., 2018). At a cycle frequency of 5 Hz, titin would be expected to remain bound to actin for the entire duration of an SSC. How titin contributes to doublet potentiation of force during isometric contractions remains unclear because activation increases titin stiffness, thus strain is required to increase titin force. Hypotheses including titin winding on actin (Nishikawa et al., 2012) or a "sticky spring" (Rode et al., 2009) could potentially explain how titin contributes to force of isometrically contracting muscle but future work is needed.

This study is also the first to test the hypothesis that titin contributes to the phase-dependence of activation. When activated at its shortest length followed by stretch-shortening, a muscle behaves like a spring in which elastic energy stored during stretch enhances work during shortening. However, when activated at its longest length followed by shortening-stretch, a muscle behaves like a motor which produces positive work (Ahn, 2012). During *in vivo* movements, the phase-dependence of activation serves the important function of allowing a muscle to function in different ways for different tasks (Dickinson et al., 2000). The observation that the phase dependence of activation is reduced in skeletal muscles from *mdm* mice suggests a contribution for titin. We suggest that binding of N2A titin to actin at different muscle lengths depending on the phase of activation is a mechanism of phase-dependence. Titin-actin binding is thought to decrease titin free length and increase titin stiffness (Dutta et al., 2018; Nishikawa et al., 2019). Binding of titin to actin at differing distances from the Z-disk would have the effect of enhancing both the spring-like and motor-like properties of muscles depending on the phase of activation.

Permeabilized Fiber Experiments

Using permeabilized fiber preparations and the myosin inhibitor BDM, we decoupled the relationships among [Ca^{2+}], cross bridge formation, and force production by activating fibers at supramaximal [Ca^{2+}] (pCa 4.2) but with reduced cross-bridge forces (Griffiths et al., 2006). We found that peak force, net work, and negative work (**Figure 6**) were greater in BDM compared to pCa-controlled fiber bundles at a given level of activation.

Early studies found that BDM decreased isometric force more than isometric stiffness. Using permeabilized rabbit psoas fibers, Seow et al. (1997) first reported that treatment with 3 mM BDM increased the stiffness to force ratio by 50%. The increased stiffness to force ratio was thought to be caused by an increase in the number of low-force (i.e., weakly bound) cross bridges that would contribute to stiffness but not active force (Bagni et al., 1992; Seow et al., 1997). However, subsequent analyses (Bagni et al., 1992, 2005; Griffiths et al., 2006) of the effects of BDM on thick and thin filament structure found that the fraction of attached cross bridges is similar between pCa- and BDM-controlled fibers at a given force. Therefore, the BDM-induced increase in the stiffness to force ratio has instead been attributed to the existence of Ca^{2+}-sensitive, non-cross bridge viscoelastic elements (Griffiths et al., 2006; Colombini et al., 2016). BDM has also been used previously to investigate residual force enhancement after isovelocity stretch (Rassier and Herzog, 2005a,b). Using BDM to decrease active force, Rassier and Herzog (2005b) found that a 50% decrease in active force led to only a 15% drop in fiber stiffness and a non-statistically significant drop in the absolute residual force enhancement. These observations are also consistent with the existence of a Ca^{2+}-sensitive, non-cross bridge, viscoelastic element that contributes to force enhancement after stretch.

One feature of SSCs is that the magnitude of peak force is positively related to force and work during the subsequent shortening phase (Seiberl et al., 2015b; Fortuna et al., 2017; Hahn and Riedel, 2018; Fukutani and Herzog, 2020a,b). A recent study (Fukutani and Herzog, 2020b) used permeabilized rabbit fibers to compare SSC mechanics between maximally activated fibers at pCa = 4.2 with or without 10 mM BDM, reducing the activation level by ~ 50%. The results showed that positive work produced during the shortening phase of SSCs was relatively larger in BDM-treated fibers, increasing from 169% of the isovelocity shortening work in 0 mM BDM to 205% in 10 mM BDM. In our study, we tested the effect of BDM on positive work during shortening across a range of activation levels from 15 to 100% maximum activation. We found that compared to pCa-controlled fibers, BDM treatment increased relative positive work only at high activation levels (>50% of the maximal isometric force). At low activation levels (<25% of maximal isometric force),

positive work of BDM-treated fibers was slightly less than for pCa-controlled fibers (**Figure 6B**).

An often neglected feature of SSCs is the history-dependent property that peak force (**Supplementary Figure S1**) is greater during the first repetition in a series of multiple SSCs (see our **Figure 2**; Campbell and Moss, 2002). This property, called thixotropy (see review by Lakie and Campbell, 2019), is enhanced at lower activation levels and leads to changes in fiber stiffness over time during multiple SSCs. In a series of two consecutive SSCs in single fibers, Campbell and Moss (2002) found that fibers were more compliant during the second stretch phase than the first. However, if a delay was introduced between the two SSCs, then the fibers recovered a portion of their initial stiffness for the second SSC. For delays >1 s, fiber stiffness became identical between the two SSCs (Campbell and Moss, 2002). They also found that fiber stiffness during the shortening phase was less dependent on length history than during the lengthening phase. The time-dependent thixotropy of fibers during SSCs was not readily predicted by cross bridge models without the addition of a Ca^{2+}-dependent parallel elastic element (Campbell and Moss, 2002).

While it is difficult to separate the contributions of cross bridge and non-cross bridge elements to force production during isometric contraction, Pinniger et al. (2006) conducted a clever set of experiments and used a cross bridge model to distinguish the relative contributions of cross bridge and non-cross bridge elastic elements to muscle force during stretch. They concluded that, after a small stretch of ~1.25–1.5% L_0, the cross bridge contribution to force enhancement reaches a maximum value, as new detachment/attachment equilibrium is reached. During length changes >1.5% L_0, force enhancement must be provided by non-cross bridge elements. Thus, the relative contribution of non-cross bridge elements increases with increasing stretch amplitude. During the SSC experiments reported here, we used strain amplitudes of 10% in whole muscles and 15% L_0 in fiber preparations. By extrapolating from Pinniger et al. (2006), the force contribution of non-cross bridge elements is expected to be ~60 and ~70% of the total force rise for whole muscles and permeabilized fibers, respectively. However, these calculations are based on maximally activated fibers, where the number of cross bridges is maximized. The calculation therefore overestimates the contribution of cross bridges for the submaximal activation levels used in our SSC experiments. For example, at an activation level of 50%, the contribution of cross bridges to peak force would be reduced by half, suggesting that cross bridges might contribute as little as 15 or 20% to peak force in SSCs for permeabilized fibers or whole muscles, respectively.

Titin as a Tunable Viscoelastic Element in Muscle Sarcomeres

Over the past 20 years, mounting evidence has suggested the existence of a Ca^{2+}-sensitive, non-cross bridge, viscoelastic element in muscle sarcomeres. This element is engaged in the earliest stages of muscle activation at [Ca^{2+}] levels below those required to activate thin filaments and permit cross bridge interactions (Bagni et al., 1994, 2002; Colombini et al., 2016). Single myofibril studies also demonstrate that the increase in stiffness with activation following active stretch persists for up to several minutes following deactivation (Joumaa et al., 2007, 2008). Recent estimates suggests that the Ca^{2+}-sensitive non-cross bridge stiffness is 100 times greater than the passive stiffness in isometrically contracting single fibers (Powers et al., 2019). In their study, Powers et al. (2019) used high-frequency length oscillations (4 kHz) in isometrically contracting single muscle fibers to measure fiber stiffness, and found that the I-band stiffness increased by two orders of magnitude in isometrically contracting fibers compared to the passive stiffness of the same fibers at a sarcomere length of 2.7 μm SL.

Accumulating evidence further suggests that the giant sarcomeric titin protein is a Ca^{2+}-sensitive, non-cross bridge, viscoelastic element, which functions as a tunable spring in active muscle (Leonard and Herzog, 2010; Nishikawa et al., 2012; Herzog, 2019; Nishikawa, 2020). Numerous recent studies support the hypothesis that N2A titin is a signaling hub and mechanical linker that binds to actin in the presence of Ca^{2+} (Nishikawa et al., 2020), thereby decreasing titin's free length and increasing its stiffness (Dutta et al., 2018; Nishikawa et al., 2019, 2020; Nishikawa, 2020). Single molecule force spectroscopy experiments demonstrate that N2A-actin interactions are highly stable in the presence of Ca^{2+} (pCa < 5.0), and the off-rate is more than three times slower (4 v. 16 s^{-1}) when Ca^{2+} is present (Dutta et al., 2018). Binding of N2A titin to actin brings the titin molecule closer to actin, which may increase the likelihood of hydrostatic interactions between PEVK titin and actin as well. PEVK interactions with actin resist stretch long after Ca^{2+} has decreased (Bianco et al., 2007).

The *mdm* mouse model is unique in exhibiting a small deletion in the N2A region of titin (Garvey et al., 2002). This region appears to be critical for mediating the Ca^{2+}-dependent increase in titin stiffness that occurs upon muscle activation (Nishikawa, 2020; Nishikawa et al., 2020). Numerous studies demonstrate that active stiffness is reduced in muscles from *mdm* mice (Powers et al., 2016; Monroy et al., 2017). These muscles also exhibit reduced force enhancement following active stretch and reduced force depression following active shortening (Tahir et al., 2020), suggesting a role for titin in these history-dependent properties.

Limitations

As is common practice, experiments were conducted at room temperature (25 and 21°C for whole muscle and fiber experiments, respectively) rather than body temperature (37°C) to reduce fatigue and fiber degradation (Hakim et al., 2013). Although muscle mechanics are altered by temperature (Stephenson and Williams, 1981, 1985; James et al., 2015; Ranatunga, 2018; Caremani et al., 2021), the effect is expected to be relatively small (~10%).

2,3-butanedione monoxime is only one way to inhibit cross bridge interactions, with other approaches including the use of different inhibitors such as N-benzyl-p-toluene sulphonamide (BTS; Pinniger et al., 2005), or chemical

removal of troponin C (Joumaa et al., 2008). Because each method has its own limitations, it is important to repeat these fiber experiments with other cross-bridge inhibitors to compare with data from this study.

Conclusion

The results from both whole muscle and permeabilized fibers in SSC experiments suggest the existence of a tunable viscoelastic element that enhances muscle force and stores strain energy during active stretch, and recovers stored energy during subsequent shortening to increase positive and net work per cycle. A tunable viscoelastic element such as titin can account for: (1) the persistence of force at low [Ca^{2+}] with doublet potentiation; the phase- and length- and phase-dependence of doublet potentiation observed in whole wild type muscles and the absence of these effects in *mdm* muscles; and lastly, the increased peak force and work per cycle in both whole muscles and permeabilized fibers in SSC experiments. While it has been suggested that other non-cross bridge elements, such as nebulin (Kawai et al., 2018), microtubules (Kerr et al., 2015), and myosin binding protein C (Harris, 2021), may increase muscle stiffness during activation, no studies have demonstrated definitive mechanisms that could help to explain the increase in muscle force and work during dynamic length changes. So far, titin is the only known non-cross bridge viscoelastic element in muscle sarcomeres that has been shown to interact with Ca^{2+} and actin.

By combining SSC experiments in whole muscles and permeabilized fibers, we gain a better understanding of the Ca^{2+}-dependent viscoelastic elements that contribute to the mechanical properties exhibited by active muscles during dynamic changes in length. Whole muscle studies have the advantage of simulating *in vivo* muscle activation and length changes, whereas in fiber preparations, we can quantify the relative contributions of cross bridge and non-cross bridge elements to dynamic force during SSCs. Both preparations showed an increase in peak force and work per cycle with increasing activation (adding a doublet in whole muscle experiments and decreasing pCa in permeabilized fibers), which was enhanced during lengthening contractions. It is important to point out that phase dependence could only be measured in whole muscle studies since muscles were activated with a duty cycle of 0.5, whereas fibers were activated with a duty cycle of 100% throughout the entire SSC protocol. Thus, work loops from fiber preparations more closely resembled eccentric work loops of whole muscles. Form these studies, it appears that perturbing activation in SSCs provides an experimental paradigm for quantifying the contributions of calcium-sensitive non-cross bridge viscoelastic elements to muscle force during dynamic length changes.

DATA AVAILABILITY STATEMENT

The raw data supporting the conclusions of this article will be made available by the authors, without undue reservation.

ETHICS STATEMENT

The animal study was reviewed and approved by the Institutional Animal Care and Use Committees of Northern Arizona University (NAU IACUC Protocol #18-002), the Claremont Colleges (CC IACUC Protocol #017-003), and the University Clinic Muenster (LANUV NRW, 81-02.04.2019.A472).

AUTHOR CONTRIBUTIONS

JM and AH contributed equally to this work and were responsible for data collection and analysis. JM, AH, and KN all contributed to the conception and design of the experiments and interpretation of the data. All authors contributed to the article and approved the submitted version.

FUNDING

The authors gratefully acknowledge financial support from the National Science Foundation (IOS-1731917 awarded to JM, IOS-2016049 awarded to KN).

ACKNOWLEDGMENTS

Dr. WA Linke (University of Muenster) provided mouse muscles and research facilities for the fiber study. D. Enright assisted in data collection from whole muscles. A. Good provided critical text editing.

SUPPLEMENTARY MATERIAL

The Supplementary Material for this article can be found online at: https://www.frontiersin.org/articles/10.3389/fphys.2021.648019/full#supplementary-material

REFERENCES

Abbate, F., Bruton, J. D., De Haan, A., and Westerblad, H. (2002). Prolonged force increase following a high-frequency burst is not due to a sustained elevation of [Ca^{2+}]i. *Am. J. Phys. Cell Physiol.* 283, C42–C47. doi: 10.1152/ajpcell.00416.2001

Abbott, B. C., and Aubert, X. M. (1952). The force exerted by active striated muscle during and after change of length. *J. Physiol.* 117, 77–86.

Ahn, A. N. (2012). How muscles function—the work loop technique. *J. Exp. Biol.* 215, 1051–1052. doi: 10.1242/jeb.062752

Askew, G. N., and Marsh, R. L. (1997). The effects of length trajectory on the mechanical power output of mouse skeletal muscles. *J. Exp. Biol.* 200, 3119–3131.

Askew, G. N., and Marsh, R. L. (1998). Optimal shortening velocity (V/Vmax) of skeletal muscle during cyclical contractions: length-force effects and velocity-dependent activation and deactivation. *J. Exp. Biol.* 201, 1527–1540.

Bagni, M. A., Cecchi, G., Colombini, B., and Colomo, F. (2002). A non-cross-bridge stiffness in activated frog muscle fibers. *Biophys. J.* 82, 3118–3127. doi: 10.1016/S0006-3495(02)75653-1

Bagni, M. A., Cecchi, G., Colomo, F., and Garzella, P. (1992). Effects of 2,3-butanedione monoxime on the crossbridge kinetics in frog single muscle fibres. *J. Muscle Res. Cell Motil.* 13, 516–522. doi: 10.1007/BF01737994

Bagni, M. A., Cecchi, G., Colomo, F., and Garzella, P. (1994). Development of stiffness precedes cross-bridge attachment during the early tension rise in single frog muscle fibres. *J. Physiol.* 481, 273–278. doi: 10.1113/jphysiol.1994.sp020437

Bagni, M. A., Colombini, B., Colomo, F., Berlinguer Palmini, R., and Cecchi, G. (2005). Non cross-bridge stiffness in skeletal muscle fibres at rest and during activity. *Adv. Exp. Med. Biol.* 565, 141–154. doi: 10.1007/0-387-24990-7_11

Bakker, A. J., Cully, T. R., Wingate, C. D., Barclay, C. J., and Launikonis, B. S. (2017). Doublet stimulation increases Ca^{2+} binding to troponin C to ensure rapid force development in skeletal muscle. *J. Gen. Physiol.* 149, 323–334. doi: 10.1085/jgp.201611727

Bang, M. L., Centner, T., Fornoff, F., Geach, A. J., Gotthardt, M., McNabb, M., et al. (2001). The complete gene sequence of titin, expression of an unusual approximately 700-kDa titin isoform, and its interaction with obscurin identify a novel Z-line to I-band linking system. *Circ. Res.* 89, 1065–1072. doi: 10.1161/hh2301.100981

Bianco, P., Nagy, A., Kengyel, A., Szatmári, D., Mártonfalvi, Z., Huber, T., et al. (2007). Interaction forces between F-actin and titin PEVK domain measured with optical tweezers. *Biophys. J.* 93, 2102–2109. doi: 10.1529/biophysj.107.106153

Binder-Macleod, S., and Kesar, T. (2005). Catchlike property of skeletal muscle: recent findings and clinical implications. *Muscle Nerve* 31, 681–693. doi: 10.1002/mus.20290

Burke, R. E., Rudomin, P., and Zajac, F. E. (1970). Catch property in single mammalian motor units. *Science* 168, 122–124. doi: 10.1126/science.168.3927.122

Burke, R. E., Rudomin, P., and Zajac, F. E. (1976). The effect of activation history on tension production by individual muscle units. *Brain Res.* 109, 515–529. doi: 10.1016/0006-8993(76)90031-7

Butler, T. M., and Siegman, M. J. (2010). Mechanism of catch force: tethering of thick and thin filaments by twitchin. *J. Biomed. Biotechnol.* 2010:725207. doi: 10.1155/2010/725207

Campbell, K. S., and Moss, R. L. (2002). History-dependent mechanical properties of permeabilized rat soleus muscle fibers. *Biophys. J.* 82, 929–943. doi: 10.1016/S0006-3495(02)75454-4

Caremani, M., Fusi, L., Linari, M., Reconditi, M., Piazzesi, G., Irving, T. C., et al. (2021). Dependence of thick filament structure in relaxed mammalian skeletal muscle on temperature and interfilament spacing. *J. Gen. Physiol.* 153:e202012713. doi: 10.1085/jgp.202012713

Chen, J., Hahn, D., and Power, G. A. (2019). Shortening-induced residual force depression in humans. *J. Appl. Physiol.* 126, 1066–1073. doi: 10.1152/japplphysiol.00931.2018

Cheng, A. J., Place, N., Bruton, J. D., Holmberg, H.-C., and Westerblad, H. (2013). Doublet discharge stimulation increases sarcoplasmic reticulum Ca^{2+} release and improves performance during fatiguing contractions in mouse muscle fibres. *J. Physiol.* 591, 3739–3748. doi: 10.1113/jphysiol.2013.257188

Colombini, B., Nocella, M., and Bagni, M. A. (2016). Non-crossbridge stiffness in active muscle fibres. *J. Exp. Biol.* 219, 153–160. doi: 10.1242/jeb.124370

Daley, M. A., and Biewener, A. A. (2011). Leg muscles that mediate stability: mechanics and control of two distal extensor muscles during obstacle negotiation in the Guinea fowl. *Philos. Trans. R. Soc. Lond. Ser. B Biol. Sci.* 366, 1580–1591. doi: 10.1098/rstb.2010.0338

Dick, T. J. M., Biewener, A. A., and Wakeling, J. M. (2017). Comparison of human gastrocnemius forces predicted by hill-type muscle models and estimated from ultrasound images. *J. Exp. Biol.* 220, 1643–1653. doi: 10.1242/jeb.154807

Dickinson, M. H., Farley, C. T., Full, R. J., Koehl, M. A., Kram, R., and Lehman, S. (2000). How animals move: an integrative view. *Science* 288, 100–106. doi: 10.1126/science.288.5463.100

Dutta, S., Tsiros, C., Sundar, S. L., Athar, H., Moore, J., Nelson, B., et al. (2018). Calcium increases titin N2A binding to F-actin and regulated thin filaments. *Sci. Rep.* 8:14575. doi: 10.1038/s41598-018-32952-8

Edman, K. A. (1975). Mechanical deactivation induced by active shortening in isolated muscle fibres of the frog. *J. Physiol.* 246, 255–275. doi: 10.1113/jphysiol.1975.sp010889

Edman, K. A., Elzinga, G., and Noble, M. I. (1982). Residual force enhancement after stretch of contracting frog single muscle fibers. *J. Gen. Physiol.* 80, 769–784. doi: 10.1085/jgp.80.5.769

Fortuna, R., Groeber, M., Seiberl, W., Power, G. A., and Herzog, W. (2017). Shortening-induced force depression is modulated in a time- and speed-dependent manner following a stretch-shortening cycle. *Phys. Rep.* 5:e13279. doi: 10.14814/phy2.13279

Fox, J., and Weisberg, S. (2010). *An R companion to applied regression. 2nd Edn*. Thousand Oaks, Calif: SAGE Publications, Inc.

Fukutani, A., and Herzog, W. (2020a). Differences in stretch-shortening cycle and residual force enhancement between muscles. *J. Biomech.* 112:110040. doi: 10.1016/j.jbiomech.2020.110040

Fukutani, A., and Herzog, W. (2020b). The stretch-shortening cycle effect is prominent in the inhibited force state. *J. Biomech.* 115:110136. doi: 10.1016/j.jbiomech.2020.110136

Garvey, S. M., Rajan, C., Lerner, A. P., Frankel, W. N., and Cox, G. A. (2002). The muscular dystrophy with myositis (mdm) mouse mutation disrupts a skeletal muscle-specific domain of titin. *Genomics* 79, 146–149. doi: 10.1006/geno.2002.6685

Gordon, A. M., Huxley, A. F., and Julian, F. J. (1966). The variation in isometric tension with sarcomere length in vertebrate muscle fibres. *J. Physiol.* 184, 170–192. doi: 10.1113/jphysiol.1966.sp007909

Granzier, H. L., and Irving, T. C. (1995). Passive tension in cardiac muscle: contribution of collagen, titin, microtubules, and intermediate filaments. *Biophys. J.* 68, 1027–1044. doi: 10.1016/S0006-3495(95)80278-X

Griffiths, P. J., Bagni, M. A., Colombini, B., Amenitsch, H., Bernstorff, S., Funari, S., et al. (2006). Effects of the number of actin-bound S1 and axial force on X-ray patterns of intact skeletal muscle. *Biophys. J.* 90, 975–984. doi: 10.1529/biophysj.105.068619

Hahn, D., and Riedel, T. N. (2018). Residual force enhancement contributes to increased performance during stretch-shortening cycles of human plantar flexor muscles in vivo. *J. Biomech.* 77, 190–193. doi: 10.1016/j.jbiomech.2018.06.003

Hakim, C. H., Wasala, N. B., and Duan, D. (2013). Evaluation of muscle function of the extensor digitorum longus muscle ex vivo and tibialis anterior muscle in situ in mice. *J. Vis. Exp.* 50183. doi: 10.3791/50183

Harris, S. P. (2021). Making waves: a proposed new role for myosin-binding protein C in regulating oscillatory contractions in vertebrate striated muscle. *J. Gen. Physiol.* 153:e202012729. doi: 10.1085/jgp.202012729

Heidlauf, T., Klotz, T., Rode, C., Siebert, T., and Röhrle, O. (2017). A continuum-mechanical skeletal muscle model including actin-titin interaction predicts stable contractions on the descending limb of the force-length relation. *PLoS Comput. Biol.* 13:e1005773. doi: 10.1371/journal.pcbi.1005773

Hennig, R., and Lømo, T. (1987). Gradation of force output in normal fast and slow muscles of the rat. *Acta Physiol. Scand.* 130, 133–142. doi: 10.1111/j.1748-1716.1987.tb08119.x

Herzog, W. (2018). The multiple roles of titin in muscle contraction and force production. *Biophys. Rev.* 10, 1187–1199. doi: 10.1007/s12551-017-0395-y

Herzog, W. (2019). The problem with skeletal muscle series elasticity. *BMC Biomed. Eng.* 1:28. doi: 10.1186/s42490-019-0031-y

Hessel, A. L., Joumaa, V., Eck, S., Herzog, W., and Nishikawa, K. C. (2019). Optimal length, calcium sensitivity and twitch characteristics of skeletal muscles from mdm mice with a deletion in N2A titin. *J. Exp. Biol.* 222:jeb200840. doi: 10.1242/jeb.200840

Hessel, A. L., and Nishikawa, K. C. (2017). Effects of a titin mutation on negative work during stretch-shortening cycles in skeletal muscles. *J. Exp. Biol.* 220, 4177–4185. doi: 10.1242/jeb.163204

Horowits, R., Kempner, E. S., Bisher, M. E., and Podolsky, R. J. (1986). A physiological role for titin and nebulin in skeletal muscle. *Nature* 323, 160–164. doi: 10.1038/323160a0

Huxley, H. E. (1957). The double array of filaments in cross-striated muscle. *J. Biophys. Biochem. Cytol.* 3, 631–648. doi: 10.1083/jcb.3.5.631

Huxley, H., and Hanson, J. (1954). Changes in the cross-striations of muscle during contraction and stretch and their structural interpretation. *Nature* 173, 973–976. doi: 10.1038/173973a0

Huxley, A. F., and Niedergerke, R. (1954). Structural changes in muscle during contraction; interference microscopy of living muscle fibres. *Nature* 173, 971–973. doi: 10.1038/173971a0

James, R. S., Altringham, J. D., and Goldspink, D. F. (1995). The mechanical properties of fast and slow skeletal muscles of the mouse in relation to their locomotory function. *J. Exp. Biol.* 198, 491–502.

James, R. S., Tallis, J., and Angilletta, M. J. (2015). Regional thermal specialisation in a mammal: temperature affects power output of core muscle more than that of peripheral muscle in adult mice (*Mus musculus*). *J. Comp. Physiol. B, Biochem. Syst. Environ. Physiol.* 185, 135–142. doi: 10.1007/s00360-014-0872-6

Joumaa, V., Rassier, D. E., Leonard, T. R., and Herzog, W. (2007). Passive force enhancement in single myofibrils. *Pflugers Arch.* 455, 367–371. doi: 10.1007/s00424-007-0287-2

Joumaa, V., Rassier, D. E., Leonard, T. R., and Herzog, W. (2008). The origin of passive force enhancement in skeletal muscle. *Am. J. Phys. Cell Physiol.* 294, C74–C78. doi: 10.1152/ajpcell.00218.2007

Kawai, M., Karam, T. S., Kolb, J., Wang, L., and Granzier, H. L. (2018). Nebulin increases thin filament stiffness and force per cross-bridge in slow-twitch soleus muscle fibers. *J. Gen. Physiol.* 150, 1510–1522. doi: 10.1085/jgp.201812104

Kerr, J. P., Robison, P., Shi, G., Bogush, A. I., Kempema, A. M., Hexum, J. K., et al. (2015). Detyrosinated microtubules modulate mechanotransduction in heart and skeletal muscle. *Nat. Commun.* 6:8526. doi: 10.1038/ncomms9526

Kuhn, T. S. (1962). *The structure of scientific revolutions*. Chicago, USA: University of Chicago Press.

Lakie, M., and Campbell, K. S. (2019). Muscle thixotropy-where are we now? *J. Appl. Physiol.* 126, 1790–1799. doi: 10.1152/japplphysiol.00788.2018

Lee, S. S. M., Arnold, A. S., de Boef Miara, M., Biewener, A. A., and Wakeling, J. M. (2013). Accuracy of gastrocnemius muscles forces in walking and running goats predicted by one-element and two-element hill-type models. *J. Biomech.* 46, 2288–2295. doi: 10.1016/j.jbiomech.2013.06.001

Leonard, T. R., and Herzog, W. (2010). Regulation of muscle force in the absence of actin-myosin-based cross-bridge interaction. *Am. J. Phys. Cell Physiol.* 299, C14–C20. doi: 10.1152/ajpcell.00049.2010

Li, Y., Hessel, A. L., Unger, A., Ing, D., Recker, J., Koser, F., et al. (2020). Graded titin cleavage progressively reduces tension and uncovers the source of A-band stability in contracting muscle. *elife* 9:e64107. doi: 10.7554/eLife.64107

Linari, M., Woledge, R. C., and Curtin, N. A. (2003). Energy storage during stretch of active single fibres from frog skeletal muscle. *J. Physiol.* 548, 461–474. doi: 10.1113/jphysiol.2002.032185

Linke, W. A. (2018). Titin gene and protein functions in passive and active muscle. *Annu. Rev. Physiol.* 80, 389–411. doi: 10.1146/annurev-physiol-021317-121234

Linke, W. A., Ivemeyer, M., Mundel, P., Stockmeier, M. R., and Kolmerer, B. (1998a). Nature of PEVK-titin elasticity in skeletal muscle. *Proc. Natl. Acad. Sci. U. S. A.* 95, 8052–8057. doi: 10.1073/pnas.95.14.8052

Linke, W. A., Stockmeier, M. R., Ivemeyer, M., Hosser, H., and Mundel, P. (1998b). Characterizing titin's I-band Ig domain region as an entropic spring. *J. Cell Sci.* 111, 1567–1574.

Lopez, M. A., Pardo, P. S., Cox, G. A., and Boriek, A. M. (2008). Early mechanical dysfunction of the diaphragm in the muscular dystrophy with myositis (Ttnmdm) model. *Am. J. Phys. Cell Physiol.* 295, C1092–C1102. doi: 10.1093/icb/icr008

Monroy, J. A., Powers, K. A., Gilmore, L. A., Uyeno, T. A., and Nishikawa, K. C. (2012). Ca^{2+}–activation of skeletal muscle: not just the thin filament? *Integr. Comp. Biol.* 52:E94.

Monroy, J. A., Powers, K. A., Gilmore, L. A., Uyeno, T., and Nishikawa, K. C. (2017). Effects of activation on the elastic properties of intact soleus muscles with a deletion in titin. *J. Exp. Biol.* 220, 828–836. doi: 10.1242/jeb.139717

Nishikawa, K. (2016). Eccentric contraction: unraveling mechanisms of force enhancement and energy conservation. *J. Exp. Biol.* 219, 189–196. doi: 10.1242/jeb.124057

Nishikawa, K. C. (2018). Muscle function from oraganisms to molecules. *Integr. Comp. Biol.* 58, 194–206. doi: 10.1093/icb/icy023

Nishikawa, K. (2020). Titin: a tunable spring in active muscle. *Physiology* 35, 209–217. doi: 10.1152/physiol.00036.2019

Nishikawa, K., Dutta, S., DuVall, M., Nelson, B., Gage, M. J., and Monroy, J. A. (2019). Calcium-dependent titin–thin filament interactions in muscle: observations and theory. *J. Muscle Res. Cell Motil.* 41, 125–139. doi: 10.1007/s10974-019-09540-y

Nishikawa, K., Lindstedt, S. L., Hessel, A., and Mishra, D. (2020). N2A Titin: signaling hub and mechanical switch in skeletal muscle. *Int. J. Mol. Sci.* 21:3974. doi: 10.3390/ijms21113974

Nishikawa, K. C., Lindstedt, S. L., and LaStayo, P. C. (2018). Basic science and clinical use of eccentric contractions: history and uncertainties. *J. Sport Health Sci.* 7, 265–274. doi: 10.1016/j.jshs.2018.06.002

Nishikawa, K. C., Monroy, J. A., Powers, K. L., Gilmore, L. A., Uyeno, T. A., and Lindstedt, S. L. (2013). A molecular basis for intrinsic muscle properties: implications for motor control. *Adv. Exp. Med. Biol.* 782, 111–125. doi: 10.1007/978-1-4614-5465-6_6

Nishikawa, K. C., Monroy, J. A., Uyeno, T. E., Yeo, S. H., Pai, D. K., and Lindstedt, S. L. (2012). Is titin a "winding filament"? A new twist on muscle contraction. *Proc. Biol. Sci.* 279, 981–990. doi: 10.1098/rspb.2011.1304

Nocella, M., Cecchi, G., Bagni, M. A., and Colombini, B. (2014). Force enhancement after stretch in mammalian muscle fiber: no evidence of cross-bridge involvement. *Am. J. Phys. Cell Physiol.* 307, C1123–C1129. doi: 10.1152/ajpcell.00290.2014

Parmiggiani, F., and Stein, R. B. (1981). Nonlinear summation of contractions in cat muscles. II. Later facilitation and stiffness changes. *J. Gen. Physiol.* 78, 295–311. doi: 10.1085/jgp.78.3.295

Paternoster, F. K., Seiberl, W., Hahn, D., and Schwirtz, A. (2016). Residual force enhancement during multi-joint leg extensions at joint- angle configurations close to natural human motion. *J. Biomech.* 49, 773–779. doi: 10.1016/j.jbiomech.2016.02.015

Pinniger, G. J., Bruton, J. D., Westerblad, H., and Ranatunga, K. W. (2005). Effects of a myosin-II inhibitor (N-benzyl-p-toluene sulphonamide, BTS) on contractile characteristics of intact fast-twitch mammalian muscle fibres. *J. Muscle Res. Cell Motil.* 26, 135–141. doi: 10.1007/s10974-005-2679-2

Pinniger, G. J., Ranatunga, K. W., and Offer, G. W. (2006). Crossbridge and non-crossbridge contributions to tension in lengthening rat muscle: force-induced reversal of the power stroke. *J. Physiol.* 573, 627–643. doi: 10.1113/jphysiol.2005.095448

Powers, J. D., Bianco, P., Pertici, I., Reconditi, M., Lombardi, V., and Piazzesi, G. (2019). Contracting striated muscle has a dynamic I-band spring with an undamped stiffness one hundred times larger than the passive stiffness. *J. Physiol.* 598, 331–345. doi: 10.1113/JP278713

Powers, K., Nishikawa, K., Joumaa, V., and Herzog, W. (2016). Decreased force enhancement in skeletal muscle sarcomeres with a deletion in titin. *J. Exp. Biol.* 219, 1311–1316. doi: 10.1242/jeb.132027

Ranatunga, K. W. (2018). Temperature effects on force and actin−myosin interaction in muscle: a look back on some experimental findings. *Int. J. Mol. Sci.* 19:1538. doi: 10.3390/ijms19051538

Rassier, D. E., and Herzog, W. (2005a). Force enhancement and relaxation rates after stretch of activated muscle fibres. *Proc. Biol. Sci.* 272, 475–480. doi: 10.1098/rspb.2004.2967

Rassier, D. E., and Herzog, W. (2005b). Relationship between force and stiffness in muscle fibers after stretch. *J. Appl. Physiol.* 99, 1769–1775. doi: 10.1152/japplphysiol.00010.2005

Rivas-Pardo, J. A., Li, Y., Mártonfalvi, Z., Tapia-Rojo, R., Unger, A., Fernández-Trasancos, Á., et al. (2020). A HaloTag-TEV genetic cassette for mechanical phenotyping of proteins from tissues. *Nat. Commun.* 11:2060. doi: 10.1038/s41467-020-15465-9

Rode, C., Siebert, T., and Blickhan, R. (2009). Titin-induced force enhancement and force depression: a "sticky-spring" mechanism in muscle contractions? *J. Theor. Biol.* 259, 350–360. doi: 10.1016/j.jtbi.2009.03.015

Sandercock, T. G., and Heckman, C. J. (1997). Doublet potentiation during eccentric and concentric contractions of cat soleus muscle. *J. Appl. Physiol.* 82, 1219–1228. doi: 10.1152/jappl.1997.82.4.1219

Seiberl, W., Paternoster, F., Achatz, F., Schwirtz, A., and Hahn, D. (2013). On the relevance of residual force enhancement for everyday human movement. *J. Biomech.* 46, 1996–2001. doi: 10.1016/j.jbiomech.2013.06.014

Seiberl, W., Power, G. A., and Hahn, D. (2015a). Residual force enhancement in humans: current evidence and unresolved issues. *J. Electromyogr. Kinesiol.* 25, 571–580. doi: 10.1016/j.jelekin.2015.04.011

Seiberl, W., Power, G. A., Herzog, W., and Hahn, D. (2015b). The stretch-shortening cycle (SSC) revisited: residual force enhancement contributes to increased performance during fast SSCs of human m. adductor pollicis. *Phys. Rep.* 3:e12401. doi: 10.14814/phy2.12401

Seow, C. Y., Shroff, S. G., and Ford, L. E. (1997). Detachment of low-force bridges contributes to the rapid tension transients of skinned rabbit skeletal muscle fibres. *J. Physiol.* 501, 149–164. doi: 10.1111/j.1469-7793.1997.149bo.x

Siebert, T., Rode, C., Herzog, W., Till, O., and Blickhan, R. (2008). Nonlinearities make a difference: comparison of two common hill-type models with real muscle. *Biol. Cybern.* 98, 133–143. doi: 10.1007/s00422-007-0197-6

Stein, R. B., and Parmiggiani, F. (1981). Nonlinear summation of contractions in cat muscles. I. Early depression. *J. Gen. Physiol.* 78, 277–293. doi: 10.1085/jgp.78.3.277

Stephenson, D. G., and Williams, D. A. (1981). Calcium-activated force responses in fast- and slow-twitch skinned muscle fibres of the rat at different temperatures. *J. Physiol. Lond.* 317, 281–302. doi: 10.1113/jphysiol.1981.sp013825

Stephenson, D. G., and Williams, D. A. (1985). Temperature-dependent calcium sensitivity changes in skinned muscle fibres of rat and toad. *J. Physiol.* 360, 1–12. doi: 10.1113/jphysiol.1985.sp015600

Stevens, E. D. (1996). Effect of phase of stimulation on acute damage caused by eccentric contractions in mouse soleus muscle. *J. Appl. Physiol.* 80, 1958–1962. doi: 10.1152/jappl.1996.80.6.1958

Tahir, U., Monroy, J. A., Rice, N. A., and Nishikawa, K. C. (2020). Effects of a titin mutation on force enhancement and force depression in mouse soleus muscles. *J. Exp. Biol.* 223:jeb197038. doi: 10.1242/jeb.197038

Taylor-Burt, K. R., Monroy, J., Pace, C., Lindstedt, S., and Nishikawa, K. C. (2015). Shiver me titin! Elucidating titin's role in shivering thermogenesis. *J. Exp. Biol.* 218, 694–702. doi: 10.1242/jeb.111849

Tsuchiya, T., and Sugi, H. (1988). Muscle stiffness changes during enhancement and deficit of isometric force in response to slow length changes. *Adv. Exp. Med. Biol.* 226, 503–511.

Zajac, F. E., and Young, J. L. (1980). Properties of stimulus trains producing maximum tension-time area per pulse from single motor units in medial gastrocnemiu muscle of the cat. *J. Neurophysiol.* 43, 1206–1220. doi: 10.1152/jn.1980.43.5.1206

Conflict of Interest: The authors declare that the research was conducted in the absence of any commercial or financial relationships that could be construed as a potential conflict of interest.

frontiers in Physiology

ORIGINAL RESEARCH
published: 31 March 2021
doi: 10.3389/fphys.2021.644981

Power Amplification Increases With Contraction Velocity During Stretch-Shortening Cycles of Skinned Muscle Fibers

André Tomalka[1], Sven Weidner[1], Daniel Hahn[2,3], Wolfgang Seiberl[4] and Tobias Siebert[1,5]*

[1] Department of Motion and Exercise Science, University of Stuttgart, Stuttgart, Germany, [2] Human Movement Science, Faculty of Sports Science, Ruhr University Bochum, Bochum, Germany, [3] School of Human Movement and Nutrition Sciences, University of Queensland, Brisbane, QLD, Australia, [4] Human Movement Science, Bundeswehr University Munich, Neubiberg, Germany, [5] Stuttgart Center for Simulation Science, University of Stuttgart, Stuttgart, Germany

Muscle force, work, and power output during concentric contractions (active muscle shortening) are increased immediately following an eccentric contraction (active muscle lengthening). This increase in performance is known as the stretch-shortening cycle (SSC)-effect. Recent findings demonstrate that the SSC-effect is present in the sarcomere itself. More recently, it has been suggested that cross-bridge (XB) kinetics and non-cross-bridge (non-XB) structures (e.g., titin and nebulin) contribute to the SSC-effect. As XBs and non-XB structures are characterized by a velocity dependence, we investigated the impact of stretch-shortening velocity on the SSC-effect. Accordingly, we performed *in vitro* isovelocity ramp experiments with varying ramp velocities (30, 60, and 85% of maximum contraction velocity for both stretch and shortening) and constant stretch-shortening magnitudes (17% of the optimum sarcomere length) using single skinned fibers of rat soleus muscles. The different contributions of XB and non-XB structures to force production were identified using the XB-inhibitor Blebbistatin. We show that (i) the SSC-effect is velocity-dependent—since the power output increases with increasing SSC-velocity. (ii) The energy recovery (ratio of elastic energy storage and release in the SSC) is higher in the Blebbistatin condition compared with the control condition. The stored and released energy in the Blebbistatin condition can be explained by the viscoelastic properties of the non-XB structure titin. Consequently, our experimental findings suggest that the energy stored in titin during the eccentric phase contributes to the SSC-effect in a velocity-dependent manner.

Keywords: contractile behavior, muscle stretch, muscle shortening, muscle damping, mechanical power, performance enhancement, eccentric contractions

OPEN ACCESS

Edited by:
Kenneth Scott Campbell, University of Kentucky, United States

Reviewed by:
Alf Mansson, Linnaeus University, Sweden
Marco Caremani, University of Florence, Italy
Kiisa Nishikawa, Northern Arizona University, United States

****Correspondence:***
André Tomalka
andre.tomalka@inspo.uni-stuttgart.de

Specialty section:
This article was submitted to Striated Muscle Physiology, a section of the journal Frontiers in Physiology

Received: *22 December 2020*
Accepted: *08 March 2021*
Published: *31 March 2021*

Citation:
Tomalka A, Weidner S, Hahn D, Seiberl W and Siebert T (2021) Power Amplification Increases With Contraction Velocity During Stretch-Shortening Cycles of Skinned Muscle Fibers. Front. Physiol. 12:644981. doi: 10.3389/fphys.2021.644981

Abbreviations: ATP, adenosine 5′ triphosphate disodium salt hydrate; CK, creatine phosphokinase; Ca^{2+}, calcium; CP, creatine phosphate; E-64, *trans*-epoxysuccinyl-L-leucylamido(4-guanidino)butane; EGTA, ethylene glycol-bis(2-aminoethylether)-N,N,N′,N′-tetraacetic acid; F/F_0, maximum isometric muscle force; *F-l*-r, force-length-relation; *F-v*-r, force-velocity-relation; rFD, residual force depression; rFE, residual force enhancement; GLH, glutathione; HDTA, 1,6-diaminohexane-N,N,N′,N′-tetraacetic acid; *h*, height; IMID, imidazole; KOH, potassium hydroxide; KP potassium propionate; L/L_0, optimum muscle fiber length associated with F/F_0; L/L_{S0}, optimum sarcomere length associated with F/F_0; L_S, individual sarcomere length; non-XB, non-cross-bridge; P_0, maximum power output; PMSF, phenylmethanesulfonyl fluoride; *P-v*-r, power-velocity-relation; SSC, stretch-shortening cycle; TES, *N*-[Tris(hydroxymethyl)methyl]-2-aminoethanesulfonic acid; v/v, volume/volume; v_0, maximum shortening velocity; w/v, weight/volume; *w*, width; XB, cross-bridge.

INTRODUCTION

The most common form of muscle action during terrestrial locomotion is characterized by eccentric muscle action (active lengthening) immediately followed by concentric muscle action (active shortening). Such stretch-shortening cycles (SSCs) occur in both cyclical and non-cyclical locomotion at the level of the muscle-tendon unit (Komi, 2000; Ishikawa et al., 2005; Aeles and Vanwanseele, 2019; Navarro-Cruz et al., 2019) and the muscle fiber (Gillis and Biewener, 2001; Nikolaidou et al., 2017). So far, a large number of experiments at the level of the muscle-tendon unit have shown an increase in muscle force, work, and power output during the shortening phase of SSCs compared with pure shortening contractions (Cavagna et al., 1968; Bosco et al., 1981; Gregor et al., 1988; Seiberl et al., 2015). This SSC-effect (i.e., increased muscular performance) is further associated with amplified muscular efficiency accompanied by reduced metabolic energy consumption (Cavagna et al., 1968; Holt et al., 2014). The underlying mechanisms of the SSC-effect that have been discussed in the literature include activation dynamics, contributions of stretch reflexes, storage and release of elastic energy, and history-dependent effects of muscle action associated with residual force enhancement (rFE) (Van Ingen Schenau et al., 1997; Cormie et al., 2011; Seiberl et al., 2015).

In contrast to a large number of SCC studies at the level of the muscle-tendon unit, there are only a few studies at the level of the skinned muscle fibers that examined the SSC-effect in the sarcomere itself (Fukutani et al., 2017a; Fukutani and Herzog, 2019, 2020a; Tomalka et al., 2020). An SSC-effect of about 30% of work enhancement relative to pure shortening was reported for slow stretch-shortening velocities [about 10% maximum shortening velocity (v_0)] and long muscle fiber lengths [2.4–3.3 μm, descending limb of the force-length relation (*F-l*-r)] of skinned rabbit soleus muscle fibers (Fukutani et al., 2017a; Fukutani and Herzog, 2019). Tomalka et al. (2020) demonstrated that the SSC-effect in skinned rat soleus muscle fibers also occurs in the more physiological working range (plateau region and ascending limb of the *F-l*-r) at fast contraction velocities (∼85% v_0). Mechanisms related to activation dynamics, reflex activity, and elastic recoil from tendons—as discussed for *in vivo* muscle action—cannot be responsible for the SSC-effect in skinned muscle fiber experiments. Thus, an additional mechanism needs to be found within the sarcomere itself. Using Blebbistatin for XB-inhibition, Tomalka et al. (2020) further showed that both XBs- and non-XB structures contribute to the SSC-effect on the skinned muscle fiber level, which is supported by other studies (Fukutani et al., 2017a; Fukutani and Herzog, 2020a).

These findings nicely fit into our current understanding of eccentric muscle action, as there is experimental evidence that non-XB structures like titin also account for increased forces during the stretch (Leonard and Herzog, 2010; Tomalka et al., 2017) and after the stretch (rFE) (Herzog, 2018; Freundt and Linke, 2019; Tahir et al., 2020). By definition, rFE describes the phenomenon of increased steady-state isometric forces after active muscle lengthening compared with the corresponding force during a purely isometric contraction (Abbott and Aubert, 1952; Edman et al., 1982). Several model approaches (Rode et al., 2009; Nishikawa et al., 2012; Schappacher-Tilp et al., 2015; Heidlauf et al., 2017) and experimental evidence of physiological mechanisms (Herzog et al., 2014; Mártonfalvi et al., 2014; Rivas-Pardo et al., 2016; Dutta et al., 2018) support the idea that titin plays an essential role in active muscle force generation (for recent reviews, see Linke, 2017; Nishikawa, 2020; Fukutani et al., 2021). Moreover, it is known that titin is a viscoelastic protein that interacts with the XBs, stores energy, and preserves force upon muscle stretch (Bianco et al., 2007; Chung et al., 2011; Herzog et al., 2014). Based on recent findings, it is assumed that the mechanisms of enhanced force generation triggered by muscle stretch are the same as triggered during the stretch-phase of SSCs and thus contribute to the SSC-effect on the level of the muscle fiber (Fukutani and Herzog, 2019; Tomalka et al., 2020).

Further, Tomalka et al. (2020) suggested that XB-kinetics are related to the SSC-effect at the single skinned muscle fiber level by XB-cycling that allows titin-actin interactions (Astier et al., 1998; Nagy, 2004; Bianco et al., 2007; Dutta et al., 2018; Li et al., 2018; Powers et al., 2020). Additionally, the elastic energy stored in elongated XBs during active muscle stretching (Huxley et al., 1994; Wakabayashi et al., 1994) might contribute to the SSC-effect during shortening (Cavagna et al., 1981). However, while only the XBs can produce active force, titin's viscoelastic behavior is likely to contribute to the SSC-effect (by storage and release of elastic energy) in a velocity-dependent manner (Freundt and Linke, 2019).

Therefore, variations in XB and non-XB kinetics with increasing stretch velocity associated with a decrease in XB-binding and detachment of bound XBs (muscle "give") (Katz, 1939; Flitney and Hirst, 1978; Choi and Widrick, 2010) might have an impact on the SSC-effect. Consequently, the influence of different stretch-shortening velocities on mechanical work and power output in the SSC should be examined. Thus, experiments in the physiological range (along the ascending limb to the plateau region) of the *F-l*-r with different ramp velocities (30, 60, and 85% v_0) and the same ramp lengths (lengthening, shortening) were performed in this study to characterize the velocity dependence of the SSC-effect. The different contributions of XB- and non-XB structures to single skinned muscle fiber force and performance amplification were identified using the XB-inhibitor Blebbistatin. We hypothesize that the SSC-effect decreases with increasing SSC-velocity due to the force-velocity-relationship (*F-v*-r) on single muscle fiber force. Thus, the muscle forces, mechanical work, and power output should decrease in a non-linear manner as a function of increasing SSC-velocity.

MATERIALS AND METHODS

Preparation, Handling, and Experimental Setup

Muscle preparation, storage, and activation techniques for permeabilized single muscle fibers were in line with Tomalka et al. (2017, 2020). Briefly, experiments were performed on glycerinated skinned single fiber segments from soleus muscles of

six freshly killed female Wistar rats (age: 3 months, weight: 428–520 g, cage-sedentary, 12–12 h light: dark cycle, housing-temperature: 22°C). The skeletal muscle fibers from rats used for this study have been provided by another animal study approved according to the German animal protection law [Tierschutzgesetz, §4 (3); Permit Number: 35-9185.81/0491]. The small bundles (50–100 fibers) were stored in a storage solution (see section "Solutions") containing 50% glycerol at –20°C for 4–6 weeks. As previously described, single fibers were prepared before the experiment (Tomalka et al., 2020). The fibers were treated with a relaxing solution (see section "Solutions") containing Triton X-100 (1% v/v) for 1–2 min at 4°C to chemically disrupt the muscle membranes without affecting the contractile apparatus (Fryer et al., 1995). Afterward, a fiber segment 0.8–1.2 mm long was cut from the fiber, and T-shaped aluminum clips were mounted at its extremities for attachment between the lever arms of a high-speed length controller (322 C-I, Aurora Scientific, Canada) and a force transducer (403a, Aurora Scientific, Canada) (**Figure 1A**). The two ends of the fiber were fixed with glutaraldehyde in rigor solution and glued to the clips with fingernail polish diluted with acetone (Burmeister Getz et al., 1998). The length (L), width (w), and height (h) of the fiber were measured at 0.1 mm intervals in the central segment of the relaxed fiber with a 10 × dry-objective (NA 0.30, Nikon) and a 10× eyepiece. The individual sarcomere length (L_S) was set to 2.4 ± 0.05 μm, which is within the optimal sarcomere length (L_{S0}) range for maximal isometric force (F_0) development in the activated state (pCa 4.5) (Stephenson and Williams, 1982). The fiber cross-sectional area was determined assuming an elliptical cross-section of single muscle fibers ($\pi hw/4$) and was 4,844 ± 1,246 μm^2 (mean ± standard deviation). The L_S was measured using a high-speed camera system (901B, Aurora Scientific, Canada) in combination with a 20 × ELWD dry-objective (NA 0.40, Nikon) and an accessory lens (2.5×, Nikon).

Experimental Protocol

Stretch-shortening cycle experiments comprised two conditions of repeated measurements. The control condition (**Figures 1B–D**) was designed to investigate the dynamic total

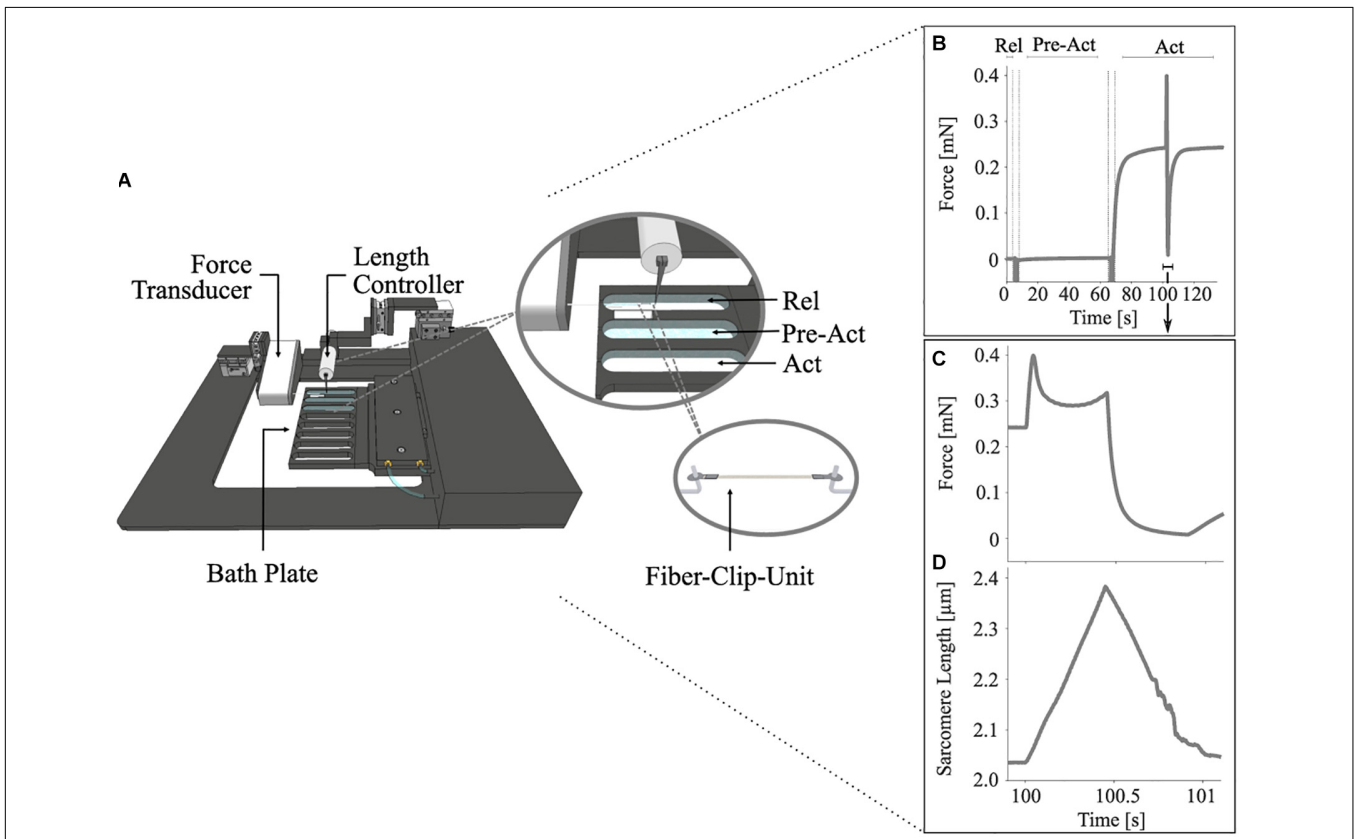

FIGURE 1 | Schematic diagram of the permeabilized fiber apparatus **(A)** and a diagram showing the control experiments' protocol **(B–D)**. **(A)** Close-up cut-away view of the eight-well bath plate (top right) showing three chambers filled with solutions and a single fiber mounted onto the hooks with T-clips (bottom right). **(B)** Representative force-time trace showing the changes in muscle force during an entire stretch-shortening cycle (SSC) with previous pre-activation (Pre-Act) and relaxation period (Rel) (n = 1, raw, unfiltered data). Enlarged views of the force response **(C)** and the change in sarcomere length **(D)** for an SSC with 85% maximum contraction velocity at supramaximal activation level (Act; pCa = 4.5). Each of these experiments consists of an isometric phase, then a ramp transient, and then an isometric phase. The force is shown in mN, and the sarcomere length is recorded at maximal activation and is shown in μm. All ramp experiments have been conducted at a constant stretch/shortening magnitude of 0.17 L_S/L_{S0} on permeabilized single fiber segments from rat soleus muscles at 12°C experimental temperature. The vertical lines indicate the time for solution change. The arrow indicates the onset of activation.

force response during varying isovelocity SSCs. The experiments with the XB-inhibitor (Blebbistatin condition) repeated the control condition and suggested the contribution of non-XB elements to force production during isovelocity SSCs. Each SSC experiment consisted of an isometric phase, followed by a ramp phase (lengthening and shortening) and a final isometric phase (**Figure 1B**).

For the control condition, single skinned fibers (six rats, 14 fibers) were activated at ∼2.0 μm L_S, stretched to L_{S0} of ∼2.4 μm [in the activated state (pCa 4.5)], and then immediately shortened to ∼2.0 μm L_S with varying stretch-shortening velocities of 30, 60, and 85% v_0 in a randomized order.

An identical protocol was repeated for the same skinned muscle fibers (five rats, 13 fibers), in the presence of 20 μmol l^{-1} Blebbistatin in all solutions (see section "Solutions") to identify non-XB contributions to muscle force (Cornachione and Rassier, 2012; Shalabi et al., 2017; Tomalka et al., 2020). Blebbistatin is a photosensitive chemical that blocks the force-generating transition of the bound actomyosin complex from a weakly to a strongly bound state and causes myosin heads to bind to actin without exerting any isometric force (Iwamoto, 2018; Tomalka et al., 2020). Thus (a major population of) XBs remain in the pre-power-stroke state weakly attached to actin (Minozzo and Rassier, 2010; Rahman et al., 2018). Blebbistatin does not affect titin mobility (Shalabi et al., 2017).

Only the data of one muscle fiber were discarded due to insufficient inhibition of force generation capability by Blebbistatin (remaining active isometric force at $L_{S0} > 20\%\ F_0$).

The average active isometric force at optimum sarcomere length L_{S0} was 0.29 ± 0.08 mN, while the mean optimum muscle fiber length was 0.77 ± 0.09 mm. The isometric force corresponds to relative average stress of 60.04 ± 9.49 kPa. The maximum shortening velocity of the skinned soleus muscle fibers from adult male Wistar rats was 0.46 ± 0.13 $L_0\ s^{-1}$ ($n = 6$), and the curvature factor of the force-velocity-relation was $curv$ = 0.07 ± 0.02. In separate experiments, the fiber specific v_0 was calculated based on our experimental data from six to eight isotonic contractions against forces in the range of 0.1 F_0 to 0.9 F_0 (two fibers each from two rats and one fiber each from two other rats).

To preserve the structural and mechanical properties in maximally activated fibers over a longer period and to reduce sarcomere inhomogeneities, the "cycling protocol" by Brenner (1983) was used. To ensure the structural and mechanical integrity of fibers in the experiments, the following criteria were applied to discard fibers: (1) isometric force in reference contractions was decreased by more than 10%; (2) aberrant behavior of force-traces, evidenced by artifacts, oscillations, or abrupt flattening was noted; and (3) lesions, ruptures, or fiber contortion were identified visually. For the determination of force degradation, isometric reference contractions at L_{S0} were performed before and after each ramp contraction. In the ramp experiments (control condition), the isometric force in successive activations decreased at an average rate of approximately 3.2% per activation. All experiments were conducted at a constant temperature of 12 ± 0.1°C. At this temperature, the fibers proved very stable and were able to withstand rapid ramp perturbations over an extended period as well as prolonged activations (Ranatunga, 1982, 1984; Bottinelli et al., 1996; Tomalka et al., 2017).

Calculations of XB- and Non-XB Forces

To separate XB and non-XB forces during SSCs, the forces obtained during the Blebbistatin condition were subtracted from the forces obtained during the control condition. This rather simple method was used previously (Tomalka et al., 2017) and is based on the following assumptions: First, XBs produce a constant average force during isokinetic stretch after an initial equilibrium of XB-distributions (Huxley, 1957; Huxley and Simmons, 1971). Second, Blebbistatin suppresses the active XB-based forces to a negligible level. This was assessed by comparing the initial isometric force at 2.0 μm L_S with and without XB-inhibitors. Administering Blebbistatin suppressed active XB forces by 98%, so it can be expected that Blebbistatin suppresses active forces during SSCs to a similar extent. Third, is assumed that Blebbistatin does only affect the active XB-based force production during SSCs (see section "'Isolated XB' Forces During the SSC").

Solutions

The relaxing solution contained (in mM) 100 TES, 7.7 $MgCl_2$, 5.44 Na_2ATP, 25 EGTA, 19.11 Na_2CP, and 10 GLH (pCa 9.0). The preactivating solution contained (in mM) 100 TES, 6.93 $MgCl_2$, 5.45 Na_2ATP, 0.1 EGTA, 19.49 Na_2CP, 10 GLH, and 24.9 HDTA. The activating solution contained (in mM) 100 TES, 6.76 $MgCl_2$, 5.46 Na_2ATP, 19.49 Na_2CP, 10 GLH, and 25 CaEGTA (pCa 4.5). The skinning solution contained (in mM) 170 potassium propionate, 2.5 $MgCl_2$, 2.5 Na_2ATP, 5 EGTA, 10 IMID, and 0.2 PMSF. The storage solution is the same as the skinning solution, except for the presence of 10 mM GLH and 50% glycerol (v/v). Cysteine and cysteine/serine protease inhibitors [*trans*-epoxysuccinil-L-leucylamido-(4-guanidino) butane, E-64, 10 mM; leupeptin, 20 μg ml^{-1}] were added to all solutions to preserve lattice proteins and thus sarcomere homogeneity (Linari et al., 2007; Tomalka et al., 2017). pH (adjusted with KOH) was 7.1 at 12°C. 450 U ml^{-1} of CK was added to all solutions, except for skinning and storage solutions. CK was obtained from Roche (Mannheim, Germany), and Blebbistatin was obtained from Enzo Life Sciences Inc. (NY, United States). All other chemicals were obtained from Sigma (St. Louis, MO, United States).

Data Processing and Statistics

Data were collected at 1 kHz with real-time software (600A, Aurora Scientific, Canada) and an A/D Interface (600A, Aurora Scientific, Canada). A custom-written MATLAB (MathWorks, Natick, MA, United States) script was utilized for data analysis. Unless stated otherwise, forces are expressed in absolute values (mN) or normalized to the individual maximum muscle force (F/F_0). The shortening velocity is reported in relative units ($\Delta L_S/L_{S0}\ s^{-1}$) or normalized to the fiber specific maximal shortening velocity (v/v_0). Fiber lengths are expressed relative to the optimum fiber length (L/L_0). Sarcomere lengths are expressed relative to the optimum sarcomere length (L_S/L_{S0}) or are reported in absolute values (μm). Mechanical work was calculated as the line integral of the changing force over the entire shortening

distance during the SSCs and the pure shortening contractions and is expressed in relative values ($\frac{F}{F_0} \cdot \frac{\Delta L_S}{L_{S0}}$). The power output as a function of velocity (*P-v*-r, orange solid line of **Figure 2**) was calculated based on the force-velocity-relation for shortening contractions (*F-v*-r, blue solid line of **Figure 2**). Power is reported as relative values ($\frac{F}{F_0} \cdot \frac{\Delta L_S}{L_{S0}}$) s^{-1} or normalized to the maximal individual power (P/P_0). The maximum mean power output P_0 was 0.018 ± 0.005 ($\frac{F}{F_0} \cdot \frac{\Delta L_S}{L_{S0}}$) s^{-1} at 20% v_0.

The power output of single skinned muscle fibers as a function of velocity calculated during isovelocity SSCs with varying velocities ranging from 30 to 85% v_0 results from the work that was done within a particular time, delta [Δ] *t*:

$$\frac{F}{F_0} \cdot \frac{\Delta L_S}{L_{S0}} \cdot \frac{1}{\Delta t}$$

To avoid ambiguity and misinterpretations of the terminology of "positive work" and "negative work" in the following text, they are defined as follows: positive work is performed when an active muscle shortens by internal forces. Negative work is performed when an active muscle lengthens by external forces (Cavagna et al., 1965).

All data are presented as mean ± standard deviation (SD) unless stated otherwise. To test whether the work (and power) significantly differs between the two conditions (control vs. Blebbistatin), a repeated-measures ANCOVA (factor 1 phase and covariate velocity) was used. Significant differences in the forces at the end of the stretch (control vs. Blebbistatin) were tested using a paired *t*-test. To test for differences in the energy recovery (defined as the ratio of elastic energy storage and release in the SSC; W_{con}/W_{ecc}) between both conditions, a paired *t*-test was used on data pooled across velocities in respective condition. To test whether the work and power output differ between the varying SSC velocities (30%, 60%, and 85% v_0), a two-way repeated-measures ANOVA (factor 1 velocity and factor 2 phase) was calculated. In case that the ANOVA demonstrated significant main effects, *post hoc* analyses were performed using the student's *t*-test with Bonferroni correction. The statistical tests were likewise performed for the control and the Blebbistatin experiments and a comparison of both conditions. The level of significance was set at $p < 0.05$. Statistical analyses were realized using SPSS 26 (IBM Corp., Armonk, NY, United States). The effect sizes of Cohen's *d* were calculated as $d = \frac{M_1 - M_2}{S_{pooled}}$, where *M* is the mean and $S_{pooled} = \sqrt{\frac{SD_1^2 + SD_2^2}{2}}$ (Cohen, 1988). The effect sizes were classified as small ($d = 0.2$), medium ($d = 0.5$), and large ($d = 0.8$) (Cohen, 1988).

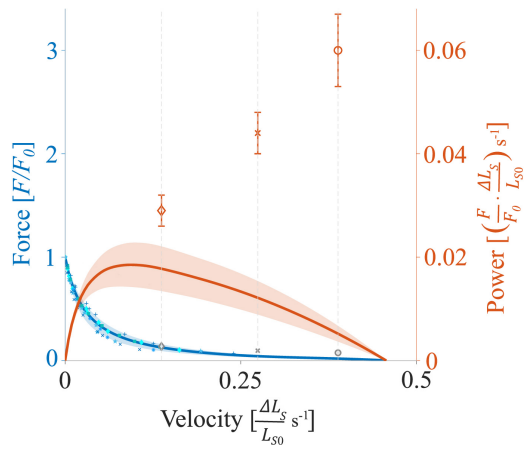

FIGURE 2 | Representative force-velocity-relationship (*F-v*-r) and power-velocity-relationship (*P-v*-r) for soleus muscle. The blue solid line (and underlying individual data points) indicates the mean *F-v*-r for shortening contractions (positive velocities), while force declines as a function of shortening velocity (two fibers each from two rats and one fiber each from two other rats). The orange solid line indicates the mean *P-v*-r for shortening contractions. Power is maximum at intermediate shortening velocities at about 0.09 $\frac{\Delta L_S}{L_{S0}}$ s^{-1} (~20% v_0). The shaded regions around the solid lines indicate the corresponding standard deviations (SD). Orange diamonds, crosses, and circles (mean ± SD) indicate maximum power output obtained during the shortening phase of SSCs with 30% v_0, 60% v_0, and 85% v_0, respectively. Gray diamonds, crosses, and circles indicate the mean calculated XB-based forces (section "Contributions of 'Isolated XB' Force to Work and Power as a Function of Velocity") obtained during the shortening phase of SSCs at respective velocities. F_0 is the maximum isometric muscle force, velocity is given in relative units ($\frac{\Delta L_S}{L_{S0}}$ s^{-1}), and power is reported as relative values ($\frac{F}{F_0} \cdot \frac{\Delta L_S}{L_{S0}}$) s^{-1}.

RESULTS

Significant differences between the control and the Blebbistatin condition ($p < 0.001$) were observed for all parameters tested. Negative mechanical work during the stretch [control: −0.20 ± 0.01 vs. Blebbistatin: −0.04 ± 0.01 $\frac{F}{F_0} \cdot \frac{\Delta L_S}{L_{S0}}$], positive mechanical work during shortening [control: 0.03 ± 0.00 vs. Blebbistatin: 0.01 ± 0.00 $\frac{F}{F_0} \cdot \frac{\Delta L_S}{L_{S0}}$], negative power output during the stretch [control: −0.32 ± 0.13 vs. Blebbistatin: 0.07 ± 0.04 ($\frac{F}{F_0} \cdot \frac{\Delta L_S}{L_{S0}}$) s^{-1}], positive power output during shortening [control: 0.04 ± 0.01 vs. Blebbistatin: 0.02 ± 0.01 ($\frac{F}{F_0} \cdot \frac{\Delta L_S}{L_{S0}}$) s^{-1}], and force at the end of the stretch were larger in the control condition (1.16 ± 0.20 F_0) compared with the Blebbistatin condition (0.42 ± 0.14 F_0). In contrast, energy recovery (W_{con}/W_{ecc}) was significantly lower in the control condition (−0.15 ± 0.02) compared with the Blebbistatin condition (−0.25 ± 0.06).

Control Condition: Effects of Velocity on Mechanical Work and Power Output

The negative mechanical work during the stretching phase of the SSCs, when work is done on the muscle, increased significantly (+8.5 ± 2.5%, $p < 0.001$, $d = 1.19$, $R^2 = 0.99$) with increasing stretch velocity (**Figure 3A** and **Table 1**).

Negative work was significantly larger for fast (−85% v_0) compared with moderate (−60% v_0) stretching velocities (+4.1% ± 2.2%, $p < 0.001$, $d = 0.61$; yellow vs. red circles of **Figure 3A**) and for moderate compared with slow (−30% v_0) stretching velocities (+4.3% ± 2.7%, $p < 0.001$, $d = 0.63$; red vs. blue circles of **Figure 3A**).

For the shortening phase of the SSCs, the positive mechanical work, when work is done by the muscle, decreased significantly

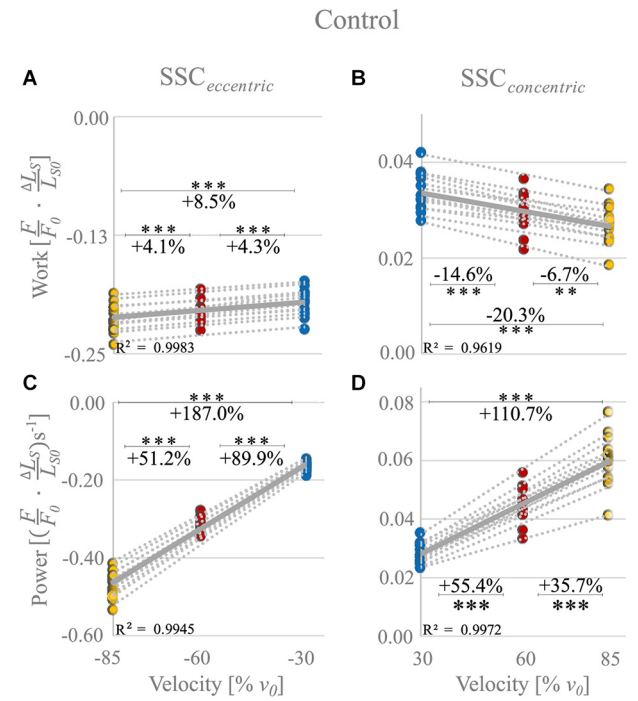

FIGURE 3 | Control condition. Influence of varying stretch-shortening velocities on work and power during the lengthening phase ($SSC_{eccentric}$; negative work/power; **A,C)** and the shortening phase ($SSC_{concentric}$; positive work/power; **B,D)** of SSCs, respectively. The gray dotted lines of the scatterplots shown in **(A–D)** indicate the individual paired data values, and solid gray lines indicate the mean values (n = 14 fibers from six rats). The blue circles indicate the SSC at (±)30% v_0, the red circles at (±)60% v_0, and the yellow circle at (±)85% v_0. Work/power values are expressed in relative values ($\frac{F}{F_0} \cdot \frac{\Delta L_S}{L_{S0}}$) and ($\frac{F}{F_0} \cdot \frac{\Delta L_S}{L_{S0}}$)$s^{-1}$, respectively. Asterisks mark differences in work/power with varying velocities in the intergroup comparison. Significance levels are marked as follows: $^{**}p < 0.01$ and $^{***}p < 0.001$. The control condition refers to the experiments without XB-inhibition.

(−20.3% ± 5.9%, $p < 0.001$, $d = 1.19$, $R^2 = 0.96$) with increasing shortening velocity. Positive work was significantly smaller for moderate compared with slow velocities (−14.6% ± 4.2%, $p < 0.001$, $d = 1.28$; **Figure 3B**) and for fast compared with moderate shortening velocities (−6.7% ± 5.6%, $p < 0.01$, $d = 0.51$; **Figure 3B**). The mean negative work output during muscle stretch was about seven times the amount of positive work during muscle shortening of SSCs (**Table 1**).

The negative power output increased successively with increasing stretch velocities (+187.0% ± 6.7%, $p < 0.001$, $d = 12.88$, $R^2 = 0.99$) for the stretching phase of the SSC (**Figure 3C**). Negative power was significantly larger for fast compared with moderate stretching velocities (+51.2% ± 3.2%, $p < 0.001$, $d = 6.05$; **Figure 3C**) and for moderate compared with slow stretching velocities (+89.9% ± 4.9%, $p < 0.001$, $d = 9.12$; **Figure 3C**).

For the shortening phase of the SSCs, the positive power output increased significantly (110.7% ± 15.6%, $p < 0.001$, $d = 4.89$, $R^2 = 0.99$) with increasing shortening velocity. Power was significantly larger for moderate compared with slow shortening velocities (+55.4% ± 7.6%, $p < 0.001$, $d = 3.36$; **Figure 3D**) and for fast compared with moderate shortening velocities (+35.7% ± 8.1%, $p < 0.001$, $d = 2.18$; **Figure 3D**).

The force-length traces of single muscle fibers are characterized by a steep rise in force in the early phase of active muscle stretching (red arrow in **Figure 4**), followed by a negative slope (up to about half the stretching time, **Figure 4**). Then the forces recovered relative to the initial drop in force to large parts toward the end of the stretch of the SSCs. The peak force during stretch increased with increasing stretch velocity (+10.7% ± 4.1%, $p < 0.001$, $d = 2.49$). Furthermore, maximum forces were reached at longer sarcomere lengths with increasing stretching velocity (+0.4% ± 0.2%, $p < 0.001$, $d = 3.00$; colored unfilled circles, **Figure 4**). During approximately 87% of the shortening phase, the highest forces were produced at the slowest shortening velocity (**Figure 4**, blue line).

Blebbistatin Condition: Effects of XB-Inhibition on Work and Power as a Function of Velocity

The XB-inhibitor Blebbistatin decreased the maximum isometric forces to 0.02 F_0 at 2.0 µm L_S (**Figure 5**). Accordingly, eccentric and concentric forces during the SSCs in the Blebbistatin condition were decreased (**Figure 5**) in comparison to the control condition (**Figure 4**). Maximum forces were reached at the end of the stretch and increased with increasing stretching velocity (colored circles, **Figure 5**).

The negative work increased significantly with increasing velocities from slow to fast stretching velocities (+48.8% ± 12.4%, $p < 0.001$, $d = 1.27$, $R^2 = 0.99$) during the stretching phase of the SSCs (cf. blue vs. yellow circles of **Figure 6A** and **Table 2**). Thus, negative work was significantly larger for fast compared with moderate velocities (+17.0% ± 7.61%, $p < 0.01$, $d = 0.59$; yellow vs. red circles of **Figure 6A**) and for moderate compared with slow stretching velocities (+27.6% ± 13.2%, $p < 0.001$, $d = 0.83$; red vs. blue circles of **Figure 6A**).

For the shortening phase of the SSCs, the mechanical work increased significantly with increasing velocity (+70.7% ± 35.0%, $p < 0.001$, $d = 1.74$, $R^2 = 0.98$, **Figure 6B**). Thus, positive work was significantly larger for moderate compared with slow velocities (+30.9%± 24.1%, $p < 0.01$, $d = 0.89$, **Figure 6B**) and for fast compared with moderate shortening velocities (+31.2% ± 18.4%, $p < 0.01$, $d = 1.02$). The overall negative work output during muscle stretch was about four times the amount of positive work during muscle shortening of SSCs.

The negative power output during muscle stretch of the SSCs increased significantly (+293.5% ± 32.7%, $p < 0.001$, $d = 3.43$, $R^2 = 0.99$) with increasing stretching velocities (**Figure 6C** and **Table 2**). Negative power was significantly larger for fast compared with moderate stretching velocities (+70.0% ± 11.1%, $p < 0.001$, $d = 1.78$; **Figure 6C**) and for moderate compared with slow stretching velocities (+132.2% ± 24.0%, $p < 0.001$, $d = 2.79$; **Figure 6C**).

TABLE 1 | Descriptive statistics and pairwise comparisons of work and power values obtained during the control experiments.

Control								
Descriptive statistics				**Pairwise comparisons work** $[\frac{F}{F_0} \cdot \frac{\Delta L_S}{L_{S0}}]$				***p*-values**
				Mean differences	**SD**	**95% Confidence interval of the difference**		
Variable	**Mean**	**SD**				**Lower**	**Upper**	
W_{ecc} 30% v_0	−0.195	0.014	W_{ecc} 30% v_0 −W_{ecc} 60% v_0	−0.008*	0.005	0.003	0.013	<0.001
W_{ecc} 60% v_0	−0.204	0.013	W_{ecc} 60% v_0 −W_{ecc} 85% v_0	−0.008*	0.005	0.004	0.013	<0.001
W_{ecc} 85% v_0	−0.212	0.014	W_{ecc} 30% v_0 −W_{ecc} 85% v_0	−0.017*	0.005	0.012	0.021	<0.001
W_{con} 30% v_0	0.034	0.004	W_{con} 30% v_0 −W_{con} 60% v_0	−0.005*	0.001	0.004	0.006	<0.001
W_{con} 60% v_0	0.029	0.004	W_{con} 60% v_0 −W_{con} 85% v_0	−0.002*	0.002	0.000	0.003	0.008
W_{con} 85% v_0	0.027	0.004	W_{con} 30% v_0 −W_{con} 85% v_0	−0.007*	0.002	0.005	0.009	<0.001
				Power $[(\frac{F}{F_0} \cdot \frac{\Delta L_S}{L_{S0}})\mathbf{s^1}]$				
P_{ecc} 30% v_0	−0.164	0.012	P_{ecc} 30% v_0 −P_{ecc} 60% v_0	−0.147*	0.010	0.138	0.157	<0.001
P_{ecc} 60% v_0	−0.312	0.020	P_{ecc} 60% v_0 −P_{ecc} 85% v_0	−0.160*	0.014	0.146	0.173	<0.001
P_{ecc} 85% v_0	−0.471	0.032	P_{ecc} 30% v_0 −P_{ecc} 85% v_0	−0.307*	0.021	0.287	0.327	<0.001
P_{con} 30% v_0	0.029	0.003	P_{con} 30% v_0 −P_{con} 60% v_0	0.016*	0.003	−0.019	−0.013	<0.001
P_{con} 60% v_0	0.044	0.006	P_{con} 60% v_0 −P_{con} 85% v_0	0.016*	0.004	−0.020	−0.012	<0.001
P_{con} 85% v_0	0.060	0.009	P_{con} 60% v_0 −P_{con} 85% v_0	0.032*	0.006	−0.037	−0.026	<0.001

*Work/power values ± SD are expressed in relative values ($\frac{F}{F_0} \cdot \frac{\Delta L_S}{L_{S0}}$) and ($\frac{F}{F_0} \cdot \frac{\Delta L_S}{L_{S0}}$) s^{-1}, respectively. W, mechanical work; P, power output; ecc, eccentric phase during active muscle stretch; con, concentric phase during active muscle shortening; %V_0, percentage of maximum contraction velocity; ns, not significant. *The mean difference is significant at the 0.05 level.*

For the shortening phase of the SSCs, positive power output increased significantly (+351.5% ± 92.7%, $p < 0001$, $d = 3.92$, $R^2 = 0.97$) with increasing shortening velocity. Power was significantly larger for moderate compared with slow shortening velocities (+138.1% ± 43.9%, $p < 0.001$, $d = 2.89$; **Figure 6D**) and for fast compared with moderate shortening velocities (+90.7% ± 26.7%, $p < 0.001$, $d = 2.24$; **Figure 6D**).

Contributions of 'Isolated XB' Force to Work and Power as a Function of Velocity

To investigate the 'isolated XB' contributions to the total force response (**Figure 7** and **Table 3**), Blebbistatin-suppressed forces (**Figure 5**) were subtracted from the total forces of control ramps (**Figure 4**) (see section "Calculations of XB- and Non-XB Forces"). Accordingly, differences in force, work, and power between control and Blebbistatin condition were referred to as 'isolated XB' forces, work, and power in the following.

'Isolated XB' forces reached at the end of the stretches decreased with increasing stretching velocity (colored circles, **Figure 7**). During the stretch phase of the SSCs (cf. blue vs. yellow circles of **Figure 8A**) negative work performed by 'isolated XBs' did not change with increasing velocities (+0.6% ± 3.9%, $p = 1.00$, $d = 0.06$, $R^2 = 0.39$).

For the shortening phase of the SSCs, positive work of 'isolated XBs' decreased significantly with increasing velocity (−45.9% ± 7.6%, $p < 0.001$, $d = 4.00$, $R^2 = 0.99$, **Figure 8B**). Thus, mechanical work of 'isolated XBs' was significantly smaller for moderate compared with slow velocities (−26.9% ± 5.0%, $p < 0.01$, $d = 2.33$, **Figure 8B**) and smaller for fast compared with moderate shortening velocities (−25.8% ± 9.6%, $p < 0.01$, $d = 1.67$).

The negative power output of 'isolated XBs' during muscle stretch of the SSCs increased significantly (+166.0% ± 10.4%, $p < 0.001$, $d = 8.22$, $R^2 = 0.99$) with increasing stretching velocities (**Figure 8C**). Negative power of 'isolated XBs' was significantly larger for fast compared with moderate stretching velocities (+46.5% ± 4.6%, $p < 0.001$, $d = 3.88$; **Figure 8C**) and larger for moderate compared with slow stretching velocities (+81.6% ± 7.0%, $p < 0.001$, $d = 6.20$; **Figure 8C**).

For the shortening phase of the SSCs, the positive power output of 'isolated XBs' increased significantly (+43.2% ± 20.1%, $p < 0001$, $d = 1.86$, $R^2 = 0.95$) with increasing shortening velocity. Power was significantly larger for moderate compared with slow shortening velocities (+33.0% ± 9.1%, $p < 0.001$, $d = 1.98$; **Figure 8D**). However, there was no change in positive power output of 'isolated XBs' for moderate compared with fast shortening velocities (+7.8% ± 13.9%, $p = 0.611$, $d = 0.53$; **Figure 8D**).

DISCUSSION

In contrast to our hypothesis, the power output during the shortening phase of the SSCs increased almost linearly (**Figure 2**, orange symbols) with increasing stretch-shortening velocity. This increase is contrary to the typical parabolic shape of the *P-v*-r for the same range of shortening velocities (**Figure 2**, orange

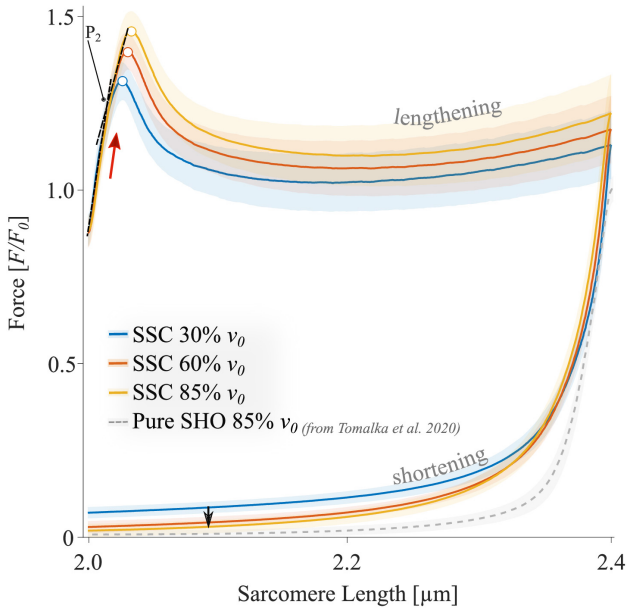

FIGURE 4 | The mean ± standard deviation (SD) of force-length traces of SSC-contractions with varying velocities (control condition). Solid blue, red, and yellow lines indicate the means. The shaded regions around the solid lines indicate the corresponding SD during active SSCs (n = 14, raw data). Negative work was determined for a period of 1,190 ms (blue line), 650 ms (red line), and 450 ms (yellow line) during the lengthening phase from the onset of stretch until the end of stretch using numerical integration of force with respect to sarcomere length. Positive work was determined for equivalent periods during the shortening phase from the onset of release until the end of the release. The red arrow indicates the steep rise in force in the early phase of active muscle stretching during SSCs. The black arrow indicates the decrease in force with increasing shortening velocity (i.e., due to the F-v-r). The colored circles indicate the peak forces at the end of the stretch. The sarcomere length is recorded at maximal activation (pCa 4.5) and is shown in µm. Additionally, pure shortening contractions of 2.4–2.0 µm with 85% v_0 of rat soleus muscle fibers, derived from Tomalka et al. (2020), show forces that are obviously below the forces obtained during the shortening phase preceded by stretch (SSC).

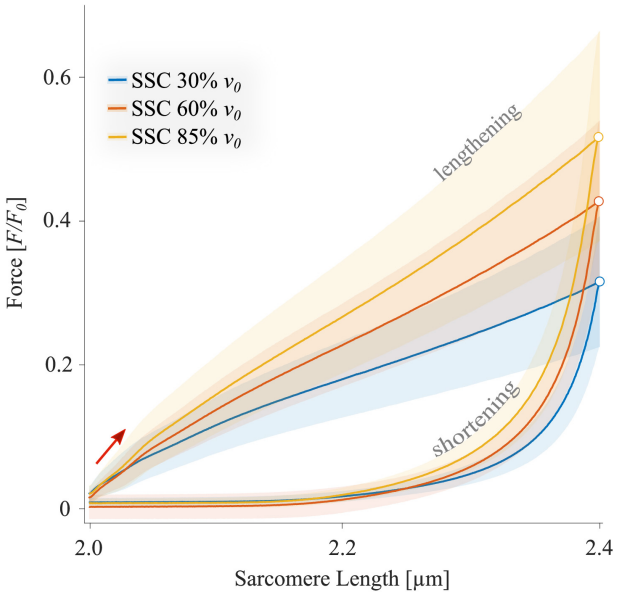

FIGURE 5 | The mean ± standard deviation (SD) of force-length traces of SSC contractions with varying velocities (Blebbistatin condition). Blue, red, and yellow solid lines indicate the means. The shaded regions around the solid lines indicate the corresponding SD during active SSCs (n = 13, raw data). Negative work was determined for a period of 1,190 ms (blue line), 650 ms (red line), and 450 ms (yellow line) during the lengthening phase from the onset of stretch until the end of stretch using numerical integration of force with respect to sarcomere length. Positive work was determined for equivalent periods during the shortening phase from the onset of release until the end of the release. Peak forces at the end of the stretch are marked by colored circles in the presence of Blebbistatin.

solid line), which is based on the hyperbolic shape of the F-v-r (Hill, 1938). Accordingly, our main result does not comply with the cross-bridge theories of muscle contraction based on the interaction of the contractile proteins actin and myosin (Huxley, 1957). Based on the results from our experiments with the XB-inhibitor Blebbistatin, we suggest that the elastic protein titin plays a significant role in power output during SSCs. In the following, we discuss potential mechanisms that explain the increased power output during muscle shortening of SSCs.

Control Condition: Influence of Muscle Fiber Kinetics on Mechanical Work and Power Output

Muscle Shortening

During the shortening phase of the SSCs, the positive work decreased (by 20%) with increasing velocities from 30 to 85% v_0 (**Figure 3B**). The F-v-r can partly explain this decrease in work since forces decrease with increasing shortening velocity (**Figure 2**, blue line). Lower forces produced over the same shortening distance will result in decreasing work with increasing velocity. However, since power is work per unit of time, this ≈20% decrease in work is overcompensated by reducing the duration of the shortening phase (by 65%) from 30 to 85% v_0. Thus, despite a decrease in work, the power output during the shortening phase significantly increased with increasing ramp velocities (**Figure 3D**).

Muscle Stretch

For all tested velocities in our study, fiber kinetics was characterized by a steep rise in force during the early phase of the stretch, immediately followed by a relatively compliant transient phase until the stretching has stopped. The initial linear phase (**Figure 4**, red arrow) is biphasic with a steep force slope followed by a more shallow slope (P_2 transition; **Figure 4**). This observation is consistent with recent investigations of stretch-induced force responses (5% L_{S0} stretch amplitude) in intact and skinned muscle fibers (mammalian and amphibian) and over a wide range of velocities (Lombardi and Piazzesi, 1990; Burmeister Getz et al., 1998; Linari et al., 2003; Pinniger et al., 2006; Tomalka et al., 2020). Both force slopes mainly arise from XB characteristics and can be attributed to the extension of all attached myosin heads to actin (Pinniger et al., 2006). Remarkably, we observed a significant rightward shift of the

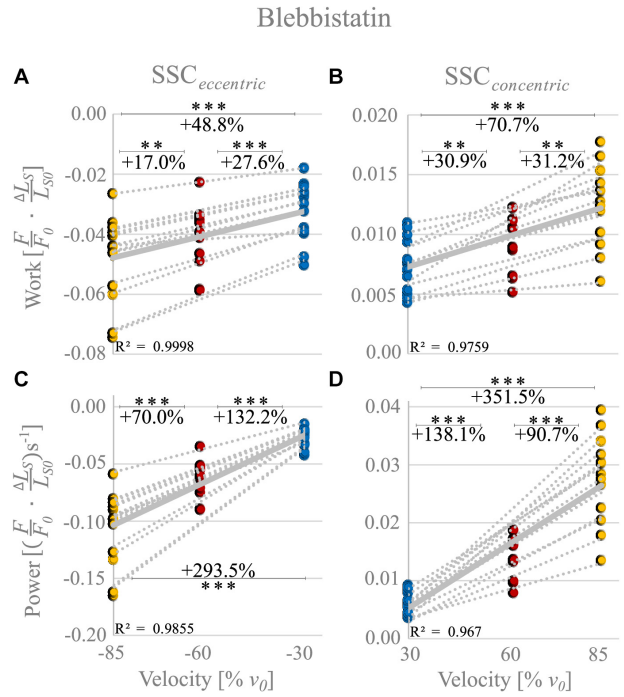

FIGURE 6 | Blebbistatin condition. Influence of varying stretch-shortening velocities on work and power during the lengthening phase [$SSC_{eccentric}$; negative work/power; **(A,C)**] and the shortening phase [$SSC_{concentric}$; positive work/power; **(B,D)**] of SSCs, respectively. The gray dotted lines of the scatterplots shown in **(A–D)** indicate the individual paired data values, and solid gray lines indicate the mean values (n = 13 fibers from five rats). The blue circles indicate the SSC at (±)30% v_0, the red circles at (±)60% v_0, and the yellow circle at (±)85% v_0. Statistical analyses are based on muscle fiber experiments in the presence of Blebbistatin. Work/power values are expressed in relative values ($\frac{F}{F_0} \cdot \frac{\Delta L_S}{L_{S0}}$) and ($\frac{F}{F_0} \cdot \frac{\Delta L_S}{L_{S0}}$)$s^{-1}$, respectively. Asterisks mark differences in work/power with varying velocities in the intergroup comparison. Significance levels are marked as follows: $^{**}p < 0.01$ and $^{***}p < 0.001$. *ns* means not significant. The Blebbistatin condition suggests the contribution of non-XB elements.

initial force peak to longer muscle lengths with increasing velocity (**Figure 4**, unfilled colored circles), accompanied by an increased peak force (ranging from 1.3 to 1.45 F_0). This rise in force after the P2 transition (≈1.5% L_{S0}; Lombardi and Piazzesi, 1990) is attributed to the continuous stretch of non-XB elements (Edman and Tsuchiya, 1996; Pinniger et al., 2006; Roots et al., 2007). Thus, elastic energy stored in viscoelastic structures, such as titin, increases with increasing stretching velocity (Edman et al., 1978; Sugi and Tsuchiya, 1988; Pinniger et al., 2006).

Further, continuous muscle lengthening beyond P_2, as investigated in this study, resulted in a negative force slope until the force recovers by the end of the stretching phase of SSCs. This characteristic transition phase has been referred to as muscle "give" (Flitney and Hirst, 1978). Muscle "give" is attributed to the detachment of myosin heads from thin filaments when the stretching velocity exceeds a particular threshold value that seems to be above 30% v_0 (Huxley, 1969; Sugi, 1972). However, the continuous rise in force after the previous "give" suggests the contribution of non-XB elements (Roots et al., 2007). This assumption is in line with previous work by Linari et al. (2003), who measured heat production and force of muscle fibers from frogs during ramp stretches. They suggested that XBs account for only ≈12% of the total energy storage during the active stretch. This amount includes the contribution of XB-elasticity (2.2% of total energy storage, Linari et al., 2000) and the redistribution of XB-states (≈9.8% of total energy storage, Linari et al., 2003), while XBs are pulled into states of higher energy during stretching.

Accordingly, more than 80% of energy storage cannot be explained by XB mechanisms, particularly since attached XBs detach quickly from actin filaments (Huxley and Simmons, 1971), and their stored elastic energy is lost (Bosco et al., 1982; Wilson et al., 1991). Consequently, non-XB structures, such as titin, may store and release most of the elastic energy during the SSCs' eccentric and concentric phases, respectively, thereby increasing power output during the shortening phase (section "Blebbistatin Condition: Influence of Non-XB Structures on Mechanical Work and Power Output").

'Isolated XB' Forces During the SSC

Based on the assumption that muscle force during a stretch is the sum of XB- and non-XB forces (Nocella et al., 2014; Tomalka et al., 2017, 2020), and that a high proportion of XB-based forces is switched off in the presence of Blebbistatin, subtraction of forces in the Blebbistatin condition from the forces in the control condition leads to XB-forces (**Figure 7**). Large parts of the stretch (≈2.1–2.4 μm L_S) show XB forces clearly below 1.0 F/F_0. This might be explained by muscle "give" since a fraction of XBs is torn off due to initial stretch. After the initial peak, the XB force continuously decreases until the end of the stretch for each stretch velocity (unfilled colored circles, **Figure 7**). Interestingly, in the second half of the stretch (2.2–2.4 μm L_S), where an almost regular XB-cycling may be restored due to the constant stretching velocity, forces are lower ($p < 0.001$) for highest stretch velocity (85% v_0, dashed yellow line, **Figure 7**) compared with the slowest stretch velocity (30% v_0, blue dashed line, **Figure 7**). This contrasts with our typical understanding of the eccentric F-v-r, where forces increase with increasing negative velocities and plateau at a certain threshold (Joyce et al., 1969; Haeufle et al., 2014). One possible reason why this behavior is not yet mentioned in the literature might be that the decreasing XB contribution with increasing stretch velocity is overcompensated by an increasing non-XB contribution (**Figure 5**) to generate enhanced muscle fiber force as found in the control condition (**Figure 4**, second half of the stretch). However, this reasoning requires the basic assumption that Blebbistatin completely inhibits XB contributions to force production, which is further discussed below.

In the SSCs' shortening phase, and in line with the F-v-r for shortening contractions (Hill, 1938), higher forces were produced at lower shortening velocity (30% v_0, **Figure 7**, blue dashed line) compared with higher shortening velocity (85% v_0, **Figure 7**, yellow dashed line). Consequently, the 'isolated XB'-based work decreased with increasing shortening

TABLE 2 | Descriptive statistics and pairwise comparisons of work and power values obtained during the Blebbistatin experiments.

Blebbistatin								
Descriptive statistics				**Pairwise comparisons work** $[\frac{F}{F_0} \cdot \frac{\Delta L_S}{L_{S0}}]$				***p*-values**
				Mean differences	**SD**	**95% Confidence interval of the difference**		
Variable	**Mean**	**SD**				**Lower**	**Upper**	
W_{ecc} 30% v_0	−0.032	0.010	W_{ecc} 30% v_0 −W_{ecc} 60% v_0	−0.008*	0.003	0.005	0.012	<0.001
W_{ecc} 60% v_0	−0.041	0.010	W_{ecc} 60% v_0 −W_{ecc} 85% v_0	−0.007*	0.005	0.003	0.012	0.002
W_{ecc} 85% v_0	−0.048	0.014	W_{ecc} 30% v_0 −W_{ecc} 85% v_0	−0.016*	0.006	0.010	0.021	<0.001
W_{con} 30% v_0	0.007	0.002	W_{con} 30% v_0 −W_{con} 60% v_0	0.002*	0.001	−0.004	−0.001	0.004
W_{con} 60% v_0	0.010	0.002	W_{con} 60% v_0 −W_{con} 85% v_0	0.003*	0.002	−0.005	−0.001	0.002
W_{con} 85% v_0	0.012	0.003	W_{con} 30% v_0 −W_{con} 85% v_0	0.005*	0.002	−0.007	−0.003	<0.001
				Power $[(\frac{F}{F_0} \cdot \frac{\Delta L_S}{L_{S0}})s^1]$				
P_{ecc} 30% v_0	−0.027	0.008	P_{ecc} 30% v_0 −P_{ecc} 60% v_0	−0.035*	0.008	0.027	0.043	<0.001
P_{ecc} 60% v_0	−0.062	0.016	P_{ecc} 60% v_0 −P_{ecc} 85% v_0	−0.044*	0.017	0.028	0.061	<0.001
P_{ecc} 85% v_0	−0.107	0.032	P_{ecc} 30% v_0 −P_{ecc} 85% v_0	−0.079*	0.024	0.055	0.104	<0.001
P_{con} 30% v_0	0.006	0.002	P_{con} 30% v_0 −P_{con} 60% v_0	0.008*	0.002	−0.011	−0.006	<0.001
P_{con} 60% v_0	0.015	0.004	P_{con} 60% v_0 −P_{con} 85% v_0	0.013*	0.005	−0.018	−0.008	<0.001
P_{con} 85% v_0	0.028	0.007	P_{con} 60% v_0 −P_{con} 85% v_0	0.021*	0.006	−0.028	−0.015	<0.001

Work/power values ± SD are expressed in relative values $(\frac{F}{F_0} \cdot \frac{\Delta L_S}{L_{S0}})$ *and* $(\frac{F}{F_0} \cdot \frac{\Delta L_S}{L_{S0}})$ s^{-1}, *respectively. W, mechanical work; P, power output; ecc, eccentric phase during active muscle stretch; con, concentric phase during active muscle shortening; %V_0, percentage of maximum contraction velocity; ns, not significant. *The mean difference is significant at the 0.05 level.*

velocity (**Figure 8B**). However, the power produced by XBs increased with increasing shortening velocities (**Figure 8D**). This increase in power output can be explained by calculated XB forces (**Figure 2**, gray symbols) slightly above the *F-v-r* (**Figure 2**, blue line). Multiplication of these slightly higher forces with the respective shortening velocity results in the observed XB-based power output ($P = F \times v$) (**Figure 8D**). One possible explanation for the slightly enhanced XB forces (**Figure 2**, gray symbols) might be that too little non-XB forces were subtracted from control forces. Titin–actin interaction might be enabled (at least partially) by strong XB-binding (Leonard and Herzog, 2010; Powers et al., 2014; Tomalka et al., 2020). A reduced amount of strong XBs in the Blebbistatin condition might reduce non-XB-based forces and, thus, explains the slightly overestimated XB forces (**Figure 2**, gray symbols).

However, it cannot be taken for granted that Blebbistatin completely eliminates XB-based force production, since Blebbistatin [and similar drugs as butanedione monoxime (BDM) (Rassier and Herzog, 2004; Rassier, 2008) and benzyl-toluene sulfonamide (BTS) (Roots et al., 2007)] seems to affect the contractile apparatus in a complex manner (Minozzo and Rassier, 2010; Månsson et al., 2015). There are indications that Blebbistatin leads, among other things, to a considerable reduction of v_0 under certain conditions (Stewart et al., 2009; Rahman et al., 2018). Furthermore, with Blebbistatin the relative force enhancement increases during the ramp stretch of 3–5% L_{S0} (Pinniger et al., 2006; Minozzo and Rassier, 2010). An effect that is explainable by the potential influence of an increased population of weakly bound XBs, which are suggested to contribute to an increase in stiffness and non-XB-based force while strained during muscle stretch (Pinniger et al., 2006; Rassier, 2008; Minozzo and Rassier, 2010; Rahman et al., 2018).

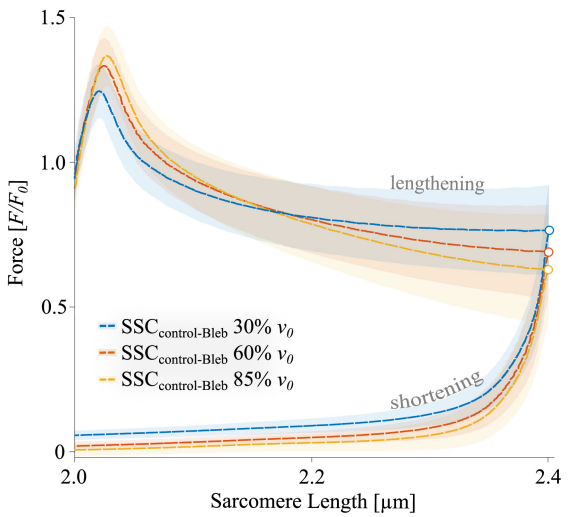

FIGURE 7 | The mean ± standard deviation (SD) of force-length traces of 'isolated XB' forces in SSCs contractions with varying velocities. 'Isolated XB' forces were calculated by subtracting the inhibited forces of the Blebbistatin condition (**Figure 5**) from the total force responses during the SSCs of the control condition (**Figure 4**) (colored dashed lines, subtractions) (see section "Calculations of XB- and Non-XB Forces"). The shaded regions around the dashed lines indicate the corresponding SD during active SSCs. The colored circles indicate the peak forces at the end of the stretch.

TABLE 3 | Descriptive statistics and pairwise comparisons of XB contributions to work and power.

Control minus Blebbistatin								
				Pairwise comparisons work $[\frac{F}{F_0} \cdot \frac{\Delta L_S}{L_{S0}}]$				***p*-values**
Descriptive statistics				**Mean differences**	**SD**	**95% Confidence interval of the difference**		
Variable	**Mean**	**SD**				**Lower**	**Upper**	
W_{ecc} 30% v_0	−0.163	0.015	W_{ecc} 30% v_0 −W_{ecc} 60% v_0	0.000	0.006	−0.007	0.006	1.000
W_{ecc} 60% v_0	−0.163	0.014	W_{ecc} 60% v_0 −W_{ecc} 85% v_0	0.001	0.005	−0.004	0.007	1.000
W_{ecc} 85% v_0	−0.164	0.017	W_{ecc} 30% v_0 −W_{ecc} 85% v_0	0.001	0.006	−0.005	0.007	1.000
W_{con} 30% v_0	0.026	0.003	W_{con} 30% v_0 −W_{con} 60% v_0	0.007*	0.002	0.005	0.009	<0.001
W_{con} 60% v_0	0.019	0.003	W_{con} 60% v_0 −W_{con} 85% v_0	0.005*	0.002	0.003	0.006	<0.001
W_{con} 85% v_0	0.014	0.003	W_{con} 30% v_0 −W_{con} 85% v_0	0.012*	0.002	0.010	0.014	<0.001
				Power $[(\frac{F}{F_0} \cdot \frac{\Delta L_S}{L_{S0}})s^1]$				
P_{ecc} 30% v_0	−0.137	0.013	P_{ecc} 30% v_0 −P_{ecc} 60% v_0	0.112*	0.011	0.100	0.123	<0.001
P_{ecc} 60% v_0	−0.249	0.022	P_{ecc} 60% v_0 −P_{ecc} 85% v_0	0.116*	0.017	0.099	0.133	<0.001
P_{ecc} 85% v_0	−0.365	0.037	P_{ecc} 30% v_0 −P_{ecc} 85% v_0	0.228*	0.025	0.202	0.254	<0.001
P_{con} 30% v_0	0.022	0.003	P_{con} 30% v_0 −P_{con} 60% v_0	−0.007*	0.002	−0.010	−0.005	<0.001
P_{con} 60% v_0	0.029	0.004	P_{con} 60% v_0 −P_{con} 85% v_0	−0.003	0.004	−0.006	0.001	0.611
P_{con} 85% v_0	0.032	0.007	P_{con} 60% v_0 −P_{con} 85% v_0	−0.010*	0.005	−0.015	−0.005	<0.001

*XB contributions were calculated by subtraction of forces obtained during Blebbistatin condition from forces during control condition (section "Calculations of XB- and **N**on-XB Forces"). Work/power values ± SD are expressed in relative values ($\frac{F}{F_0} \cdot \frac{\Delta L_S}{L_{S0}}$) and ($\frac{F}{F_0} \cdot \frac{\Delta L_S}{L_{S0}}$) s^{-1}, respectively. W, mechanical work; P, power output; ecc, eccentric phase during active muscle stretch; con, concentric phase during active muscle shortening; %v_0, percentage of maximum contraction velocity; ns, not significant. *The mean difference is significant at the 0.05 level.*

Regardless of the effect of Blebbistatin on the contractile apparatus, a contribution of weakly bound XBs to force during the stretch (Rassier, 2008; Minozzo and Rassier, 2010) seems to be likely only for small stretch amplitudes (≈1.5% L_{S0}) (see section "Muscle Stretch"). For rather extensive ramp amplitudes of 17% L_{S0}, as used in this study, weakly bound XBs rapidly detach (Schoenberg, 1985; Bagni et al., 2002). Thus, it seems unlikely that weakly bound XBs are primarily responsible for the observed significant peak forces at the end of the lengthening phase of the SSCs.

However, our approach does not clearly separate XB- and non-XB contributions. Accordingly, other inhibitors such as BTS or alternative approaches like the depletion of non-XB structures (e.g., selective digestion of titin by trypsin; Higuchi, 1992) should be considered for further studies attempting to separate XB- and non-XB contributions (Iwamoto, 2018; Ma et al., 2018).

Blebbistatin Condition: Influence of Non-XB Structures on Mechanical Work and Power Output

Linari et al. (2003) observed an increase in energy storage with increasing stretch velocity in frog muscle fibers and suggested that non-XB structures may be responsible for this observation. Recently, there is increasing support that contributions of non-XB structures, such as titin, are (at least partially) responsible for the observed SSC-effect on the muscle fiber level (Fukutani et al., 2017b; Fukutani and Herzog, 2019, 2020b; Tomalka et al., 2020). It is essential to separate XB and non-XB contributions to total muscle force to approach the physiological mechanisms. Our Blebbistatin experiments, which suppress XB contributions, confirm these recent observations on the importance of non-XB structures for the stretch phase of SSCs and point to a velocity dependence of the SSC-effect in the control condition.

In the presence of Blebbistatin, when actin–myosin cycling is negligible, we found a quasi-linear force response during the SSCs' stretch phase (**Figure 5**) with no muscle "give" upon active stretching (cf. section "Muscle Stretch"). Therefore, the increasing forces with increasing stretch velocities (**Figure 5**) point to higher loading of non-XB structures. This increased loading of titin or other non-XB structures with increasing stretch velocity contributes to increased energy storage during the stretch phase of SSCs, associated with amplified negative work and power (Linari et al., 2003; Pinniger et al., 2006; Tomalka et al., 2017).

Consequently, when a spring recoils, stored elastic energy is recovered in the shortening phase of SSCs and thus contributes to the observed performance amplification (**Figures 3**, **6**), which was also suggested by Lindstedt (2016) and Hessel et al. (2017). However, significantly more work is done on the muscle upon active muscle stretching (negative work) than work generated by the muscle during the shortening phase of SSCs (positive work), typical for viscoelastic materials. Viscoelastic titin behavior during SSCs has been reported in previous studies (Bianco et al., 2007; Chung et al., 2011; Herzog et al., 2014) and may be attributed to titin's mechano-structural properties. Thus, at low stretch velocities, temporary energy storage in viscoelastic elements leads to a significant reduction of muscle fiber's negative power (**Figures 3C**, **6C**), which agrees with Roberts and Azizi (2010).

Previous work showed that maximum eccentric forces in the XB-inhibited conditions are enhanced by 11-fold than passive experiments (without Blebbistatin and calcium) at 85% v_0 (Tomalka et al., 2020). This enhancement is partly attributed to

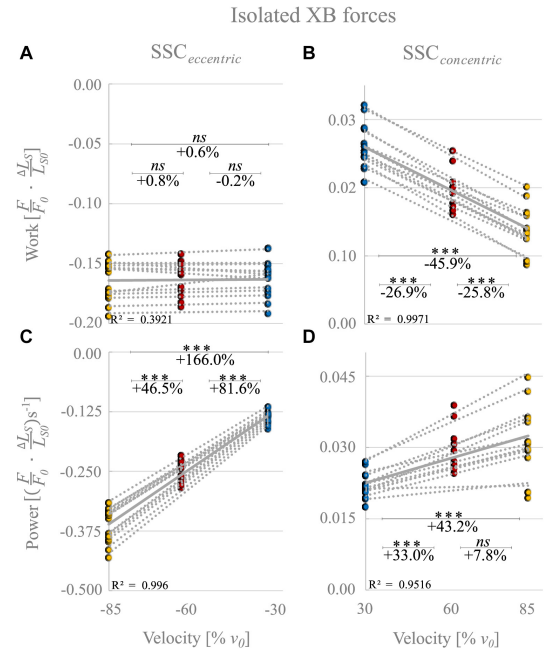

FIGURE 8 | 'Isolated XB' forces calculated by subtraction of forces obtained from control and Blebbistatin conditions. Influence of varying stretch-shortening velocities on work and power output during the lengthening phase **(A,C)** and the shortening phase **(B,D)** of SSCs, respectively. The gray dotted lines of the scatterplots shown in **(A–D)** indicate the individual paired data values, and gray solid lines indicate the mean values (n = 13 fibers from five rats). The blue circles indicate the SSC at 30% v_0, the red circles at 60% v_0, and the yellow circle at 85% v_0. Statistical analyses are based on calculations of XB forces by subtraction of Blebbistatin-suppressed forces from control forces. Work/power values are expressed in relative values ($\frac{F}{F_0} \cdot \frac{\Delta L_S}{L_{S0}}$) and ($\frac{F}{F_0} \cdot \frac{\Delta L_S}{L_{S0}}$)$s^{-1}$, respectively. Asterisks mark differences in work/power with varying velocities in the intergroup comparison. Significance levels are marked as follows: ***$p < 0.001$. *ns* means not significant.

calcium-induced stiffening of titin (by 20%) during activation (Labeit et al., 2003). However, more important seems to be the property of skeletal muscle titin to significantly reduce its persistence length upon activation, potentially by titin–actin interactions (Herzog, 2014; Nishikawa, 2016). As a beneficial consequence, the reduced titin length allows for increased force production during subsequent stretching (Kellermayer and Granzier, 1996; Labeit et al., 2003; Rode et al., 2009; Dutta et al., 2018; Tahir et al., 2020). These mechanisms might increase non-XB forces (presumably titin-based) during the stretch and enable the muscle to raise the total energy storage during active muscle stretching. Although many previous studies have investigated titin–actin interactions in the muscle (Kellermayer and Granzier, 1996; Astier et al., 1998; Nagy, 2004; Bianco et al., 2007; DuVall et al., 2017; Dutta et al., 2018; Li et al., 2020; Powers et al., 2020), naming of a target site for such interactions would be speculative at this time. For further information on the description of physiological mechanisms for the increase of titin stiffness in the active muscle, we refer to recent reviews (Linke, 2017; Herzog, 2018; Nishikawa, 2020).

Energy Recovery

The energy recovery (W_{con}/W_{ecc}; calculated by dividing the work output obtained during the shortening phase of the SSC by the work done during the lengthening phase) significantly decreases in the control condition with increasing velocity (from 17.4% at 30% v_0 to 12.8% at 85% v_0). This decrease is partly due to the XBs' dissipative properties, as dissipation increases with velocity. Thus, inhibiting XB-cycling by Blebbistatin leads to an increase in energy recovery. The ratio (W_{con}/W_{ecc}) is higher in the Blebbistatin condition compared with the control experiments. Interestingly, in the Blebbistatin condition, the energy recovery (W_{con}/W_{ecc}) tends to increase slightly with increasing velocity (from 23.9% at 30% v_0 to 26.4% at 85% v_0, *ns*). This increase suggests that titin can be mechanically understood as a spring in series with a damper (Millard et al., 2019; Brunello and Fusi, 2020; Powers et al., 2020). For such a spring-damper system, at a higher velocity, due to the serial damper, the spring is stretched with higher force (and can store more energy in the spring element) and thus release more energy when it is shortened. Although the force at the end of the stretch in the Blebbistatin condition is only about a third of the force in the control experiments (cf. **Figure 4** vs. **Figure 5**), the work during the XB-inhibited shortening phase of SSCs (at 85% v_0) reached nearly 50% of the work reported in the control condition. This finding implies a comparatively high energy recovery by titin.

Implications for *in vivo* Muscle Action

Despite clear evidence of the SSC-effect across all structural muscle levels (for a recent review, see Groeber et al., 2019), the contraction modalities (such as, e.g., the stretch-shortening amplitude and contraction velocity) might have important implications on experimental findings of comparable studies in the literature. In general, there are conflicting results regarding the occurrence of active SSCs in the muscle fascicles themselves during *in vivo* human movements. Depending on movement tasks studied, SSCs without (Cronin and Finni, 2013; Lai et al., 2015; Aeles and Vanwanseele, 2019) and with fascicle stretch (Ishikawa et al., 2005; Rubenson et al., 2012; Nikolaidou et al., 2017) have been reported. To date, no mechanism exclusively explains the SSC-effect and there likely is an interaction of mechanisms at different structural levels, with a dominance, e.g., depending on involved muscle (group) or movement dynamics. The transfer of experimental *in vitro* findings on *in vivo* SSC-effects should be considered with caution; however, the existence of an SSC-effect on the fiber level cannot be neglected. Since many (cyclical) everyday movements occur at submaximal muscle activation levels (Groeber et al., 2019), future studies should be done in skinned muscle fibers at different calcium concentrations to better understand the meaning of the SSC-effect in *in vivo* situations.

CONCLUSION

In the present study, we found work and power amplification in the shortening phase of SSCs in control- and Blebbistatin conditions. Interestingly, (i) this SSC-effect is velocity-dependent

since the power output increases with increasing velocity. (ii) The energy recovery (ratio of elastic energy storage and release in the SSC) is higher in the Blebbistatin condition compared with the control condition. This amplified energy recovery in the Blebbistatin condition can be explained by the viscoelastic properties of the non-XB structure titin.

This SSC-effect study promotes a basic understanding of human locomotion since SSCs are part of the most basic, everyday-type of muscle contraction. The separation of XB- and non-XB structures is of primary importance to give a more detailed understanding of the potential involvement of viscoelastic elements, such as titin, working as an energy-storing spring during lengthening contractions and SSCs. This information is required for the improvement of muscle models (Heidlauf et al., 2016; Tahir et al., 2018; Seydewitz et al., 2019) as well as for improved predictions by multi-body models (Röhrle et al., 2017; Haeufle et al., 2020) concerning, e.g., movement control and efficiency of locomotion.

DATA AVAILABILITY STATEMENT

The original contributions presented in the study are included in the article. Further inquiries can be directed to the corresponding author/s.

ETHICS STATEMENT

The skeletal muscle fibers from rats used for this study have been provided by another animal study that was approved according to the regulations of the German Animal Protection Law (Tierschutzgesetz, §4 (3); Permit Number: 35-9185.81/0491) by the Regierungspräsidium Stuttgart, Department of Landwirtschaft, Ländlicher Raum, Veterinär- und Lebensmittelwesen.

AUTHOR CONTRIBUTIONS

AT, TS, DH, and WS contributed to the conceptualization of the study and edited and revised the manuscript. SW and AT performed the experiments. AT analyzed the data, prepared the figures, and drafted the first version of the manuscript. AT and TS analyzed and discussed the results. All authors contributed to the article and approved the submitted version.

FUNDING

This work was supported by the Deutsche Forschungsgemeinschaft (DFG) under grants SI841/15-1, SI841/17-1, HA 5977/5-1, and SE 2109/2-1 as well as partially funded by the DFG as part of the German Excellence Strategy – EXC 2075 – 390740016.

ACKNOWLEDGMENTS

The authors would like to thank Annika Klotz for technical help with **Figure 1A**.

REFERENCES

Abbott, B. C., and Aubert, X. M. (1952). The force exerted by active striated muscle during and after change of length. *J. Physiol.* 117, 77–86. doi: 10.1113/jphysiol.1952.sp004733

Aeles, J., and Vanwanseele, B. (2019). Do stretch-shortening cycles really occur in the medial gastrocnemius? A detailed bilateral analysis of the muscle-tendon interaction during jumping. *Front. Physiol.* 10:1504. doi: 10.3389/fphys.2019.01504

Astier, C., Raynaud, F., Lebart, M. C., Roustan, C., and Benyamin, Y. (1998). Binding of a native titin fragment to actin is regulated by PIP2. *FEBS Lett.* 429, 95–98. doi: 10.1016/S0014-5793(98)00572-9

Bagni, M. A., Cecchi, G., Colombini, B., and Colomo, F. (2002). A non-cross-bridge stiffness in activated frog muscle fibers. *Biophys. J.* 82, 3118–3127. doi: 10.1016/S0006-3495(02)75653-1

Bianco, P., Nagy, A., Kengyel, A., Szatmári, D., Mártonfalvi, Z., Huber, T., et al. (2007). Interaction forces between F-actin and titin PEVK domain measured with optical tweezers. *Biophys. J.* 93, 2102–2109. doi: 10.1529/biophysj.107.106153

Bosco, C., Ito, A., Komi, P. V., Luhtanen, P., Rahkila, P., Rusko, H., et al. (1982). Neuromuscular function and mechanical efficiency of human leg extensor muscles during jumping exercises. *Acta Physiol. Scand.* 114, 543–550.

Bosco, C., Komi, P. V., and Ito, A. (1981). Prestretch potentiation of human skeletal muscle during ballistic movement. *Acta Physiol. Scand.* 111, 135–140. doi: 10.1111/j.1748-1716.1981.tb06716.x

Bottinelli, R., Canepari, M., Pellegrino, M. A., and Reggiani, C. (1996). Force-velocity properties of human skeletal muscle fibres: myosin heavy chain isoform and temperature dependence. *J. Physiol.* 495(Pt 2), 573–586.

Brenner, B. (1983). Technique for stabilizing the striation pattern in maximally calcium-activated skinned rabbit psoas fibers. *Biophys. J.* 41, 99–102.

Brunello, E., and Fusi, L. (2020). A new spring for titin. *J. Physiol.* 598, 213–214. doi: 10.1113/JP279314

Burmeister Getz, E., Cooke, R., and Lehman, S. L. (1998). Phase transition in force during ramp stretches of skeletal muscle. *Biophys. J.* 75, 2971–2983. doi: 10.1016/S0006-3495(98)77738-0

Cavagna, G. A., Citterio, G., and Jacini, P. (1981). Effects of speed and extent of stretching on the elastic properties of active frog muscle. *J. Exp. Biol.* 91, 131–143.

Cavagna, G. A., Dusman, B., and Margaria, R. (1968). Positive work done by a previously stretched muscle. *J. Appl. Physiol.* 24, 21–32.

Cavagna, G. A., Saibene, F. P., and Margaria, R. (1965). Effect of negative work on the amount of positive work performed by an isolated muscle. *J. Appl. Physiol.* 20, 157–158.

Choi, S. J., and Widrick, J. J. (2010). Calcium-activated force of human muscle fibers following a standardized eccentric contraction. *Am. J. Physiol. Cell Physiol.* 299, 1409–1417. doi: 10.1152/ajpcell.00226.2010

Chung, C., Methawasin, M., Nelson, O., Radke, M., Hidalgo, C., Gotthardt, M., et al. (2011). Titin based viscosity in ventricular physiology: an integrative investigation of PEVK-actin interactions. *J. Mol. Cell. Cardiol.* 51, 428–434. doi: 10.1016/j.yjmcc.2011.06.006

Cohen, J. (1988). *Statistical Power Analysis for the Behavioral Sciences*, 2nd Edn. Hoboken, NJ: Taylor and Francis.

Cormie, P., Mcguigan, M., and Newton, R. (2011). Developing maximal neuromuscular part 1 – biological basis of maximal power production. *Sports Med.* 41, 17–39.

Cornachione, A. S., and Rassier, D. E. (2012). A non-cross-bridge, static tension is present in permeabilized skeletal muscle fibers after active force inhibition

or actin extraction. *Am. J. Physiol. Cell Physiol.* 302, C566–C574. doi: 10.1152/ajpcell.00355.2011

Cronin, N. J., and Finni, T. (2013). Treadmill versus overground and barefoot versus shod comparisons of triceps surae fascicle behaviour in human walking and running. *Gait Posture* 38, 528–533. doi: 10.1016/j.gaitpost.2013.01.027

Dutta, S., Tsiros, C., Sundar, S. L., Athar, H., Moore, J., Nelson, B., et al. (2018). Calcium increases titin N2A binding to F-actin and regulated thin filaments. *Sci. Rep.* 8:14575. doi: 10.1038/s41598-018-32952-8

DuVall, M. M., Jinha, A., Schappacher-Tilp, G., Leonard, T. R., and Herzog, W. (2017). Differences in titin segmental elongation between passive and active stretch in skeletal muscle. *J. Exp. Biol.* 220:jeb160762. doi: 10.1242/jeb.160762

Edman, K. A. P., Elzinga, G., and Noble, M. (1978). Enhancement of mechanical performance by stretch during tetanic contractions of vertebrate skeletal muscle fibres. *J. Physiol.* 281, 139–155. doi: 10.1113/jphysiol.1978.sp012413

Edman, K. A. P., Elzinga, G., and Noble, M. (1982). Residual force enhancement after stretch of contracting frog single muscle fibers. *J. Gen. Physiol.* 80, 769–784. doi: 10.1085/jgp.80.5.769

Edman, K. A. P., and Tsuchiya, T. (1996). Strain of passive elements during force enhancement by stretch in frog muscle fibres. *J. Physiol.* 490, 191–205. doi: 10.1113/jphysiol.1996.sp021135

Flitney, F., and Hirst, D. (1978). Cross-bridge detachment and sarcomere 'give' during stretch of active frog's muscle. *J. Physiol.* 276, 449–465.

Freundt, J. K., and Linke, W. A. (2019). Passive properties of muscle titin as a force-generating muscle protein under regulatory control. *J. Appl. Physiol.* 126, 1474–1482. doi: 10.1152/japplphysiol.00865.2018

Fryer, M. W., Owen, V. J., Lamb, G. D., and Stephenson, D. G. (1995). Effects of creatine phosphate and P(i) on Ca2+ movements and tension development in rat skinned skeletal muscle fibres. *J. Physiol.* 482, 123–140. doi: 10.1113/jphysiol.1995.sp020504

Fukutani, A., and Herzog, W. (2019). Influence of stretch magnitude on the stretch-shortening cycle in skinned fibres. *J. Exp. Biol.* 222:jeb206557. doi: 10.1242/jeb.206557

Fukutani, A., and Herzog, W. (2020a). Differences in stretch-shortening cycle and residual force enhancement between muscles. *J. Biomech.* 112:110040. doi: 10.1016/j.jbiomech.2020.110040

Fukutani, A., and Herzog, W. (2020b). The stretch-shortening cycle effect is prominent in the inhibited force state. *J. Biomech.* 115:110136. doi: 10.1016/j.jbiomech.2020.110136

Fukutani, A., Isaka, T., and Herzog, W. (2021). Evidence for muscle cell-based mechanisms of enhanced performance in stretch-shortening cycle in skeletal muscle. *Front. Physiol.* 11:609553. doi: 10.3389/fphys.2020.609553

Fukutani, A., Joumaa, V., and Herzog, W. (2017a). Influence of residual force enhancement and elongation of attached cross-bridges on stretch-shortening cycle in skinned muscle fibers. *Physiol. Rep.* 5:e13477. doi: 10.14814/phy2.13477

Fukutani, A., Misaki, J., and Isaka, T. (2017b). Both the elongation of attached crossbridges and residual force enhancement contribute to joint torque enhancement by the stretch-shortening cycle. *R. Soc. Open Sci.* 4:161036. doi: 10.1098/rsos.161036

Gillis, G. B., and Biewener, A. A. (2001). Hindlimb muscle function in relation to speed and gait: in vivo patterns of strain and activation in a hip and knee extensor of the rat (*Rattus norvegicus*). *J. Exp. Biol.* 204, 2717–2731.

Gregor, R. J., Roy, R. R., Whiting, W. C., Lovely, R. G., Hodgson, J. A., and Edgerton, V. R. (1988). Mechanical output of the cat soleus during treadmill locomotion: in vivo vs in situ characteristics. *J. Biomech.* 21, 721–732. doi: 10.1016/0021-9290(88)90281-3

Groeber, M., Reinhart, L., Kornfeind, P., and Baca, A. (2019). The contraction modalities in a stretch-shortening cycle in animals and single joint movements in humans: a systematic review. *J. Sports Sci. Med.* 18, 604–614.

Haeufle, D. F. B., Günther, M., Bayer, A., and Schmitt, S. (2014). Hill-type muscle model with serial damping and eccentric force-velocity relation. *J. Biomech.* 47, 1531–1536. doi: 10.1016/j.jbiomech.2014.02.009

Haeufle, D. F. B., Wochner, I., Holzmüller, D., Driess, D., Günther, M., and Schmitt, S. (2020). Muscles reduce neuronal information load: quantification of control effort in biological vs. robotic pointing and walking. *Front. Robot. AI* 7:77. doi: 10.3389/frobt.2020.00077

Heidlauf, T., Klotz, T., Rode, C., Altan, E., Bleiler, C., Siebert, T., et al. (2016). A multi-scale continuum model of skeletal muscle mechanics predicting force enhancement based on actin–titin interaction. *Biomech. Model. Mechanobiol.* 15, 1423–1437. doi: 10.1007/s10237-016-0772-7

Heidlauf, T., Klotz, T., Rode, C., Siebert, T., and Röhrle, O. (2017). A continuum-mechanical skeletal muscle model including actin-titin interaction predicts stable contractions on the descending limb of the force-length relation. *PLoS Comput. Biol.* 13:e1005773. doi: 10.1371/journal.pcbi.1005773

Herzog, J., Leonard, T., Jinha, A., and Herzog, W. (2014). Titin (Visco-) elasticity in skeletal muscle myofibrils Titin (Visco-) elasticity in skeletal muscle myofibrils. *Mol. Cell. Biomech.* 11, 1–17. doi: 10.3970/mcb.2014.011.001.html

Herzog, W. (2014). Mechanisms of enhanced force production in lengthening (eccentric) muscle contractions. *J. Appl. Physiol.* 116, 1407–1417. doi: 10.1152/japplphysiol.00069.2013

Herzog, W. (2018). The multiple roles of titin in muscle contraction and force production. *Biophys. Rev.* 10, 1187–1199. doi: 10.1007/s12551-017-0395-y

Hessel, A. L., Lindstedt, S. L., and Nishikawa, K. C. (2017). Physiological mechanisms of eccentric contraction and its applications: a role for the giant titin protein. *Front. Physiol.* 8:70. doi: 10.3389/fphys.2017.00070

Higuchi, H. (1992). Changes in contractile properties with selective digestion of connectin (titin) in skinned fibers of frog skeletal muscle. *J. Biochem.* 111, 291–295. doi: 10.1093/oxfordjournals.jbchem.a123752

Hill, A. V. (1938). The heat of shortening and the dynamic constants of muscle. *Proc. R. Soc. B Biol. Sci.* 126, 136–195. doi: 10.1098/rspb.1938.0050

Holt, N. C., Roberts, T. J., and Askew, G. N. (2014). The energetic benefits of tendon springs in running: is the reduction of muscle work important? *J. Exp. Biol.* 217, 4365–4371. doi: 10.1242/jeb.112813

Huxley, A. F. (1957). Muscle structue and theories of contraction. *Prog. Biophys. Biophys. Chem.* 7, 255–318.

Huxley, A. F., and Simmons, R. M. (1971). Proposed mechanism of force generation in striated muscle. *Nature* 233, 533–538. doi: 10.1038/233533a0

Huxley, H. E. (1969). The mechanism of muscular contraction. *Science* 164, 1356–1366.

Huxley, H. E., Stewart, A., Sosa, H., and Irving, T. (1994). X-ray diffraction measurements of the extensibility of actin and myosin filaments in contracting muscle. *Biophys. J.* 67, 2411–2421. doi: 10.1016/S0006-3495(94)80728-3

Ishikawa, M., Niemelä, E., and Komi, P. V. (2005). Interaction between fascicle and tendinous tissues in short-contact stretch-shortening cycle exercise with varying eccentric intensities. *J. Appl. Physiol.* 99, 217–223. doi: 10.1152/japplphysiol.01352.2004

Iwamoto, H. (2018). Effects of myosin inhibitors on the X-ray diffraction patterns of relaxed and calcium-activated rabbit skeletal muscle fibers. *Biophys. Physicobiol.* 15, 111–120. doi: 10.2142/biophysico.15.0_111

Joyce, G., Rack, P., and Westbury, D. (1969). The mechanical properties of cat soleus muscle during controlled lengthening and shortening movements. *J. Physiol.* 204, 461–474.

Katz, B. (1939). The relation between force and speed in muscular contraction. *J. Physiol.* 96, 45–64. doi: 10.1113/jphysiol.1939.sp003756

Kellermayer, M., and Granzier, H. L. (1996). Calcium-dependent inhibition of in vitro thin-filament motility by native titin. *FEBS Lett.* 380, 281–286. doi: 10.1016/0014-5793(96)00055-5

Komi, P. V. (2000). Stretch-shorting cycle:a powerful model to study normal and fatigued muscle. *J. Biomech.* 33, 1197–1206.

Labeit, D., Watanabe, K., Witt, C., Fujita, H., Wu, Y., Lahmers, S., et al. (2003). Calcium-dependent molecular spring elements in the giant protein titin. *Proc. Natl. Acad. Sci. U.S.A.* 100, 13716–13721. doi: 10.1073/pnas.2235652100

Lai, A., Lichtwark, G. A., Schache, A. G., Lin, Y. C., Brown, N. A. T., and Pandy, M. G. (2015). In vivo behavior of the human soleus muscle with increasing walking and running speeds. *J. Appl. Physiol.* 118, 1266–1275. doi: 10.1152/japplphysiol.00128.2015

Leonard, T. R., and Herzog, W. (2010). Regulation of muscle force in the absence of actin-myosin-based cross-bridge interaction. *Am. J. Physiol. Cell Physiol.* 299, C14–C20. doi: 10.1152/ajpcell.00049.2010

Li, Y., Hesseit, A. L., Unger, A., Ing, D., Recker, J., Koser, F., et al. (2020). Graded titin cleavage progressively reduces tension and uncovers the source of A-band stability in contracting muscle. *Elife* 9:e64107. doi: 10.7554/eLife.64107

Li, Y., Unger, A., von Frieling-Salewsky, M., Rivas Pardo, J. A., Fernandez, J. M., and Linke, W. A. (2018). Quantifying the titin contribution to muscle force generation using a novel method to specifically cleave the titin springs in situ. *Biophys. J* 114:645. doi: 10.1016/j.bpj.2017.11.3480

Linari, M., Caremani, M., Piperio, C., Brandt, P., and Lombardi, V. (2007). Stiffness and fraction of Myosin motors responsible for active force in permeabilized

muscle fibers from rabbit psoas. *Biophys. J.* 92, 2476–2490. doi: 10.1529/biophysj.106.099549

Linari, M., Lucii, L., Reconditi, M., Casoni, M. E., Amenitsch, H., Bernstorff, S., et al. (2000). A combined mechanical and X-ray diffraction study of stretch potentiation in single frog muscle fibres. *J. Physiol.* 526, 589–596. doi: 10.1111/j.1469-7793.2000.00589.x

Linari, M., Woledge, R. C., and Curtin, N. A. (2003). Energy storage during stretch of active single fibres from frog skeletal muscle. *J. Physiol.* 548, 461–474. doi: 10.1113/jphysiol.2002.032185

Lindstedt, S. L. (2016). Skeletal muscle tissue in movement and health: positives and negatives. *J. Exp. Biol.* 219, 183–188. doi: 10.1242/jeb.124297

Linke, W. A. (2017). Titin gene and protein functions in passive and active muscle. *Annu. Rev. Physiol.* 80, 389–411. doi: 10.1146/annurev-physiol-021317-121234

Lombardi, V., and Piazzesi, G. (1990). The contractile response during steady lengthening of stimulated frog muscle fibres. *J. Physiol.* 431, 141–171.

Ma, W., Gong, H., and Irving, T. (2018). Myosin head configurations in resting and contracting murine skeletal muscle. *Int. J. Mol. Sci.* 19:2643. doi: 10.3390/ijms19092643

Månsson, A., Rassier, D., and Tsiavaliaris, G. (2015). Poorly understood aspects of striated muscle contraction. *Biomed. Res. Int.* 2015:245154. doi: 10.1155/2015/245154

Mártonfalvi, Z., Bianco, P., Linari, M., Caremani, M., Nagy, A., Lombardi, V., et al. (2014). Low-force transitions in single titin molecules reflect a memory of contractile history. *J. Cell Sci.* 127, 858–870. doi: 10.1242/jcs.138461

Millard, M., Franklin, D., and Herzog, W. (2019). A continuous and differentiable mechanical model of muscle force and impedance. *Biosyst. Biorobotics* 22, 262–266. doi: 10.1007/978-3-030-01887-0_50

Minozzo, F. C., and Rassier, D. E. (2010). Effects of blebbistatin and Ca2+ concentration on force produced during stretch of skeletal muscle fibers. *Am. J. Physiol. Cell Physiol.* 299, C1127–C1135. doi: 10.1152/ajpcell.00073.2010

Nagy, A. (2004). Differential actin binding along the PEVK domain of skeletal muscle titin. *J. Cell Sci.* 117, 5781–5789. doi: 10.1242/jcs.01501

Navarro-Cruz, R., Alcazar, J., Rodriguez-Lopez, C., Losa-Reyna, J., Alfaro-Acha, A., Ara, I., et al. (2019). The effect of the stretch-shortening cycle in the force-velocity velocity relationship and its association with physical function in older adults with COPD. *Front. Physiol.* 10:316. doi: 10.3389/fphys.2019.00316

Nikolaidou, M. E., Marzilger, R., Bohm, S., Mersmann, F., and Arampatzis, A. (2017). Operating length and velocity of human M. vastus lateralis fascicles during vertical jumping. *R. Soc. Open Sci.* 4:170185. doi: 10.1098/rsos.170185

Nishikawa, K. (2016). Eccentric contraction: unraveling mechanisms of force enhancement and energy conservation. *J. Exp. Biol.* 219, 189–196. doi: 10.1242/jeb.124057

Nishikawa, K. (2020). Titin: a tunable spring in active muscle. *Physiology* 35, 209–217. doi: 10.1152/physiol.00036.2019

Nishikawa, K. C., Monroy, J. A., Uyeno, T. E., Yeo, S. H., Pai, D. K., and Lindstedt, S. L. (2012). Is titin a "winding filament"? A new twist on muscle contraction. *Proc. R. Soc. B Biol. Sci.* 279, 981–990. doi: 10.1098/rspb.2011.1304

Nocella, M., Cecchi, G., Bagni, M. A., and Colombini, B. (2014). Force enhancement after stretch in mammalian muscle fiber: no evidence of cross-bridge involvement. *Am. J. Physiol. Cell Physiol.* 307, C1123–C1129. doi: 10.1152/ajpcell.00290.2014

Pinniger, G. J., Ranatunga, K. W., and Offer, G. W. (2006). Crossbridge and non-crossbridge contributions to tension in lengthening rat muscle: force-induced reversal of the power stroke. *J. Physiol.* 573, 627–643. doi: 10.1113/jphysiol.2005.095448

Powers, J. D., Bianco, P., Pertici, I., Reconditi, M., Lombardi, V., and Piazzesi, G. (2020). Contracting striated muscle has a dynamic I-band spring with an undamped stiffness 100 times larger than the passive stiffness. *J. Physiol.* 598, 331–345. doi: 10.1113/JP278713

Powers, K., Schappacher-Tilp, G., Jinha, A., Leonard, T., Nishikawa, K., and Herzog, W. (2014). Titin force is enhanced in actively stretched skeletal muscle. *J. Exp. Biol.* 217, 3629–3636. doi: 10.1242/jeb.105361

Rahman, M. A., Ušaj, M., Rassier, D. E., and Månsson, A. (2018). Blebbistatin effects expose hidden secrets in the force-generating cycle of actin and myosin. *Biophys. J.* 115, 386–397. doi: 10.1016/j.bpj.2018.05.037

Ranatunga, K. W. (1982). Temperature-Dependence of shortening velocity skeletal muscle. *J. Physiol.* 329, 465–483.

Ranatunga, K. W. (1984). The force-velocity relation of rat fast- and slow-twitch muscles examined at different temperatures. *J. Physiol.* 351, 517–529. doi: 10.2170/jjphysiol.34.1

Rassier, D., and Herzog, W. (2004). Active force inhibition and stretch-induced force enhancement in frog muscle treated with BDM. *J. Appl. Physiol.* 97, 1395–1400. doi: 10.1152/japplphysiol.00377.2004

Rassier, D. E. (2008). Pre-power stroke cross bridges contribute to force during stretch of skeletal muscle myofibrils. *Proc. R. Soc. B Biol. Sci.* 275, 2577–2586. doi: 10.1098/rspb.2008.0719

Rivas-Pardo, J. A., Eckels, E. C., Popa, I., Kosuri, P., Linke, W., and Fernández, J. M. (2016). Work done by titin protein folding assists muscle contraction. *Cell Rep.* 14, 1339–1347. doi: 10.1016/j.celrep.2016.01.025

Roberts, T. J., and Azizi, E. (2010). The series-elastic shock absorber: tendons attenuate muscle power during eccentric actions. *J. Appl. Physiol.* 109, 396–404. doi: 10.1152/japplphysiol.01272.2009

Rode, C., Siebert, T., and Blickhan, R. (2009). Titin-induced force enhancement and force depression: a "sticky-spring" mechanism in muscle contractions? *J. Theor. Biol.* 259, 350–360. doi: 10.1016/j.jtbi.2009.03.015

Röhrle, O., Sprenger, M., and Schmitt, S. (2017). A two-muscle, continuum-mechanical forward simulation of the upper limb. *Biomech. Model. Mechanobiol.* 16, 743–762. doi: 10.1007/s10237-016-0850-x

Roots, H., Offer, G. W., and Ranatunga, K. W. (2007). Comparison of the tension responses to ramp shortening and lengthening in intact mammalian muscle fibres: crossbridge and non-crossbridge contributions. *J. Muscle Res. Cell Motil.* 28, 123–139. doi: 10.1007/s10974-007-9110-0

Rubenson, J., Pires, N. J., Loi, H. O., Pinniger, G. J., and Shannon, D. G. (2012). On the ascent: the soleus operating length is conserved to the ascending limb of the force-length curve across gait mechanics in humans. *J. Exp. Biol.* 215, 3539–3551. doi: 10.1242/jeb.070466

Schappacher-Tilp, G., Leonard, T., Desch, G., and Herzog, W. (2015). A novel three-filament model of force generation in eccentric contraction of skeletal muscles. *PLoS One* 10:e0117634. doi: 10.1371/journal.pone.0117634

Schoenberg, M. (1985). Equilibrium muscle cross-bridge behavior. Theoretical considerations. *Biophys. J.* 48, 467–475. doi: 10.1016/S0006-3495(85)83802-9

Seiberl, W., Power, G. A., Herzog, W., and Hahn, D. (2015). The stretch-shortening cycle (SSC) revisited: residual force enhancement contributes to increased performance during fast SSCs of human m. adductor pollicis. *Physiol. Rep.* 3:e12401. doi: 10.14814/phy2.12401

Seydewitz, R., Siebert, T., and Böl, M. (2019). On a three-dimensional constitutive model for history effects in skeletal muscles. *Biomech. Model. Mechanobiol* 18, 1665–1681. doi: 10.1007/s10237-019-01167-9

Shalabi, N., Cornachione, A., Leite, F., Vengallatore, S., and Rassier, D. E. (2017). Residual force enhancement is regulated by titin in skeletal and cardiac myofibrils. *J. Physiol.* 595, 2085–2098. doi: 10.1113/JP272983

Stephenson, D. G., and Williams, D. A. (1982). Effects of sarcomere length on the force-pCa relation in fast- and slow-twitch skinned muscle fibres from the rat. *J. Physiol.* 333, 637–653.

Stewart, M., Franks-Skiba, K., and Cooke, R. (2009). Myosin regulatory light chain phosphorylation inhibits shortening velocities of skeletal muscle fibers in the presence of the myosin inhibitor blebbistatin. *J. Muscle Res. Cell Motil.* 30, 17–27. doi: 10.1007/s10974-008-9162-9

Sugi, H. (1972). Tension changes during and after stretch in frog muscle fibres. *J. Physiol.* 225, 237–253.

Sugi, H., and Tsuchiya, T. (1988). Stiffness changes during enhancement and deficit of isometric force by slow length changes in frog skeletal muscle fibres. *J. Physiol.* 407, 215–229. doi: 10.1113/jphysiol.1988.sp017411

Tahir, U., Hessel, A. L., Lockwood, E. R., Tester, J. T., Han, Z., Rivera, D. J., et al. (2018). Case study: a bio-inspired control algorithm for a robotic foot-ankle prosthesis provides adaptive control of level walking and stair ascent. *Front. Robot. AI* 5:36. doi: 10.3389/frobt.2018.00036

Tahir, U., Monroy, J. A., Rice, N. A., and Nishikawa, K. C. (2020). Effects of a titin mutation on force enhancement and force depression in mouse soleus muscles. *J. Exp. Biol.* 223:jeb197038. doi: 10.1242/jeb.197038

Tomalka, A., Rode, C., Schumacher, J., and Siebert, T. (2017). The active force – length relationship is invisible during extensive eccentric contractions in

skinned skeletal muscle fibres. *Proc. R. Soc. B Biol. Sci.* 284:20162497. doi: 10.1098/rspb.2016.2497

Tomalka, A., Weidner, S., Hahn, D., Seiberl, W., and Siebert, T. (2020). Cross-Bridges and sarcomeric non-cross-bridge structures contribute to increased work in stretch-shortening cycles. *Front. Physiol.* 11:921. doi: 10.3389/fphys.2020.00921

Van Ingen Schenau, G. J., Bobbert, M. F., and de Haan, A. (1997). Mechanics and energetics of the stretch-shortening cycle: a stimulating discussion. *J. Appl. Biomech.* 13, 484–496.

Wakabayashi, K., Sugimoto, Y., Tanaka, H., Ueno, Y., Takezawa, Y., and Amemiya, Y. (1994). X-ray diffraction evidence for the extensibility of actin and myosin filaments during muscle contraction. *Biophys. J.* 67, 2422–2435. doi: 10.1016/S0006-3495(94)80729-5

Wilson, G., Elliott, B., and Wood, G. (1991). The effect on performance of imposing a delay during an SSC movement. *Med. Sci. Sports Exerc.* 23, 364–370.

Conflict of Interest: The authors declare that the research was conducted in the absence of any commercial or financial relationships that could be construed as a potential conflict of interest.

Advantages of publishing in Frontiers

OPEN ACCESS
Articles are free to read for greatest visibility and readership

FAST PUBLICATION
Around 90 days from submission to decision

HIGH QUALITY PEER-REVIEW
Rigorous, collaborative, and constructive peer-review

TRANSPARENT PEER-REVIEW
Editors and reviewers acknowledged by name on published articles

Frontiers
Avenue du Tribunal-Fédéral 34
1005 Lausanne | Switzerland

Visit us: www.frontiersin.org
Contact us: frontiersin.org/about/contact

REPRODUCIBILITY OF RESEARCH
Support open data and methods to enhance research reproducibility

DIGITAL PUBLISHING
Articles designed for optimal readership across devices

FOLLOW US
@frontiersin

IMPACT METRICS
Advanced article metrics track visibility across digital media

EXTENSIVE PROMOTION
Marketing and promotion of impactful research

LOOP RESEARCH NETWORK
Our network increases your article's readership